# INVESTIGATING THE EFFECTS OF POLYCYCLIC AROMATIC HYDROCARBON EXPOSURE ON AVIAN PRE-MIGRATORY FUELLING AND MIGRATION

A Thesis Submitted to the College of

Graduate and Postdoctoral Studies

In Partial Fulfillment of the Requirements

For the Degree of Doctor of Philosophy

In the Toxicology Graduate Program

University of Saskatchewan

Saskatoon, Saskatchewan, Canada

By

**Kristin Bianchini**

© Copyright Kristin Bianchini, December 2018. All rights reserved.

## PERMISSION TO USE

In presenting this thesis in partial fulfillment of the requirements for a postgraduate degree from the University of Saskatchewan, I agree that the Libraries of the University may make it freely available for inspection. I further agree that permission for copying of this thesis in any manner, in whole or in part, for scholarly purpose may be granted by the professor or professors who supervised this thesis work or, in their absence, by the Head of the Department or the Dean of the College in which this thesis work was done. It is understood that any copying or publication or use of this thesis or parts thereof for financial gain shall not be allowed without my written permission. It is also understood that due recognition shall be given to me and to the University of Saskatchewan in any scholarly use which may be made of any material in this thesis.

Requests for permission to copy or to make other use of material in this thesis in whole or parts should be addressed to:

Chair of the Toxicology Graduate Program
Toxicology Centre
University of Saskatchewan
44 Campus Drive
Saskatoon, Saskatchewan S7N 5B3
Canada

OR

Dean
College of Graduate and Postdoctoral Studies
University of Saskatchewan
116 Thorvaldson Building, 110 Science Place
Saskatoon, Saskatchewan S7N 5C9
Canada

## ABSTRACT

Long-distance avian migrants travel vast distances between their breeding and wintering grounds. Often this involves non-stop flights of thousands of kilometers without access to supplementary food or water. During these periods, birds rely almost exclusively on endogenously stored fuel to sustain several hours to days of migration flight. Accomplishing these extreme feats of endurance requires that birds rapidly accumulate fat stores prior to migration and at discrete sites (i.e., staging sites) along the migration route. Rapidly storing enough fat is crucial for long-distance migrants. Adequate fuel accumulation increases the probability of surviving migration. As well, fat deposition rates and departure fuel loads affect migration pace, and earlier arrival on the breeding grounds in the spring increases reproductive performance. As a result, impaired pre-migratory fuelling has been identified as an important factor in the ongoing declines of long-distance migratory bird populations.

There is evidence to suggest that polycyclic aromatic hydrocarbons (PAHs), the toxic constituents of oil pollution, can impair refuelling physiology and limit pre-migratory fat accumulation. Despite this evidence, however, a link between PAH exposure and impaired pre-migratory fuelling had yet to be established. Therefore, the objectives of this research were (1) to directly assess whether PAH ingestion impairs pre-migratory fuelling, (2) to investigate the physiological mechanisms of PAH-induced pre-migratory fuelling impairment, and (3) to characterize the impacts of impaired fuelling on avian migration timing.

My first objective was addressed using a captive dosing experiment. Sanderling (*Calidris alba*), a long-distance migratory shorebird, were orally dosed with environmentally-relevant PAH concentrations and mixtures. I found that oral exposure to PAHs during staging lowered Sanderling pre-migratory body mass gains, with individuals in the high dose group (dosed with 1260 µg PAH/kg-bw/day) gaining 4.4 ± 3.7 g less than controls. More specific investigations into the mechanisms underlying this result showed that serum bile acid concentrations and the hepatic mRNA expression of liver basic fatty acid binding protein 1 (*Lbfabp*) and hepatic lipase (*Lipc)* were reduced by PAH exposure. This suggested that sublethal PAH ingestion impaired fuelling by disrupting cholesterol and lipid homeostasis. These results confirmed that PAH exposure can limit deposition of the fuel loads that influence staging durations, departure decisions, and migratory speed. Therefore, further research was warranted to characterize the effects of PAH exposure and fuelling impairment on avian migration timing. For this work, I

first examined the relationship between PAH contamination and staging site quality for fuelling shorebirds. I trapped Sanderling and Red knots (*C. canutus*) from six staging sites along the Texas and Louisiana Gulf Coast, which were variably affected by the Deepwater Horizon oil spill and which are susceptible to frequent and repeated oil pollution. Upon capture, I collected blood samples to measure Sanderling and Red knot plasma metabolite levels. I estimated PAH ingestion from foraging by measuring sediment total PAH concentrations at each site. Staging sites in Louisiana had the highest total sediment PAH concentrations (3.41 – 640 ng/g sediment). Metabolite data suggested that Sanderling in Louisiana exhibited the lowest refuelling rates, and both Sanderling and Red knots departed later than average from Louisiana. Next, I investigated the relationship between fuelling and migration timing in northward-migrating Sanderling using radio-telemetry techniques. I attached coded nanotags to Sanderling at the six Gulf of Mexico staging sites and at Chaplin Lake, Saskatchewan, a more northern staging site along Sanderlings' migration route. Fuel loads were negatively correlated with stopover durations and departure dates at both sites. I also found that individuals that departed later from the Gulf of Mexico also arrived later and subsequently departed later from Saskatchewan. Model estimates suggested that a bird that was 5 g lighter at capture departed 2 days later from the Gulf of Mexico, arrived 1.5 days later in Saskatchewan, and then departed 16 hours later for its breeding grounds. There is thus evidence that fuel loads affect Sanderling migration timing and that slower birds do not catch up with earlier individuals.

Fully understanding how PAHs affect pre-migratory fuelling, and ultimately avian populations, requires a mechanistic approach that links molecular-level events to adverse outcomes at the population-level. Therefore, the fourth objective of this research was to synthesize multiple datasets on how PAHs can affect avian pre-migratory fuelling into a biologically plausible mode of action that is useful to avian ecotoxicological risk assessment. This was accomplished by organizing the data of this thesis and existing knowledge into a putative adverse outcome pathway linking the molecular mechanisms underlying pre-migratory fuelling impairment to the effects of impaired fuelling on migratory bird populations. Organizing data into a progression of toxicity events increases our understanding of how PAHs and compounds with similar mechanisms of action can affect avian populations. Therefore, this thesis provides new information to guide avian ecotoxicological risk assessments and to increase our understanding of the toxicological threats to long-distance migratory bird populations.

## ACKNOWLEDGEMENTS

This work would not have been possible, or half as enjoyable, without the support of many excellent people. First, I would like to like to extend my sincere gratitude to my advisor, Dr. Christy Morrissey. When I started a PhD in Avian Ecotoxicology, I had no formal background in birds, ecology, or toxicology, but Christy welcomed me to her lab without hesitation. Her passion for birds and ecotoxicology is contagious, and I cannot thank her enough for fuelling my own enthusiasm for these topics. Christy's mentorship and encouragement have helped me to grow as a scientist. She has shown unwavering confidence in my research and my abilities, which was especially reassuring when my own confidence was lacking. Christy always inspired me to push myself beyond where I thought my limits were and showed me that with enough effort, no problem is insurmountable. Next, I would like to extend my sincere appreciation to my committee members, Drs. Jane Alcorn, Jorge Chedrese, Markus Hecker, and Dave Janz. Their advice and expertise helped to shape and improve my thesis. They have been an invaluable resource throughout my PhD.

I am deeply indebted to Lori Wilson, David Newstead, and Delaina Leblanc, who showed me genuine hospitality in Chaplin, Texas, and Louisiana, and without whom none of my field work would have been possible. Lori is one of the kindest and most unfailingly generous people I have ever met. I wish to thank Lori for her enthusiasm and cheerfulness, for sharing her local knowledge, for her amazing home cooking, and for bringing us midnight hot chocolate and scones. Lori is a true gem. A very special thanks to David for helping me to catch Red knots and "trash birds" in the Gulf of Mexico. David is forever busy working on multiple projects, but he always found time to drive us around on the beach to catch birds. I cannot thank him enough for his contribution to my project. I would also like to thank David for his kindness and patience, for sharing his extensive local birding knowledge, and for introducing me to fun with explosives. I would like to thank Delaina for hosting us and coordinating the work in Louisiana. Delaina's warm and welcoming personality, her enthusiasm for everyone's research, and her positivity made Grand Isle feel more like summer camp with friends than hard work.

I have been incredibly lucky to have met and worked with a number of stellar individuals for this project. My field work in Chaplin Lake can be a true test of the spirit, and I would like to thank everyone who suffered through mud, cold, and sleep deprivation to help me catch Sanderling in Saskatchewan. I would also like to thank all the wonderful people who helped

catch Sanderling and Red knots in the Gulf of Mexico. Thanks to the landowners in Saskatchewan for generously donating a portion of their land and for volunteering their time to help set up Motus towers. A special thanks to my fellow peep, Jessica Howell. No matter how frustrating things became with those "dang" towers, noose carpets, driving birds across the province, or preventing Texans from running us over, your friendship and positive attitude helped me every step of the way. I would also like to thank everyone who contributed to my captive work. Thanks to Gwen Roy and Mackenzie Clarke for spending their summer with me and the Sanderling in FAAR. It was a tough job with long hours and no days off, but Gwen and Mackenzie's dedication, engagement, and positivity were an enormous motivation.

I am extremely grateful to the Natural Science and Engineering Research Council of Canada (NSERC), the University of Saskatchewan, and the Toxicology Centre for providing stipend support for my PhD. I would also like to acknowledge NSERC and Environment and Climate Change Canada for financially supporting this project.

My success in graduate school would not have been possible without the support of my family and friends. I am incredibly thankful to the Morrissey lab members, both past and present, for their friendship and support throughout my project. I am very fortunate to have been part of such a solid group of people. The fun and laughter that we shared are what I will remember and cherish most about my PhD. Thanks to "everyJuan" in the Core Four for the adventures, music, and red velvet cupcakes, and thanks the Meewasin Wheelers for the movie nights, dinners, and perpetual puppy peer pressure. My deepest thanks to my parents, Andy and Linda, and my brother, Eric, for their unwavering support and encouragement throughout university. Your love, patience, and continual reassurance are the reason that I have made it this far in grad school. Thanks to my niece, Lyra, for bringing everyone happiness with her silliness and energy. Thank you to my pup, Maggie, for being the perfect writing buddy and for forcing me to be present in the moment.

Finally, to my partner and best friend, Tim. Thank you for following me across the country and for sticking it out with me in Saskatoon. Thank you for supporting me through every success and frustration. You continually reminded me that there is a life outside of grad school. It has been an intense and interesting journey, and I'm glad that I could share it with you.

## TABLE OF CONTENTS

## LIST OF TABLES

## LIST OF FIGURES

## LIST OF ABBREVIATIONS

| | |
|---|---|
| ºC | degrees Celsius |
| α | significance level |
| Acenthy | acenaphthylene |
| Aceph | acenaphthene |
| *Acsl5* | acyl-CoA synthetase long-chain family member 5 |
| AhR | aryl hydrocarbon receptor |
| AICc | Akaike's information criterion corrected for small sample size |
| AMPK | AMP-activated protein kinase |
| Anth | anthracene |
| AO | adverse outcome |
| AOP | adverse outcome pathway |
| *ApoB* | apolipoprotein B |
| AST | aspartate aminotransferase |
| ASY | after second year |
| *β* | beta coefficient |
| BaA | benz[*a*]anthracene |
| BaP | benzo[*a*]pyrene |
| BbF | benzo[*b*]fluoranthene |
| BF | Bolivar Flats |
| BghiP | benzo[*ghi*]perylene |
| BkF | benzo[*k*]fluoranthene |
| BOHB | β-hydroxybutyrate |
| bw | body weight |
| cDNA | complementary DNA |
| Chry | chrysene |
| CK | creatine kinase |
| cm | centimetre |
| $CO_2$ | carbon dioxide |
| cos | cosine |
| Ct | threshold cycle |

| | |
|---|---|
| CYP | cytochrome P450 |
| *Cyp1a* or CYP1A | cytochrome P450 1A |
| *Cyp1a4* or CYP1A4 | cytochrome P450 1A4 |
| CYP1B | cytochrome P450 1B |
| *Cyp7a1* | cytochrome P450 7a1 |
| *Cyp7b1* or CYP7B1 | cytochrome P450 7B1 |
| DahA | dibenz[*ah*]anthracene |
| ΔAICc | delta AICc |
| DCCO | double-crested cormorant |
| DCM | dichloromethane |
| DNA | deoxyribonucleic acid |
| δ*R* | uncertainty in the difference in mass |
| δX | standard error of the mean control group mass |
| δY | standard error of the mean high dose group mass |
| EDTA | ethylenediaminetetraacetic acid |
| *Eefa1a1* | elongation factor 1 alpha 1 |
| EI | Elmer's Island |
| EROD | ethoxyresorufin-*O*- deethylase |
| eV | electron volt |
| *F* | F statistic |
| F | forward |
| FAAR | Facility for Applied Avian Research |
| FABP | fatty acid binding protein |
| FAT/CD36 | fatty acid translocase |
| FI | fattening index |
| Fluor | fluorene |
| g | gram |
| GC/MS | gas chromatography/mass spectrometry |
| GGT | gamma-glutamyl transferase |
| GI | Grand Isle |
| GOM | Gulf of Mexico |
| GPx | glutathione peroxidase |

| | |
|---|---|
| *Gpx3* or GPX3 | glutathione peroxidase 3 |
| *Gstm3* or GSTM3 | glutathione S-transferase 3 |
| h | hour |
| Hct | hematocrit |
| HEPES | 4-(2-hydroxyethyl)-1-piperazineethanesulfonic acid |
| HIS | hepatosomatic index |
| *Hmgcr* or HMGCR | 3-hydroxy-3-methylglutaryl-coenzyme A reductase |
| HPLC | high performance liquid chromatography |
| IcdP | indeno[1,2,3-*cd*]pyrene |
| k | number of estimated parameters in the model |
| KE | key event |
| KE1 | key event 1 |
| KE2 | key event 2 |
| KE3 | key event 3 |
| KE4 | key event 4 |
| KE5 | key event 5 |
| KER | key event relationship |
| kg | kilogram |
| $KH_2PO_4$ | potassium dihydrogen phosphate |
| kJ | kilojoule |
| km | kilometer |
| l | litre |
| *Lbfabp* or LBFABP | liver basic fatty acid binding protein 1 |
| *Lipc* or LIPC | hepatic lipase |
| log | logarithm |
| m | meters |
| M | molar |
| MAPK | mitogen-activated protein kinase |
| MC252 | Mississippi Canyon 252 oil |
| mg | milligram |
| MHz | megahertz |
| MI | Mustang Island |

| | |
|---|---|
| MIE | molecular initiating event |
| min | minute |
| ml | millilitre |
| mm | millimetre |
| mM | millimolar |
| mmol | millimole |
| mRNA | messenger ribonucleic acid |
| ms | milliseconds |
| n | sample size |
| NaCl | sodium chloride |
| NADPH | nicotinamide adenine dinucleotide phosphate |
| Naph | naphthalene |
| NEFA | non-esterified fatty acids |
| ng | nanogram |
| nm | nanometre |
| nM | nanomolar |
| NPI | North Padre Island |
| NTC | no template control |
| O.C.T. | optimal cutting temperature |
| OECD | Organisation for Economic Co-operation and Development |
| ON | Ontario |
| ORO | oil red O |
| *p* | probability value |
| PAH | polycyclic aromatic hydrocarbon |
| PC | principal component |
| PC1 | principal component axis 1 |
| PC2 | principal component axis 2 |
| PC3 | principal component axis 3 |
| PCA | principal component analysis |
| PCR | polymerase chain reaction |
| PERMANOVA | permutational multivariate analysis of variance |
| Phen | penanathrene |

| | |
|---|---|
| PPAR | peroxisome proliferator-activated receptor |
| PPARγ | peroxisome proliferator-activated receptor gamma |
| R | reverse |
| $R^2$ | coefficient of determination |
| *Rpl4* or RPL4 | ribosomal protein L4 |
| s | second |
| SE | standard error |
| *Slco1a2* or | solute carrier organic anion transporter family, member 1A2 |
| SY | second year |
| t | tonnes |
| TCDD | 2,3,7,8-tetrachlorodipenzo-*p*-dioxin |
| TG | triglyceride |
| tPAH | total PAH |
| U | unit |
| UA | uric acid |
| µg | microgram |
| µl | microlitre |
| µm | micrometre |
| µmol | micromole |
| w | AICc weight |
| $x^2$ | number raised to the second power |
| $x^4$ | number raised to the fourth power |
| x g | centrifugal force |

## NOTE TO READERS

This thesis is organized and formatted to follow the University of Saskatchewan College of Graduate Studies and Research guidelines for a manuscript-style thesis. Chapter 1 is a general introduction and literature review, including project goals and objectives. Chapter 6 contains a general discussion and overall conclusion. Chapters 2, 3, 4, and 5 of this thesis are organized as manuscripts for publication in peer-reviewed scientific journals. Chapter 2 was published in the journal, *Ecotoxicology and Environmental Safety*, and Chapter 4 was published in the journal, *Environmental Science & Technology*. Chapter 3 and 5 are in preparation for submission for publication. Full citations for the research papers and a description of author contributions are provided following the preface of each chapter. As a result of the manuscript-style format, there is some repetition of material in the introduction and material and methods sections of the thesis. The tables, figures, supporting information, and references cited in each chapter have been reformatted here to a consistent thesis style. References cited in each chapter are combined and listed in the 'References' section of the thesis. Supporting information associated with research chapters are presented in the 'Appendix' section at the end of this thesis. Tables and figures included in the Appendix are numbered consecutively as A.1, A.2, etc.

# 1 CHAPTER 1: GENERAL INTRODUCTION

## PREFACE

Chapter 1 is a general introduction and literature review of the topics of avian migration, pre-migratory fuelling, oil pollution, and polycyclic aromatic hydrocarbon toxicity. Chapter 1 also discusses shorebird ecology and the utility of shorebirds as a model for studying oil contaminant effects in birds. Chapter 1 also includes the overall goals and objectives of the thesis and the hypotheses and predictions tested in the subsequent chapters.

### 1.1 Avian migration

Migration is one of the most remarkable life history features of birds. An estimated 19% of the world's extant bird species are migratory and make annual, cyclical movements between distinct breeding and wintering ranges (Kirby et al., 2008). Migration is thought to have evolved to exploit predictable seasonal changes in resource availability that improve overall fitness (Alerstam et al., 2003). Birds migrate to higher latitudes to avoid density-dependent nest predation and increase their reproductive output, and migration to lower latitudes allows migrants to avoid inclement weather and to benefit from higher foraging opportunities and better roosting sites (Fretwell, 1980; Klaassen et al., 2012). Such spatial opportunism can give migrants a selective advantage over resident species (Alerstam et al., 2003).

To achieve this selective advantage, some avian migrants undertake astounding endurance flights. For example, the ruby-throated hummingbird (*Archilochus colubris*), a bird weighing only 3 – 3.5 g, flies non-stop for over 800 km when it migrates directly across the Gulf of Mexico (Robinson et al., 1996). Bar-tailed godwits (*Limosa lapponica*) make extreme 11,700 km non-stop flights between Alaska and New Zealand (Gill et al., 2005). Great snipes (*Gallinago media*) sustain very fast ground speeds of 15 – 27 m/s for 4300 – 6800 km non-stop flights, which they accomplish in only 48 to 96 hours (Klaassen et al., 2011). It is important to remember that birds accomplish these highly aerobic, non-stop, multi-day flights without access to supplementary food or water (Newton, 2008). Therefore, storing adequate fuel loads prior to migration is critical for avian migrants.

Despite the advantages that birds gain by migrating, migration is not without its risks. During migration, birds can experience a higher risk of mortality due to starvation, predation, storms, or adverse weather en route (Newton, 2006), and previous work shows that rates of mortality are higher on migration than during the breeding and wintering periods (Sillett and Holmes, 2002). It has also been suggested that poor conditions on migration could act as a bottleneck that limit migrant bird populations (Newton, 2006). Indeed, long-distance migratory bird populations are currently experiencing population declines globally (Holmes, 2007; Sanderson et al., 2006; Zockler et al., 2003). These declines are largely attributed to anthropogenic activities that impair birds' ability to efficiently fuel prior to migration (Klaassen et al., 2012).

### 1.2 Pre-migratory fuelling

Most long-distance migratory birds rely on endogenously stored energy to fuel prolonged migration flights. Therefore, migration is typically composed of alternating periods of migration flight and periods where birds stop at specific locations (i.e., staging sites) to rest and refuel (Warnock, 2010). Pre-migratory refuelling involves a series of behavioural and physiological adjustments, including increasing food consumption (hyperphagia) and fuel assimilation efficiency, that enable the rapid accumulation of fuel stores (Bairlein, 2002). The predominant fuel used for long-distance avian migration is fat. Fat contributes to about 90% of total migration energy expenditure, and protein catabolism provides the remaining 10% of the energy for migration (Jenni and Jenni-Eiermann, 1998) and also supplies migrants with glucose, key metabolic intermediates, and metabolic water (Guglielmo et al., 2017). Fat is the ideal fuel for long-distance migration. Because fatty acids are stored with relatively less water than protein and carbohydrates, fat has a higher energy density than either other energy source (37 kJ/g versus 4-5 kJ/g; Jenni and Jenni-Eiermann, 1998). Therefore, by storing energy as fat, long-distance migratory birds maximize the amount of energy stored per unit mass (Guglielmo, 2018; Jenni and Jenni-Eiermann, 1998).

Many migratory bird species have remarkable fat storage capabilities. The amount of fat that an individual stores depends on several factors, including its age, sex, body size, season, whether it will cross an ecological barrier (e.g., large bodies of water, deserts, or mountain ranges), predation risk, and habitat quality (Newton, 2008). For instance, passerines preparing to migrate over hospitable habitats store 20 – 30% of their lean body mass as fat, whereas passerines preparing to cross an ecological barrier typically store 50 – 70% of their lean body mass as fat (reviewed in Guglielmo, 2018). Long-distance migratory shorebirds commonly show extreme pre-migratory fat gains. For example, fat makes up over half of the total body mass of bar-tailed godwits (mean fat mass is 201 g on birds that have an average total body mass of 367 g) prior to departure for their non-stop migration between Alaska and New Zealand (Piersma and Gill, 1998). Similarly, Red knots (*Calidris canutus*) staging in Iceland increase in body mass by almost 50% (144 to 215 g) as they prepare to migrate to their high arctic breeding grounds, and fat contributes to over 100% these body mass increases due to the loss of lean mass (intestinal, leg muscle, liver and stomach mass) at the end of staging (Piersma et al., 1999). Therefore, long-

distance avian migrants, and shorebirds in particular, truly are “obese super athletes” (Guglielmo, 2018).

### 1.2.1 Physiological mechanisms of pre-migratory fuelling

Pre-migratory fuelling requires that birds quickly and efficiently absorb, transport, and store fats. The fat for refuelling is primarily derived from dietary sources (Price, 2010). After a meal, dietary triglycerides are partially digested, emulsified with bile, and then hydrolyzed by pancreatic lipase to non-esterified fatty acids (NEFA) and glycerol (Ramenofsky, 1990; Yen et al., 2015). NEFA and glycerol are then absorbed, primarily through passive diffusion, into enterocytes, where triglyceride re-synthesis occurs (Price, 2010; Yen et al., 2015). In birds, triglycerides are transported through the portal vein in portomicrons, large lipoprotein particles analogous to the chylomicrons of mammals (Hermier, 1997). Data from poultry suggests that due to their large size, portomicrons are likely too large to pass through the portal capillaries into the liver; therefore most portomicrons enter the systemic circulation (Fraser et al., 1986). In addition to receiving fatty acids from dietary sources, the liver is also capable of *de novo* fatty acid synthesis from carbohydrate or protein (Chong et al., 2007). In the liver, NEFA, triglycerides, phospholipids, and other lipids are repackaged into very low density lipoproteins (VLDL) for transport in the systemic circulation to other tissues (Guglielmo, 2018; Price, 2010). Adipose tissue is the primary storage site for lipids. When portomicrons or VLDLs reach the adipose tissue, they are hydrolyzed to free fatty acids by lipoprotein lipases (Ramenofsky, 1990). Free fatty acids enter adipose tissues through both passive diffusion and protein-facilitated transport (e.g., by fatty acid transport proteins or fatty acid translocase/CD36; Koutsari et al., 2011). Fatty acids are then re-esterified and stored in adipose tissues as triglycerides (Ramenofsky, 1990).

During pre-migratory fuelling, several physiological changes occur to optimize fat deposition. In many migratory bird species, the size and functional capacity of the intestine and liver increase during refuelling to enable higher levels of digestion and nutrient processing into fat (Guglielmo, 2018). During staging, digestive efficiency can be elevated by modifying the activity of digestive enzymes and transporters, prolonging gut retention times, and increasing intestinal leakiness (Guglielmo, 2018). The activity of many hepatic enzymes, including fatty acid synthase and glucose-6-phosphate dehydrogenase, increases during the pre-migratory period, resulting in an increased capacity for *de novo* fatty acid production (Guglielmo and

Williams, 2003; Shah et al., 1978). Interestingly, nightly torpor and seasonal hypothermia have been documented in hummingbirds (Carpenter et al., 1993; Hiebert, 1993) and barnacle geese (*Branta leucopsis;* Butler and Woakes, 2001), respectively, which is thought to enhance fat deposition by lowering energy expenditure on thermoregulation. It is unclear whether other pre-migratory bird species also use seasonal or nightly hypothermia to enhance refuelling (Guglielmo, 2018).

### 1.2.2 Optimal fat loads for migration

Rapidly storing sufficient fat reserves is critical for long-distance migrants. However, an individual's optimal departure fat load will depend on whether it behaves according to a time- or energy-minimization migration strategy. Most spring migrants employ a time-minimization migration strategy (Hedenström and Alerstam, 1997; Nilsson et al., 2013; Zhao et al., 2017) because early arrival on the breeding grounds in the spring is associated with higher reproductive success and greater reproductive performance. Birds that arrive earlier have access to higher quality territories and mates (Smith and Moore, 2005). Earlier arrival dates are associated with earlier breeding, bigger clutches, and larger offspring, which are more likely to survive and become breeding adults (McKellar et al., 2013; Norris et al., 2004; Smith and Moore, 2005). As well, earlier arriving females have additional time for renesting or to produce a second brood (Cooper et al., 2010; Smith and Moore, 2005), and earlier males have an increased likelihood of extra-pair mating success or polygyny (Canal et al., 2012; Cooper et al., 2010; Reudink et al., 2009).

Individuals following a time minimization migration strategy are expected to maximize migration speeds by maximizing refuelling rates and departure fuel loads (Alerstam and Lindström, 1990). During migration, relatively more time is spent at staging sites than in migration flight. Therefore, fuel deposition rate, rather than flight speed, determines the overall pace of migration (Houston, 2000; Nilsson et al., 2013; Schmaljohann et al., 2017). Departure fuel loads are also important determinants of migration pace. This is because larger fuel loads maximize an individual's potential flight range, allowing birds to make more direct flights with fewer stopovers en route, which ultimately increases overall migration speeds (Alerstam, 2011, 2001; Gómez et al., 2017). Given that time-minimizers store the maximum amount of fuel in the shortest possible time, the fuelling rates, and ultimately the departure fuel loads, of time-

minimizers are highly dependent on staging site quality (Hedenström and Alerstam, 1997; Weber and Houston, 1997).

Alternatively, avian migrants can also behave according to an energy-minimization migration strategy (Hedenström and Alerstam, 1997; Nilsson et al., 2013; Zhao et al., 2017). There are two types of energy-minimizers: those that minimize the energy costs of flight (transport energy-minimizers) and those that minimize the total energy costs of migration (total energy-minimizers; Hedenström and Alerstam, 1997). Transport energy-minimizers minimize flight costs by only accumulating the minimum amount of fat needed to travel to the next closest staging site (Hedenström and Alerstam, 1997). Total energy-minimizers minimize the energy required for both flight and staging. This involves a trade-off between minimizing the energy used to fly, which increases as fuel loads and flight speeds increase, and minimizing energy spent during staging, which decreases as fuel loads and flight speeds increase (Hedenström and Alerstam, 1997). Transport energy-minimizers are expected to have the most circuitous migration routes and the smallest departure fuel loads, which are not affected by refuelling rates during staging, while total energy-minimizers are expected to have intermediate migration speeds and departure fuel loads, which are affected by refuelling rates during staging (Hedenström and Alerstam, 1997; Weber et al., 1998). Therefore, factors that reduce staging site quality and lower refuelling rates and departure fuel loads are more likely to negatively impact individuals following a time-minimization migration strategy.

### 1.2.3 Consequences of impaired pre-migratory fuelling

Impaired pre-migratory refuelling can have serious population-level consequences for migratory birds. Many long-distance migrants must attain a fat load threshold before departure, especially before crossing an ecological barrier (Baker et al., 2004; Schaub et al., 2008). For example, Red knots staging in Delaware Bay require a departure mass of 180 to 200 g to have enough energy to fly to the breeding grounds and survive inclement conditions upon arrival (Baker et al., 2004). Red knots in Delaware Bay, like many other species of long-distance migrants (Both and Visser, 2001; Gill et al., 2001), have a strict migration schedule and leave on a specific date regardless of their condition (Baker et al., 2004, 2001). Failure to reach a mass threshold by the time of departure is associated with reduced adult survival, lower recruitment of young, and rapid population declines (Baker et al., 2004).

Fuel loads and fuelling rates can also influence individual departure decisions. In many cases, individuals with lower refuelling rates and fat loads depart later from wintering and staging sites, and, in turn, arrive later on the breeding grounds and show lower reproductive success (Cooper et al., 2015; Deppe et al., 2015; Dossman et al., 2016; Goymann et al., 2010; Norris et al., 2004; Schmaljohann and Naef-Daenzer, 2011). Alternatively, Duijns et al. (2017) found that fatter Red knots departed later than thinner birds, yet fatter birds still arrived earlier on the breeding grounds by waiting to select more favourable wind conditions at departure, which increased overall migration speeds. Fatter Red knots consequently experienced higher breeding success and lower mortality than thinner birds. Although it is possible for thinner individuals to 'catch up' by increasing fuel deposition rates during staging (Atkinson et al., 2007) or to successfully reproduce following late arrival on the breeding grounds (Senner et al., 2015), these compensatory effects are not typically observed. Therefore, fuel loads and fuelling rates are important drivers of migratory population demographics.

There are several factors that can impair avian pre-migratory fuelling. Reduced food availability, for instance, directly limits pre-migratory fat deposition (Klaassen et al., 2012). This can be caused by the phenological mismatches produced by climate change (Both and Visser, 2001) or the overharvesting of avian prey sources (Baker et al., 2004). Other factors can impair refuelling by reducing foraging times. For example, habitat loss increases density-dependent food competition (Dolman and Sutherland, 1994) and predator densities (Andren, 1992), which disrupts foraging and negatively affects refuelling rates (Lind and Cresswell, 2006; Moore and Yong, 1991; Pomeroy et al., 2006). Similarly, human disturbance during staging can flush birds from foraging areas and reduce their access to food (Burger et al., 2007). It is also possible for factors to impair pre-migratory fuelling physiology. Staging site contamination by environment toxicants, like petroleum products, pesticides, and persistent organic pollutants, is associated with lower body stores and fat accumulation (Bursian et al., 2017a; Elliott et al., 2007; Eng et al., 2017; Harris and Elliott, 2011). Although long-distance migrants may be particularly vulnerable to toxicants during staging and migration (Klaassen et al., 2012), the relationship between toxicant exposure and impaired pre-migratory fuelling is poorly understood. Given the strong association between staging site quality, fat deposition, migration timing, and avian population dynamics, understanding the factors that reduce staging site quality and affect pre-migratory fuelling will have important implications for migratory bird conservation.

### 1.3 Oil pollution

Oil pollution in the marine environment poses a serious threat to birds in coastal wintering and staging habitats. Oil enters marine ecosystems from natural sources (i.e., natural seeps) and anthropogenic activities, including offshore drilling and production operations, spills from ships and pipelines, and run off from land (GESAMP, 2007; Morandin and O'Hara, 2016; National Research Council, 2003). It is estimated that between 0.5 and 8.4 million t of oil enter marine ecosystems globally every year (National Research Council, 2003). Large-scale catastrophic oil spills, such as the Exxon Valdez, Prestige, and Deepwater Horizon oil spills, are associated with mass avian mortality events (Balseiro et al., 2005; Burger, 1993; Deepwater Horizon Natural Resource Damage Assessment Trustees, 2016; Piatt et al., 1990), yet chronic, small-scale oil pollution may trigger comparable or greater cumulative bird mortalities (reviewed in Troisi et al., 2016).

The acutely lethal effects of heavy oiling to birds are well studied. Birds die from oil spills when they are smothered in oil and suffocated (Camphuysen and Leopold, 2004). Birds also die from heavy external oiling, which disrupts the water-proofing, thermal insulation, and buoyancy properties of feathers, rendering birds flightless and unable to forage. Mortality from external oiling ultimately results from hypothermia, dehydration, and severe emaciation (Balseiro et al., 2005; Jenssen, 1994; Piatt and Van Pelt, 1997). Mortality from ingested oil results from kidney, liver, and gastrointestinal tract damage (Briggs et al., 1996). Although many birds are killed immediately following an oil spill, it has been suggested that chronic and sublethal exposure to oil and its toxic constituents, most notably polycyclic aromatic hydrocarbons (PAHs), may more seriously impact avian populations than acute mortalities (Bursian et al., 2017a). However, the physiological effects of chronic, sublethal oil and PAH exposure in birds are relatively less well characterized.

#### 1.3.1 Polycyclic aromatic hydrocarbons

PAHs are considered the most toxic constituents of oil pollution (Leighton, 1993). PAHs are made up of carbon and hydrogen atoms arranged in two or more fused aromatic rings (Abdel-Shafy and Mansour, 2016; Douben, 2003; Eisler, 1987) (Figure 1.1). The PAHs in crude oil are formed naturally over geological time scales by low temperature, high pressure reactions of organic matter. PAHs are also produced by the incomplete combustion of organic matter (e.g., fossil fuels, wood, refuse; Albers, 2006; Latimer and Zheng, 2003). These compounds have high

melting and boiling points, low vapour pressures, and low hydrophobicity, which decreases with increasing molecular weight (Eisler, 1987; Latimer and Zheng, 2003). This property gives PAHs a higher affinity for organic phases than for water, and in the environment PAHs thus partition into the organic fractions in sediments, soil, and biota (Douben, 2003; Eisler, 1987).

PAHs can thus bioaccumulate in marine organisms and enter higher trophic levels. The potential for PAH bioaccumulation increases in organisms with lower metabolic capabilities, higher lipid contents, and life history patterns that increase PAH exposures (Eisler, 2000; McElroy et al., 1989). For instance, marine invertebrates show high rates of PAH uptake but relatively inefficient PAH metabolism, which results in bioaccumulation (Meador et al., 1995). Recent work has shown that PAH bioaccumulation in avian invertebrate prey sources results in dietary PAH exposure in birds (Willie et al., 2017). Similarly, radiocarbon analyses have shown that oil from the Deepwater Horizon spill was incorporated into a terrestrial bird species, the seaside sparrow (*Ammodramus maritimus*), suggesting that Deepwater Horizon oil also entered terrestrial food webs (Bonisoli-Alquati et al., 2016). Although avian PAH exposure is expected following an oil spill, PAH bioaccumulation in birds is unlikely because birds efficiently metabolize and excrete PAHs (Albers, 2006).

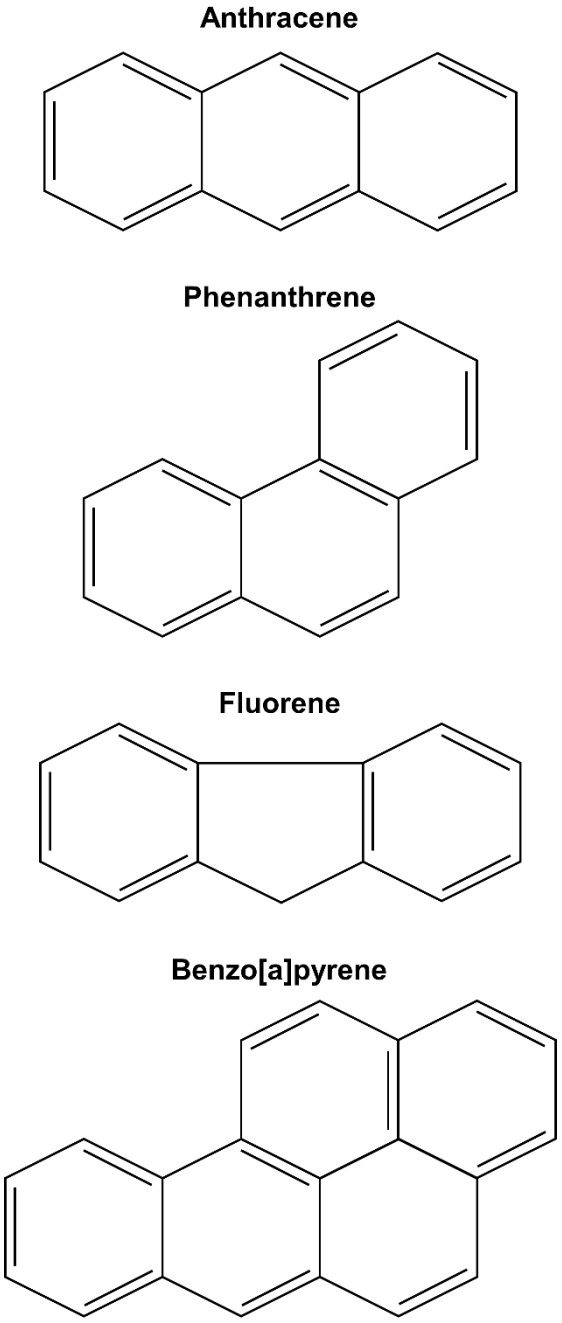


**Figure 1.1.** Examples of petrogenic PAHs, showing the typified PAH structure of carbon and hydrogen atoms arranged into fused aromatic rings.

Oil and PAHs can persist in the environment for decades following a spill. Oil can be sequestered into areas where it is sheltered from physical removal or weathering processes (Owens et al., 2008; Peterson et al., 2003). For instance, oil and elevated PAH concentrations were detected in subsurface sediments 16 years after the Exxon Valdez oil spill (Short et al., 2007), and oil persisted on exposed and sheltered beaches in Chedabucto Bay, Nova Scotia, 36 years after a spill from the Arrow oil tanker (Owens et al., 2008). Measurements of ethoxyresorufin-*O*-deethylase (EROD) activity, a sensitive biomarker of PAH exposure in birds (Esler et al., 2010; Head et al., 2015; Willie et al., 2017), indicated that harlequin ducks (*Hisrionicus histrionicus*) in Prince William Sound, Alaska, were exposed to oil contaminants up to 22 years after the Exxon Valdez oil spill (Esler et al., 2017). Therefore, chronic oil and PAH exposure is possible for birds that refuel at contaminated staging sites.

### 1.3.2 Sublethal PAH toxicity in birds

PAHs and other cyclic hydrocarbons share similar toxic mechanisms of action (Sikkema et al., 1995). This involves an interference with cellular membrane function and with enzyme systems associated with the membrane (Neff, 1985). Many aromatic hydrocarbons are biotransformed to reactive metabolites, such as epoxides, which bind to cellular proteins and DNA, causing a dysregulation of gene expression and protein function, and can lead to oxidative stress (Abdel-Shafy and Mansour, 2016; Mchale et al., 2012; Sikkema et al., 1995). Another proposed mechanism of PAH toxicity in birds is an aryl hydrocarbon receptor (AhR)-mediated biochemical response (Albers, 2006), which can affect toxicities similar to other AhR ligands (Brunstrom, 1991).

PAH and oil exposure produce a wide range of sublethal effects in birds. External oiling of the feathers is associated with impaired flight performance, including lower takeoff speeds (Maggini et al., 2017a), elevated flight energy costs (Maggini et al., 2017b), and taking less efficient flight paths (Perez et al., 2017a). Well-documented effects of oil and PAH ingestion include hemolytic anemia (Newman et al., 2000; Seiser et al., 2000; Troisi et al., 2007) and immunosuppression (Briggs et al., 1997; Newman et al., 2000; Rocke et al., 1984). Oil and PAH ingestion is also associated with reproductive impairment in birds, and effects include infertility (Hough et al., 1993), reduced egg laying, and loss of incubation behaviour (reviewed in Leighton, 1993).

There is also evidence to suggest that PAH and oil exposure could impair avian pre-migratory fuelling physiology. Observational post-spill work and experimental oiling studies provide evidence of impaired fuel deposition in the field. Loss of body condition is often observed in birds following an oil spill (Golet et al., 2002; Harris et al., 2011; Newman et al., 2000; Troisi et al., 2016). For instance, following the Prestige oil spill, birds with heavy external oiling were emaciated, showing reduced abdominal, subcutaneous, and pericardial fat stores (Balseiro et al., 2005). Similarly, light application of crude oil to the feathers of homing pigeons (*Columba livia*) reduced mass gains between repeated experimental flights (Perez et al., 2017a, 2017b). As well, circulating PAH levels were negatively correlated with body condition in birds at previously oiled sites (Alonso-Alvarez et al., 2007; Paruk et al., 2016), indicating that oil contaminant ingestion also influences avian fuel loads.

There are several mechanisms by which oil and PAHs could impair pre-migratory fuelling. Hyperphagia is a crucial behaviour for pre-migratory birds, and both external (Burger and Tsipoura, 1998; Hughes et al., 1990) and oral (Cunningham et al., 2017) dosing studies measured reduced food intake following oil exposure. However, this is not always observed (e.g., Cunningham et al., 2017; Horak et al., 2017). PAHs also have the potential to impair fat absorption in fuelling migrants. This is suggested by work showing gastrointestinal damage and impaired nutrient absorption following oral and dermal oil exposure (Balseiro et al., 2005; Briggs et al., 1997, 1996; Bursian et al., 2017b; Crocker et al., 1975; Fry and Lowenstine, 1985; Harr et al., 2017a; Maggini et al., 2017c). External and oral PAH and oil exposure also cause thermal stress in birds, which is characterized by elevated heat loss and hypothermia and is associated with a compensatory increase in metabolic rates and mass loss (Balseiro et al., 2005; Bursian et al., 2017a; Butler et al., 1986; Cunningham et al., 2017; Harr et al., 2017b; Hughes et al., 1990; Jenssen, 1994; Maggini et al., 2017c). Furthermore, PAHs have the potential to disrupt the endocrine control of pre-migratory fuelling. PAHs alter estrogen activity (Lee et al., 2017; Zhang et al., 2016) and thyroid hormone (Troisi et al., 2016), prolactin (Cavanaugh et al., 1983; Cavanaugh and Holmes, 1987; Harvey and Philips, 1981), and corticosterone levels (Fowler et al., 1995; Lattin and Romero, 2014; Peakall et al., 1981), which regulate migratory fattening, nocturnal activity, and departure decisions (Cornelius et al., 2012). Finally, PAHs can also bind the AhR and generate the same responses as other AhR agonists (Soshilov and Denison, 2014). AhR activation can inhibit fatty acid synthesis (Tanos et al., 2012), adipose and muscle fatty acid

uptake (Brewster and Matsumura, 1988), and pre-adipocyte differentiation into mature fat cells (Brodie and Azarenko, 1996; Vogel and Matsumura, 2003). Ultimately, this results in peripheral fat mobilization and hepatic steatosis (Lee et al., 2010).

Head et al. (2015) ranked the relative potency of eight PAHs to induce AhR-mediated EROD activity in chicken (*Gallus domesticus*), Pekin duck (*Anas platyrhynchos*), and greater scaup (*Aythya marila*) embryonic hepatocyte cultures. In all species, the relative AhR mediated PAH potency, in order from high to low potency, was: dibenz[*ah*]anthracene > benzo[*k*]fluoranthene > indeno[1,2,3-*cd*]pyrene >benzo[*a*]pyrene > chrysene ≈ benz[*a*]anthracene ≈ benz[*ghi*]perylene > benzo[*b*]naphto[2,3-*d*]thiophene, which is similar to the rank order potency for AhR-mediated responses in mammalian and fish cell lines (Bols et al., 1999; Till et al., 1999; Villeneuve et al., 2002).

Liver damage is a well documented effect of PAH and oil exposure (Albers, 2006; Harr et al., 2017a; Leighton, 1993). This has important implications for pre-migratory fuelling because the liver is an essential metabolic organ and plays a key role in energy and lipid homeostasis. Some important liver functions include *de novo* lipogenesis, triglyceride synthesis and storage, ketone body production, and bile acid synthesis (Hofmann, 1999; Rui, 2014). Correspondingly, recent work by Crump et al. (2017) found that exposure to Athabasca Oil Sands petcoke extracts, a major source of PAHs (Zhang et al., 2016), reduced the mRNA expression of lipid and cholesterol homeostasis genes in chicken (*Gallus gallus domesticus*) and double-crested cormorant (*Phalacrocorax auritus*) embryonic hepatocytes.

### 1.4 Shorebirds as a pre-migratory fuelling model

Shorebirds (Order Charadriifomes) are a useful model for studying the effects of PAHs on avian pre-migratory fuelling. Shorebirds are particularly vulnerable to the toxic constituents of oil exposure because they are dependent on intertidal shoreline habitats, which are highly susceptible to oil spills (Henkel et al., 2012; Peterson et al., 2003). For example, the Gulf of Mexico provides key wintering and staging habitats to 28 migratory shorebird species (Withers, 2002), but shorelines in this region are subject to frequent and recurrent oil pollution (Henkel et al., 2012). At least 2100 km of shoreline in the northern Gulf of Mexico (Louisiana, Mississippi, Alabama, and Florida) received an estimated 10,000 to 30,000 t of oil following the Deepwater Horizon oil spill (Beyer et al., 2016). As well, due to the ongoing and extensive oil extraction

and transportation activities in this region, Gulf of Mexico shorelines are subject to chronic and repeated exposure to smaller oil spills (Burger, 2017).

The foraging ecology of shorebirds also increases their susceptibility to oil and PAH exposure. Many shorebird species feed primarily on marine invertebrates by picking and probing in subsurface sediments (Grond et al., 2015; Macwhirter et al., 2002), and incidental sediment ingestion during foraging is common in shorebirds (Mathot et al., 2010; Schultz et al., 1994). Shorebirds thus have a high potential for chronic PAH exposure at contaminated sites because PAHs tend to partition into subsurface sediments (Douben, 2003; Eisler, 1987) where they can persist for decades following a spill (Owens et al., 2008; Short et al., 2007). Shorebirds are exposed to higher PAH concentrations following the ingestion of contaminated prey as marine invertebrates are unable to efficiently metabolize PAHs and consequently bioaccumulate these compounds (Meador et al., 1995). Moreover, shorebirds generally exhibit high staging site fidelity, with large proportions of their populations wintering and staging together at specific locations (Drake et al., 2001). This behaviour increases the probability of repeated PAH exposure as shorebird populations return to contaminated sites every year (Henkel et al., 2012).

Finally, shorebirds are of high conservation concern. This group is currently experiencing worldwide population declines (Clemens et al., 2016; Mackinnon et al., 2012; Thomas et al., 2006; Zockler et al., 2003), and at least 61% of shorebird populations in North America are in decline (Andres et al., 2012). Impaired pre-migratory fuelling has been identified as an important factor in shorebird declines (Baker et al., 2004). Many arctic breeding shorebirds tend to use a time-minimization migration strategy in the spring. These birds therefore have high refuelling rates, extreme departure fat loads (see Section 1.2), and make direct flights between relatively few staging sites (Farmer and Weins, 1999; Gudmundsson et al., 1991; Jehl, 1997; Lyons and Haig, 1995). Time constraints commonly dictate that shorebirds leave on a specific date regardless of their current fat load (Baker et al., 2004, 2001), and reduced pre-migratory refuelling rates have been associated with a slower migration pace, lower departure masses, lower adult survival and fitness, and, ultimately, population declines (Baker et al., 2004; Gómez et al., 2017; Houston, 2000; Nilsson et al., 2013; Schmaljohann et al., 2017). Shorebirds therefore represent ecologically relevant sentinel species for investigating the effects of PAHs on pre-migratory fuelling.

### 1.5 Research needs

Although there is evidence to suggest that PAHs could limit pre-migratory fuel loads and refuelling rates, we have yet to establish a link between PAH exposure and impaired pre-migratory fuelling. Moreover, whether sublethal PAH ingestion during staging ultimately influences migration timing is unknown. Long-distance migratory birds are currently experiencing global population declines (Holmes, 2007; Sanderson et al., 2006; Zockler et al., 2003), and both impaired pre-migratory fuelling (Baker et al., 2004) and staging site oil pollution (Bursian et al., 2017a; Henkel et al., 2012) have been identified as important factors contributing to these declines. There is therefore an urgent need to directly assess and characterize the impacts of PAH exposure on pre-migratory birds, and this thesis aims to fill this knowledge gap.

### 1.6 Thesis objectives and major hypotheses

The overarching question of this thesis was: does sublethal PAH exposure impair avian pre-migratory fuelling? This was addressed through a series of captive and field studies that evaluated sub-organismal mechanisms and organismal- and population-level responses using Sanderling (*Calidris alba*), a long-distance migratory shorebird species, as a primary model.

My first objective was to evaluate whether sublethal PAH ingestion affects pre-migratory mass gains. I addressed my first objective in Chapter 2, where I used a controlled dosing experiment to simulate dietary PAH exposure during staging. For this experiment, I orally exposed wild-caught Sanderling to environmentally-relevant PAH mixtures and concentrations for the duration of their autumn pre-migratory fuelling period. I hypothesized that sublethal PAH ingestion lowers Sanderling pre-migratory mass gains. My second objective was to investigate the physiological mechanisms of PAH-induced pre-migratory fuelling impairment. I also addressed my second objective in Chapter 2 by measuring EROD activity, serum biochemical profiles, and liver mass and lipid content in Sanderling from my captive dosing experiment. In Chapter 3, I examined possible molecular pathways for pre-migratory fuelling impairment by measuring the hepatic mRNA expression of eight target genes related to fat deposition and oil exposure in liver subsamples from these same birds.

My third objective was to explore the effects of impaired fuelling on avian migration timing. In Chapter 4, I examined the relationship between PAH contamination and staging site quality for fuelling shorebirds. Because shorebirds typically maximize refuelling rates during staging (Baker et al., 2004; Farmer and Weins, 1999; Gudmundsson et al., 1991; Lyons and

Haig, 1995), differences in fuelling rates and staging durations reflect differences in staging site quality (Seaman, 2004). Therefore, I trapped Sanderling and Red knots at six key coastal staging sites in the Gulf of Mexico and assessed the quality of each site by measuring the current fuel loads, relative fuel deposition rates, and migratory departure dates of each species. I then estimated dietary PAH exposure by measuring total sediment PAH concentrations at these same sites. I hypothesized that PAH contamination lowers staging site quality for migratory shorebirds. I predicted that at staging sites with higher total sediment PAH concentrations, both species would exhibit lower fuel loads, lower fuelling rates, and later departure dates.

In Chapter 5, I investigated whether pre-migratory fuel loads influence Sanderling migration timing. I used a combination of radio-telemetry and field measurements to examine the relationship between fuel loads and staging duration in Sanderling at six staging sites in the Gulf of Mexico and in Chaplin Lake, Saskatchewan. I hypothesized that fuel loads influence Sanderling migration timing by testing the prediction that stopover durations and departure dates are correlated with fuel loads at capture. I also tracked Sanderling movements to see if delays in departures from the Gulf of Mexico influenced arrivals and departures in Saskatchewan. I hypothesized that delays in migration carry-over from one staging site to the next. I tested the predictions that Gulf of Mexico departure dates are positively associated with Saskatchewan arrival dates and that Saskatchewan arrival and departure dates are positively related.

My final objective was to synthesize the multiple datasets of the preceding chapters in a way that is useful to ecotoxicological risk assessment. Fully understanding how PAHs affect pre-migratory fuelling, and ultimately avian populations, requires a mechanistic approach that links molecular-level events to adverse outcomes at the population-level. Therefore, the goal of my final chapter (Chapter 6) was to develop a putative adverse outcome pathway (AOP) that links the molecular mechanisms underlying pre-migratory fuelling impairment to the effects of impaired fuelling on migratory bird populations. By organizing the data of preceding chapters and existing knowledge into a progression of toxicity events, we gain a better understanding of how PAHs and toxicants with similar mechanisms of action can affect avian populations. Therefore, this thesis provides new information to help inform avian ecotoxicological risk assessments and to advance our understanding of the contaminant-related threats affecting the conservation of long-distance migratory birds.

# 2 CHAPTER 2: POLYCYCLIC AROMATIC HYDROCARBON EXPOSURE IMPAIRS PRE-MIGRATORY FUELLING IN CAPTIVELY-DOSED SANDERLING

## PREFACE

Although previous research suggests that PAHs have the potential to limit fat deposition and disrupt lipid homeostasis, whether PAHs impair avian pre-migratory fuelling still required direct investigation. The aim of Chapter 2 was to directly assess the effects of sublethal dietary PAH exposure on avian pre-migratory fat deposition and fuelling physiology. This work used a controlled dosing study to eliminate confounding variables that can complicate the interpretation of results in the field. At the same time, every effort was made to replicate environmentally relevant conditions (i.e., PAH concentrations, exposure routes, and exposure durations) to more accurately evaluate the effects of PAHs on wild birds staging at a contaminated site. Directly measuring whether individuals that ingest PAHs during staging gain less mass was necessary to confirm the overall hypothesis of this thesis that PAHs impair avian pre-migratory fuelling. Chapter 2 also served as a foundation for subsequent experiments that anchored molecular-level results and field observations to effects at the individual level.

The content of Chapter 2 was reprinted (adapted) from *Ecotoxicology and Environmental Safety*, (10.1016/j.ecoenv.2018.05.036), K. Bianchini, C. Morrissey, "Polycyclic aromatic hydrocarbon exposure impairs pre-migratory fuelling in captively-dosed Sanderling (*Calidris alba*)" 161, 383-391. Copyright (2018), with permission from Elsevier.

Author contributions:

Kristin Bianchini (University of Saskatchewan) conceived, designed, and managed the experiment, generated and analyzed the data, prepared all figures, and drafted the manuscript.

Christy A. Morrissey (University of Saskatchewan) provided inspiration, scientific input, and guidance, commented on and edited the manuscript, and provided funding for the research.

## 2.1 Abstract

Efficient fuelling is essential for migratory birds because fuel loads and fuelling rates affect individual fitness and survival during migration. Many migrant shorebirds are exposed to oil pollution and its toxic constituents, polycyclic aromatic hydrocarbons (PAHs), at migratory staging sites, which has the potential to interfere with avian refuelling physiology. In this study, we orally dosed birds with environmentally-relevant PAH mixtures to simulate dietary shorebird exposure during staging. Forty-nine wild-caught Sanderling (*Calidris alba*) were orally dosed with 0 (control), 12.6 (low), 126 (medium), or 1260 (high) μg total PAH/kg body weight/day. Birds were dosed during a 21-day period of autumn pre-migratory fuelling to mimic the typical staging duration of Sanderling. We measured daily changes in mass and fat loads, as well as ethoxyresorufin-*O*-deethylase (EROD) activity, serum biochemical profiles, and liver mass and lipid content following dosing. All dose groups gained fat and increased in mass (size-corrected) during the study period, with females having a higher average body mass than males. However, mass gain was 3.9, 5.4, and 3.8 times lower in the low, medium, and high dose groups, respectively, relative to controls, and body mass in the medium and high dose groups significantly declined near the end of the experiment. EROD activity showed a dose-dependent increase and was significantly elevated in the high dose group relative to controls. Higher individual EROD activity was associated with reduced serum bile acid and elevated serum creatine kinase concentrations in both sexes, and with elevated serum lipase concentrations in females. These results suggest that PAH exposure in Sanderling can interfere with mechanisms of lipid transport and metabolism, can cause muscle damage, and can lead to reduced overall fat loads that are critical to staging duration, departure decisions, migratory speed, and flight range. Given that many shorebirds migrate thousands of kilometers between the breeding and wintering grounds and frequently aggregate at key staging sites that are subject to contamination, PAH exposure likely represents a significant threat to shorebird migratory success.

## 2.2 Introduction

One incredible life history feature of birds is their ability to migrate. Most migrants rely exclusively on endogenously stored energy to fuel long-distance migration flights. As such, the pre-migratory period in birds is characterized by intense food consumption (hyperphagia) and a rapid accumulation of fuel stores as fat (Sandberg and Moore, 1996). Proper fuelling is critical for migrants because attaining a threshold fat load prior to departure, and particularly before crossing an ecological barrier (e.g., desert, large water body), increases the probability of surviving migration (Baker et al., 2004). Moreover, fat deposition rates are positively correlated with migration speed (Hedenström and Alerstam, 1997), and early arrival at the breeding grounds in spring increases reproductive performance (Sandberg and Moore, 1996). Therefore, migratory success and the demographics of migratory bird populations are closely related to the quality of re-fuelling (i.e., staging) sites along migration routes.

For shorebirds (Order Charadriiformes), an ongoing threat to the quality of their staging sites is oil pollution. Many intertidal shoreline habitats are key staging sites for migrant shorebirds. Coastal environments, however, are subject to small, regularly occurring oil spills and to chronic exposure to residual oil from large spills (Henkel et al., 2012). PAHs have the potential to bioaccumulate in marine invertebrates and to be incorporated into the avian food chain (Willie et al., 2017). Biomarkers of oil exposure (measured as ethoxyresorufin-*O*-deethylase (EROD) activity) indicate that birds are exposed to PAHs up to two decades following a spill (Esler et al., 2010). Shorebirds thus have a high potential for chronic PAH exposure at many coastal staging sites. Many migrant shorebird species also tend to exhibit high staging site fidelity, which makes them susceptible to repeated oil exposure at coastal staging sites that experience high levels of oil contamination (Henkel et al., 2012).

PAHs are typically identified as the major source of toxicity in oil spills (Boehm et al., 1998). Despite their relatively rapid metabolism and excretion in avian species (Albers, 2006), PAHs have many known toxic effects in birds and could interfere with avian pre-migratory fuelling physiology. Field studies on birds at previously oiled relative to unoiled sites reported lower body masses and parameters indicative of liver damage (e.g., elevated plasma aspartate aminotransferase, AST, and gamma-glutamyl transferase, GGT), and the magnitude of these effects were related to circulating PAH concentrations (Alonso-Alvarez et al., 2007). A well-documented effect of oil and PAH ingestion is liver damage (Albers, 2006), which has the

potential to impair *de novo* fatty acid synthesis and to disrupt the production of bile and other digestive products (Duffy et al., 1996). Experimental oiling studies have also shown effects on nutrient absorption and fat deposition by reducing intestinal function, causing inflammation, and increasing metabolic rates (reviewed in Bursian et al., 2017a). A recent series of experiments that dosed double-crested cormorants (*Phalacrocorax auratus*), laughing gulls (*Leucophaeus atricilla*), western sandpipers (*Calidris mauri*), and rock pigeons (*Columba livia*) with artificially weathered Deepwater Horizon oil (Mississippi Canyon 252; MC252) reported several fuelling-related effects, including reduced appetite; lower mass; changes in plasma chemistry and oxidative stress; higher relative liver weights; adrenal, kidney, liver, and thyroid lesions; and higher cytochrome P4501A (CYP1A) protein expression and catalytic activity (Bursian et al., 2017a). Furthermore, oral oil and PAH doses increase corticosterone, thyroxine, and adrenocorticotropic hormone activities (Yanyan Zhang et al., 2016), which can influence rates of fat and protein metabolism and the regulation of pre-migratory fattening (Cornelius et al., 2012). PAHs can also bind to the aryl hydrocarbon receptor (AhR; Head et al., 2015) and have the potential to affect the responses of other AhR agonists. These include inhibiting fatty acid synthesis and increasing peripheral fat mobilization and hepatic steatosis (Lee et al., 2010).

Despite this evidence, however, researchers have yet to establish a direct link between PAH exposure and impaired avian pre-migratory fuelling ability. Shorebirds are of particular conservation concern because many species of long-distance migrant shorebirds have demonstrated declines throughout their range (Zockler et al., 2003). Additionally, reduced fuelling ability has been associated with delayed migration and population declines in migrant shorebird species (Baker et al., 2004). Here, we used a controlled dosing study to examine individual responses to varying degrees of dietary PAH exposure in wild-caught Sanderling (*Calidris alba*), a long-distance migrant shorebird species. We measured changes in fattening, AhR activation, serum biochemical profiles, and liver steatosis following chronic exposure to environmentally-relevant PAH dosages during a period of autumn pre-migratory fattening. We hypothesized that PAH ingestion impairs Sanderling pre-migratory fuelling. We tested the predictions that Sanderling mass loads and fuelling rates would decrease with increasing levels of PAH exposure and that physiological indicators associated with fuelling would be impaired upon administration of higher PAH dosages. We discuss how observed effects could potentially affect shorebird migration.

## 2.3 Materials and methods

### 2.3.1 Study species capture and husbandry

Sanderling are a long-distance migratory shorebird species, capable of extreme pre-migratory mass gains (e.g., 70% body mass increase during staging at Delaware Bay; Robinson et al., 2003). This species also has a high risk of oil exposure due to its heavy reliance on intertidal shoreline habitats (Henkel et al., 2012). As well, Sanderling are relatively abundant (Macwhirter et al., 2002), easy to trap and to keep in captivity (AL-Mansour, 2005), and have an adequate body size for dosing and sample collection. Based on these factors, Sanderling are suitable model organisms and ecologically relevant sentinel species for investigating how PAH exposure affects avian pre-migratory fuelling.

Sanderling were trapped during northward migration from 21 May to 2 June, 2016, at Chaplin Lake, Saskatchewan, Canada (50°26′28.36″, -106°40′9.37″), using mist nets and noose carpets. Sanderling were captured under Scientific Banding Permit #10268L. All animal care protocols follow the Canadian Council on Animal Care guidelines for humane animal use, were approved by the University of Saskatchewan Animal Research Ethics Board and adhere to University of Saskatchewan Policy on Care and Use of Animals in Research (Animal Use Protocol #20120021).

Sanderling can experience substantial mass loss following capture (~10% body mass loss in 13 hours; Schick, 1983). Therefore, individuals were only selected for use in this study if they weighed at least 50 g and had a fat score of at least 2 on a scale of 0 to 5. Because second year (SY) birds can exhibit different foraging and fuelling efficiencies than older, after second year (ASY) birds (Sandberg and Moore, 1996), only ASY birds were collected for this study. Fifty Sanderling were captured and transported to the Facility for Applied Avian Research (FAAR) at the University of Saskatchewan. One Sanderling died of unknown causes following transfer, and the remaining 49 birds were used for subsequent experiments. Sanderling were maintained in groups of 8 to 12 birds in outdoor aviaries designed to hold ponded fresh water with an artificial shoreline. Birds were fed commercial 3 mm trout chow pellets *ad libitum*, supplemented with mealworms. Following a two-week acclimation period, food consumption was recorded daily, and mass and fat scores were measured every four days to monitor for signs of autumn pre-migratory fuelling. Following acclimation to captivity, masses remained stable until the onset of fuelling.

Birds were considered to have started their southward fuelling when they showed sustained increases in mass, fat, and food consumption, with at least a 10% increase in mass and 1-point increase in fat score within four days. Experimental dosing treatments (described below) began once individuals started fuelling. Fuelling commenced between 11 – 31 July, which constituted a minimum of 40 days between capture and dosing. This was well above the typical two week depuration period of other oil and PAH dosing studies (e.g., Lattin and Romero, 2014), and, given the rapid metabolism of PAHs in birds (e.g., chicken embryos metabolize 100% of injected PAHs in 18 days; Albers, 2006), this amount of time was considered sufficient for depuration.

### 2.3.2 Dosing procedure

Generally, avian migrants tend to exhibit slower and less synchronous migration in autumn than in the spring (Hedenström and Alerstam, 1997). Likewise, the onset of pre-migratory fuelling was staggered in our group of wild-caught Sanderling. Individuals were thus assigned to one of six cohorts for dosing, based on when they started to exhibit pre-migratory fuelling. First, each cohort was food restricted (fed 3.5 g food/bird/day) for four days to ensure that the process of fuelling was more fully captured by the dosing period. After four days, birds were again fed *ad libitum*, and individuals within each cohort were randomly assigned to one of four treatment groups.

Treatment concentrations and conditions were chosen to simulate environmentally-relevant PAH exposure levels and scenarios following an oil spill. During migration, the primary food source of Sanderling is aquatic invertebrates (Macwhirter et al., 2002), which can bioaccumulate total PAH (tPAH) concentrations of over 6000 μg/kg after a spill (Allan et al., 2012). We therefore chose dosages that represent a dietary exposure range of 60 to 6000 μg tPAH/kg food/day. Fuelling Sanderling have ingestion rates as high as 12.6 g/day during staging (based on a 60 g bird; Vanermen et al., 2009). Therefore, assuming maximum fuel ingestion rates, dose solution volumes were adjusted daily according to each individual's body mass to maintain nominal dosages of 0 (control), 12.6 (low), 126 (medium), and 1260 (high) μg tPAH/kg body weight/day.

The PAH composition and concentration of every crude oil source is unique. Moreover, the fate, transport, composition, and persistence of PAH mixtures in the environment following an oil spill is a product of many complex processes, including the location of the spill and the

physical, chemical, and biological weathering processes affecting oil in that location (Reddy et al., 2012). It is consequently very difficult to perfectly mimic chronic PAH exposures from any one spill. Therefore, we chose a dose solution that closely matched the compositional mixture of PAHs detected following the Exxon Valdez (Boehm et al., 1998) and Deepwater Horizon (Reddy et al., 2012) oil spills. For this, we used a commercial PAH mixture (QTM PAH Mix, Sigma-Aldrich) composed of 2,000 µg/ml each of acenaphthene, acenaphthylene, anthracene, benz[*a*]anthracene, benzo[*b*]fluoranthene, benzo[*ghi*]perylene, benzo[*a*]pyrene, 2-bromonaphthalene, chrysene, dibenz[*a,h*]anthracene, fluoranthene, fluorene, indeno[1,2,3-*cd*]pyrene, naphthalene, phenanthrene, and pyrene in dichloromethane (DCM; tPAH = 32,000 µg/ml).

The commercial mixture was diluted in food-grade organic sunflower oil (Compliments brand, Sobeys Canada) to produce three target dose solutions of 164.57 (low), 1,645.71 (med), and 16,457.14 (high) µg/ml tPAH. DCM was also added to the control (sunflower oil only), low, and medium dose solutions to ensure that all solutions contained equal ratios of oil:DCM and that the only variable amongst dose groups was the tPAH concentration. Daily dosages were administered by force-feeding each Sanderling a mealworm injected with a small (µl) volume of the appropriate dose solution. For 2 cohorts on day 9 (n = 8) and day 7 (n = 12) of dosing, we discovered that our Hamilton syringes were not drawing up the dosing solution. We confirmed this was due to the syringes being faulty for an unknown period of time. Therefore, we switched to using disposable 0.3 insulin syringes for injection and extended the dosing by 6 and 4 days, respectively, for these first cohorts only. All other birds in subsequent cohorts (n = 29) were dosed for 21 days to mimic the typical staging duration of Sanderling (Robinson et al., 2003).

### 2.3.3 Body measurements and sample collection

Sanderling mass was measured daily during dosing to calculate mass gain and fuelling rates, and tarsus and bill lengths were measured to calculate size-corrected body masses. Sanderling were humanely euthanized by $CO_2$ asphyxiation 24 hours after the final dosing day. Birds were immediately exsanguinated by cardiac puncture. Whole blood samples were left to clot at room temperature for 1 h, and serum samples were collected following centrifugation and stored at -80°C until further processing. During exsanguination, small subsamples of whole blood (two per bird) were drawn into heparinized microhematocrit tubes and centrifuged for hematocrit measurements. For each bird, the average of both tubes' hematocrit values was used

for analysis. Whole liver masses were recorded. Livers were cut into pieces (~ 0.03 g each), which were flash frozen on dry ice and stored at -80°C for EROD activity and histochemical analyses. Sex was determined by post-mortem examination of the gonads.

### 2.3.4 Serum chemistry

To determine the physiological fuelling status of birds, we tested the serum levels of eleven key analytes: aspartate aminotransferase (AST), bile acids, β-hydroxybutyrate (BOHB), cholesterol, creatine kinase, gamma-glutamyl transferase (GGT), glucose, lipase, non-esterified fatty acids (NEFA), triglyceride (TG), and uric acid (UA). Circulating TG, lipase, and NEFA are directly indicative of lipid storage, metabolism, and mobilization, respectively. BOHB and UA are the products of NEFA and protein metabolism, and high levels of these analytes suggest energy shortages (reviewed in Landys et al., 2005). Bile acids, which are synthesized from cholesterol, facilitate the digestion and absorption of fats (Staels and Fonseca, 2009). We also measured glucose, which is involved in energy production and fatty acid synthesis, and circulating glucose concentrations are negatively correlated with body mass (Braun and Sweazea, 2008). High creatine kinase levels suggest high energy metabolism and also indicate muscle damage (Baird et al., 2012). Finally, given the liver's key role in regulating lipid levels and the known hepatotoxic effects of PAHs (see above), we also measured GGT and AST levels, which can be elevated in response to liver damage (Alonso-Alvarez et al., 2007). Samples were analyzed by Prairie Diagnostic Services, Saskatoon, SK, using the Cobas c311 Chemistry Analyzer (Roche Diagnostics, Laval, Quebec). Samples were scored for levels of lipemia, hemolysis, and hyperbilirubinemia using the scale: none, slight, 1+, 2+, and 3+. These three factors can affect serum chemistry results and were included as random effects in our analyses where appropriate (see below).

### 2.3.5 EROD assay

Frozen liver samples (~ 30 mg) were homogenized on ice in 200 µl of ice-cold Tris buffer (0.05 M Tris, 8.6% sucrose, pH 7.4). Homogenates were centrifuged at 10,000 x g for 10 min at 4°C. The supernatant of each sample was transferred to pre-chilled ultracentrifuge tubes and centrifuged again at 100,000 x g for 30 min at 4°C. The resulting supernatant was discarded, and the microsomal pellet was re-suspended in ice-cold microsome stabilizing buffer (20%

glycerol, 0.1 M $KH_2PO_4$, 1 mM EDTA, 1 mM dithiothreitol) at a volume of 3 ml buffer per gram of tissue originally used (dilution was accounted for during final EROD activity calculation).

The microsomal EROD activity and protein concentration of each sample were analyzed simultaneously following the methods of Kennedy and Jones (1994), which were modified for use in 96-well plates by Doering et al. (2012). EROD and protein standard curves were generated using dilutions of resorufin and bovine serum albumin, respectively. For EROD measurement, all reaction wells contained 16 µl of microsome, 30 µl of 7-ethoxyresorufin working solution, and 65 µl HEPES buffer (0.05 M HEPES, pH 7.8). Following incubation for 10 min at 37°C, EROD reactions were initiated by addition of 30 µl nicotinamide adenine dinucleotide phosphate (NADPH). Resorufin was quantified at 5, 7, 10, 15, 20, 25, 30, 40, and 45 min at 530 nm excitation and 590 nm emission wave-lengths in a fluorescence plate reader (POLARstar OPTIMA, BMG LAB-TECH, Cary, NC, USA) at 37°C. EROD reactions were then stopped by the addition of 60 µl florescamine. Plates were incubated at room temperature in the dark for 10 min, and then protein was quantified at 400 nm excitation and 460 nm emission. All samples were analyzed in triplicate and averaged for analyses.

### 2.3.6 Liver lipid content

Hepatic lipid content was quantified as described in Mehlem et al. (2013). Briefly, frozen tissue samples were embedded in Tissue-Tek® O.C.T. compound (Electron Microscopy Sciences). At least 10 cryo-sections (12 µm) were obtained from different depths of each sample. Sections were mounted onto Superfrost Plus microscope slides (VWR) and were stained for neutral lipids using oil red O (ORO, Sigma-Aldrich). Tissue images were taken using a digital camera mounted on a microscope (Zeiss Axioplan, Cal Zeiss Canada Ltd., Toronto, Canada) and ZEN 2 software (Carl Zeiss Microscopy GmbH, Jena, Germany), and lipid droplet quantification was performed using Image J software.

### 2.3.7 Statistical analyses

Changes in size-corrected body mass over time with treatment were assessed using a longitudinal mixed effects model. Body mass (size-corrected) was calculated as the residuals of a linear regression of body mass against tarsus and bill length. We assessed changes in mass over time (i.e., experimental dosing day) among treatment groups (nominal factor) and included an interaction term for treatment and time as fixed effects in our global model. We also tested for

possible differences among sexes and the interaction of sex and treatment as fixed effects. Given that mass increases over time were not linear, we also added a quadratic term for time and the interaction between this quadratic term and treatment as fixed effects. Individuals in our captive cohort showed large variations in body mass at the start of the experiment and in mass changes over time. This variation was controlled for statistically by applying a random intercept of bird identity nested within cohort and a random slope of time. Inclusion of these random effects better fit the data as determined by lower AICc scores (Akaike's information criterion corrected for small sample size; Burnham and Anderson, 2002). Model selection was determined by lowest AICc scores, model weights, and deviance scores, following Burnham and Anderson (2002).

Differences in liver EROD activity among treatment groups were analyzed using a linear mixed effects model. We tested the effect of tPAH treatment and sex on EROD activity by including treatment group, sex, and their interaction as fixed effects in the global model. We controlled for possible differences among dosing cohorts and for possible diurnal variations in EROD activity by including random intercepts for cohort and sampling time. AICc scores, model weights, and deviance scores were used for model selection (Burnham and Anderson, 2002). More than one model best described the variance in EROD activity ($\Delta$AICc < 2). Therefore, weighted model-averaged estimates (i.e., relationships among variables) were calculated for fixed effects in the top model set. EROD data were log transformed to ensure that model residuals met the assumptions of normality and heteroscedasticity. For all subsequent analyses, EROD was used as a marker of PAH exposure, as we found that EROD better reflected exposure than the categorical dose group, likely due to differences in metabolism and possibly gut absorption efficiency of the dosing solution among individuals.

For all other variables, we used linear mixed effects models to assess whether variation was related to changes in EROD activity or sex. Global models thus included fixed effects of EROD activity (log transformed), sex, and the interaction between EROD and sex. We controlled for any influence of dosing period by including cohort as a random effect. In all serum analyte models, we accounted for any diurnal fluctuations in serum analytes by including sampling time as a random effect. The analysis of some serum analytes can be affected by lysed red blood cells (hemolysis) and by the presence of fat (lipemia) and bilirubin (hyperbilirubinemia) and these factors were included as random effects where applicable. Lipemia was included in the models for BOHB, bile acid, hematocrit, NEFA, and triglyceride;

hemolysis was included in the models for bile acid, creatine kinase, GGT, and UA; and hyperbilirubinemia was included in the models for AST and lipase. Serum analyte response variables were transformed where necessary to ensure that model residuals met the assumptions of normality and heteroscedasticity: BOHB, creatine kinase, TG, hepatosomatic index (HSI), and liver lipid content were log transformed; UA was cube root transformed; lipase and hematocrit were power transformed ($x^4$ and $x^2$, respectively); and GGT and AST were cos-transformed. The methods used for serum analyte model selection and weighted model-averaged estimate calculation were the same as the methods described above for the EROD activity analysis.

Serum analytes were further evaluated using a multivariate principal component analysis (PCA). The PCA converts a set of possibly correlated variables into a smaller number of uncorrelated variables called principal components (PC; Smith, 2002). The PCA allows us to visualize how serum analytes are related to each other and to analyze how they vary together with changes in EROD activity and with sex. The first 3 principal components (PC) were retained and individual PC1, PC2, and PC3 axis scores (see Smith, 2002) were extracted to use in above models as response variables. All modelling was performed in R version 3.2.5 (R Core Team, 2017).

**2.4 Results**

Average values for all whole body, liver, and serum responses by treatment group are shown in Table 2.1. The best approximating model for body mass (size-corrected) included fixed effects of time, time$^2$ (describes the non-linear change in Sanderling mass over time), treatment, sex, and the interaction of time and treatment (Table 2.2). Mass increased over time ($\beta = 0.60 \pm 0.15$, $p < 0.001$), indicating fuelling occurred, and the polynomial term time$^2$ indicated that this was a curvilinear relationship ($\beta = -0.011 \pm 0.004$, $p = 0.007$), which plateaued at about Day 20, near the end of dosing (Figure 2.1A). tPAH exposure reduced Sanderling body mass by 3.9 (low dose), 5.4 (medium dose) and 3.8 (high dose) times that of controls (Table 2.2, Figure 2.1A). Interactions between time and treatment indicated that early fuelling rates were more rapid in the medium and high dose groups (medium dose: $\beta = 0.76 \pm 0.18$, $p < 0.001$; high dose: $\beta = 0.33 \pm 0.18$, $p = 0.06$), but interactions between time$^2$ and treatment in the medium and high dose groups also indicated a decline in fuelling rates at the end of the experiment (medium dose: $\beta = -0.030 \pm 0.006$, $p < 0.001$; high dose: $\beta = -0.015 \pm 0.006$, $p = 0.006$). For example, mass peaked at

**Table 2.1.** Measured whole body, liver, and serum responses in Sanderling at the end of a 21-day exposure to nominal dosages of 0 (n = 12), 12.6 (n = 12), 126 (n = 12), and 1260 (n = 13) µg/kg-bw/day of a commercial PAH mixture. Values are mean ± standard error.

| | tPAH dosage (µg/kg body weight/day) | | | |
|---|---|---|---|---|
| Response | 0 | 12.6 | 126 | 1260 |
| *Whole body measurements* | | | | |
| Mass (g) | 73.2± 2.7 | 69.4± 2.5 | 67.7± 2.7 | 68.8± 2.6 |
| Body mass (size-corrected) | 4.05± 2.71 | -0.74± 2.75 | -2.98± 2.99 | -0.311± 2.35 |
| *Gross liver measurements* | | | | |
| Liver lipid content (% pixels in image) | 32.2± 4.2 | 28.5± 4.2 | 38.3± 6.1 | 29.3± 3.2 |
| HSI (%) | 2.76± 0.18 | 2.58± 0.09 | 2.56± 0.24 | 3.2± 0.51 |
| *Serum analytes* | | | | |
| AST (U/l) | 532± 47 | 464± 55 | 579± 43 | 545± 59 |
| Bile acid (µmol/l) | 76.8± 20.1 | 62.8± 10.6 | 54.3± 7.5 | 50.8± 9.4 |
| BOHB (mmol/l) | 0.93± 0.133 | 1.18± 0.16 | 1.85± 0.35 | 1.41± 0.25 |
| Cholesterol (mmol/l) | 15.3± 0.8 | 15.1± 0.6 | 16.4± 0.7 | 16.3± 0.7 |
| Creatine kinase (U/l) | 641± 249 | 703± 132 | 721± 126 | (1.06± 2.17) x $10^3$ |
| Glucose (mmol/l) | 19.1± 0.7 | 19.9± 0.6 | 20.2± 0.7 | 19.7± 0.7 |
| GGT (U/l) | 0.83± 0.366 | 1.42± 0.50 | 0.92± 0.417 | 0.462± 0.268 |
| Hematocrit (%) | 54.4± 2.2 | 55.1± 2.5 | 52.4± 2.1 | 51.6± 2.5 |
| Lipase (U/l) | 7.18± 0.18 | 7.08± 0.15 | 7.17± 0.17 | 7.00± 0.28 |
| NEFA (mmol/l) | 0.69± 0.052 | 0.775± 0.087 | 0.98± 0.085 | 0.733± 0.099 |
| Triglyceride (mmol/l) | 3.52± 0.82 | 2.79± 0.38 | 2.37± 0.51 | 2.26± 0.34 |
| Uric Acid (µmol/l) | 691± 107 | 595± 84 | 593± 99 | 549± 92 |

**Table 2.2** Summary of parameter estimates and significance ($p < 0.05$) for the terms retained in the best-approximating model (based on lowest Akaike's information criterion corrected for small sample sizes, AICc) to explain variation in body mass (size-corrected) over time and EROD activity in Sanderling orally exposed to nominal treatment dosages of 0 (n = 12), 12.6 (n = 12), 126 (n = 12), and 1260 (n = 13) µg/kg-bw/day of a commercial PAH mixture for 21 days.

| Response | Parameter | β estimate ± SE | *p* |
|---|---|---|---|
| Body mass (size-corrected)[a] | time | (5.96 ± 1.45) x $10^{-1}$ | **<0.001**[*] |
| | time$^2$ | (-1.08 ± 0.40) x $10^{-2}$ | **0.007** |
| | sex (male) | -5.59 ± 1.42 | **<0.001** |
| | treatment 12.6 | -3.90 ± 2.00 | 0.06 |
| | treatment 126 | -5.35 ± 2.01 | **0.01** |
| | treatment 1260 | -3.84 ± 1.96 | 0.06 |
| | time x treatment 12.6 | 0.228 ± 0.178 | 0.2 |
| | time x treatment 126 | 0.760 ± 0.178 | **<0.001** |
| | time x treatment 1260 | 0.331 ± 0.175 | 0.06 |
| | time$^2$ x treatment 12.6 | (-9.94 ± 5.65) x $10^{-3}$ | 0.08 |
| | time$^2$ x treatment 126 | (-2.96 ± 0.57) x $10^{-2}$ | **<0.001** |
| | time$^2$ x treatment 1260 | (-1.52 ± 0.59) x $10^{-2}$ | **0.006** |
| EROD[b] | treatment 12.6 | 0.106 ± 0.249 | 0.7 |
| | treatment 126 | (0.899 ± 2.49) x $10^{-1}$ | 0.7 |
| | treatment 1260 | 0.616 ± 0.243 | **0.01** |
| | sex (male) | 0.152 ± 0.189 | 0.4 |

[a] Global model included fixed effects of treatment group, time, sex, a quadratic (non-linear) term for time (time$^2$), and all interaction terms in addition to a random slope of time and a random intercept of bird identity nested within cohort.

[b] Global model included fixed effects of treatment group, sex, and the interaction of treatment and sex, in addition to random intercepts for cohort and sampling time.

[*] Boldface type indicates statistical significance ($p < 0.05$).

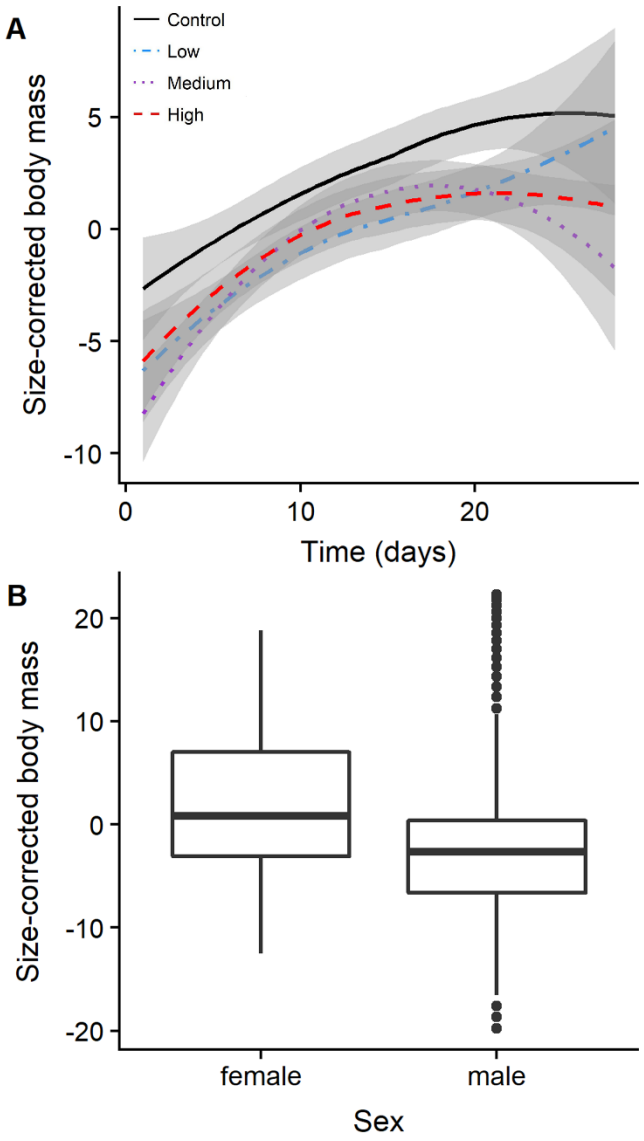


**Figure 2.1.** Changes in Sanderling pre-migratory size-corrected body mass over time (A) and by sex (B; females n = 27, males n = 22) during a 21-day oral exposure to nominal dosages of 0 (Control, n = 12), 12.6 (Low, n = 12), 126 (Medium, n = 12), or 1260 (High, n = 13) µg/kg-bw/day of a commercial PAH mixture. Lines and boxes indicate model-based estimates of the weighted model-averaged means ± a 95% confidence interval. In panel A, line colours indicate treatment group (black = Control, blue = Low dose, purple = Medium dose, and red = High dose). In panel B, dots represent points outside of the 95% confidence interval.

approximately 18 and 20 days in the medium and high dose groups, respectively, and decreased thereafter, whereas controls gained mass throughout dosing and achieved and maintained their peak mass at the end of the experiment (Figure 2.1A). At the end of the experiment, male birds had a lower mean body mass than females ($\beta$ = -5.6 ± 1.4, $p < 0.001$; Figure 2.1B), but there was no interaction between sex and treatment.

EROD activity was best predicted by dose group (Table 2.2; see Table A.1 for model selection results). Higher tPAH dosages caused an induction of EROD activity relative to controls, which was significantly higher in the high dose group (low dose: $\beta$ = 0.11 ± 0.25, $p$ = 0.68; medium dose: $\beta$ = 0.09 ± 0.25, $p$ = 0.73; high dose: $\beta$ = 0.62 ± 0.24, $p$ = 0.01; Figure 2.2).

EROD, a reliable indicator of PAH exposure (Head et al., 2015), was further supported as a predictor of effects on serum analytes and liver endpoints. EROD was consistently in the best-supported model sets for most liver and serum responses, including liver lipid content, bile acid, cholesterol, creatine kinase, GGT, hematocrit, lipase, NEFA, and uric acid, but not AST, BOHB, triglyceride, and HSI (see Tables A.2 and A.3 for model selection results). Increasing EROD activity was significantly associated with lower concentrations of bile acid ($\beta$ = -13.5 ± 6.4, $p$ = 0.04; Figure 2.3A) and with higher concentrations of creatine kinase ($\beta$ = 0.41 ± 0.15, $p$ = 0.01; Figure 2.3B). In female birds, EROD activity was positively correlated with lipase concentrations ($\beta$ = 560 ± 249, $p$ = 0.03; Figure 2.3C). At increasing levels of EROD activity, plasma cholesterol, GGT, and NEFA tended to increase, and hematocrit, UA, and liver lipid content tended to decrease, but these trends were not statistically significant ($p > 0.05$). In addition, sex explained variance in the top model sets predicting BOHB, bile acid, cholesterol, glucose, lipase, and liver lipid content but was not formally significant ($p > 0.05$). Triglyceride, AST, and HSI were not explained by differences in EROD, sex, or the interaction of EROD and sex (i.e., the null model was the top model for these responses; Table 2.3).

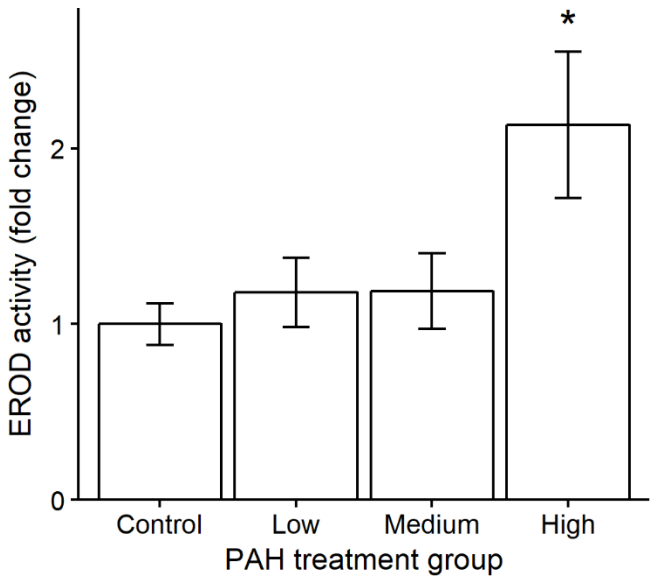


**Figure 2.2.** Induction of hepatic EROD activity in Sanderling orally exposed to nominal dosages of 0 (Control, n = 12), 12.6 (Low, n = 12), 126 (Medium, n = 12), or 1260 (High, n = 13) µg/kg-bw/day of a commercial PAH mixture for 21 days. Values are model-based estimates of the weighted model-averaged means ± a 95% confidence interval. Asterisk indicates a statistically significant difference from controls ($p < 0.05$).

**Table 2.3.** Summary of parameter ($\beta$) estimates and significance ($p < 0.05$) for terms retained in the best-approximating models (based on lowest Akaike's information criterion corrected for small sample sizes, AICc) to explain variation in physiological response variables in Sanderling exposed to nominal dosages of 0 (n = 12), 12.6 (n = 12), 126 (n = 12), and 1260 (n = 13) µg/kg-bw/day of a commercial PAH mixture for 21 days.

| | Parameter $\beta$ estimate ± SE | | |
|---|---|---|---|
| Response[a] | EROD | sex (male) | EROD x sex (female) |
| *Liver measurements* | | | |
| Liver lipid content | -0.142 ± 0.109 | 0.140 ± 0.144 | x |
| HSI | x | x | x |
| *Serum analytes* | | | x |
| AST | x | x | x |
| Bile acid | -13.5 ± 6.4* | -14.1 ± 8.1 | x |
| BOHB | x | 0.176 ± 0.134 | x |
| Cholesterol | 0.496 ± 0.584 | 0.636 ± 0.749 | x |
| Creatine kinase | 0.410 ± 0.145* | x | x |
| Glucose | x | -0.716 ± 0.676 | x |
| GGT | 0.117 ± 0.128 | x | x |
| Hematocrit | -214 ± 200 | x | x |
| Lipase | 418 ± 286 | 450 ± 225 | 560 ± 249* |
| NEFA | 0.110 ± 0.058 | x | x |
| TG | x | x | x |
| Uric Acid | -0.600 ± 0.310 | x | x |

[a] Global models included fixed effects of EROD activity, sex, and the interaction of EROD activity and sex. All models included cohort as a random intercept, all serum analytes included sampling time as a random intercept, and lipemia, hemolysis, and hyperbilirubinemia were included as random intercepts where appropriate (see Section 2). x indicates that a fixed effect was not included in that response's top model. Asterisks indicate statistical significance ($p < 0.05$).

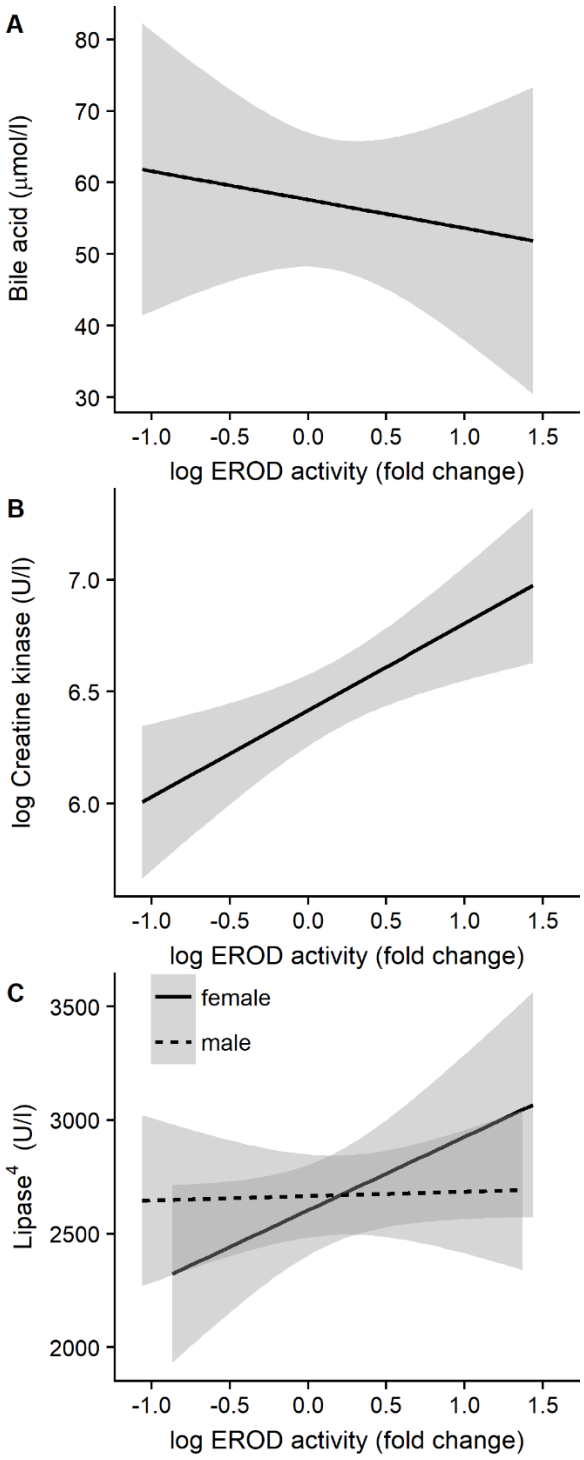


**Figure 2.3.** Relationship between EROD activity and serum bile acid (A), EROD activity and serum creatine kinase (B), and the effect of the interaction between EROD activity and sex (females n = 27, males n = 22) on serum lipase (C) in Sanderling treated with nominal dosages of 0 (n = 12), 12.6 (n = 12), 126 (n = 12), or 1260 (n – 13) µg/kg-bw/day of a commercial PAH mixture for 21 days. Lines indicate best-fit linear trends with 95% confidence intervals (shaded areas).

A multivariate PCA was performed to evaluate the relationship among all serum analytes (Table A.4; Figure A.1). Principal component (PC) axis 1, PC2, and PC3 explained 29.5, 13.7, and 10.7% of the variance among the serum analytes, respectively. There was no clear separation of birds into clusters based on treatment group, although birds in the control and low dose groups tended to have more positive scores along PC2 relative to birds in the medium and high dose groups (Figure A.1). Increasing EROD activity was associated with lower scores along PC 2 ($\beta$ = -0.39 ± 0.20, $p$ = 0.06), which was unaffected by sex and the interaction of EROD and sex. Changes in PC1 and PC3 were not explained by differences in EROD, sex, nor the interaction of EROD and sex (i.e., the null model was the top model for these responses; see Table A.5 for model selection results).

## 2.5 Discussion

We hypothesized that PAH ingestion would impair Sanderling pre-migratory fuelling. This study is unique in tracking the effects of sublethal oral PAH exposure in a wild shorebird species during its pre-migratory fuelling period, which has important implications for understanding the effects of ongoing oil spills on migrant birds. Our dosing concentrations were within the range of environmental levels measured in marine species in the Gulf of Mexico following the Deepwater Horizon oil spill (ranging from 21 – 143 μg/kg in finfish to 3676 μg/kg in oysters; Gohlke et al., 2011). The compositional mixture of PAHs used in this study also closely match those detected following the Exxon Valdez and Deepwater Horizon oil spills (Boehm et al., 1998; Reddy et al., 2012). Furthermore, the 21-day experimental period represents the average staging duration of Sanderling (Robinson et al., 2003). This study thus simulated the ingestion of a PAH-contaminated food source during staging. Lastly, experiments were conducted on wild-caught Sanderling, which, like other wild avian populations, are more genetically polymorphic, and have different ages, dietary histories, and previous xenobiotic exposures, relative to many uniform captive lab populations. Therefore, these results are likely more representative of how a wild Sanderling population might respond to PAH ingestion and the type of variance that may be expected among wild birds.

### 2.5.1 PAH Exposure

EROD activity is a common and sensitive biomarker for oil contaminant and PAH exposure in birds (e.g., Esler et al., 2010; Head et al., 2015; Willie et al., 2017). Induction of

EROD activity occurs when PAHs and related halogenated aromatic hydrocarbons bind to the AhR, which promotes the transcription of several genes, including the enzyme CYP1A. The activity of CYP1A is commonly measured as EROD activity (reviewed in Head et al., 2015). Therefore, statistically significant increases in EROD activity in the high dose group relative to controls confirmed PAH exposure in these captively-dosed Sanderling. Liver EROD activity is thus a strong measure of PAH exposure for the analysis of all liver and serum response variables.

### 2.5.2 Fuel loads and fuelling rates

Our body mass results show that PAH exposure produced whole-organism-level changes in Sanderling fuelling ability. At the end of the 21-day dosing period, we found that body mass (size-corrected) gain was 3.9, 5.4, and 3.8 times lower in the low, medium, and high dose groups, respectively, relative to controls. PAH effects on mass gain were not formally dose-dependent; however, all treatment groups showed impairment relative to controls. Perez et al. (2017a) similarly observed reduced post-flight mass gains in homing pigeons (*Columba livia*) following external oiling, but did not test various levels of exposure. Previous work in wintering western sandpipers observed a dose-dependent mass loss following 20 days of oral exposure to artificially weathered Deepwater Horizon oil (Bursian et al., 2017b). However, the mechanisms regulating mass gain during the pre-migratory period differ from those that maintain mass during wintering and breeding (Cornelius et al., 2012). It is therefore unknown why PAH effects on mass gain were not strictly dose-dependent, but individual variation in the high dose group may have contributed. Nevertheless, fuelling rates in the medium and high dose groups decreased towards the end of the experimental dosing period (after days 18 and 20, respectively), suggesting that higher PAH dosages affected the threshold timing of fat deposition. We also found that male Sanderling had a lower mean body mass than females. This sexual size dimorphism has been observed previously in Sanderling (Lourenço et al., 2016). However, we did not observe PAHs differentially affecting the sexes in terms of fuelling rates and total mass gain.

It is important to note that our measurements were taken in older Sanderling (after second year, ASY) and during the Sanderling's autumn pre-migratory fuelling period. Juvenile (< 3 months old) and first time migrating birds (second year, SY) birds appear to exhibit different strategies and efficiencies in foraging, fuelling, and fat deposition than older birds (Sandberg and Moore, 1996). Similarly, the physiological regulation of avian pre-migratory fuelling varies

between spring and autumn migrants (for review, see Cornelius et al., 2013). Therefore, PAH ingestion in younger birds or in spring migrants could produce results that vary from those of this study.

These fuelling results could have important implications for migrant birds, with the potential for seasonally dissimilar outcomes. Spring migrants tend to exhibit a time-minimization strategy, depositing as much fat as possible as quickly as possible to meet the nutritional requirements for migration and breeding (Hedenström and Alerstam, 1997). Time-minimizers appear to have relatively fixed departure dates and can leave their staging site at a specific time regardless of whether they have reached the threshold mass required for migration and for initiating breeding (Baker et al., 2004). In spring-migrating Red knots (*Calidris canutus*), for example, lower fuelling and departure masses were associated with reduced adult survival, lower recruitment of young, and, ultimately, population declines (Baker et al., 2004). Conversely, autumn migrants tend to exhibit an energy-minimization migration strategy, and migration pace should not be influenced by fuel loads or refuelling rates (Hedenström and Alerstam, 1997). Given the differences between spring and autumn migrants, we predict that PAH ingestion in the spring is more likely to have survival and fitness consequences and possible population-level effects from "flying lean". Investigating seasonal differences in toxicant effects in migrant birds could be an important area for future avian ecotoxicological research.

### 2.5.3 Mechanisms for fuelling impairment

Our serum analyte results provide insight into the mechanisms by which the above body mass changes may have occurred. The observed changes in serum bile acid concentrations are a clear indication of altered fatty acid metabolism and absorption in dosed Sanderling. Bile acids are potent emulsifiers and play a key role in solubilizing hydrophobic compounds, including lipids and fat-soluble vitamins, and in facilitating their digestion and absorption (Staels and Fonseca, 2009). Previous studies found that the AhR agonist TCDD alters the expression of genes related to cholesterol synthesis and metabolism (Sato et al., 2008), and that TCDD administration in rats inhibits the synthesis and excretion of bile acids (Fletcher et al., 2005). Therefore, PAH ingestion may have lowered bile acid concentrations in Sanderling through an AhR-mediated pathway.

The changes in circulating creatine kinase suggest a change in overall energy metabolism and muscle damage in dosed Sanderling. Previous studies confirm that oil and PAH exposure

can increase circulating creatine kinase concentrations (Duffy et al., 1996). Creatine kinase is a central regulatory enzyme in energy metabolism. Creatine kinase is found in high concentrations in the cytosol of tissues with a high energy demand, like the skeletal muscle, and cellular disturbances can cause creatine kinase to leak from cells into the blood (reviewed in Baird et al., 2012). For this reason, elevated creatine levels are a widely used marker of skeletal muscle damage (Guglielmo et al., 2001).

This PAH-induced muscle damage can have functional consequences for exposed birds. Alderman et al. (2017b) found that swimming performance was reduced in Sockeye salmon (*Oncorhynchus nerka*), a migratory fish species, exposed to 66.7 µg/l tPAH for 4 weeks. Similarly, muscle damage due to PAH ingestion during staging could reduce a bird's migratory flight performance. PAH-induced muscle damage also has the potential to affect overall migration speeds. Previous work by Guglielmo et al. (2001) found that migration flights cause muscle damage that must be repaired during staging and that the time spent repairing muscle damage upon arrival can influence 'settling times' (the time between arrival and initiating fuelling). Settling times strongly influence overall staging durations, which, in turn, affect total migration speeds (Hedenström and Alerstam, 1997). Presumably the added muscle damage caused by staging site PAH exposure would limit a bird's ability to also repair migration-induced muscle damage and could delay departure.

Although serum lipase concentrations were positively associated with EROD activity in female Sanderling, it is unlikely that these results reflect a meaningful change in pre-migratory fuelling physiology. Overall males tended to have higher lipase concentrations than females ($\beta$ = 450 ± 225; $p$ = 0.05; Table 3), and untransformed female lipase concentrations (7.00 ± 0.26, 7.00 ± 0.22, 7.20 ± 0.37, and 6.88 ± 0.44 in the control, low, medium, and high dose groups, respectively) only show a marginal increase in the medium dose group (+2.9%) and a slight decrease in the high dose group (-1.7%) relative to controls. Serum lipase concentrations in our Sanderling also remain within the normal physiological range of other avian species (Van Gils, 2004). As well, any PAH-induced changes in female serum lipase concentrations and any related changes in lipid metabolism or in pancreatic and/or renal function, did not reduce female size-corrected body mass relative to males.

Several serum analytes were unaltered by PAH ingestion, and changes in many of the typical biological markers of PAH exposure (e.g. elevated AST and GGT, reduced hemoglobin,

liver steatosis; Albers, 2006; Alonso-Alvarez et al., 2007; Lee et al., 2010), were not observed. This is in accordance with recent work by Bursain et al. (2017b), who orally dosed wintering western sandpipers with artificially weathered MC252 oil for 20 days, and also found that plasma chemistry was largely unaltered by oil ingestion. The authors concluded that either the high gut transit time of shorebirds likely led to low PAH absorption or that western sandpipers are relatively insensitive to ingested oil, both of which may be similar for our closely related Sanderling. Nevertheless, it is interesting to note that our PCA results corroborate the changes commonly observed in serum biomarkers following PAH exposure: the significant negative association between PC2 and EROD activity suggest a positive association between EROD activity and serum markers of liver damage (AST and GGT; Alonso-Alvarez et al., 2007) and a negative association between EROD activity and hematocrit. Additionally, the negative association between PC2 and EROD activity suggests a positive association between EROD activity and cholesterol, which is metabolised into bile acids (Staels and Fonseca, 2009), and creatine kinase, which further confirms that the overall effects of PAH ingestion were a disruption of lipid homeostasis and muscle damage.

### 2.5.4 Possible alternative mechanisms for impaired fuelling

It is important to consider alternative physiological mechanisms that could be affecting pre-migratory fuel loads and fuelling rates in PAH-dosed Sanderling. Here, we measured EROD activity, which is a biomarker of AhR activation (Head et al., 2015), but other non-AhR-mediated pathways not explored here are also affected by PAHs. For example, PAHs can increase the expression of the peroxisome proliferator-activated receptor gamma (PPARγ; Zhang et al., 2016), which regulates fatty acid storage and glucose metabolism (Wang, 2010). PAHs are also recognized endocrine disruptors that have been shown to alter thyroid, sex steroid, adrenocorticotropic, and corticosterone hormone activities (Yanyan Zhang et al., 2016), all of which can affect fat metabolism and the regulation of pre-migratory fuelling (Cornelius et al., 2012). As well, we focussed on the liver as a target of PAH toxicity because a typical and well-documented effect of PAH exposure is liver damage (Albers, 2006; Bursian et al., 2017a). However, PAHs and their reactive metabolites could affect other tissues and organs related to fuelling. For example, dietary benzo[*a*]pyrene intake causes intestinal damage (Ribiere et al., 2016). Similar damage in exposed birds could reduce the absorptive capacity of the intestine, lowering the ability for PAH-exposed birds to absorb dietary nutrients, particularly over time.

## 2.6 Conclusions

Pre-migratory fuelling is an essential and tightly regulated event in the life history of migrant birds. Because long distance migrants operate at the limits of physiological endurance exercise, even subtle changes in fuelling ability or fuelling speeds could negatively impact these birds. This study confirms that ingestion of environmentally-relevant PAH concentrations interferes with mechanisms for pre-migratory fuelling. We saw that PAH exposure over a 21-day period of pre-migratory fuelling reduced overall Sanderling body mass and the rate of body mass increase. As well, our measured serum analytes suggest that PAH ingestion affected the physiological mechanisms involved in lipid absorption and metabolism and can cause muscle damage. Our study thus highlights the negative impacts that chronic dietary exposure to PAHs can have on the fuelling physiology of migratory birds.

# 3 CHAPTER 3: POLYCYCLIC AROMATIC HYDROCARBON INGESTION ALTERS THE HEPATIC EXPRESSION OF GENES INVOLVED IN SANDERLING (*CALIDRIS ALBA*) PRE-MIGRATORY FUELLING

## PREFACE

Oral dosing with environmentally-relevant PAH concentrations lowered Sanderling pre-migratory mass gains and interfered with mechanisms for lipid absorption and metabolism (Chapter 2). Although serum biochemistry results suggested possible mechanisms by which PAHs may have impaired Sanderling pre-migratory fat deposition, further research was needed to characterize the molecular pathways underlying changes observed at the organismal level. Therefore, using liver subsamples from the same individuals in the previous oral dosing experiment, this study measured the hepatic mRNA expression of eight target genes related to fat deposition and oil exposure.

## 3.1 Abstract

In a previous study, oral dosing with a polycyclic aromatic hydrocarbon mixture reduced Sanderling (*Calidris alba*) pre-migratory mass gains and interfered with lipid homeostasis. We measured the expression of eight target genes related to fattening and PAH exposure in liver subsamples from these same birds. Cytochrome P450 1A4 (*Cyp1a4*) expression was upregulated, which confirmed aryl hydrocarbon receptor activation. We also found that liver basic fatty acid binding protein 1 (*Lbfabp*) and hepatic lipase (*Lipc*) expression were reduced in orally dosed Sanderling. This reveals possible molecular-level pathways for the observed impairment of pre-migratory refuelling and lipid homeostasis.

## 3.2 Introduction

Long-distance migrant shorebirds make non-stop flights of thousands of kilometers as they travel between their wintering and breeding grounds (Piersma, 1987). Completing these long-distance flights requires that shorebirds stop along the way to rest and replenish fuel stores as fat (Jenni and Jenni-Eiermann, 1998). However, shorebird refuelling ability appears to be impaired at certain key staging sites, with consequences for survival and reproductive performance (Baker et al., 2004). Impaired pre-migratory fuelling is therefore identified as an important factor in the ongoing global declines of shorebird populations (Zockler et al., 2003).

Shorebirds stage on migration at intertidal shoreline habitats, which are susceptible to contamination from oil spills (Henkel et al., 2012). The primary constituents of toxicity in oil are polycyclic aromatic hydrocarbons (PAHs; Leighton, 1993). PAHs can persist in subsurface sediments for decades following an oil spill (Short et al., 2007) and can accumulate in intertidal invertebrates (Willie et al., 2017). Shorebirds forage on intertidal invertebrates by probing in subsurface sediments (Grond et al., 2015) and commonly ingest sediments while foraging (Mathot et al., 2010). Therefore, shorebirds are vulnerable to chronic dietary PAH exposure at contaminated staging sites. Many shorebird species also exhibit strong staging site fidelity, which puts them at risk of reoccurring PAH exposures as they return to contaminated sites every year (Henkel et al., 2012).

Recent work in our lab (Bianchini and Morrissey, 2018) provides evidence that PAH ingestion impairs shorebird pre-migratory fuelling. In this study, we orally dosed Sanderling (*Calidris alba*), a long-distance migrant shorebird species, with environmentally-relevant PAH concentrations over a 21-day pre-migratory fuelling period to simulate dietary PAH exposures during staging. We found that pre-migratory mass gains were reduced in all treatment groups relative to controls. We also saw a dose-dependent increase in ethoxyresorufin-*O*-deethylase (EROD) activity, which confirmed aryl hydrocarbon receptor (AhR) activation in these birds. Higher individual EROD activity was correlated with lower serum bile acid concentrations and elevated serum creatine kinase concentrations in both sexes. EROD activity was also correlated with elevated serum lipase concentrations in female birds, however, this was not thought to have meaningfully affected Sanderling pre-migratory fuelling physiology (see Bianchini and Morrissey, 2018). These results suggested that the ingestion of a PAH-contaminated food source during staging can reduce overall fat deposition in pre-migratory shorebirds, and serum analyte

results suggested that PAH exposure interfered with mechanisms for lipid absorption and metabolism and caused muscle damage.

Here, our objective was to explore the molecular mechanisms underlying the serum and whole-body effects observed in our previous study. Using liver subsamples from the same individuals in our previous dosing experiment, we successfully optimized nine primer pairs (eight target genes and one housekeeping gene) for use in Sanderling, a wild bird species. We measured the hepatic mRNA expression of eight target genes related to fat deposition and oil exposure. To date, most molecular toxicology work in birds has acutely dosed pooled embryonic hepatocyte cultures from domestic/model avian species or wild avian embryos (e.g., Crump et al., 2017, 2016; Porter et al., 2014). Although this work is vital for determining a baseline response, there is a need to phenotypically anchor *in vitro* findings with whole-animal studies (Buesen et al., 2017). It is also important to assess toxicological outcomes in ecologically relevant wild species and in older birds, which can show different responses to PAH exposure than earlier life stages (Albers, 2006). This study is unique in assessing the molecular response of individual wild adult birds to chronic, sublethal PAH exposure in a system where molecular-level responses can be compared to known whole organism-level results. We discuss how observed changes in mRNA expression are related to effects previously observed at the whole organism-level. We also discuss the potential avian physiological refuelling mechanisms affected by PAH exposure.

## 3.3 Materials and methods

### 3.3.1 Sanderling capture, husbandry, and dosing

All field work and experimental procedures were approved by the University of Saskatchewan Animal Research Ethics Board, followed the Canadian Council on Animal Care guidelines for humane animal use, and adhered to the University of Saskatchewan Policy on Care and Use of Animals in Research (Animal Use Protocol #20120021). Birds were captured under Scientific Banding Permit #10268L.

Please see Bianchini and Morrissey (2018) for a detailed description of the methods used to trap, hold, and dose Sanderling. Briefly, between 21 May to 2 June, 2016, we used mist nets and noose carpets to trap 50 northward-migrating Sanderling from Chaplin Lake, Saskatchewan, Canada (50°26′28.36″, -106°40′9.37″). Sanderling were maintained in groups of 8 to 12 birds in outdoor aviaries at the Facility for Applied Avian Research (FAAR) at the University of

Saskatchewan. After transfer to captivity, one individual died of unknown causes, and the 49 remaining birds were used for the dosing study and tissue collections.

Dosing experiments began when birds showed signs of autumn pre-migratory fuelling. Individual birds began fuelling at different times (between 11 and 31 July). We therefore sorted birds into one of six cohorts for dosing, based when the onset of pre-migratory fuelling occurred. Individuals within each cohort were randomly assigned to one of four treatment groups: a control, low, medium, and high dose group that were dosed daily with 0, 12.6, 126, and 1260 µg total PAH (tPAH)/kg body weight/day, respectively, for 21 days. These dosages represent environmentally relevant dietary PAH exposure concentrations for Sanderling (see Bianchini and Morrissey, 2018), and the dosing period mimics the typical staging duration of Sanderling (Robinson et al., 2003). Daily dosages were administered by injecting a mealworm with the appropriate dose solution volume (3 – 8 µl; adjusted daily according to each individual's body mass) to mimic dietary exposure through ingestion of a contaminated food source. Twenty-four hours after the final dosing day, Sanderling were humanely euthanized by $CO_2$ asphyxiation. Liver samples were collected and immediately flash-frozen on dry ice. Samples were held at -80ºC until analysis.

Dose solutions were produced by diluting a commercial PAH mixture (QTM PAH Mix, Sigma-Aldrich; composition: 2,000 µg/ml each of acenaphthene, acenaphthylene, anthracene, benz[*a*]anthracene, benzo[*b*]fluoranthene, benzo[*ghi*]perylene, benzo[*a*]pyrene, 2-bromonaphthalene, chrysene, dibenz[*a,h*]anthracene, fluoranthene, fluorene, indeno[1,2,3-*cd*]pyrene, naphthalene, phenanthrene, and pyrene in dichloromethane; tPAH concentration was 32,000 µg/ml) in food-grade organic sunflower oil (Compliments brand, Sobeys, Canada). All dose solutions contained equal ratios of sunflower oil and dichloromethane to ensure that only the tPAH concentration varied amongst the dosing solutions. The control, low, medium, and high dose solutions had target concentrations of 0, 164.57, 1,645.71, and 16,457.14 µg/ml tPAH, respectively.

### 3.3.2 RNA extraction and cDNA synthesis

Total RNA was extracted from approximately 30 mg liver tissue using the RNeasy Mini Kit (Qiagen) according to the manufacturer's protocol. RNA purity and concentration were assessed by measuring the A260/A280 absorbance ratio using a NanoDrop ND-1000 Spectrophotometer (Thermo Scientific). Only samples with an A260/A280 ratio between 1.8 and

2.2 were used for cDNA synthesis (n = 9 for the control, low, and medium dose group, and n = 10 for the high dose group). Purified RNA was stored at -80ºC until analysis. Total RNA (1 µg) was reverse transcribed to cDNA using the QuantiTect Reverse Transcription Kit (Qiagen) according to the manufacturer's protocols. cDNA samples were stored at -80ºC until analysis.

### 3.3.3 Quantitative real-time PCR

Real-time PCR was performed in 96-well plates using the QuantStudio 6 Flex Real-Time PCR System (Applied Biosystems). Initially, we tested primer sequences for 12 genes of interest, which were obtained from the double-crested cormorant (DCCO) ToxChip PCR array designed by Crump et al. (2016). The primers selected for analysis are involved in lipid and cholesterol homeostasis, two pathways that would directly affect pre-migratory fuelling and that were previously impacted in orally-dosed Sanderling (Bianchini and Morrissey, 2018). We also selected primers that are indicative of oxidative stress or AhR activation, which are typical biomarkers of PAH exposure (Bursian et al., 2017a; Willie et al., 2017). We also tested two housekeeping genes. DCCO primer sequences for apolipoprotein B (*ApoB*), acyl-CoA synthetase long-chain family member 5 (*Acsl5*), and eukaryotic translation elongation factor 1 alpha 1 (*Eefa1a1*) failed to sufficiently amplify in Sanderling tissues. Nine primers (eight target genes and one housekeeping gene) successfully amplified and were used in subsequent experiments (Table 3.1).

**Table 3.1.** Description of the nine amplified gene targets and their associated pathways[a]

| Pathways | Gene symbol | Description | Accession number |
|---|---|---|---|
| Phase I metabolism | CYP1A4 | cytochrome P450 1A4 | |
| Lipid homeostasis | LBFABP | liver basic fatty acid binding protein 1 | |
| | LIPC | hepatic lipase | |
| Cholesterol homeostasis | CYP7B1 | cytochrome P450 7B1 | KT886919 |
| | HMGCR | 3-hydroxy-3-methylglutaryl-coenzyme A reductase | KT886908 |
| | SLCO1A2 | solute carrier organic anion transporter family, member 1A2 | |
| Oxidative stress | GPX3 | glutathione peroxidase 3 | |
| | GSTM3 | glutathione S-transferase | |
| Control | RPL4 | ribosomal protein L4 | KT886917 |

[a] Table adapted from Crump et al. (2016).

Primer sets were optimized using standard curves and primer optimization matrices. A standard curve in 2X cDNA dilution series (ranging from 0.125 to 20 ng of cDNA, assuming 100% reverse transcription efficiency) was used to determine the amplification efficiency of each primer. Assay conditions that yielded a $R^2 > 0.95$ and an amplification efficiency between 90 and 110% were considered acceptable. Primer optimisation matrices were run with 300, 450, and 650 nM forward (F) and reverse (R) primer combinations. Primer combinations that yielded the greatest amplification (i.e., the lowest threshold cycle (Ct) value) were used in subsequent analyses. In our Sanderling tissues, optimal F:R primer concentrations were: 600 nM:600 nM for *Lipc*, *Gstm3*, and *Lbfabp*; 300 nM:300 nM for *Cyp7b1*, *Gpx3*, and *Hmgcr*; and 650 nM:650 nM for *Cyp1a4*, *Rpl4*, and *Slco1a2*. Primer specificity was verified by a single melt curve peak and a single band on an agarose gel.

Optimized real-time PCR reactions contained 10 µl PowerUp SYBR Green Master Mix (Applied Biosystems), 5 µl diluted cDNA (at 12.5 ng/well), 300 – 650 nM of the gene-specific forward and reverse primer (Life Technologies Inc.), and nuclease-free water, for a final reaction volume of 20 µl/well. The PCR reaction mixture was denatured at 95ºC for 10 min, followed by 40 cycles of denaturing at 95ºC or 15 s and extension at 60ºC for 1 min. All reactions were run in triplicate.

### 3.3.4 PCR quality control

We tested for genomic DNA contamination by including a no-reverse transcriptase control with every cDNA synthesis preparation, which was run in a PCR reaction containing primers for the *Rpl4* reference gene. Reagent contamination was controlled for by including a no template control (NTC) well on every PCR plate. This reaction mixture included 5 µl of nuclease-free water instead of the cDNA template and contained primers for the *Rpl4* reference gene.

### 3.3.5 Data analysis

The relative expression of each gene target was calculated using the comparative Ct method, where the gene expression of each sample was normalized to *Rpl4* and to control samples according to the methods described by Livak and Schmittgen (Livak and Schmittgen, 2001) and Schmittgen and Livak (Schmittgen and Livak, 2008). The effect of PAH treatment concentration on relative gene expression was analyzed using linear mixed effects models.

Treatment group was included as a fixed effect, and we controlled for possible differences among cohorts and for diurnal variations in mRNA expression by including random intercepts for cohort and sampling time. A preliminary screen of the data revealed no differences among sexes. Therefore, sexes were grouped for the full analysis. To meet the assumptions of normality and heteroscedasticity, the expression levels of *Cyp1a4*, *Gpx3*, *Hmgcr*, *Lbfabp*, *Lipc*, and *Slco1a2* were log transformed, and *Cyp7b1* and *Gstm3* were square root transformed. Model selection was determined by lowest AICc (Akaike's information criterion corrected for small sample size) scores, model weights, and deviance scores according to Burnham and Anderson (2002). When global and intercept only (null) models were equivalent ($\Delta$AICc < 2), the weighted model-averaged estimate for treatment group was calculated using model.avg in the MuMIn package (Barton, 2017). All modelling was performed in R version 3.4.2 (R Core Team, 2017) using the lme4 package (Bates et al., 2015), and results were plotted using package ggplot2 (Wickham, 2009) and cowplot (Wilke, 2017).

### 3.4 Results

We found that *Cyp1a4*, *Lbfabp*, and *Lipc* were affected by PAH treatment (see Table A.6 for model results). *Cyp1a4* mRNA expression was 18-fold greater in the high dose group relative to controls ($\beta$ = 1.59 ± 0.67, $p$ = 0.02; Figure 3.1). The mRNA expression of both lipid homeostasis pathway genes, *Lbfabp* and *Lipc*, was 0.4- and 0.2-fold less, respectively, in the high dose group relative to controls (*Lbfabp*: $\beta$ = -1.78 ± 0.66, $p$ = 0.01, Figure 3.2A; *Lipc*: $\beta$ = -1.68 ± 0.51, $p$ = 0.002, Figure 3.2B). Changes in mRNA expression for genes in the cholesterol homeostasis pathway (*Hmgcr, Slco1a2, and Cyp7b1*; Figure 3.3) and oxidative stress pathway (*Gstm3* and *Gpx3*; Figure 3.4) were not explained by treatment. Both *Hmgcr* (Figure 3.3A) and *Slco1a2* (Figure 3.3B) tended to decrease with increasing PAH dosages, while *Cyp7b1* mRNA expression showed no discernible change in with treatment (Figure 3.3C). *Gstm3* (Figure 3.4A) expression tended to decrease while *Gpx3* (Figure 3.4B) tended to increase at increasing PAH dosages. However, these changes were not statistically significant (the intercept only (null) model was the best-approximating model for these responses). Expression of the internal control gene, *Rpl4*, was not altered by PAH treatment. Neither the genomic DNA contamination control nor the NTC showed amplification.

**Table 3.2.** Summary of parameter ($\beta$) estimates and significance ($p < 0.05$) for the terms retained in the best-approximating models to explain variation in Sanderling hepatic mRNA expression among PAH treatment groups.[a]

| Response[1] | Parameter | $\beta$ estimate ± SE | $p$[b] |
|---|---|---|---|
| *Cyp1a4* | treatment 12.6 | 0.654 ± 0.669 | 0.3 |
| | treatment 126 | (-6.96 ± 66.88) x $10^{-2}$ | 0.9 |
| | treatment 1260 | 1.59 ± 0.67 | **0.02** |
| *Lbfabp* | treatment 12.6 | (8.21 ± 66.44) x $10^{-2}$ | 0.9 |
| | treatment 126 | -0.379 ± 0.664 | 0.6 |
| | treatment 1260 | -1.78 ± 0.66 | **0.01** |
| *Lipc* | treatment 12.6 | (9.57 ± 50.18) x $10^{-2}$ | 0.9 |
| | treatment 126 | -0.435 ± 0.507 | 0.4 |
| | treatment 1260 | -1.68 ± 0.51 | **0.002** |

[a] Model selection was based on lowest AICc values (Akaike's information criterion corrected for small sample sizes). Global models included the fixed effect of treatment group and random intercepts for cohort and sampling time.

[b] Boldface type indicates a statistically significant difference ($p < 0.05$) in mRNA expression from the control.

*Cyp1a4* = cytochrome P450 1A4; *Lbfabp* = liver basic fatty acid binding protein 1; *Lipc* = hepatic lipase.

Samples sizes: 0, 12.6, and 126 n = 9; 1260 n = 10.

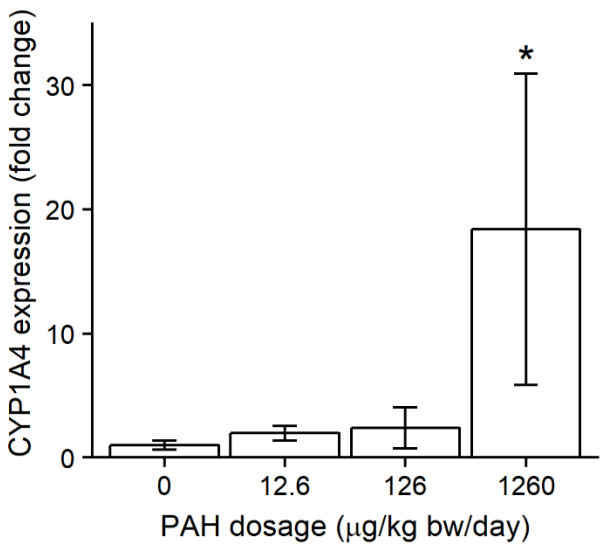


**Figure 3.1.** Cytochrome P450 1A4 (CYP1A4) hepatic mRNA expression in Sanderling orally exposed to increasing dosages of a commercial PAH mixture during a 21-day period of pre-migratory fuelling. Data are given as relative fold change in mRNA expression (mean ± standard error) relative to the control group. Asterisk indicates a significant difference from controls.

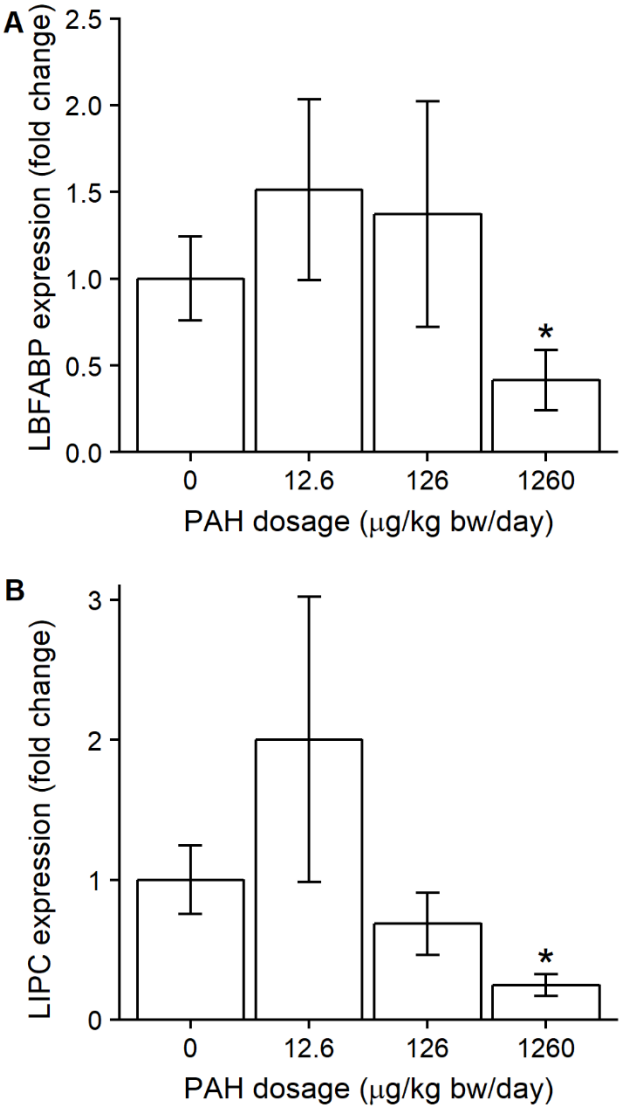


**Figure 3.2.** Hepatic mRNA expression of lipid homeostasis pathway genes, liver basic fatty acid binding protein 1 (LBFABP; A) and hepatic lipase (LIPC; B), in Sanderling orally exposed to increasing dosages of a commercial PAH mixture during a 21-day period of pre-migratory fuelling. Data are given as relative fold change in mRNA expression (mean ± standard error) relative to the control group. Asterisks indicate a significant difference from controls.

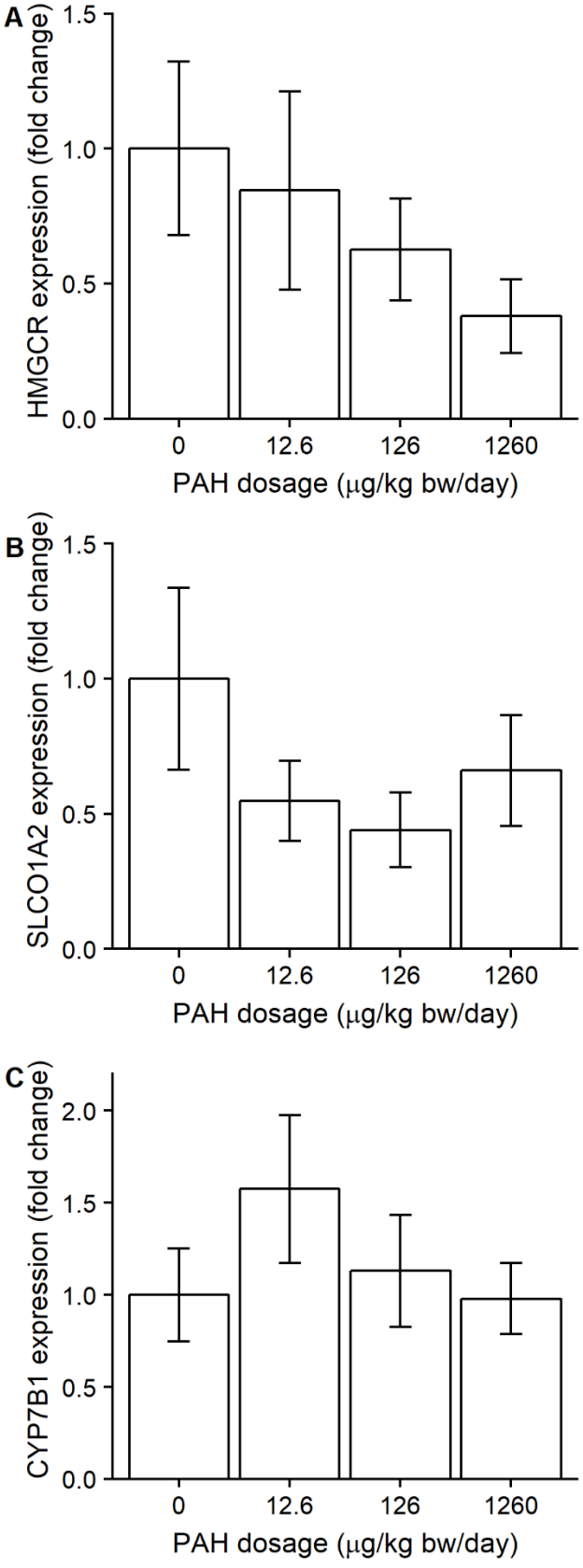


**Figure 3.3.** Hepatic mRNA expression of cholesterol homeostasis pathway genes, 3-hydroxy-3-methylglutaryl-coenzyme A reductase (HMGCR; A), solute carrier organic anion transporter family, member 1A2 (SLCO1A2; B), and cytochrome P450 7B1 (CYP7B1; C), in Sanderling orally exposed to increasing dosages of a commercial PAH mixture during a 21-day period of pre-migratory fuelling. Data are given as relative fold change in mRNA expression (mean ± standard error) relative to the control group.

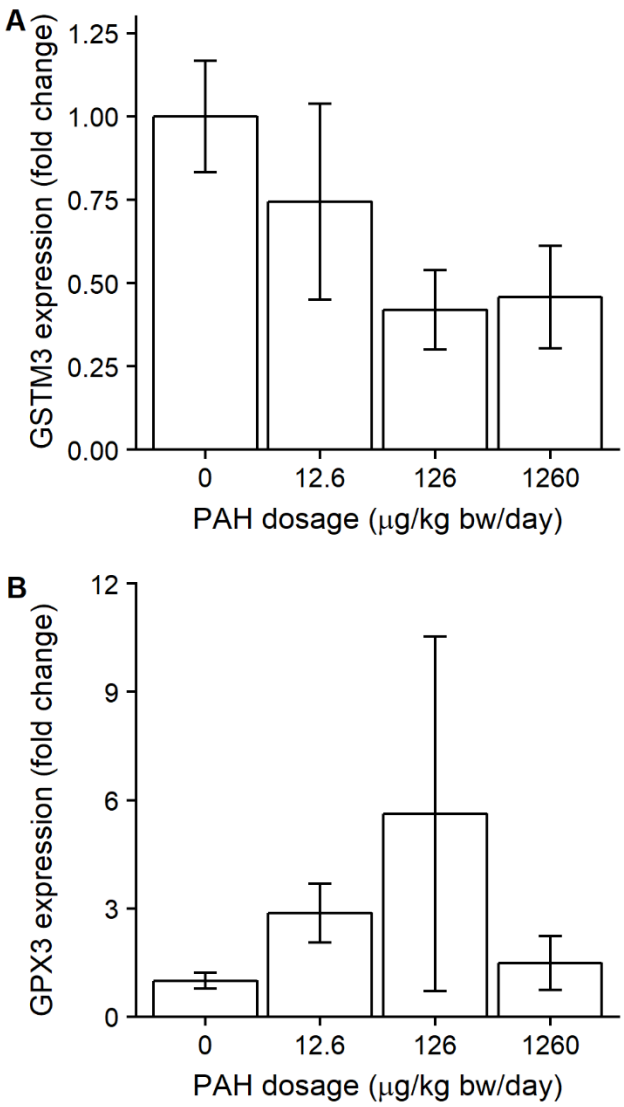


**Figure 3.4.** Hepatic mRNA expression of oxidative stress pathway genes, glutathione S-transferase (GSTM3) and glutathione peroxidase 3 (GPX3), in Sanderling orally exposed to increasing dosages of a commercial PAH mixture during a 21-day period of pre-migratory fuelling. Data are given as relative fold change in mRNA expression (mean ± standard error) relative to the control group.

## 3.5 Discussion

This study is unique in measuring gene expression changes in a wild shorebird species following sublethal oral PAH exposure during its pre-migratory fuelling period. Changes in the expression of eight target genes related to fat deposition and PAH exposure were measured in orally dosed Sanderling at the end of a 21-day dosing experiment when birds should have maximized fat deposition. Of the 12 DCCO primer sequences tested, nine successfully optimized in Sanderling tissues, suggesting a high degree of sequence overlap in these species. Throughout the discussion, changes in mRNA expression were considered physiologically relevant if they were statistically significant ($\alpha < 0.05$) and if transcript abundance was at least 0.5-fold less or 2-fold greater than controls. We saw that the expression of genes indicative of AhR activation and lipid homeostasis were significantly altered by PAH exposure. Because our Sanderling were wild-caught, they have different ages, dietary histories, and previous xenobiotic exposures, and are expected to be genetically polymorphic. Our birds likely show more variability in than the uniform captive populations typically used in gene expression studies. The treatment concentrations and conditions used in this experiment simulated environmentally-relevant PAH exposure levels and scenarios for staging shorebirds following an oil spill (Bianchini and Morrissey, 2018). Therefore, our results are likely representative of the effects of sublethal PAH ingestion in wild shorebird populations.

### 3.5.1 AhR activation

Bioactivation of PAHs to more toxic metabolites is primarily mediated by the xenobiotic-metabolizing monooxygenases, cytochrome P450 (CYP) 1A and 1B, following AhR activation (Schimada and Fujii-Kuiyama, 2004). PAHs are known bind to and activate the AhR, which promotes *Cyp1a* transcription. CYP1A activity is frequently measured as EROD activity, and EROD induction is a common biomarker for PAH exposure in birds (Head et al., 2015). On average, we observed 18-fold greater *Cyp1a4* mRNA expression in the high dose group relative to controls, and *Cyp1a4* was the most responsive transcript tested. This agrees with our previous study, where we saw significantly elevated EROD activity in the high dose group relative to controls (Bianchini and Morrissey, 2018). Therefore, the highest level of PAH exposure upregulated *Cyp1a4* expression and there was an associated increase in CYP1A activity. This further confirms AhR activation and PAH exposure in our captively-dosed Sanderling.

### 3.5.2 Lipid homeostasis

For the two genes involved in lipid homeostasis, *Lbfabp* and *Lipc*, mRNA expression was 0.4- and 0.2-fold lower, respectively, in the high dose group relative to controls. Similarly, Crump et al. (2017) observed reduced *Lbfabp* expression on the Chicken and DCCO ToxChip PCR Arrays following exposure of embryonic hepatocytes to petroleum coke, a major source of PAHs, and previous work in salmonid species also observed reduced lipase activity following PAH exposure (de Gelder et al., 2017; Meador et al., 2006). Microarray experiments in mice suggest that the observed reduction in *Lipc* and *Lbfabp* may be due to AhR agonism (Nault et al., 2017). In the liver, fatty acid binding proteins (FABP) are intracellular lipid chaperones and contribute to lipid homeostasis by enhancing fatty acid uptake, transport, storage, and metabolism (Atshaves et al., 2010). Hepatic lipase (LIPC) is a lipolytic enzyme that facilitates plasma lipid metabolism by hydrolyzing triglycerides (TG) and phospholipids in circulating lipoproteins. LIPC also contributes to lipid uptake in a variety of cell types by enhancing the interaction of lipoproteins with cell surface receptors (Santamarina-Fojo et al., 2004). Therefore, reduced expression of these two genes suggests that lipid metabolism and uptake were impaired in dosed Sanderling.

Given that Sanderling are long-distance migrants, this effect may be particularly detrimental to this species' survival and fitness. Maximizing migration speeds requires that birds rapidly deposit fat in adipose tissues prior to flight (Smith and Moore, 2005) and rapidly transport fats from adipose tissues to muscles during flight (Guglielmo, 2010). Long-distance migratory birds support the efficient movement of fatty acids during migration by increasing the expression and activity of the proteins involved in fat storage and transportation, including adipose tissue lipoprotein lipase, an enzyme that regulates adipose tissue fatty acid uptake (Ramenofsky et al., 1999), and fatty acid transport proteins on the membranes of muscles (fatty acid translocase (FAT/CD36) and plasma-membrane FABP) and in the cytosol of the heart (heart-type FABP) (Guglielmo, 2010). Whether the expression and activity of hepatic lipase and FABP similarly increases during migration is unknown. Nevertheless, these results suggest that PAH exposure may have impaired fatty acid uptake, transport, and metabolism during the migratory phase when rapid and efficient lipid transport is vitally important.

### 3.5.3 Cholesterol homeostasis

In our previous whole organism-level study, bile acid concentrations were significantly reduced by PAH exposure (Bianchini and Morrissey, 2018). Bile acids are the end products of cholesterol metabolism and play a key role in lipid absorption and in the regulation of hepatic lipid and metabolic homeostasis (Schonewille, 2016). We tested three genes in the cholesterol homeostasis pathway: *Hmgcr*, the rate-limiting enzyme in cholesterol biosynthesis; *Cyp7b1*, an enzyme involved in the conversion of cholesterol to bile acids; and *Slco1a2*, a transporter that contributes to the reuptake of bile acids from enterohepatic circulation into the liver (Schonewille, 2016). None of these genes showed statistically significant changes in mRNA expression following PAH exposure. Conversely, experiments in rodents typically report a coordinated repression of the genes responsible for cholesterol homeostasis following AhR agonism (Fader et al., 2017; Fletcher et al., 2005). Similarly, Chicken and DCCO embryonic hepatocytes show reduced *Slco1a2* and *Cyp7b1* mRNA expression following PAH exposure, however no change in *Hmgcr* expression was observed (Crump et al., 2017).

The observed downward trend in *Hmgcr* expression suggests that reduced serum bile acid levels were related to declines in cholesterol production. However, in the whole organism, we saw no significant change in serum cholesterol concentrations (Bianchini and Morrissey, 2018). As well, the downward trend in *Slco1a2* expression is expected to be associated with higher serum bile acid concentrations due to reduced hepatic bile acid reuptake (Haeusler et al., 2016). Many other enzymes regulate cholesterol and bile acid homeostasis, and our results suggests that other unexplored molecular pathways may have reduced serum bile acid concentrations.

### 3.5.4 Oxidative stress

PAH metabolism involves a complex series of enzymatic reactions that produce DNA-reactive metabolites and reactive oxygen species. Glutathione S-transferases (GSTs) and glutathione peroxidase (GPx) detoxify these reactive metabolites and protect against PAH-induced toxicity and oxidative damage (Benedetti et al., 2015). These enzymes are used as biomarkers of antioxidant capacity, and their expression typically increases in response to oxidative stress (Espin et al., 2017; Jenni-Eiermann et al., 2014). However, avian gene expression experiments have also observed both a downregulation and no change in *Gstm3* and *Gpx3* expression following PAH exposure (Crump et al., 2017). Here, we saw no statistically significant changes in the expression of *Gstm3* or *Gpx3*, but *Gstm3* tended to decrease and *Gpx3*

tended to increase in PAH-treated birds relative to controls. This was consistent at the whole organism-level, where serum gamma glutamyl transferase (GGT) and aspartate amino transferase (AST) were not significantly affected by PAH exposure. Similarly, we saw no significant change in liver lipid content or in the hepatosomatic index of PAH-treated birds relative to controls (Bianchini and Morrissey, 2018).

### 3.6 Conclusions

In our previous study, we found that environmentally-relevant PAH concentrations and exposure scenarios impaired Sanderling pre-migratory fuelling. Increases in *Cyp1a4* expression further confirmed AhR activation in dosed birds. *Lbfabp* and *Lipc* downregulation suggested that PAH exposure may have lowered pre-migratory mass gains by altering fatty acid uptake, transport, and metabolism at the molecular level which translated to whole organism effects. It is important to note that in mammals, reduced hepatic FABP and lipase activity are associated with mass gains, diabetes, and obesity. Loss of liver FABP function in mammals decreases hepatic fatty acid uptake and oxidation, which increases the availability of fatty acids for oxidation in muscle and/or storage in adipose tissues (Atshaves et al., 2010), and LIPC deficiencies in mammals are associated with hypertriglyceridemia and hypercholesterolemia (Santamarina-Fojo et al., 2004). However, in migrating bird species, individuals undergo rapid body mass gains in response to seasonal cues, and lipid metabolism differs markedly from mammals (Li, 2017).

The extreme endurance exercise of long-distance migration depends on several tightly controlled physiological processes, and even subtle alterations can have serious downstream effects. It is therefore important to identify the sub-organismal-level changes underlying effects observed at the individual level. Our study offers new insights into the pathways by which chronic dietary PAH exposure can impair avian pre-migratory fuelling in a wild bird in addition to providing important fundamental insight into the molecular changes underpinning lipid and cholesterol homeostasis.

# 4 CHAPTER 4: ASSESSMENT OF SHOREBIRD MIGRATORY FUELLING PHYSIOLOGY AND DEPARTURE TIMING IN RELATION TO POLYCYCLIC AROMATIC HYDROCARBON CONTAMINATION IN THE GULF OF MEXICO

## PREFACE

Captive dosing experiments confirmed that sublethal dietary PAH exposure lowered Sanderling pre-migratory mass gains (Chapter 2) and revealed how PAH ingestion can impair pre-migratory fuelling physiology (Chapter 2 and 3). Chapter 4 expanded on these captive results by investigating the relationship between PAH contamination and staging quality for fuelling shorebirds. PAH exposure from foraging was estimated at six key coastal staging sites in the Gulf of Mexico by measuring sediment total PAH concentrations, and the quality of these sites for pre-migratory shorebirds was evaluated by measuring metrics of pre-migratory fuelling efficiency in two shorebird species, Sanderling (*Calidris alba*) and Red knots (*C. canutus*). Field measurements were necessary to confirm that the captive results were representative of the effects observed in wild shorebirds fuelling at PAH-contaminated sites. As well, demonstrating the relationship between PAH exposure and slower refuelling was necessary to support subsequent investigations into the linkages between PAH ingestion, impaired fuelling, and slower migration timing.

The content of Chapter 4 was reprinted (adapted) from *Environmental Science & Technology*, (10.1021/acs.est.8b04571), K. Bianchini, C. Morrissey, "Assessment of shorebird migratory fuelling physiology and departure timing in relation to polycyclic aromatic hydrocarbon contamination in the Gulf of Mexico" 52, 13562-13573. Copyright (2018), with permission from ACS Publications.

Author contributions:

Kristin Bianchini (University of Saskatchewan) conceived, designed, and managed the study, generated and analyzed the data, prepared all figures, and drafted the manuscript.

Christy A. Morrissey (University of Saskatchewan) provided inspiration, scientific input, and guidance, commented on and edited the manuscript, and provided funding for the research.

## 4.1 Abstract

Over one million shorebirds depend on staging sites in the Gulf of Mexico that are frequently subject to pollution by oil and its toxic constituents, polycyclic aromatic hydrocarbons (PAHs). It was hypothesized that PAH contamination lowers staging site quality for migratory shorebirds, with consequences for fuelling and departure timing. Sediment total PAH concentrations were measured at six staging sites along the Texas and Louisiana Gulf Coast. Sites in Louisiana were expected to have higher total PAH concentrations, as they were more heavily impacted by the Deepwater Horizon oil spill. From 2015 to 2017, 170 Sanderling (*Calidris alba*) and 55 Red knots (*C. canutus*) were captured at these same sites during their northward migration (late April to mid May). Mass, fat scores and plasma metabolite measurements were taken to determine fuel loads and fuelling rates, and a subset of birds (120 Sanderling and 39 Red knots) received a coded radio tag to determine departure dates using the Motus telemetry array. Compared to Texas sites, sediment in Louisiana had higher total PAH concentrations, dominated by 6 ring indeno[1,2,3-*cd*]pyrene (48%). Plasma metabolite profiles suggested that fuelling rates for Sanderling, but not Red knots, tended to be lower in Louisiana, and both species departed later than the study average from Louisiana. However, multiple factors including migration patterns, food supply, disturbance and other contaminants likely influenced individual and species-specific differences in fuelling and departures across sites and years. PAH contamination in the Gulf of Mexico remains an ongoing issue that may be impacting the staging site quality and migration timing of long-distance migratory birds.

## 4.2 Introduction

Long-distance migratory birds are currently experiencing worldwide population declines (Sanderson et al., 2006). Birds can experience higher mortality on migration than during breeding and wintering (Sillett and Holmes, 2002), and it is possible for events on migration to carry-over and limit population levels by lowering reproductive success (Baker et al., 2004). Whether birds survive migration and successfully reproduce typically depends on a series of staging sites, where birds rest and accumulate necessary fuel for subsequent migration flights (Warnock, 2010). Therefore, long-distance migrants are sensitive to changes that limit staging site resource availability (Baker et al., 2004), and characterizing the quality of key staging areas is crucial for avian conservation (Faaborg et al., 2010).

Oil pollution is a serious threat to staging site quality for numerous bird species. The Gulf of Mexico contains some of the Western Hemisphere's most important coastline habitat for migratory birds (Burger, 2017). Over one million shorebirds winter and migrate along the Gulf coast (Withers, 2002), billions of Neotropical-Nearctic migrants stage there every year (Cohen et al., 2017), and the area is considered the most important migratory pathway in the world for waterfowl (Gallardo et al., 2004). Yet, ecosystems in the Gulf of Mexico are subject to frequent and repeated oil pollution (Henkel et al., 2012). Shorelines in the northern Gulf of Mexico (in Louisiana, Mississippi, Alabama, and Florida) were heavily impacted by the Deepwater Horizon oil spill (Beyer et al., 2016). As well, extensive oil extraction and transportation activities throughout this region cause both chronic and episodic oil exposure to migratory birds that seasonally use the area (Burger, 2017; DeLaune et al., 1990). Oil and polycyclic aromatic hydrocarbons (PAHs), the primary contaminant of concern in oil spills (Leighton, 1993), are detectible in subsurface sediments decades after an oil spill (Esler et al., 2010), and PAHs can readily bioaccumulate in avian invertebrate prey sources and incorporate into the avian food chain (Bonisoli-Alquati et al., 2016; Paruk et al., 2016; Willie et al., 2017). Therefore, oil contaminant impacts on coastal ecosystems can persist for decades following release.

The acutely lethal effects of oil exposure (e.g., hypothermia, emaciation) in birds are well known (Balseiro et al., 2005), and mass avian mortalities following large scale, catastrophic oil spills are well documented (Balseiro et al., 2005; Burger, 1993). However, it has been suggested that chronic and sublethal oil and PAH exposure may be more important to avian populations than acute mortalities (Bursian et al., 2017a). There is a growing body of work showing how

sublethal oil exposure can lower migratory bird vitality. PAH exposures have the potential to lower overall migration speeds due to external oiling of the feathers leading to reduced post-flight mass gains (Perez et al., 2017b, 2017a) and impaired flight performance, including slower take off speeds (Maggini et al., 2017b) and the selection of less efficient flight paths (Perez et al., 2017b). PAH exposure significantly reduces swimming speeds in fish, likely due to the cardiotoxic effects of this chemical class (Alderman et al., 2017b; Stieglitz et al., 2016). PAHs thus have the potential to lower the speed of flapping flight in migratory birds. Sublethal PAH and oil ingestion can also impair immune function and thermoregulation, increase metabolic rates, cause hemolytic anemia, impair nutrient absorption, and lower body mass (Bursian et al., 2017a; Paruk et al., 2016). Recent work on captively dosed Sanderling in our lab showed that PAH ingestion during staging lowered fuelling rates and overall pre-migratory mass gains near the end of a 21-day exposure period. We also found that PAHs affected Sanderling lipid homeostasis and caused muscle damage (Bianchini and Morrissey, 2018). PAHs also have endocrine disrupting effects (Lee et al., 2017) and cause liver and other organ toxicity, which is likely modulated through activation of the aryl hydrocarbon receptor (Soshilov and Denison, 2014).

Measures of avian pre-migratory fuelling can provide useful metrics for evaluating the quality of staging sites in the Gulf of Mexico with varying levels of oil pollution. Overall migration speeds are primarily determined by resting and refuelling time between flights (Schmaljohann et al., 2017). Therefore, birds minimize the time spent on migration by storing the maximum amount of fuel in the shortest possible time (Alerstam and Lindström, 1990). As a result, fuel deposition rates depend on the quality of refuelling habitats, and variations in staging site fuelling rates can correlate to local differences in food quality and availability (Aharon-Rotman et al., 2016; Schaub and Jenni, 2001). Given that fuel deposition rates directly influence departure fuel loads, stopover durations, and departure dates, these indices can provide a measure of staging site quality (Seaman, 2004). In addition to fat stores, other biotic and abiotic factors, such as weather, age and sex, can also influence departure decisions (Covino et al., 2014; Jarjour et al., 2017).

Here, we aimed to assess potential sublethal PAH exposure at key migratory staging sites and evaluated differences in staging site quality by measuring pre-migratory fuelling metrics in two shorebird species, Sanderling (*Calidris alba*) and Red knots (*C. canutus*). Both are long-

distance, arctic breeding shorebird species, that stage and/or over-winter in the Gulf of Mexico (Withers, 2002). Peak numbers of both species occur along Texas and Louisiana shorelines in late April and May (Baker et al., 2013; Macwhirter et al., 2002; Withers, 2002). Spring migrants of both species and are ecologically important for studying contaminant related effects on migration. Red knots are listed as a threatened species, with the rufa subspecies (*C. c. rufa*) listed as endangered in Canada (BirdLife International, 2017). Both species forage by picking and probing for marine invertebrates and bivalves in subsurface sediments (Grond et al., 2015; Macwhirter et al., 2002), and incidental sediment ingestion is common in shorebirds (Mathot et al., 2010). Therefore, oral PAH exposure can occur during foraging when individuals ingest contaminated prey (Bonisoli-Alquati et al., 2016; Paruk et al., 2016; Willie et al., 2017) and/or sediments (Labarrere, 2016).

In this study, we estimated potential PAH exposure by measuring total sediment PAH concentrations at six key shorebird staging sites in 2 coastal states in the Gulf of Mexico. Among our study sites, those in Louisiana were more heavily impacted by the Deepwater Horizon spill (Beyer et al., 2016), however, due to the extensive oil extraction and transportation activities in the Gulf of Mexico, smaller scale oil spills are common, and shorelines throughout the Gulf Coast are vulnerable to oil pollution from sources other than the Deepwater Horizon spill (Burger, 2017; DeLaune et al., 1990). We hypothesized that pooled sediment samples from Louisiana would have higher PAH concentrations relative to sites in the Texas Gulf. We hypothesized that oil pollution lowers staging site quality for migratory shorebirds. Although the energy for migration flight is primarily derived from lipids, body proteins are also catabolized during flight (Schaub and Jenni, 2001). Therefore, we evaluated the fuelling status of both species by testing the plasma concentrations of triglycerides (TG), β-hydroxybutyrate (BOHB), and uric acid (UA). Circulating TG and BOHB levels are indicative of fat deposition and metabolism, respectively, while UA is indicative of protein catabolism, which collectively represent the individual metabolic profile and fuelling status (Schaub and Jenni, 2001). We predicted that at staging sites with higher total sediment PAH concentrations, Sanderling and Red knots would exhibit (1) lower fuel loads at capture, (2) metabolite profiles indicative of reduced fuelling, and (3) later departure dates.

## 4.3 Materials and methods

### 4.3.1 Study sites

Sampling was conducted at six sites in the western Gulf of Mexico: North Padre Island (27º20′56.0″N 97º19′49.3″W), Mustang Island (27º40′00.3″N 97º10′25.1″W), and Bolivar Flats (29º24′05.6″N 94º42′32.7″W) in Texas, and Elmer's Island Wildlife Refuge (29º10′49.4″N 90º03′58.1″W), Grand Isle (29º13′11.2″N 90º00′59.5″W), and Port Fourchon (29º05′51.1″N 90º12′16.9″W) in Louisiana (Figure 4.1). All sites have previously been identified as important refuelling habitats for Sanderling and Red knots, and these sites are known to host large congregations of both species during wintering and particularly during spring staging (Withers, 2002). Among our six study sites, those in Louisiana were closest to the Deepwater Horizon blowout and were directly and heavily impacted by the Deepwater Horizon oil spill (Beyer et al., 2016), and sites in Bolivar Flats also exhibited high sediment PAH concentrations immediately following the Deepwater spill (Sammarco et al., 2013).

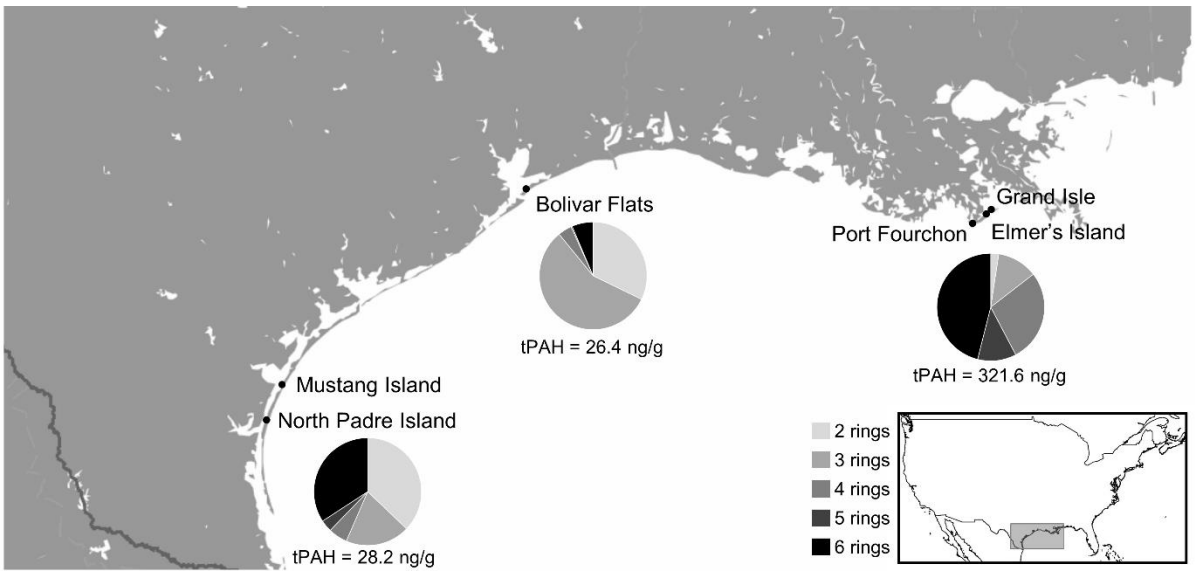


**Figure 4.1.** Sediment and bird sampling locations in the western Gulf of Mexico. Pie charts show the PAH composition of each staging area (shown as number of rings), with darker shades of grey indicating increasing structural complexity. The total sediment PAH (tPAH) concentration (in ng/g wet mass) of each staging area is indicated below the pie chart. Figure inset indicates the study area in the southeastern United States shown on the map.

### 4.3.2 PAH determination in sediment samples

Sediment samples were collected from North Padre Island in 2013 – 2015 and from Mustang Island, Bolivar Flats, Elmer's Island, and Grand Isle in 2016. No sediment samples were collected from Port Fourchon. All sampling was performed at locations where Sanderling were trapped or were observed foraging in large numbers. At each sampling location, surface cores (10 cm depth) were taken above, at, and below the waterline along three transects, approximately 100 m apart (total of 9 surface cores per sampling location). Within each study site, sediments from all sites were pooled and thoroughly mixed. Samples were frozen and kept dark during transportation to the University of Saskatchewan, where they were stored at -20ºC until analysis.

Sediment samples were processed using methods modified from Ohiozebau et al. (2017). Briefly, 20 g of wet sediment was mixed with anhydrous sodium sulfate to remove water. Samples were then extracted for 18 h with 250 ml of a 2:1 dichloromethane (DCM):hexane solution in a Soxhlet apparatus. Extracts were cleaned using a silica gel column. Glass columns were dry-packed with 6 g of activated silica gel and topped with 2 g of anhydrous sodium sulfate. Columns were conditioned with 30 ml of a 2:1 DCM:hexane solution, and extracts were loaded into the column just before the sodium sulfate layer was exposed to air. Cleaned extracts were concentrated to ~ 1 ml by rotary evaporation, followed by concentration to ~100 µl under a gentle stream of nitrogen.

Concentrations of 16 parent PAHs (naphthalene, acenaphthylene, acenaphthene, fluorene, phenanthrene, anthracene, fluoranthene, pyrene, benz[*a*]anthracene, chrysene, benzo[*b*]fluoranthene, benzo[*k*]fluoranthene, benzo[*a*]pyrene, indeno[1,2,3-*cd*]pyrene, dibenz[*ah*]anthracene, and benzo[*ghi*]perylene) were analyzed by GC/MS using a Q Exactive™ Hybrid Quadrupole-Orbitrap™ Mass Spectrometer full scan mode. PAHs were identified and quantified using a method described previously (Ohiozebau et al., 2017). PAHs were measured using a Hewlett Packard (HP) 7683 series autosampler fitted with a 60 m, 0.25 mm i.d. DB-5 silica capillary column. The injection temperature was 250ºC, and the detector temperature was 280ºC. The temperature ramp was: 60ºC for 2 min, 20ºC/min to 160ºC, followed by 5ºC/min to 268ºC and 2ºC/min to 300ºC, where it was held for 10 min for a total run time of 55.5 min. The HP 7683 series autosampler was operated in Selected Ion Mode (SIM). A 1 µl sample of

extractor or standard was injected in split/splitless mode. Mass spectra were acquired in electron impact (EI) mode at 70 eV.

All analytical data were subject to strict quality control. Method blanks and spiked blanks were used to determine background contamination, which showed no detectable PAHs. Instruments were calibrated prior to analysis with calibration standards. All glassware was hand-washed, rinsed with deionized water (Milli-Q system), and solvent-rinsed three times with HPLC grade hexane and DCM before use (Fisher Scientific, Canada). PAHs were quantified using an internal calibration method based on a five-point calibration curve of pure standards (100 ng/ml of acenaphthyene-$d_8$, p-terphenyl-$d_{14}$, benzo[e]pyrene-$d_{12}$). Surrogate recoveries averaged 75%, and final values were recovery corrected. The method detection limits ranged from 0.3 to 5.0 ng/g wet mass.

### 4.3.3 Animal capture and handling

Between 2015 and 2017, we captured 165 Sanderling from all study sites (North Padre Island: n = 89, Mustang Island: n = 2, Bolivar Flats: n = 31, Elmer's Island: n = 10, Port Fourchon: n = 15, Grand Isle: n = 18). In 2015 and 2016, we captured 55 Red knots (North Padre Island: n = 29, Mustang Island: n = 2, Grand Isle: n = 24). Permitting restrictions did not allow us to trap Red knots in Bolivar Flats; therefore, no Red knots were trapped from this site. We trapped both species from late April to mid May. Birds were trapped throughout the day using cannon nets and noose carpets. Upon capture, we took mass and body measurements and attached a unique numbered metal band and a coded alpha numeric flag. In 2015 and 2016, all birds were blood sampled, and a random subset (samples from 80 Sanderling and 35 Red knots) were analyzed for plasma metabolite concentrations. Blood was collected by puncturing the brachial vein with a sterile 27-gauge needle and collecting blood (< 100 µl) in heparinized microhematocrit tubes. Blood was transferred to heparinized 1 ml centrifuge tubes and stored on ice in the field. Samples were centrifuged within 12 h of collection before freezing. Plasma samples were stored on dry ice for transportation to the University of Saskatchewan, where they were subsequently stored at -80ºC until analysis.

We attached Lotek coded nanotags (NTQB-3-2 (Sanderling) and NTQB-4-2 (Red knots), Newmarket, ON, Canada) to a subset of 120 Sanderling (North Padre Island: n = 59, Bolivar Flats n = 31, Elmer's Island: n = 8, Port Fourchon: n = 9, Grand Isle: n = 13) and 39 Red knots (North Padre Island: n = 19, Mustang Island: n = 2, Grand Isle: n = 18). Tags were attached from

April 17 – May 6, which was a minimum and maximum of 0 to 52 and 1 to 33 days prior to departure for Sanderling and Red knots, respectively (departure date ranges from radio-telemetry data were: Sanderling May 2 – June 8, Red knot May 7 – 20). Because both species can undergo extreme variations in body mass during migration (Robinson et al., 2003), tags were glued to the birds' skin using a quick-setting marine epoxy (J-B Weld ClearWeld 5 Min Epoxy). Transmitters on Sanderling (NTQB-3-2) weighed 0.67 g, and transmitters on Red knots (NTQB-4-2) weighed 1.0 g, which represented <1.5% and approximately 0.7% of the estimated lean body mass of Sanderling (Scott et al., 2004) and Red knots (Duijns et al., 2017), respectively. All tags were programmed at a single frequency (166.380 MHz) with pulse lengths of 2.5 ms and pulse intervals of approximately 6 s (2015 and 2016) and 8 s (2017) with estimated lifespans 82 (Sanderling) and 180 days (Red knot). Only after second year (ASY) adult birds received transmitters, because second year (SY) juvenile birds can show alternative migration schedules (McKinnon et al., 2014).

All animal handling and research protocols were approved by the University of Saskatchewan Animal Care Committee (AUP 20120021) and conducted under Canadian Wildlife Service Scientific Banding Permit 12SKS009. Trapping in Texas was performed under the Texas Parks & Wildlife Department Permit SPR-0911-341. Work in Bolivar Flats was approved by the Houston Audubon Society, and trapping on the Padre Island National Seashore was approved by the National Park Service under permits 2015-SCI-0006, 2015-SCI-0007, and 2016-SCI-0005. Birds in Louisiana were trapped under the Louisiana Department of Wildlife and Fisheries Scientific Collecting Permit LNHP-16-059 and LNHP-17-011.

### 4.3.4 Plasma metabolite determination

Metabolite concentrations were determined using commercially available kits modified for small plasma volumes (3 – 20 µl). Samples from 2012 to 2014 were analyzed using kits from Sigma-Aldrich (Triglyceride Determination Kit TR0100; Beta-Hydroxybutyrate Assay Kit MAK041; Uric Acid Assay Kit MAK077), and samples from 2015 and 2016 were processed using kits from Cayman Chemical (Triglyceride Colorimetric Assay 10010303, β-Hydroxybutyrate (Ketone Body) Colorimetric Assay Kit 700190, Uric Acid Assay Kit 700320). Replicate tests on a subset of samples revealed that the Sigma-Aldrich and Cayman Chemical kits produced equivalent results. For all metabolite assays, plasma was diluted threefold in a 0.9% NaCl solution. Tests were performed using standard clear 96 well plates, and absorbance

was measured at 540, 450, and 570 nm for TG, BOHB, and uric acid determination, respectively, on a microplate spectrophotometer (Biotek ELX800).

### 4.3.5 Telemetry data collection and processing

We determined departure dates from our study sites using the Motus Wildlife Tracking System (http://motus.org/), an international array of automated radio-telemetry receiving stations maintained by a collaborative network of researchers (Taylor et al., 2017). Between 2015 and 2017, 18 receiver stations were operational in our study area. Stations have a detection radius of about 15 km (Taylor et al., 2017). Signals of radio-tagged individuals were considered true detections if at least three consecutive tag bursts were detected on a single antenna at a single receiver (Crewe et al., 2018). We caution that here we assumed that the last detections at a staging site corresponded to an individual's actual departure dates. All final detections fall within the range of expected departure dates of both species (Baker et al., 2013; Macwhirter et al., 2002; Withers, 2002). However, birds could have either died or moved outside of range of the Motus array prior departure from a site, and actual departures from the Gulf of Mexico may have been later than reported here. Further expansion of the Motus network in the Gulf of Mexico will help to more accurately assess local and migratory movements.

### 4.3.6 Data analysis

Following post-processing to remove false detections, radio-telemetry data revealed that individuals trapped in North Padre and Mustang Island moved between the nearby North Padre and Mustang Island study sites, and that individuals trapped at sites in Louisiana moved between the three Louisiana study sites. Therefore, sites were grouped into three areas for analysis, termed 'staging areas', to more accurately reflect the PAH exposure of an individual during a single staging event: (1) North Padre (composed of North Padre and Mustang Islands), (2) Bolivar Flats, and (3) Louisiana (composed of Elmer's Island, Grand Isle, and Port Fourchon). We saw no inter-site movement of individuals between the North Padre, Bolivar Flats, and Louisiana staging areas.

For each species, we evaluated differences in mass and plasma metabolite levels among staging areas using linear mixed effects models. Here, mass, rather than a size-corrected body mass index (i.e., residuals from regression of mass and body size), was used as we found a slightly higher correlation between mass and fat scores for Sanderling ($R^2 = 0.72$ for mass and

0.65 for body condition index) and for Red knots ($R^2$ = 0.61 for mass and 0.60 for body condition index). Global models included staging area, year, and age as fixed effects. All models included random effects of capture date to control for seasonal variations in mass and metabolite levels, time of capture to account for any diurnal fluctuations, and handling time, as these variables are known to be influenced by the time between capture and sampling (Dietz et al., 2009). Sanderling mass and the plasma metabolite concentrations of both species were log transformed to ensure that model residuals met the assumptions of normality and heteroscedasticity.

Multivariate principal component (PCA, run using the prcomp function in the R stats package; R Core Team, 2017) were used to further evaluate the plasma metabolite concentrations of Sanderling and Red knots in each staging area. Initially, a PCA that included TG, BOHB, and UA was run to identify any clustering of metabolites profiles (i.e., the combination of the three metabolite concentrations in each sample) by staging area. Differences in plasma metabolite profiles among staging areas were tested using a PERMANOVA (run using the adonis function in the vegan package; Oksanen et al., 2018). Previous work has shown that together plasma TG and BOHB concentrations provide an accurate representation of an individual's fuelling status (i.e., whether an individual is gaining or losing mass; Jenni-Eiermann and Jenni, 1994). Therefore, following the methods of Schaub and Jenni (2001), we also calculated a 'fattening index' as individual PCA axis scores of the first principle component (PC1) that included TG and BOHB only. More positive scores indicate that birds had higher TG levels (greater fuelling) and more negative scores indicate that birds had higher BOHB levels (lipolysis and reduced fuelling). Differences among study areas in this second PCA were also compared using a PERMANOVA. Fattening index was also compared among staging areas using linear mixed effects models. The global model included staging area, year, and age as fixed effects, plus the random effects of capture date, time of capture, and handling time.

Departure dates and stopover durations were highly correlated in both species (Sanderling $R^2$ = 0.99; Red knot $R^2$ = 0.80), and preliminary analyses revealed that models with either response gave equivalent results. Therefore, we chose to only analyze departure dates as a metric of migration timing. First, we compared Sanderling and Red knot departure dates using a linear model that included species, staging area, and year as fixed effects. We then used linear mixed effects models to evaluate the influence of staging area, mass, fattening index, and year on

Sanderling and Red knot departure dates, with capture date as a random effect. Mass at capture and fattening index were not highly correlated in either species (Sanderling $R^2 = 0.25$, Red knot $R^2 = 0.19$), and therefore both variables were included in the global models. Sanderling and Red knots were analyzed separately due to potential differences in the physiology of each species that may mask the other variables. Model selection was performed using AICc scores (Akaike's information criterion corrected for small sample size), model weights, and deviance scores (Burnham and Anderson, 2002) in the bbmle package (Bolker and R Development Core Team, 2017). When models were equivalent ($\Delta$AICc < 2), the weighted model-averaged estimates of the top model sets were calculated using model.avg in the MuMIn package (Barton, 2017). All modelling was performed in R version 3.4.2(R Core Team, 2017) using the lme4 package (Bates et al., 2015), and plots were generated using ggplot2 (Wickham, 2009), cowplot (Wilke, 2017), ggmap (Kahle and Wickam, 2013), and RgoogleMaps (Loecher and Ropkins, 2015).

## 4.4 Results

### 4.4.1 Sediment PAH concentrations

Pooled sediment total PAH (tPAH) levels were highest in the Louisiana staging area, where samples were dominated by PAHs composed of 6 rings (Figure 4.1). This was due to the high tPAH concentrations in sediment samples from Elmer's Island (640 ng tPAH/g wet mass), which were dominated by indeno[1,2,3-*cd*]pyrene. Conversely, naphthalene (2 rings) was the predominant congener in samples from Grand Isle, and tPAH concentrations were much lower at this site (3.41 ng/g; Table 4.1). The Bolivar Flats and North Padre staging areas in Texas had similar tPAH concentrations (Figure 4.1, Table 4.1). North Padre samples were dominated by PAHs composed of 2 and 6 rings (Figure 4.1). Indeed, indeno[1,2,3-*cd*]pyrene was the predominant congener in North Padre sediments in all years, and North Padre samples from 2013 and 2015 and the 2016 Mustang Island sample also had relatively high levels of naphthalene. The tPAH concentrations in North Padre also varied among years and were highest in 2013 (64.9 ng/g) and lowest in 2014 (3.15 ng/g) and 2015 (9.71 ng/g; Table 4.1). Although naphthalene was the individual congener with the highest concentration in Bolivar Flats (8.49 ng/g, 32% of tPAH; Table 4.1), collectively, 3-ringed PAHs contributed to most of the tPAH concentrations at this staging area (58% of tPAH, Table 4.1; Figure 4.1).

**Table 4.1.** PAH concentrations (ng/g wet mass)[a] in sediment samples from four Gulf of Mexico staging sites[b] and the total PAH (tPAH) concentrations in three staging area categories.

| | | Staging area | | | | | | |
|---|---|---|---|---|---|---|---|---|
| | | Bolivar Flats | North Padre | | | | Louisiana | |
| PAH congener | Ring # | BF 2016 | NPI 2013 | NPI 2014 | NPI 2015 | MI 2016 | EI 2016 | GI 2016 |
| Naph | 2 | 8.49 (32%) | 17.65 (27%) | 0.59 (19%) | 1.22 (13%) | 22.41 (64%) | 14.53 (2.3%) | 1.02 (30%) |
| Acenthy | 3 | 0.98 (3.7%) | 1.46 (2.3%) | 0.08 (2.5%) | 0.1 (1.0%) | 1.98 (5.7%) | 1.39 (0.2%) | 0.17 (5.0%) |
| Aceph | 3 | 0.62 (2.4%) | 0.46 (0.7%) | 0.08 (2.5%) | 0.08 (0.8%) | 0.57 (1.6%) | 1.02 (0.2%) | 0.07 (2.1%) |
| Fluorene | 3 | 2.00 (7.6%) | 0.93 (1.4%) | n.d. | n.d. | 1.28 (3.7%) | 5.79 (0.9%) | n.d. |
| Phen | 3 | 6.26 (24%) | 3.24 (5.0%) | 0.51 (16%) | 0.44 (4.5%) | 3.73 (11%) | 36.42 (5.7%) | 0.8 (23%) |
| Anth | 3 | 5.14 (20%) | 2.79 (4.3%) | 0.44 (14%) | 0.38 (3.9%) | 3.29 (9.4%) | 31.6 (4.9%) | 0.69 (20%) |
| Fluor | 4 | 0.62 (2.4%) | 1.94 (3.0%) | 0.05 (1.6%) | 0.07 (0.7%) | 0.55 (1.6%) | 64.09 (10%) | 0.09 (2.6%) |
| Pyrene | 4 | 0.34 (1.3%) | 1.5 (2.3%) | 0.02 (0.6%) | 0.06 (0.6%) | 0.33 (0.9%) | 53.82 (8.4%) | 0.07 (2.1%) |
| BaA | 4 | 0.04 (0.2%) | 0.63 (1.0%) | 0.02 (0.6%) | 0.06 (0.6%) | 0.07 (0.2%) | 29.59 (4.6%) | 0.01 (0.3%) |
| Chry | 4 | 0.10 (0.4%) | 0.99 (1.5%) | 0.04 (1.3%) | 0.1 (1.0%) | 0.07 (0.2%) | 30.88 (4.8%) | 0.04 (1.2%) |
| BbF | 5 | 0.02 (0.08%) | 0.85 (1.3%) | 0.01 (0.3%) | 0.17 (1.8%) | n.d. | 26.26 (4.1%) | 0.02 (0.6%) |
| BkF | 5 | 0.02 (0.08%) | 0.47 (0.7%) | 0.01 (0.3%) | 0.09 (0.9%) | n.d. | 14.79 (2.3%) | 0.01 (0.3%) |
| BaP | 5 | 0.05 (0.2%) | 0.84 (1.3%) | 0.07 (2.2%) | 0.88 (9.1%) | n.d. | 26.45 (4.1%) | n.d. |
| DahA | 5 | 0.01 (0.4%) | 0.05 (0.08%) | 0.01 (0.3%) | 0.02 (0.2%) | 0.55 (1.6%) | 7.31 (1.1%) | 0.01 (0.3%) |
| IcdP | 6 | 1.65 (6.3%) | 31.03 (48%) | 1.21 (38%) | 5.87 (60%) | 0.21 (0.6%) | 295.56 (46%) | 0.39 (11%) |
| BghiP | 6 | 0.03 (0.1%) | 0.07 (0.11%) | 0.01 (0.3%) | 0.17 (1.8%) | n.d. | 0.31 (0.1%) | 0.03 (0.9%) |
| Site tPAH | | 26.4 | 64.9 | 3.15 | 9.71 | 35.0 | 640 | 3.41 |
| Area tPAH | | 26.4 | 28.2 ± 14.0 | | | | 322 ± 318 | |

[a] Numbers in parentheses indicate % of study site total PAH (tPAH); n.d. = not detected.

[b] Staging site abbreviations: BF = Bolivar Flats, NPI = North Padre Island, MI = Mustang Island, EI = Elmer's Island, GI = Grand Isle.

[c] PAH abbreviations: Naph = naphthalene, Acenthy = acenaphthylene, Aceph = acenaphthene, Phen = phenanthrene, Anth = anthracene, Fluor = fluoranthene, BaA = benz[*a*]anthracene, Chry = chrysene, BbF = benzo[*b*]fluoranthene, BkF = benzo[*k*]fluoranthene, BaP = benzo[*a*]pyrene, DahA = dibenz[*ah*]anthracene, IcdP = indeno[1,2,3-*cd*]pyrene, BghiP = benzo[*ghi*]perylene.

### 4.4.2 Shorebird fuelling and departures

The mean and ranges of mass, plasma metabolite concentrations, and departure dates of each species are given in Table 4.2.

#### 4.4.2.1 Fuel loads

There was not strong support for differences in Sanderling nor Red knot masses among staging areas. The best-approximating model for Sanderling only included year as a fixed effect, and individuals trapped in 2017 were heavier ($\beta$ = 0.13 ± 0.04, $p$ = 0.01) than in 2016 and 2015 (see Table A.7 for model selection results). The best-approximating model for Red knots included age, staging area, and year as fixed effects. Juvenile (SY) Red knots tended to weigh less than older (ASY) birds ($\beta$ = -10.7 ± 13.7, $p$ = 0.45). Red knots in North Padre tended to weigh more than in Louisiana (4.63 ± 8.34, $p$ = 0.82) and tended to be heavier in 2016 than in 2015 ($\beta$ = 11.5 ± 8.7, $p$ = 0.59). However, these differences were not significant ($p > 0.05$).

#### 4.4.2.2 Fuelling rates

Based on the single metabolites, we did not find a difference in fuelling rates among staging areas. Top model sets for BOHB (Sanderling only) and UA (both species) included year as a fixed effect. Relative to other years, in 2016 plasma BOHB concentrations were higher in Sanderling ($\beta$ = 0.36 ± 0.12, $p$ = 0.003) and plasma UA concentrations were lower in Sanderling ($\beta$ = -0.14 ± 0.07, $p$ = 0.04) and higher in Red knots ($\beta$ = 0.31 ± 0.12, $p$ = 0.01). Variation in TG (both species) and BOHB (Red knots only) were not explained by differences in staging area, year, or age (i.e., the null model was the top model for these responses; see Table A.8 for model selection results).

Multivariate PCAs including TG, BOHB, and UA revealed the plasma metabolite profiles of Sanderling and Red knots in each staging area (Figure 4.2). In the PCA for Sanderling, principal component (PC) axis 1, PC2, and PC3 explained 46.0, 29.4, and 24.6% of the variance among plasma metabolites, respectively. Sanderling in Louisiana tended to have slightly higher plasma BOHB concentrations, although plasma metabolite profiles did not formally differ among staging areas ($F_{2,77}$ = 1.97, $p$ = 0.07). In the PCA for Red knots, PC1, PC2, and PC3 explained 59.6, 29.3, and 11.1% of the variance among plasma metabolites, respectively. Red knot plasma metabolite profiles from Louisiana compared to North Padre were

**Table 4.2.** Summary of means and ranges of mass, plasma metabolite concentrations, and departure dates of Sanderling and Red knots in the Gulf of Mexico. Mass and departure data were collected from 2015 to 2017 and plasma metabolite data were collected in 2015 and 2016.

| | Sanderling | | Red knot | |
|---|---|---|---|---|
| | mean | range | mean | range |
| mass (g) | 56.5 | 40.0 – 86.2 (n = 165) | 137 | 108 – 174 (n = 55) |
| TG (µg/µl) | 1.07 | 0.00 – 2.91 (n = 80) | 1.65 | 0.249 – 3.59 (n = 35) |
| BOHB (nmol/µl) | 1.48 | 0.521 – 4.59 (n = 80) | 1.16 | 0.390 – 2.47 (n = 35) |
| UA (nmol/µl) | 1.35 | 0.140 – 4.49 (n = 80) | 1.34 | 0.0574 – 2.68 (n = 35) |
| Departure (Julian day) | 136.0 | 123 – 159 (n = 48) | 131.0 | 117 – 144 (n = 15) |

Abbreviations: TG = triglyceride, BOHB = β-hydroxybutyrate, UA = uric acid

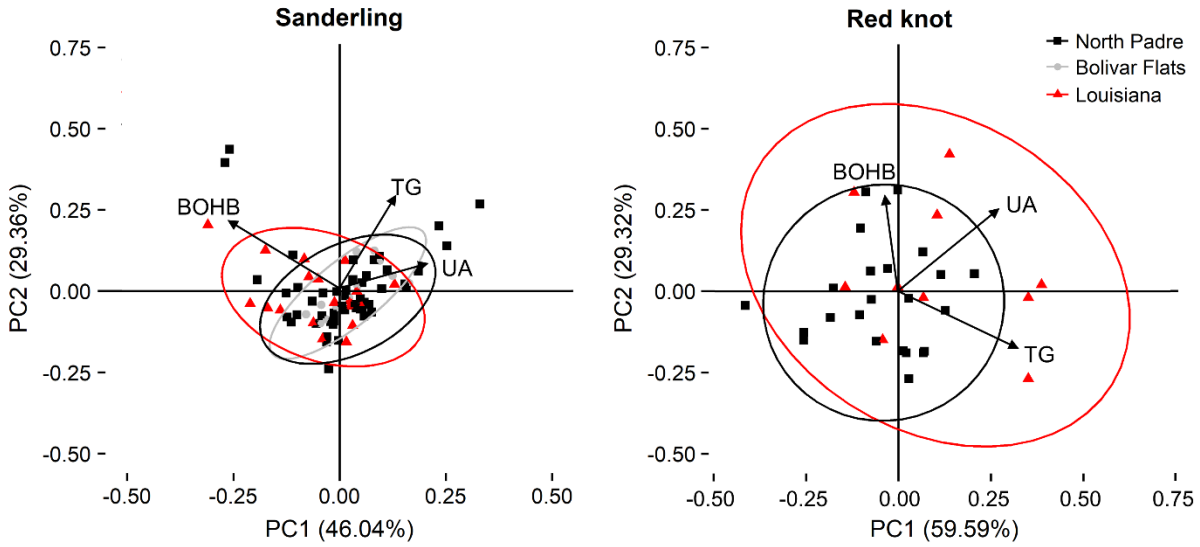


**Figure 4.2.** Plasma metabolite profiles of Sanderling and Red knots from staging areas in the Gulf of Mexico in 2015 and 2016 (North Padre = black squares, Bolivar Flats = gray circles, Louisiana = red triangles). Plasma metabolites are projected onto the first two principal component axes (PC1 and PC2) of a principal component analysis, where PC1 and PC2 explain 46.0 and 29.4% (Sanderling) and 59.6 and 29.3% (Red knots) of the variance among variables, respectively. Ellipses are the 95% confidence ellipses for the mean of each staging area. BOHB: β-hydroxybutyrate, TG: triglyceride, UA: uric acid. Sample sizes for Sanderling: n = 49 (North Padre), 12 (Bolivar Flats), 19 (Louisiana); Red knot: n = 24 (North Padre), 11 (Louisiana).

statistically different ($F_{1,31} = 4.15$, $p = 0.01$), and Red knots in Louisiana had more variable metabolite profiles relative to North Padre.

Sanderling 'fattening index' (PC1 axis score of PCA with TG and BOHB) explained 57.3% of the variance in metabolites. Model-averaged mean Sanderling fattening index was 0.15 and was significantly higher in Bolivar Flats relative to Louisiana ($\beta = 0.74 \pm 0.26$, $p = 0.005$). Although Sanderling fattening index tended to be higher in North Padre relative to Louisiana ($\beta = 0.18 \pm 0.23$), this difference was not statistically significant ($p = 0.45$; Figure 4.3; see Table A.8 for model selection results). Sanderling fattening index also varied by year, where individuals trapped in 2016 had lower fattening indices than individuals trapped in 2015 ($\beta = -0.66 \pm 0.22$, $p = 0.004$). For Red knots, fattening index explained 67.8% of the variance in metabolites. Model-averaged mean Red knot fattening index was 0.05 and was lower in North Padre than Louisiana ($\beta = -0.60 \pm 0.27$, $p = 0.04$; Figure 4.3). Red knots tended to have higher fattening indices in 2016 relative to 2015, but these differences were again not statistically significant ($\beta = 0.47 \pm 0.37$, $p = 0.23$).

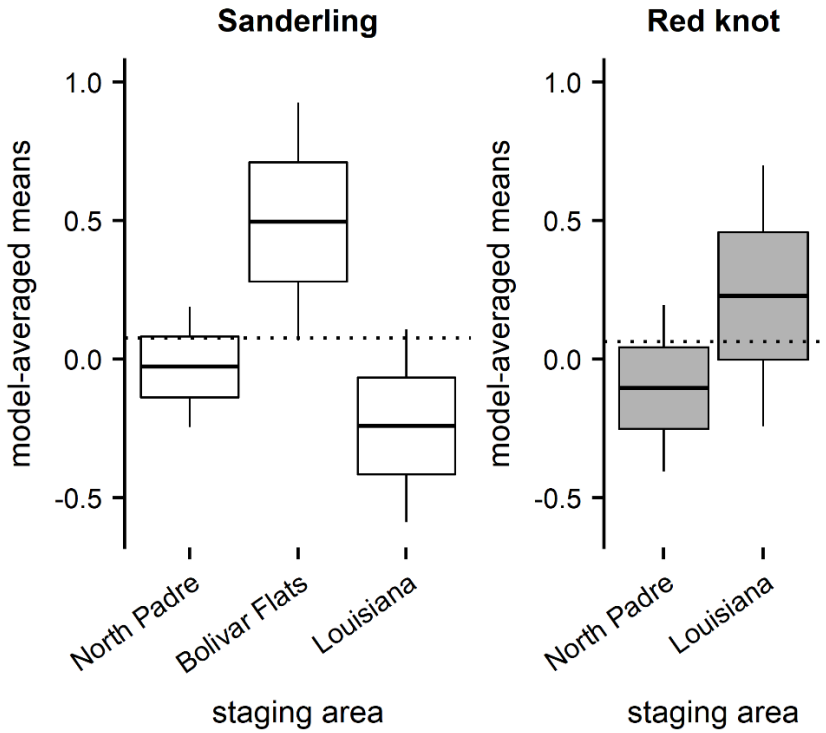


**Figure 4.3.** Fattening indices of Sanderling and Red knots from staging areas in the Gulf of Mexico in 2015 and 2016. Fattening index was calculated from the PC1 axis score of a PCA that included TG and BOHB. More positive values indicate greater fat deposition and more negative values indicate lower fat deposition. Boxes show model-averaged fattening index means ± standard error, with vertical lines indicating the 95% confidence interval. Box colours indicate species (white: Sanderling, gray: Red knot). Dotted horizonal lines show the mean model-averaged fattening index of each species. Sample sizes: Sanderling n = 49 (North Padre), 12 (Bolivar Flats), 19 (Louisiana); Red knot n = 24 (North Padre), 11 (Louisiana).

### 4.4.2 Departure dates

Initial models compared departure dates of Sanderling and Red knots among staging areas using last Motus detections. The best approximating model included species, staging area, and year as fixed effects (see Table A.9 for model selection results). Although Red knots tended to depart earlier, differences in departure dates between species were not statistically significant ($\beta$ = 3.68 ± 0.02, $p$ = 0.12). For each species, we examined departure dates among staging areas alongside physiological metrics of fuelling status (i.e., mass and fattening index; model selection results are in Table A.10). For Sanderling, the best approximating model for departure timing included fattening index, staging area, and year as fixed effects, whereas mass was not retained in the model. We found that on average, Sanderling departed on Julian day 136 (i.e., May 15/16), with birds in North Padre departing earliest ($\beta$ = -14.8 ± 2.7, $p$ < 0.0001; Figure 4.4). Sanderling also departed approximately 11 days earlier in 2016 ($\beta$ = -10.6 ± 2.7, $p$ = 0.0002) relative to 2015. There was no relationship between fattening index and departure dates ($\beta$ = -0.06 ± 1.65, $p$ = 0.97). For Red knots, the best approximating model for departure timing included staging area and year as fixed effects, and neither mass nor fattening index were retained in the model. On average, Red knots departed on Julian day 131 (i.e., May 10/11). Red knots tended to depart earlier in 2016 relative to 2015 ($\beta$ = -8.3 ± 4.8, $p$ = 0.14), and Red knots in North Padre tended to depart slightly earlier than individuals in Louisiana ($\beta$ = -8.5 ± 5.7, $p$ = 0.19; Figure 4.4), but these differences were not significant.

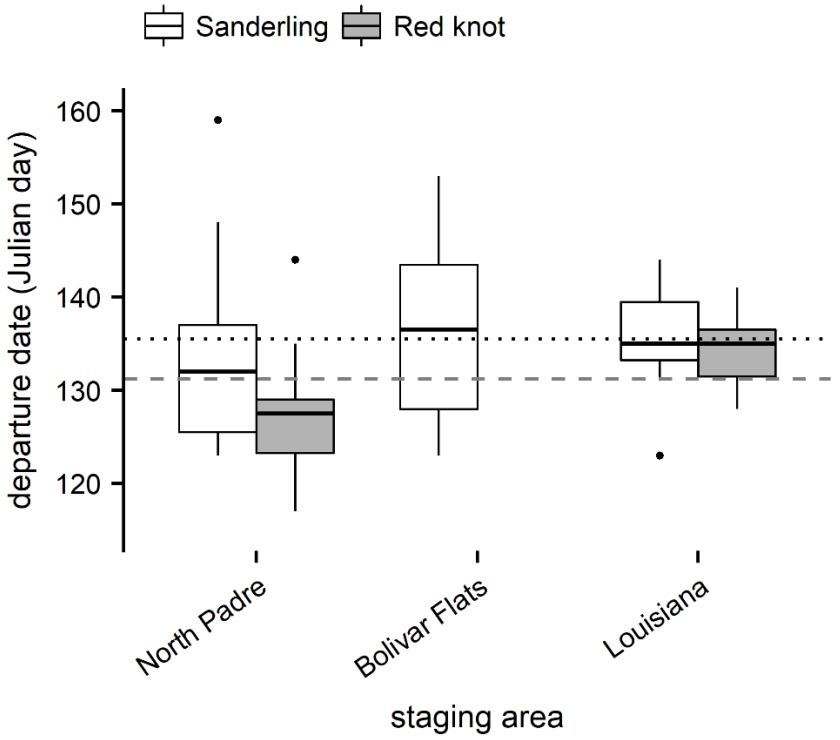


**Figure 4.4.** Sanderling and Red knot departure dates from staging areas in the Gulf of Mexico from 2015 – 2017. Boxes show median departure dates ± the first and third quartiles, with vertical lines indicating the 95% confidence interval; dots indicate values lying outside of the 95% confidence interval. Box colours indicate species (white: Sanderling, gray: Red knot). The black dotted horizontal line shows the mean departure date for Sanderling, and the gray dashed horizontal line shows the mean departure date for Red knots. Sample sizes: Sanderling n = 18 (North Padre), 17 (Bolivar Flats), 13 (Louisiana); Red knot n = 9 (North Padre), 6 (Louisiana).

## 4.5 Discussion

We hypothesized that staging site quality is lowered by PAH contamination, with consequences for shorebird refuelling and departure timing. As expected, sites in Louisiana had the highest sediment PAH concentrations, and PAHs were present at levels high enough to cause sublethal effects. Fuelling data suggested that Sanderling, but not Red knots, were fuelling less rapidly in Louisiana than birds at sites with lower PAH contamination, and both species departed later from Louisiana than from North Padre. There is thus correlative evidence to support our hypothesis that elevated PAH exposures may be associated with slower pre-migratory fuelling in Sanderling and with later departure dates in both species. However, Sanderling in Bolivar Flats departed at the same time as birds from Louisiana, suggesting that other unmeasured factors affected fuelling rates and departure dates at this site. PAH contamination remains an issue in the Gulf of Mexico and may play a role in reducing staging site quality for migratory birds. There is a strong association between staging site quality, overall migration pace, and population dynamics in avian migrants (Baker et al., 2004; Deppe et al., 2015; Gómez et al., 2017). However, many key staging sites remain poorly characterized in terms of chemical contamination. This study highlights the need to consider organic pollutants alongside other variables when assessing the quality of staging sites for refuelling in long-distance migratory birds.

### 4.5.1 Composition and concentration of PAHs in sediment samples

Our results confirm the hypothesis that pooled sediment tPAH concentrations were highest at sites in Louisiana, which were more heavily impacted by the Deepwater Horizon oil spill (Beyer et al., 2016). The average tPAH concentration in Louisiana (322 ng/g) fell within the range of tPAH concentrations measured in oil-soaked beach sands and sediments surrounding the Macondo wellhead following the Deepwater Horizon spill (300 – 2800 ng/g; Aeppli et al., 2012; Liu et al., 2012). However, much higher sediment tPAH concentrations (>500,000,000 ng/g) were also recorded (Sammarco et al., 2013; Urbano et al., 2013).

The oil released by the Deepwater Horizon spill (MC252) is a light crude, dominated by naphthalene (64% of tPAH), followed by phenanthrene and fluorene, with chrysene and other heavier PAHs occurring as relatively minor components (Liu et al., 2012). The lighter MC252 components, like naphthalene, were mostly depleted by the time oil reached the shoreline (range

0 to 9% of tPAH; Aeppli et al., 2012; Liu et al., 2012; Urbano et al., 2013). The more toxic, higher molecular weight PAHs are more recalcitrant to weathering and microbial degradation, and phenanthrene, chrysene, and other heavier PAHs were enriched in samples from oiled beaches (38-56% tPAH) up to 4 years following the spill (Aeppli et al., 2014; Liu et al., 2012; Urbano et al., 2013). Therefore, the predominance of indeno[1,2,3-*cd*]pyrene (6-rings) in Louisiana sediments may reflect ongoing MC252 weathering, whereas the relatively high concentrations of naphthalene (2-rings) in North Padre and Bolivar Flats may suggest more recent oil pollution in these areas, either from smaller scale oil spills or natural oil seeps (Beyer et al., 2016; Burger, 2017). High molecular weight PAHs (4-6 rings, including benz[*a*]anthracene, chrysene, benzo[*a*]pyrene, benzo[*ghi*]perylene, and indeno[1,2,3-*cd*]pyrene) are also abundant in pyrogenic PAHs (e.g. from gasoline and diesel combustion; Harrison et al., 1996). Sediments in the northern Gulf of Mexico that were not oiled by the Deepwater Horizon spill show tPAH concentrations similar to what we measured in Louisiana (~100 – 450 ng/g), with a predominance of high molecular weight PAHs (Wang et al., 2014). Therefore, the relatively high proportion of 4-6 ring PAHs in Louisiana and North Padre suggest that petroleum combustion may also have contributed to the tPAH concentrations in these staging areas.

Overall, our results suggest that birds in Louisiana experienced higher levels of PAH exposure than birds in Bolivar Flats and North Padre. As well, because sediment samples from Louisiana were predominated by higher molecular weight PAHs, which are more lipophilic and resistant to oxidation and reduction (Liu et al., 2012), birds staging in Louisiana may have a higher potential for chronic PAH exposure. Marine invertebrates bioaccumulate PAHs and typically show higher concentrations than the surrounding sediment (Snyder et al., 2014b). Therefore, sediment tPAH concentrations could underestimate shorebird exposures from foraging. Willie et al. (2017) found that tPAH concentrations of < 150 ng/g in the marine invertebrate food source of the sea duck, Barrow's goldeneyes (*Bucephala islandica*), were associated with elevated hepatic 7-ethoxyresorufin-O-deethylase (EROD) activity. As well, Common Loons (*Gavia immer*) with plasma PAH concentrations > 5 ng/g weighed less on average than individuals with undetectable plasma PAH concentrations (Paruk et al., 2016). This suggests that tPAH concentrations in Louisiana sediments were high enough to stimulate mass loss through mechanisms possibly associated with activation of the AhR.

We acknowledge that our sediment sample size is small. Ideally, we would have sediment samples from all staging sites and every year that birds were trapped to more accurately assess temporal and spatial trends in site-level exposure. Further work is needed to fully characterize intertidal subsurface oil contaminant levels at multiple staging areas in the Gulf of Mexico in both sediment and prey samples. Our small sample size may have contributed to the high variation in sediment tPAH concentrations in Louisiana, where sediments from Elmer's Island had tPAH concentrations 188-fold higher than Grand Isle. Previous work found that sediment samples in this region of the Gulf of Mexico tend to show high differences in PAH concentrations due to their proximity to the mouth of the Mississippi River, where a variety of newly deposited sediment types are within close proximity of each other (Wang et al., 2014). The high variation in tPAH concentrations may also result from the uneven distribution of sedimented organic detritus in the sampling area (Snyder et al., 2014a). Moreover, beach raking activities, which can expose subsurface sediments and accelerate photooxidation (Bagby et al., 2017), and beach nourishment activities, which dredge material from offshore sites and deposit it in intertidal and dune zones (Campbell et al., 2004; Louisiana Department of Wildlife and Fisheries, 2016), are common practices at many Gulf sites, including Grand Isle (Meyer-Arendt, 2011). Beach raking and nourishment activities complicate pinpointing the source of PAH contamination and assessing the long-term weathering of PAHs in any one site.

### 4.4.2 Staging area quality for fuelling shorebirds

In Sanderling, the results supported our hypothesis that elevated PAH exposures are associated with slower pre-migratory fuelling and later departures. Staging sites in Louisiana had the highest sediment PAH concentrations. Plasma metabolite profiles indicated that birds in Louisiana tended to have higher plasma BOHB concentrations, and fattening index scores tended to be lower in Louisiana relative to North Padre and Bolivar Flats, indicative of relatively lower fat deposition rates at this site. As well, Sanderling in Louisiana departed later than individuals staging in North Padre (results for Bolivar Flats are discussed below). There is thus correlative evidence showing that higher sediment PAH concentrations in Louisiana were associated with lower refuelling and later departure dates in Sanderling.

The relationship between sediment PAH concentrations and Red knot fuelling and departure data is less consistent, likely due to our small sample size. Red knots in North Padre exhibited a lower fattening index than Red knots in Louisiana, suggesting that Red knots in

North Padre fuelled more slowly. However, like Sanderling, Red knots in North Padre departed earlier than individuals in Louisiana. Louisiana plasma metabolite profiles showed high variability, likely due to the small number of Red knots sampled at this site, and thus should be interpreted with caution. There is preliminary evidence in a small number of individuals that higher PAH exposures in Louisiana were correlated with later Red knot departures, but more research is needed to confirm that the results for Sanderling are generalizable to other shorebird species.

It is important to note that there were also unexpected relationships between Sanderling site-level fuelling and departure data. Sanderling in North Padre tended to have below average model-predicted fattening indices at capture but departed earliest, and Sanderling in Bolivar Flats exhibited more positive fattening index scores at capture but departed relatively late. In both species, neither fuel loads at capture nor fattening index explained the variation in departure dates. This is unexpected, given the strong association between fuelling rates and departure dates in spring migrating shorebirds species (Baker et al., 2004), but may explain the inconsistencies between fuelling and departure data observed here. The timing of shorebird sampling likely influenced our mass and plasma metabolite results. Investigations into mass at capture over time revealed that Sanderling in the Gulf of Mexico did not initiate rapid fuelling until Julian Day 120 (April 29 – 30; Figure A.2). Unfortunately, we only trapped Sanderling after Julian Day 120 in North Padre and Bolivar Flats in 2017, but plasma metabolites were not measured. Indeed, prior to 2017, the heaviest trapped individual weighed only 64 g, which is well below the highest mass (~100 g) observed previously in fuelling Sanderling (Robinson et al., 2003). Although Red knots exhibited more linear mass increases over time (Figure A.3), the heaviest individual in this study weighed 175 g, which is also below the typical departure mass (~200 g) of this species (Baker et al., 2004; Robinson et al., 2003). It is expected that the relationship between fuel loads at capture and departure dates would be stronger closer to departure.

The timing of sampling may also explain why fuel loads at capture did not differ among staging areas with different levels of PAH contamination. Previous work in our lab orally dosed Sanderling with increasing PAH concentrations for the duration of their pre-migratory fuelling period. We found that PAH exposure over 21 days lowered fuelling rates and overall mass gains near the end of the dosing experiment (Bianchini and Morrissey, 2018), which suggests that PAH-induced reductions in fuel loads and fuelling rates may be more measurable near peak

mass, which is closer to departure. Therefore, the timing of sampling is likely important in determining PAHs effects on fuel loads and fuelling rates.

Although Sanderling in Bolivar Flats exhibited more positive fattening index scores at capture, indicative of relatively high fat deposition rates, these birds also showed highly variable departure dates (range: 30 days) and on average departed at the same time as Sanderling in Louisiana. These results suggest that other, unknown factors prolonged Sanderling staging durations in Bolivar Flats. Both the Louisiana and Bolivar Flats staging areas are relatively highly polluted (Rabalais et al., 2002; Saleh and Wilson, 1999; Santschi et al., 2001), and it is important to consider that for both species other co-contaminants not measured here may have influenced departures from these sites. The Louisiana staging area is located near the mouth of the Mississippi River. Outflows from the Mississippi River are expected to have high contaminant loads, as much of the land upstream is devoted to agriculture and industry (Rabalais et al., 2002). In addition to oil pollution, inputs of concern in the Mississippi River Basin are nitrogen fertilizers (Rabalais et al., 2002), legacy contaminants, including DDTs and polychlorinated biphenyls (Santschi et al., 2001), and heavy metals, including mercury (Bank et al., 2007). Similarly, Bolivar Flats is located in the Houston Ship Channel, a heavily polluted water body that receives significant municipal and industrial discharges. For instance, this location is known to have high concentrations of dioxins, dibenzofurans, polychlorinated biphenyls, and heavy metals (Saleh and Wilson, 1999; Suarez et al., 2006). It is therefore likely that multiple contaminants interacted in these staging areas; however, the mixture toxicity of these different classes of environmental pollutants is poorly understood, and their combinatorial effects on avian pre-migratory fuelling and departures is unknown.

It is also important to consider the multiple factors that, in addition to staging site PAH concentrations, could influence refuelling rates and departure decisions. Fuel loads and departure dates are influenced by inter-annual differences in arrival dates, foraging conditions, food quality and availability, environmental factors, such as wind direction and precipitation, and an individual's sex and age (Covino et al., 2014; Jarjour et al., 2017). A major limitation of our radio-telemetry data is that the arrival dates of individuals are unknown. Therefore, differences in time spent refuelling are uncertain. We were also unable to re-trap birds to calculate departure fuel loads (Atkinson et al., 2007; Bayly et al., 2012). Therefore, it is unknown whether individuals are staying longer to reach a departure mass threshold or if they are following a

stricter migration schedule and depart at the same time but risk migrating with inadequate fuel stores (Baker et al., 2004). As well, there is the possibility of carry-over effects from earlier staging and wintering sites. Previous work has shown that wintering and staging site habitat quality influence the subsequent migration pace (Gómez et al., 2017). Therefore, the conditions that birds experienced prior to their arrival in the Gulf of Mexico may have influenced their fuelling performance and body condition at our staging sites. More research will be needed to fully characterize the differences in refuelling rates and departure dates observed here and to definitively link staging site PAH contamination to impaired fuelling and delays in departure timing.

# 5 CHAPTER 5: FUEL LOADS, MIGRATION PACE, AND STAGING SITE CONNECTIVITY IN A LONG-DISTANCE MIGRATORY SHOREBIRD

## PREFACE

Chapter 4 found early evidence that shorebirds at staging sites with higher sediment PAH concentrations had lower refuelling rates and later departure dates. The goal of Chapter 5 was to examine whether differences in refuelling and departure timing affect the subsequent pace of Sanderling migration. Migration pace affects how early birds arrive on their breeding grounds in the spring, and earlier arrival is typically associated with greater reproductive success. Therefore, Chapter 5 provides measurements that are relevant to shorebird demographics. Combined with the data of preceding chapters, this work supports a predictive link between PAH exposure and changes in Sanderling population trajectories.

## 5.1 Abstract

Despite the link between migration pace and avian fitness, the factors that influence migration timing are not well understood, and researchers tend to study staging areas in isolation. Therefore, we investigated the relationships between fuelling, departure and arrival dates, and travel speed in northward-migrating Sanderling (*Calidris alba*) at latitudinally disparate staging sites along the Central and Mississippi Flyways. Between 2015 and 2017, we captured, measured, and attached coded nanotags to 121 Sanderling from 6 sites in the Gulf of Mexico (GOM) and 118 Sanderling from Chaplin Lake, Saskatchewan to assess staging behaviour using the Motus telemetry array. Fuel loads were negatively correlated with stopover durations and departure dates at all sites. Most (91%, n = 20) GOM-trapped Sanderling detected in more northern latitudes were in Saskatchewan. Although travel time between the GOM and Saskatchewan was negatively associated with departure dates (i.e., birds that departed later from the GOM travelled faster to reach Saskatchewan), individuals that departed later from the GOM were unable to catch up with earlier individuals and showed later arrival and subsequent departure dates in Saskatchewan. Our study provides evidence that delays in migration carry over from one staging site to the next. This work highlights how proper fuelling at staging areas along the entire migration route is essential for the conservation of migrant species.

## 5.2 Introduction

Every year, long-distance migrants travel vast distances to find better foraging opportunities, avoid predation and inclement weather, and improve fitness (Alerstam et al., 2003). Although the conditions at a migrant's destination (i.e., its breeding and wintering grounds) are significant determinants of fitness and survival (Latta and Baltz, 1997; Rappole and McDonald, 1994), there is mounting evidence to suggest that conditions along migratory routes are important drivers of population dynamics (Baker et al., 2004; Hewson et al., 2016; Newton, 2006). In particular, factors that influence migration timing in the spring have been closely linked to the fitness of migrant birds. This is because early arrival on the breeding grounds is associated with access to higher quality territories and mates, earlier breeding, additional time for renesting, and consequently, greater reproductive performance (Norris et al., 2004; Smith and Moore, 2005).

Given the link between pre-breeding migration timing and avian fitness, spring migrants are expected to minimize the time spent on migration (Alerstam and Lindström, 1990; Farmer and Weins, 1999; Hedenström and Alerstam, 1997; Lyons and Haig, 1995). Individuals behaving according to a time-minimization migration strategy (i.e., time-minimizers) are predicted to make relatively rapid migration flights with fewer stopovers en route (Alerstam, 2001; Hedenström and Alerstam, 1997). Relatively more time is spent at staging sites to refuel than in actual flight during migration (Hedenström and Alerstam, 1997; Schmaljohann et al., 2017). Therefore, time-minimizers are expected to gain the maximum amount of fuel in the least amount of time (Alerstam and Lindström, 1990), and factors affecting fuelling rates, like staging site habitat quality (Bayly et al., 2012), should strongly influence departure fuel loads and the total speed of migration (Hedenström and Alerstam, 1997; Houston, 2000). Indeed, migrants at lower quality wintering and staging sites tend to have lower fat loads, which are associated with later spring departures (Cooper et al., 2015), delayed arrival on the breeding grounds (Cooper et al., 2015; Finch et al., 2014; Norris et al., 2004), and, ultimately, lower reproductive success (Finch et al., 2014; Marra et al., 1998; McKellar et al., 2013; Norris et al., 2004). Therefore, the population dynamics of time-minimizers are sensitive to factors that limit pre-migratory fuelling (Baker et al., 2004; Cooper et al., 2015; Finch et al., 2014), and events during staging have the potential to carry-over and influence subsequent stages of the annual cycle (Finch et al., 2014; Legagneux et al., 2012).

There is thus a strong association between spring migration pace and reproductive success in birds (Norris et al., 2004; Smith and Moore, 2005), and identifying the factors influencing migration timing will have important implications for avian conservation. Indeed, evidence suggests that birds may be particularly vulnerable during migration (Hewson et al., 2016; Newton, 2006; Piersma, 1994), and species of long-distance migrant birds are currently experiencing population declines globally (Berthold et al., 1998; Robbins et al., 1989; Sanderson et al., 2006). However, studying long-distance migratory birds can be challenging. Multiple factors, such as departure fuel loads, sex, age, weather, and predator avoidance, can affect avian migration pace (Farmer and Weins, 1999; Gómez et al., 2017; Hope et al., 2014, 2011; Warnock et al., 2004). Research is further complicated by the potential for carry-over effects along the migration route, where conditions at one site affect an individual's performance at a subsequent site (Harrison et al., 2011). Moreover, studying long-distance migrants has been complicated by the logistical difficulty of tracking individuals across widely dispersed, but biologically linked, breeding, wintering, and staging sites (Marra et al., 1998; Norris et al., 2004; Webster et al., 2002).

Our goal was to examine the factors affecting migration pace in a long-distance migratory shorebird species, Sanderling (*Calidris alba*). New World Sanderling migrate up to 10,000 km annually between their wintering grounds in South and Central America and the Gulf of Mexico (GOM) and their breeding grounds in the Canadian Arctic (Macwhirter et al., 2002). Previous work suggests that arctic breeding shorebirds tend to use a time-minimization migration strategy, where birds accumulate exceptional pre-migratory fuel loads, have high fuelling rates, and rely on relatively few staging sites (Farmer and Weins, 1999; Gudmundsson et al., 1991; Jehl, 1997; Lyons and Haig, 1995). Although previous work points to the importance of the Central and Mississippi Flyways (hereafter referred to as the "mid-continental flyways") for Sanderling migration (Myers et al., 1990; Skagen et al., 1999), the quality of staging sites along these migration routes remains relatively understudied, and the migration behaviour of Sanderling on these flyways is not well understood.

Recent advancements in automated radio-telemetry systems facilitate the continuous tracking of migrants across broad geographical scales (Taylor et al., 2017). Therefore, we used a combination of field measurements and direct tracking to investigate the relationship between staging site fuel loads, departure and arrival dates, and migration timing as Sanderling migrated

between key, latitudinally dispersed staging sites along the mid-continental flyways (sites in the GOM and Saskatchewan, Canada). Given that spring-migrating shorebirds are typically time-minimizers, we hypothesized that fuel loads influence Sanderling migration timing, and we tested the predictions that (1) stopover durations and (2) departure dates are correlated with fuel loads. By monitoring individuals in both the GOM and Saskatchewan, we were also able to look for potential carry-over effects between staging sites. We hypothesized that delays in migration carry-over from one staging site to the next. We tested the predictions that (1) GOM departure dates are positively associated with Saskatchewan arrival dates and (2) Saskatchewan arrival and departure dates are positively related.

## 5.3 Materials and methods

### 5.3.1 Animal capture and handling

Between 2015 and 2017, Sanderling were trapped during northward migration from staging sites in Texas (North Padre Island, 27º20′56.0″N 97º19′49.3″W; Bolivar Flats, 29º24′05.6″N 94º42′32.7″W), Louisiana (Elmer's Island Wildlife Refuge, 29º10′49.4″N 90º03′58.1″W; Grand Isle, 29º13′11.2″N 90º00′59.5″W; Port Fourchon, 29º05′51.1″N 90º12′16.9″W), and Saskatchewan, Canada (Chaplin Lake, 50°26′28.36″, -106°40′9.37″) (Figure 5.1). We classified trapping sites in the GOM into three trapping areas: (1) North Padre Island, Texas (2) Bolivar Flats, Texas and (3) Louisiana (composed of Elmer's Island, Grand Isle, and Port Fourchon).

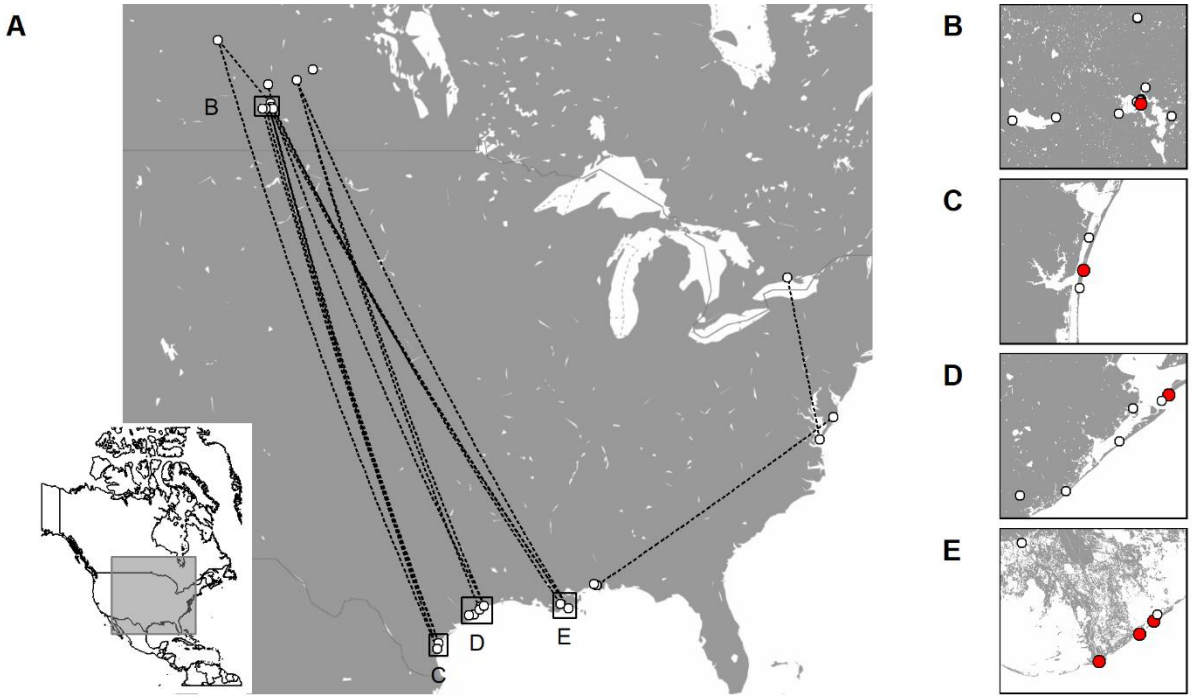


**Figure 5.1.** Sanderling trapping sites, detection locations, and spring migration patterns. (A) 185 radio-tagged Sanderling were detected at receivers throughout North America (white dots). 22 Sanderling were detected at receivers north of where they were trapped. For these birds, lines connect the great arc distances between an individual's last detection in the Gulf of Mexico and its first detection at a more northern site (lines do not necessarily indicate flight paths). The map inset indicates the area in North America shown in panel A. (B - E) Receiver locations where Sanderling were detected (white dots) and Sanderling trapping sites (red dots) in the Chaplin Lake (B), North Padre (C), Bolivar Flats (D), and Louisiana (E) trapping areas.

In the GOM, birds were trapped during the day using cannon nets and noose carpets, and in Chaplin Lake, birds were trapped at night using mist nets and during the day with noose carpets. Upon capture, individuals were weighed, measured and given a unique numbered metal band and a coded alpha numeric flag. In Chaplin Lake, birds were also given a combination of coloured leg bands representing the cohort site and year. We attached Lotek coded nanotags (NTQB-3-2, Newmarket, ON, Canada) to 59 Sanderling in North Padre, 31 Sanderling in Bolivar Flats, 30 Sanderling in Louisiana, and 118 Sanderling in Chaplin Lake. Tags weighed 0.67 g (< 1.5% of the estimated lean body mass of Sanderling; Scott et al., 2004), and were programmed with pulse lengths of 2.5 ms and pulse intervals of approximately 6 s (2015 and 2016) and 8 s (2017), at a single frequency (166.380 MHz). Sanderling undergo extreme variations in body mass during migration (Sanderling can gain over 50% of their lean body mass during a single staging event; mass ranges from ~40 to >100 g; Robinson et al., 2003). Therefore, nanotags were affixed to birds by gluing tags to birds' skin using a quick-setting marine epoxy (J-B Weld ClearWeld 5 Min Epoxy). Nanotags were only attached to adult after second year (ASY) birds, as second year (SY) juvenile birds can exhibit different migration schedules (McKinnon et al., 2014; Stewart et al., 2002).

### 5.3.2 Detection data collection and processing

We tracked Sanderling migration movements using the Motus Wildlife Tracking System (http://motus.org/), a collaborative research network that coordinates and maintains an international array of automated radio-telemetry receivers (Taylor et al., 2017). Between 2015 and 2017, over 300 receiver stations in North America were operational, which can detect birds within about 15 km of the receiver tower (Taylor et al., 2017). Detections of radio-tagged Sanderling were filtered to only include true signals with at least three consecutive tag detections on a single antenna at a single receiver (Crewe et al., 2018; Gómez et al., 2017). Our radio-tagged Sanderling were detected at 26 receiver stations during their northward, spring migration (Figure 5.1), giving us the exact time of detection and approximate location of individuals over the study period.

Detection data were used to calculate the minimum, corrected, and actual stopover durations of tagged Sanderling. Minimum stopover duration was calculated as the number of days between capture (and nanotag attachment) and the final detection of an individual in its trapping area (we saw no movement of birds between the North Padre, Bolivar Flats, and

Louisiana trapping areas). We use the term 'minimum' stopover duration because the arrival date prior to capture and tagging is unknown. We use the term 'corrected' stopover duration for all GOM birds given the mixture of individuals that were overwintering and staging. We found that Sanderling at our GOM sites ramped up fuelling on Julian day 120 (April 29 and 30), and that prior to this date Sanderling maintained their over-wintering lean mass (see Figure A.2). Therefore, for the subset of individuals trapped in the GOM before Julian day 120 (n = 80), we calculated stopover duration as the number of days between Julian day 120 and an individual's final detection in the trapping area. Finally, for birds trapped in the GOM and detected in Chaplin Lake (n = 19), 'actual' stopover duration was calculated as the number of days between the first and last detection in Chaplin Lake (i.e., departure – arrival date). Here an actual stopover event was defined as a detection period lasting at least two days, and shorter durations were considered fly-bys.

Detection data were also used to calculate the travel time for all individuals trapped in the GOM and detected in Saskatchewan. Travel time was calculated as the number of days between an individual's last detection in the GOM and an individual's first detection in Saskatchewan. We caution that throughout this paper we assumed that the last and first detections at a staging site corresponded to the actual departure and arrival dates of individuals. However, birds can move out of the range of the Motus receiver stations, and it is possible that the actual departure and arrival timing of certain individuals was not detected. Consequently, actual departures, arrivals, and travel times may be later, earlier, and faster, respectively, than those reported here. However, we cannot reliably differentiate between actual migration departures and more local movements with the current dataset. Further development of the Motus network in the GOM and along the mid-continental flyways will help to more accurately assess movements within and between staging areas along these migration routes.

### 5.3.3 Statistical analyses

Several models were used to examine differences among Sanderling from different trapping areas. Linear mixed effects models were used to compare corrected stopover durations among GOM trapping areas, actual and minimum stopover durations in Chaplin Lake, and differences in departure dates from the GOM and Chaplin Lake among individuals from different trapping areas. We used linear models to compare actual stopover durations, Chaplin Lake arrival dates, and travel times among Sanderling from different GOM trapping areas. All global

models included trapping area (North Padre Island, Bolivar Flats, Louisiana, and, where applicable, Chaplin Lake) and year as fixed effects, and mixed effects models included a random intercept for capture date. Departure dates from the GOM were log transformed and departure dates from Chaplin Lake were cube transformed to ensure that model residuals met the assumptions of normality and heteroscedasticity.

Further analyses examined the factors influencing migration timing and pace. We used a linear mixed effects model to examine the effect of mass at capture (i.e., fat loads; see Figure A.4) on stopover duration and departure timing. Global models included mass and year as fixed effects, and random intercepts were included for capture date and capture time. For Sanderling trapped in the GOM and detected in Chaplin Lake, we separated travel time into two ordered categories: 'slower' (> 11 days) and 'faster' (< 11 days), where 11 days was the median travel time between the GOM and Chaplin Lake. We used a linear model to investigate the effect of GOM departure date, travel time, and the interaction of GOM departure date and travel time on Chaplin arrival date. A linear model was also used to examine the relationship between Chaplin arrival and departure dates. Both linear models included year as a fixed effect.

All modelling was performed in R (R Core Team, 2017) using the lme4 package (Bates et al., 2015). Lower AICc scores (Akaike's information criterion corrected for small sample size), model weights, and deviance scores were used for model selection according to Burnham and Anderson (Burnham and Anderson, 2002) using the bbmle package (Bolker and R Development Core Team, 2017). Where models were equivalent, weighted model-averaged estimates were calculated for fixed effects in the top model set ($\Delta$AICc < 2) using model.avg in the MuMIn package (Barton, 2017). All plotting was performed using packages ggplot2 (Wickham, 2009) and cowplot (Wilke, 2017). Maps were created using packages ggmap (Kahle and Wickam, 2013) and RgoogleMaps (Loecher and Ropkins, 2015).

### 5.4 Results

Nanotagged Sanderling detection locations and migratory movements indicated a strong selectivity for northward migration along the mid-continental flyways (Figure 5.1). Indeed, of the 22 Sanderling tagged in the GOM and detected again in more northern latitudes, 20 individuals (91%) were detected by receivers in Saskatchewan and only 2 in the Eastern Flyway, suggesting strong connectivity between GOM and Saskatchewan staging sites.

The best approximating model to explain differences in corrected stopover duration among GOM trapping areas included trapping area and year (see Table A.11 for model selection results). North Padre birds showed significantly shorter stopover durations than birds tagged in Bolivar Flats and Louisiana ($\beta$ = -12.9 ± 3.74, $p$ = 0.001; Figure 5.2A), and corrected stopover durations in the GOM were shorter in 2016 (-12.4 ± 3.6, $p$ = 0.001) and 2017 (-18.0 ± 4.5, $p$ = 0.0003) relative to 2015. Departure dates from the GOM showed a high level of variation (range: Julian day 123 to 159; i.e., May 2/3 to June 7/8; Figure 5.2B), which was not explained by trapping area or year (i.e., the intercept only model was the top model; see Table A.11 for model selection results). Models examining the effect of mass at capture on corrected stopover duration and departure date both included mass and year in the best-supported model sets (see Table A.12 for model selection results). There was a negative association between mass at capture and corrected stopover duration in the GOM such that heavier birds had shorter stopovers ($\beta$ = -0.33 ± 0.19, $p$ = 0.08; Figure 5.2C) and departed earlier ($\beta$ = -0.35 ± 0.19, $p$ = 0.07; Figure 5.2D). Although year was in these top model sets, it was not formally significant ($p > 0.05$).

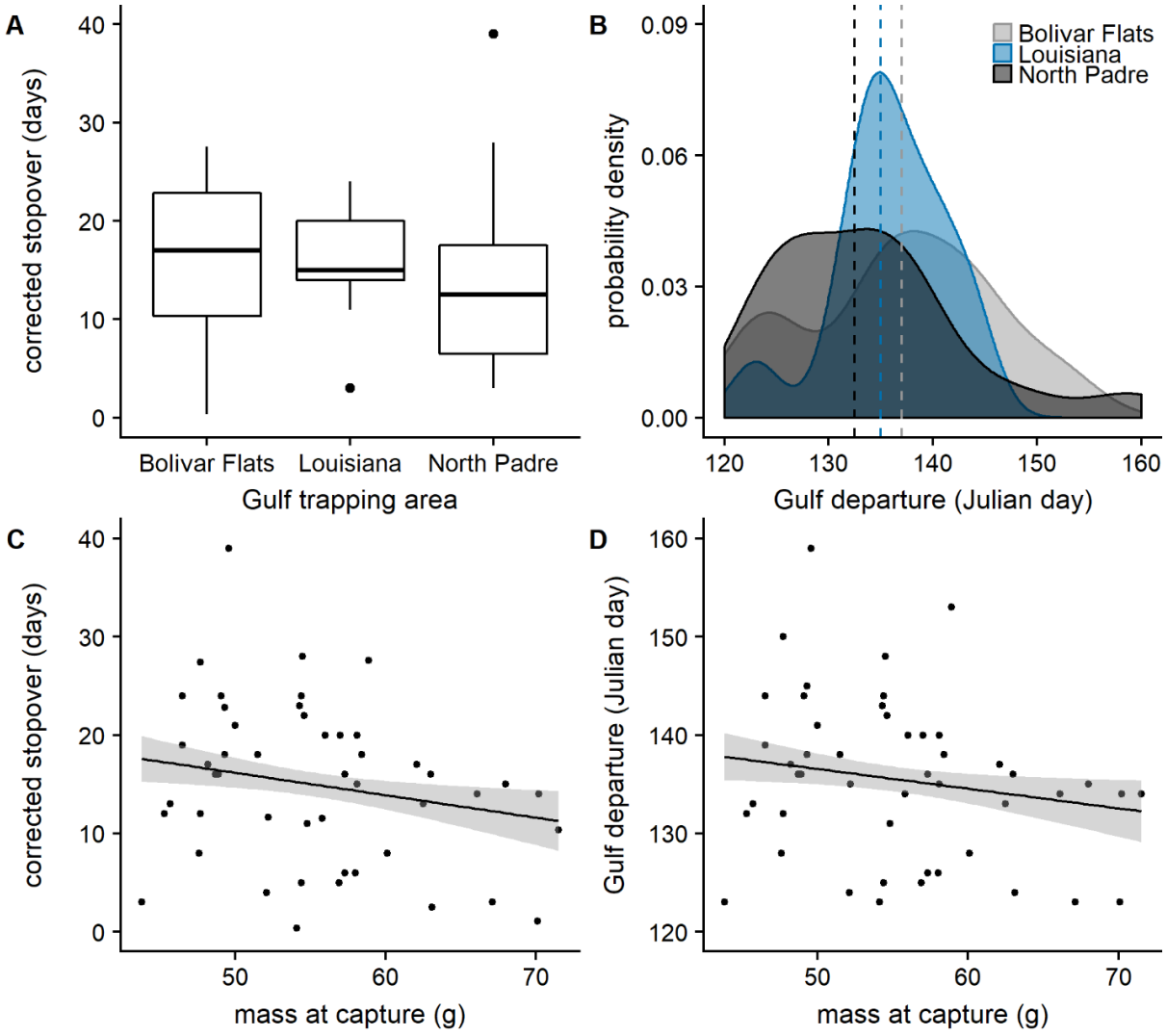


**Figure 5.2.** Fuel loads affected Sanderling stopover and departure timing in the Gulf of Mexico (GOM). (A) Corrected stopover duration of Sanderling varied among GOM trapping areas. (B) There was variation in departure dates among Sanderling in the GOM. Shaded polygons represent the probability density of departure (area under the curves = 1), and vertical lines show the median departure date from each trapping area. Mass at capture was negatively correlated with corrected stopover duration (C) and GOM departure dates (D). In panels C and D, dots indicate raw data points, and lines indicate model-based estimates of the weighted model-averaged means ± a 95% confidence interval. Sample sizes: Bolivar Flats n = 17, Louisiana n = 13, North Padre n = 18.

Twenty birds trapped in the GOM were subsequently detected in Saskatchewan, of which 15 staged for at least two days in Chaplin Lake. These birds showed a high variation in travel time between these sites (median = 11.0 days, range = 3.17 – 34.0 days). Travel time was negatively associated with GOM departure dates ($\beta$ = -0.46 ± 0.24, $p$ = 0.07), and travel times to Saskatchewan were shorter in 2015 ($\beta$ = -10.8 ± 4.5, $p$ = 0.03) and 2017 ($\beta$ = -9.75 ± 4.4, $p$ = 0.04) compared to 2016 (see Table A.13 for model selection results). Travel times to Saskatchewan did not differ among GOM trapping areas (i.e., the null model was the best approximating model for this response; see Table A.14).

Variation in Chaplin Lake arrival dates was explained by travel time, GOM departure date, and the interaction of travel time and departure date (see Table A.15 for model selection results). Chaplin arrival date was positively correlated with GOM departure date ($\beta$ = 0.75 ± 0.21, $p$ = 0.002) and negatively correlated with travel time ($\beta$ = -8.6 ± 1.9, $p$ < 0.0001), and the interaction of GOM departure date and travel time negatively influenced Chaplin Lake arrival date ($\beta$ = -0.064 ± 0.015, $p$ < 0.0001) such that birds departing the GOM on the same date that travelled more slowly arrived later in Chaplin Lake (Figure 5.3A). There was high variation in Chaplin Lake arrival dates (range = Julian day 134 to 159; i.e., May 13/14 to June 7/8). Arrival dates in Chaplin differed among Sanderling from different GOM trapping areas (see Table A.16), where individuals from North Padre arrived later ($\beta$ = 10.3 ± 2.9, $p$ = 0.002) than birds from Louisiana and Bolivar Flats (Figure 5.3B). We also found that Chaplin Lake arrival date influenced subsequent departure date (see Table A.17), with later arriving Sanderling also leaving later ($\beta$ = 0.45 ± 0.12, $p$ = 0.002; Figure 5.3C).

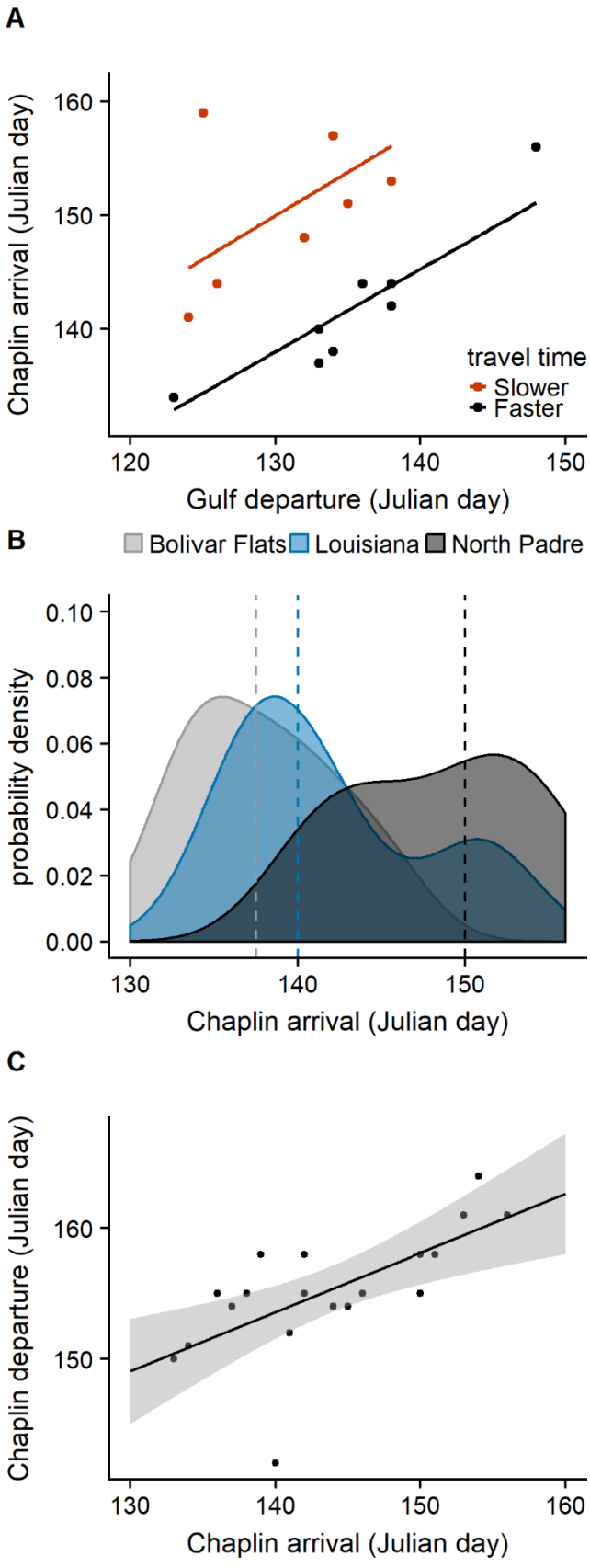


**Figure 5.3.** Evidence for carry-over of migration pace in the Gulf of Mexico (GOM) to Chaplin Lake. (A) Chaplin lake arrival date was positively correlated with GOM departure date and was negatively influenced by travel time (n = 15). Dots indicate raw data points, and line indicates model-predicted estimates for each of 2 travel time categories: slow (> 11 days; orange points) and fast (< 11 days; black points). (B) Chaplin Lake arrival dates differed among Sanderling from different GOM trapping areas. Shaded polygons represent the probability density of arrival (area under the curves = 1), and vertical lines show the median arrival date of individuals from each GOM trapping area. (C) Chaplin departure dates were positively correlated with Chaplin arrival dates. Dots indicate raw data points, and line indicates model-based estimates ± a 95% confidence interval. Samples sizes in panels b and c: Bolivar Flats n = 6, Louisiana n = 4, North Padre n = 9.

The best approximating model to explain variation in actual stopover duration in Chaplin Lake only included GOM trapping area as a fixed effect (see Table A.18). Individuals trapped in North Padre had the shortest stopover durations ($\beta$ = -7.60 ± 2.08, $p$ = 0.002). Models comparing actual and minimum stopover durations in Chaplin Lake suggested trapping area and year were important. Minimum stopover duration of Sanderling trapped in Chaplin Lake appeared longer than the actual stopover duration in North Padre ($\beta$ = -4.57 ± 1.90, $p$ = 0.02) but shorter than in Bolivar Flats ($\beta$ = 4.80 ± 2.05, $p$ = 0.02; Figure 5.4A). As in the GOM, we saw large variations in Sanderling departure dates from Chaplin Lake (range = Julian day 141 to 167; i.e., May 20/21 to June 15/16; Figure 5.4B). Although year and trapping area were included in the top model for departure dates from Chaplin Lake (see Table A.19), neither had a significant effect. The minimum stopover duration of Saskatchewan-trapped birds was negatively correlated with mass at capture such that heavier birds again had shorter stays ($\beta$ = -0.16 ± 0.04, $p$ < 0.0001; Figure 5.4C) and earlier departure dates ($\beta$ = -0.13 ± 0.04, $p$ = 0.0008; Figure 5.4D). This model correspondingly showed that minimum stopover durations were shorter in 2016 ($\beta$ = -3.13 ± 1.00, $p$ = 0.003) and 2017 ($\beta$ = -2.82 ± 1.11, $p$ = 0.01) than in 2015 (see Table A.20 for model selection results).

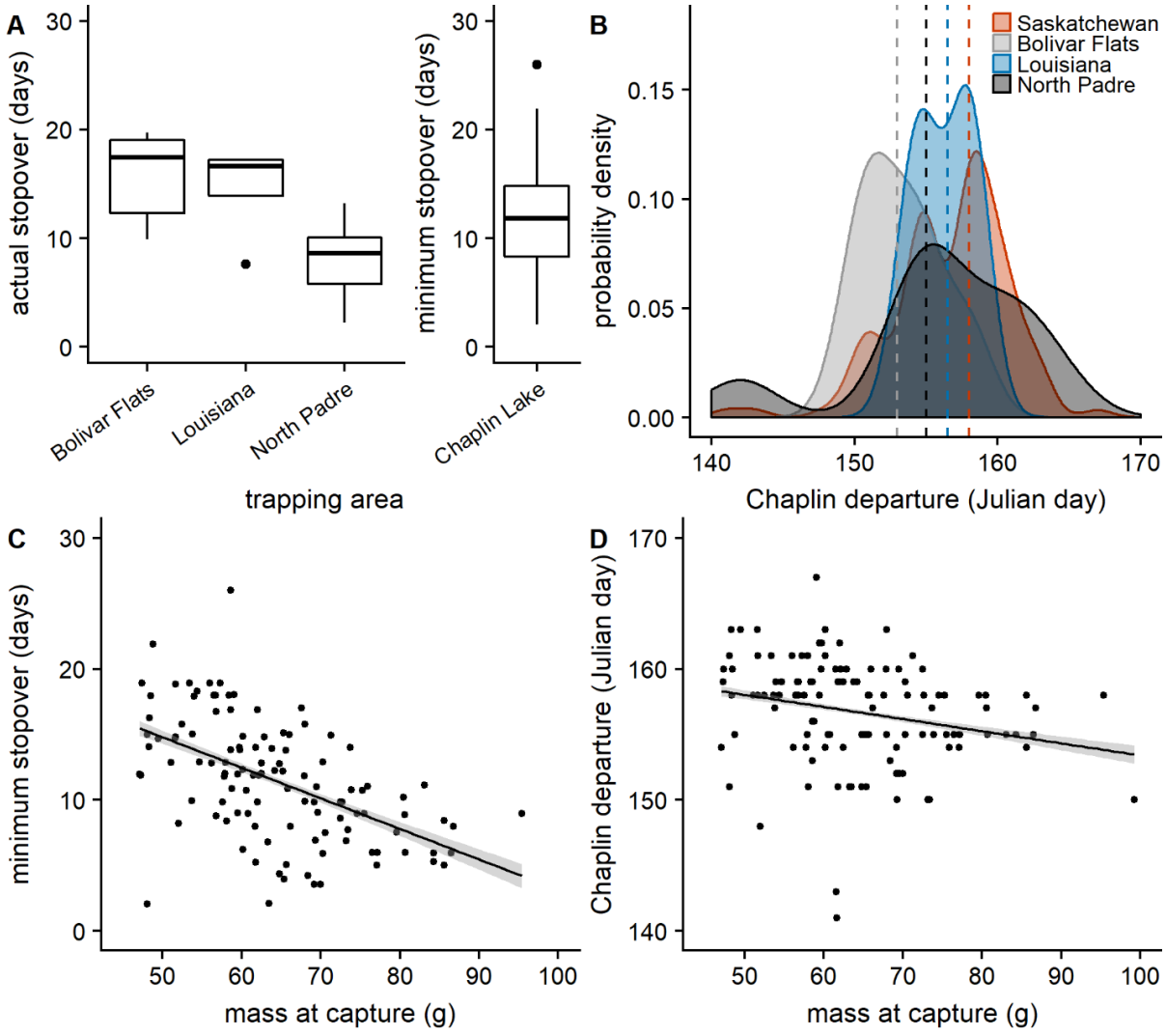


**Figure 5.4.** Fuel loads affected Sanderling stopover and departure timing in Chaplin Lake, SK. (A) Stopover durations in Chaplin Lake varied among trapping areas. (B) There was variation in departure dates from Chaplin Lake. Shaded polygons represent to probability density of departure (area under the curves = 1), and vertical lines show the median departure date from each trapping area. (C) Minimum stopover duration in Chaplin Lake was negatively correlated with mass at capture. (D) Chaplin departure dates were negatively correlated with mass at capture. In panels C and D, dots indicate raw data points, and lines indicate model-based estimates ± a 95% confidence interval. Samples sizes: Bolivar Flats n = 6, Louisiana n = 4, North Padre n = 9, Chaplin Lake n = 117.

## 5.5 Discussion

Given the logistical difficulties associated with tracking long-distance migrants, previous work has tended to study staging sites in isolation (e.g., Baker et al., 2004; Burger et al., 2007). Uniquely, our work traces individual long-distance migrants between staging sites separated by thousands of kilometers and links their migratory behaviour to the intrinsic factors that influence departure and arrival timing. The relationship between mass (i.e., fuel loads) and stopover durations and departure dates confirm that Sanderling fuel loads influence migration timing. As well, positive relationships between departure and arrival data suggests that individuals showing delays at one staging site continue to show delays at a subsequent staging site and do not "catch up". Taken together, these results highlight the importance of identifying the quality of major refuelling sites and point to the possibility for long-term consequences if migrants are delayed at a single site during migration.

We saw an association between fuel loads at capture and stopover and departure timing in the GOM and in Chaplin Lake, confirming that fuel stores consistently influenced Sanderling stopover durations and departure dates. Based on the slopes of these relationships, we can predict that a bird weighing 5 g less on the day of capture would depart 2 days later from the GOM and 1 day later from Chaplin Lake. It is possible that Sanderling were attempting to reach a certain mass prior to departure for migration. Similarly, Red knots (*Calidris canutus*) are known to require a minimum mass threshold prior to departure, and attaining this threshold is associated with greater survival on migration and a higher reproductive output (Baker et al., 2004). Previous work has found that birds that depart later leave with higher fuel loads, which allows them to migrate faster (Deppe et al., 2015; Gómez et al., 2017; Warnock, 2010). However, later departures are often associated with lower body conditions and later arrivals at subsequent sites (Cooper et al., 2015; McKinnon et al., 2014; Ouwehand and Both, 2017). We were unable to recapture individuals at our trapping sites, and therefore the fuelling rates and departure fuel loads of our Sanderling are unknown (Bayly et al., 2012; Gómez et al., 2017).

Sanderling, like other shorebird species, are expected to behave according to a time-minimization migration strategy (Farmer and Weins, 1999; Gudmundsson et al., 1991; Jehl, 1997; Lyons and Haig, 1995). Indeed, Sanderling are capable of extreme pre-migratory mass gains, putting on up to 70% of their lean body mass during a single stopover event (Robinson et al., 2003), and can overload (gain more fat than is needed to reach the next closest staging site)

in order to bypass lower-quality staging areas, which reduces the overall time spent on migration (Gudmundsson et al., 1991). As well, Sanderling travel faster, make longer flights, and have fewer stopovers during spring migration relative to autumn (Zhao et al., 2017), suggesting that this species is more time constrained during pre-breeding migration. The negative association between travel times and departure dates confirms that consistent with other arctic breeding species, Sanderling in this study were behaving according to a time-minimization migration strategy.

Our results also suggest that some individuals exhibit alternative migratory behaviours and travel at a slower pace (Gómez et al., 2017). In particular, Sanderling trapped in North Padre, Texas, appear to use a migration strategy that is different than the strategy of individuals trapped in Louisiana and Bolivar Flats. On average, North Padre Sanderling departed from the GOM at the same time as birds from the other two areas. Although there were no statistically significant differences in travel times among GOM trapping areas, North Padre birds arrived latest in Chaplin Lake. These individuals appear to have compensated for later arrival by reducing their stopover duration, ultimately departing from Chaplin Lake at the same time as individuals from other trapping areas.

A possible explanation for these differences is that a higher proportion of Sanderling trapped in North Padre were over-wintering at this site rather than in locations south of the GOM. Based on banding and feather isotope records, we have information that suggests that a proportion of the Chaplin Lake migrants are overwintering in the Texas Gulf Coast (Labarrere, 2016). They may therefore take on a slightly different migration strategy as relatively shorter distance migrants. Variable migration strategies within and between avian populations have been observed previously (Ely and Meixell, 2016; Weimerskirch et al., 2015). Sites in the North Padre area are especially important Sanderling wintering areas (Withers, 2002), and our earliest GOM trapping dates were in North Padre (only individuals in North Padre were trapped before Julian day 113 (April 22/23)). Populations that migrate shorter distances between their breeding and wintering grounds tend to face fewer time constraints and have more flexible migration schedules than populations with longer migrations (Arlt et al., 2015). This would suggest that as relatively shorter distance migrants, North Padre birds could be less time constrained and take more circuitous routes to Chaplin Lake. Indeed, shorebird populations that make shorter distance flights typically have shorter stopover durations, which are associated with lower departure fuel

loads (Battley et al., 2012; Henkel and Taylor, 2015), whereas more time-minimizing individuals depart later, leave with higher fuel loads, and consequentially travel more rapidly on migration (Deppe et al., 2015; Gómez et al., 2017; Warnock et al., 2004).

Sanderling detection data suggest that individuals that leave later from the GOM are also later in Chaplin Lake. Although based on only 15 GOM-tagged birds that staged in Chaplin Lake, we saw a strong positive association between GOM departures and Chaplin Lake arrivals. Therefore, birds departing later from the GOM arrived later in Chaplin Lake. This resulted in up to a 23-day span in arrival dates at the northern stopover. We also saw a strong positive association between Chaplin Lake arrival and departure dates, where later arrivals in Chaplin Lake were associated with later departures from this site. This provides early evidence that delays in migration could carry over from one staging site to the next. These carry-over effects have the potential to negatively impact Sanderling populations, particularly if individuals are behaving according to a time-minimization migration strategy, where birds leave on a certain date regardless of their condition (Both and Visser, 2001; Gill et al., 2001). However, it is important to consider that multiple factors influence the departure decisions of migratory birds. Departure fuel loads, refuelling rates, and departure dates are influenced by an individual's age, sex, and arrival date, as well as the quality and availability of food during staging, and environmental factors, such as wind direction and precipitation (Atkinson et al., 2007; Covino et al., 2014; Jarjour et al., 2017). A major limitation of radio-telemetry data is that it is not possible to accurately determine an individual's date of arrival. Therefore, differences in the total time spent refuelling are unknown. Another limitation was that we were unable to retrap individuals to estimate departure fuel loads, therefore we do not know the condition of birds at the time of departure. More research will be needed to fully characterize why some Sanderling were later than others.

Finally, this research confirms the importance of the mid-continental flyways for Sanderling migration. Of the 120 Sanderling tagged in the GOM, 22 were detected in more northern sites, with 20 individuals (91%) detected in Saskatchewan, suggesting a strong connectivity between GOM and Saskatchewan staging areas. Band resight data corroborate the importance of the mid-continental flyways for Sanderling and suggest that most individuals staging in the Gulf Coast and migrating north through the Canadian Prairies overwinter in Chile and Peru (Myers et al., 1990). The percentage of birds tagged in the GOM and then detected in

more northern latitudes (18.3%) was lower than the recovery rates of previous studies using the Motus telemetry network (Gómez et al., 2017; Taylor et al., 2017) and was likely related to the small number of shorebird staging areas along the mid-continental flyways that are outfitted with Motus radio-telemetry receivers (Taylor et al., 2017). Further expansion of the Motus network and future advancements in tracking technology will aid in identifying key shorebird staging areas and determining avian migration routes along the mid-continental flyways.

### 5.6 Conclusions

Our study highlights the link between fuel loads and migration timing and provides early evidence that delays at one staging site can carry over to subsequent sites. These findings underscore the need to characterize the factors that impair avian pre-migratory fuelling and, ultimately, to identify the initial cause of migration delays. A significant cause of migration delays is reduced staging site quality. Staging site quality is closely linked to fuel deposition rates (Bayly et al., 2012) and consequentially affects stopover duration, departure fuel loads, and the subsequent pace of migration (Bayly et al., 2012; Gómez et al., 2017; Norris et al., 2004). Several factors can influence staging site quality and the ability of migrants to fuel. Reduced food availability, for instance, is a major issue for migrants and has been attributed to anthropogenic factors, like climate change (Both and Visser, 2001), habitat loss (Studds et al., 2017), and the overharvesting of avian prey sources (Baker et al., 2004). Reduced food availability can limit fuel deposition and delay departure (Cooper et al., 2015) or cause individuals to leave underweight (Baker et al., 2004). Similarly, human disturbance and high predator abundance at staging sites can reduce and delay fuelling by flushing birds from a foraging area (Burger et al., 2007; Fransson and Weber, 1997). There is also evidence that staging site contamination by toxicants, such as pesticides, petroleum products, and persistent organic pollutants, can reduce migrant vitality and impair fat deposition (Bursian et al., 2017b; Eng et al., 2017; Harris and Elliott, 2011). Given the association between staging site quality, fuelling, migration pace, and migrant population dynamics, there is a vital need to identify and maintain the quality of stopover habitats used by long-distance migrants.

# 6 CHAPTER 6: GENERAL DISCUSSION

## 6.1 Summary

The main hypothesis of this thesis was that PAH exposure can impair avian pre-migratory fuelling. I focused on Sanderling (*Calidris alba*) as a model because of its long-distance migratory behaviour, its extreme fuelling ability, and its ecological relevance. A controlled dosing experiment confirmed that dietary exposure to environmentally-relevant PAH concentrations and mixtures during staging lowered Sanderling pre-migratory mass gains (Chapter 2). To my knowledge, this study is the first to directly link PAH ingestion to impaired pre-migratory fuelling. More specific investigations into the mechanisms underlying this result suggested that PAHs impaired pre-migratory fat deposition by disrupting cholesterol and lipid homeostasis. Serum bile acids, which facilitate lipid absorption and digestion (Staels and Fonseca, 2009), were reduced with increasing PAH exposure (Chapter 2). As well, the hepatic mRNA expression of liver basic fatty acid binding protein 1 (*Lbfabp*), a lipid chaperone that enhances fatty acid uptake, transport, storage, and metabolism (Atshaves et al., 2010), and hepatic lipase (*Lipc*), an enzyme involved in lipid metabolism and uptake (Santamarina-Fojo et al., 2004), were reduced in PAH-dosed Sanderling relative to controls (Chapter 3).

The results of the oral dosing study served as a foundation for broader investigations into effects that may occur in the field. I found early evidence that PAHs or other co-contaminants lower staging site quality for fuelling shorebirds (Chapter 4). At staging sites in Louisiana, which had the highest total sediment PAH concentrations, metabolite data suggested that Sanderling exhibited lower refuelling rates, and both Sanderling and Red knots (*C. canutus*) departed later from Louisiana compared to North Padre. However, the data suggested that other unmeasured factors (e.g., the presence of other co-contaminants) were also influencing departure dates from the study sites. Radio-telemetry data revealed an association between Sanderling fuel loads and migration pace (Chapter 5). Mass at capture was negatively correlated with Sanderling stopover durations and departure dates in the Gulf of Mexico and Chaplin Lake. Moreover, individuals that departed later from the Gulf of Mexico also arrived later and subsequently departed later from Saskatchewan. This work thus provided evidence that delays in migration carry over from one staging site to the next and that birds have a limited ability to "catch up".

This thesis highlights the risk of pollution to long-distance avian migrants that are extreme endurance athletes, capable of making non-stop flights of several thousand kilometers without access to supplementary food or water. Long distance migratory birds are currently

experiencing worldwide population declines (Holmes, 2007; Sanderson et al., 2006). Birds may experience higher risks of mortality on migration than during other parts of their life cycle (Newton, 2006; Sillett and Holmes, 2002), and migration delays may have unfavourable fitness consequences if they result in delayed arrival on the breeding grounds (Norris and Marra, 2007). It has therefore been suggested that migration could act as a bottleneck that limits migratory bird populations (Newton, 2006). Given the link between pre-migratory fuelling ability and avian population dynamics, identifying and understanding the factors that limit pre-migratory fat deposition represents a key research and conservation priority.

### 6.2 Adverse outcome pathway development

The objective of this chapter, and indeed the thesis as a whole, was to synthesize multiple datasets on how PAHs could affect avian pre-migratory fuelling by organizing events into a biologically plausible mode of action that is useful to avian ecotoxicological risk assessment. Specifically, I propose a putative adverse outcome pathway (AOP) linking the molecular mechanisms underlying pre-migratory fuelling impairment to the effects of impaired fuelling on migratory bird populations. Guidelines for AOP development and evaluation are outlined by the Organisation for Economic Co-operation and Development (OECD, 2018, 2017). As a general rule, AOPs start at a molecular initiating event (MIE), in which a toxicant interacts with a biological molecule, and proceeds to an adverse outcome (AO), an apical outcome that is relevant to risk assessment (Ankley et al., 2010; Villeneuve et al., 2014a; Vinken et al., 2017). MIEs and AOs are linked by key events (KEs) and key event relationships (KERs). A KE is a measurable biological change that is required for a MIE to progress to an AO (Villeneuve et al., 2014a; Vinken et al., 2017). KERs provide directional associations that link together adjacent MIEs, KEs, and AOs (Groh et al., 2015; Villeneuve et al., 2014a; Vinken et al., 2017). Ideally, AOPs should not be chemical specific. Thus, any chemical that initiates a MIE can activate the subsequent procession of KEs and the AO (Villeneuve et al., 2014b). However, case studies limited to a single chemical can be submitted to the OECD AOP program with the goal of applying an AOP to a category of chemicals as new data is acquired (OECD, 2017). This thesis thus served as a case study that, along with existing data regarding PAH mechanisms of action and avian migration ecology, can be used for the development of a putative AOP linking PAH exposure to avian population declines.

In this chapter, I present a putative AOP linking PAH-induced molecular-level effects to impaired pre-migratory fat deposition, migration delays, and population declines (Figure 6.1). The progression from the MIE to individual-level effects is the most speculative section of the AOP (discussed in Section 6.2.1). This thesis focused on the AhR as a biologically plausible mediator of PAH-induced pre-migratory fuelling impairment. I predicted that AhR activation would lead to changes in lipid and cholesterol homeostasis (KE1), which lower pre-migratory mass gains (KE2). Conversely, the progression from individual- to population-level effects is well supported by data from this thesis and the literature (discussed in Section 6.2.2). This involves a progression from lower fuel loads (KE2), to migration delays (KE3) and late arrival on the breeding grounds (KE4) and then to lower reproductive success (KE5), and ultimately to population declines (AO). Each component of this putative AOP is discussed below in greater detail and in temporal sequence. Uncertainties are identified throughout to highlight areas that require further investigation. Possible alternative pathways for fuelling impairment and migration delays are also discussed (Section 6.2.3).

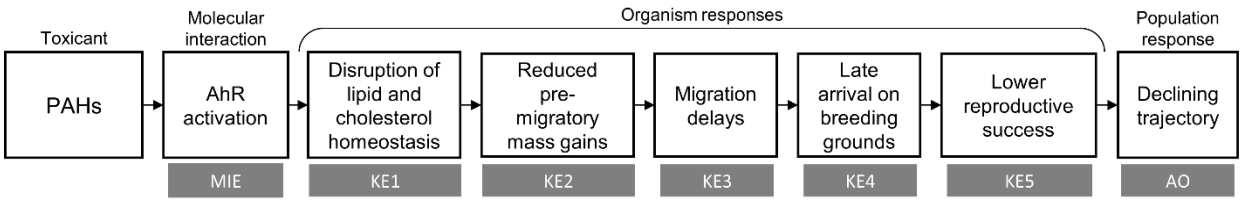


**Figure 6.1** Schematic of a putative AOP linking PAH-mediated AhR activation to pre-migratory fuelling impairment and to the impact of impaired fuelling on migration timing and migratory bird populations. The molecular initiating event (MIE), intermediate key events (KE), and the adverse outcome (AO) are indicated. See Figure 6.4 for possible alternative or co-occurring pathways.

### 6.2.1 Biological cascade from MIE to impaired pre-migratory fuelling

This thesis focused on AhR activation as one biologically plausible mediator of PAH-induced pre-migratory fuelling impairment. PAHs are known AhR ligands (Denison and Nagy, 2003; Head et al., 2015), and the observed increase in hepatic cytochrome P450 (*Cyp*) 1A4 expression (Chapter 3) and hepatic ethoxyresorufin-*O*-deethylase (EROD) activity (Chapter 2) confirmed AhR activation in PAH-dosed Sanderling. Evidence from the literature supports the inclusion of AhR activation as a plausible MIE. In mice and rats, AhR activation causes hepatic steatosis, changes the lipid composition of the liver, increases peripheral fat mobilization, and inhibits β-oxidation and the secretion of very low-density lipoproteins (Angrish et al., 2012; Lee et al., 2010; Nault et al., 2017). Microarray experiments have shown that AhR agonism is responsible for a coordinated repression of the genes responsible for lipid and cholesterol homeostasis (Fader et al., 2017; Fletcher et al., 2005; Nault et al., 2017), including *Lipc* and *Lbfabp* (Nault et al., 2017), as well as *Cyp7a1* (Fader et al., 2017; Fletcher et al., 2005; Iwano et al., 2006), the rate limiting enzyme in the metabolism of cholesterol to bile acids (Schonewille, 2016). Interestingly, contrary to the results of this thesis, rodent studies typically report elevated serum bile acid concentrations following AhR induction (Brewster et al., 1988; Couture et al., 1988; Fader et al., 2017; Gao et al., 2016), which is likely due to the concurrent repression of blood-to-hepatocyte transporters and induction of hepatocyte-to-blood transporters (Fader et al., 2017; Fletcher et al., 2005). Further research is required in migratory bird species that can undergo rapid major increases in body mass in response to seasonal migratory cues to fully understand these interspecies differences.

Captive dosing experiments measured changes in gene expression and higher order effects in the same individuals. Therefore, although this thesis had insufficient data to specifically and causally link AhR activation with later KEs in pre-migratory Sanderling, it was possible to map how gene expression changes were related to changes in Sanderling serum biochemistry, organ responses, and individual-level changes in mass. The correlative strength of associations among responses at different levels of biological organization were visualized using a Sankey diagram (created using R packages networkD3 (Allaire et al., 2017) and scales (Wickham, 2017); Figure 6.2). The Sankey diagram visualizes each variable as a rectangle (called a “node”), and nodes are joined together by lines (termed “paths”). To compare variables with dissimilar units, all results were rescaled to have a mean of zero and a standard deviation of

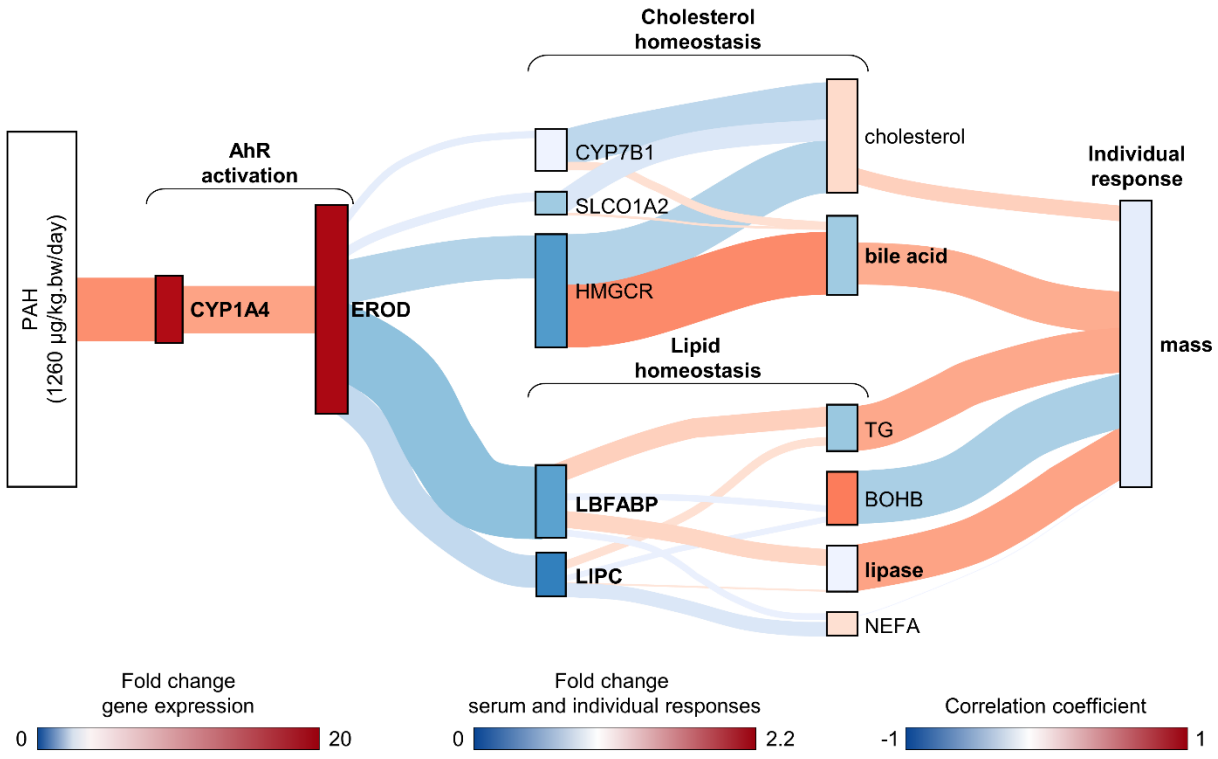


**Figure 6.2.** Sankey diagram showing the correlative strength of associations between gene expression, serum, and individual responses indicative of AhR activation, cholesterol homeostasis, lipid homeostasis pathways, and fuel loads in Sanderling orally dosed with 1260 µg/kg bw/day of a commercial PAH mixture over a 21-day pre-migratory fuelling period. Node colours indicate response values, expressed as fold change from controls (range: 0 – 20 for changes in gene expression, 0 – 2.2 for changes serum analytes and mass). Darker reds indicate increases relative to controls, and darker blues indicate decreases relative to controls. Path colours indicate the correlation coefficient between variables: darker blues indicate a more negative correlation (closer to -1) and darker reds indicate a more positive correlation (closer to +1). Path widths are proportional to the strength of the correlation between variables. Boldface type indicates that there was a statistically significant change in a response following PAH dosing. Paths do not necessarily represent a direct biological association between variables.

one. Variables were then grouped into three pathways (AhR activation, lipid homeostasis, and cholesterol homeostasis), and the correlation coefficients were calculated for adjacent variables in each pathway. The strength of these correlations is represented by path colours and widths.

The Sankey diagram illustrates that there was a negative correlation between AhR-mediated EROD activity and the expression of genes in the lipid and cholesterol homeostasis pathways. Elevated EROD activity was most strongly correlated with changes in *Lbfabp*, *Lipc*, and 3-hydroxy-3-methylglutaryl-coA (*Hmgcr*) hepatic mRNA expression ($R^2$ = -0.40, -0.20, and -0.26, respectively). In the lipid homeostasis pathway, changes in hepatic *Lbfabp* and *Lipc* expression were weakly correlated ($-0.09 < R^2 < 0.13$) with changes in the serum concentrations of triglyceride (TG), β-hydroxybutyrate (BOHB), lipase, and non-esterified fatty acids (NEFA), suggesting that these hepatic genes played little role in regulating the concentrations of these serum analytes. This is not surprising, given that TG, BOHB, and NEFA concentrations were not statistically altered by PAH treatments and that changes in serum lipase concentrations were not considered physiologically relevant (see Chapter 2). In the cholesterol homeostasis pathway, the strongest gene-serum analyte correlations were between *Hmgcr* expression and serum cholesterol ($R^2$ = -0.30) and bile acid ($R^2$ = 0.37) concentrations and between *Cyp7b1* expression and serum cholesterol concentrations ($R^2$ = -0.22). *Hmgcr* is the rate limiting enzyme in cholesterol biosynthesis, and *Cyp7b1* is involved in the conversion of cholesterol to bile acids (Schonewille, 2016). There is therefore a direct biological association among these variables. The negative correlation between *Hmgcr* mRNA expression and serum cholesterol concentrations is unexpected. It is expected that other, untested enzymes and/or transporters in the cholesterol homeostasis pathway could be affecting changes in these variables. Overall, no one pathway stands out as being most strongly correlated with changes in Sanderling mass. Serum TG, lipase, and bile acid concentrations showed the strongest positive correlations with Sanderling mass ($R^2$ = 0.26, 0.27, and 0.24, respectively), while BOHB showed the strongest negative correlation with Sanderling mass ($R^2$ = -0.30). Several interrelated physiological pathways are likely responsible for the effects observed in dosed individuals, and this would be an interesting area for further AOP network development.

### 6.2.2 Reduced pre-migratory mass gains leading to population declines

The data from Chapters 2, 4, and 5 provide a preliminary link between PAH ingestion, reduced mass gains during staging, and migration delays. The correlative strength of associations between Sanderling fuel loads in the Gulf of Mexico, departure dates from the Gulf of Mexico, arrival dates in Chaplin Lake, and subsequent departure dates from Chaplin Lake can also be visualized using a Sankey diagram (Figure 6.3). Here, correlations among organismal and population responses grew stronger over time, with Chaplin Lake arrivals and departures showing the strongest association ($R^2 = 0.50$).

The relationship among fuel loads, departure dates, and migration pace has been documented previously in a variety of long-distance migratory bird species (e.g., Grey-cheeked thrush, *Catharus minimus*, (Gómez et al., 2017); American Redstart, *Setophaga ruticilla* (Cooper et al., 2015); Hermit thrush, *Catharus guttatus*, (Smith and Mcwilliams, 2014), Red knots (Baker et al., 2004)). In the captive dosing study, Sanderling in the high dose group gained 4.4 ± 3.7 g less than controls[1] (Chapter 2). Using model-based estimates, we can predict that an individual Sanderling weighing 5 g less on the day of capture would depart approximately 2 days later from the Gulf of Mexico, would then arrive 1.5 days later in Saskatchewan, and would subsequently depart 16 hours later toward its arctic breeding grounds. These knock on effects suggest that contaminants like PAHs could have a direct and measurable effect on an individual's migration pace.

The progression of events from changes in fuelling rates and fuel loads to effects on reproductive success and avian populations is supported by a body of avian ecological research in numerous migratory bird species. Lower fuelling rates and departure fuel loads are associated with delays in departure from wintering and staging sites, later arrivals on the breeding grounds, and ultimately lower reproductive success (Cooper et al., 2015; Deppe et al., 2015; Dossman et al., 2016; Goymann et al., 2010; Norris et al., 2004; Schmaljohann and Naef-Daenzer, 2011). This is because birds that arrive later on the breeding grounds have less access to higher quality

[1] Sanderling in the control and high dose groups weighed 73.2 ± 2.7 and 68.8 ± 2.6 g, respectively, at the end of the 21-day captive dosing experiment. Standard error for the difference in mass was calculated using the error propagation formula: $\delta R = ((\delta X)^2 + (\delta Y)^2)^{1/2}$ (Lindberg, 2000). $\delta R$ = uncertainty in the difference in mass, $\delta X$ = standard error of the mean control group mass, $\delta Y$ = standard error of the mean high dose group mass.

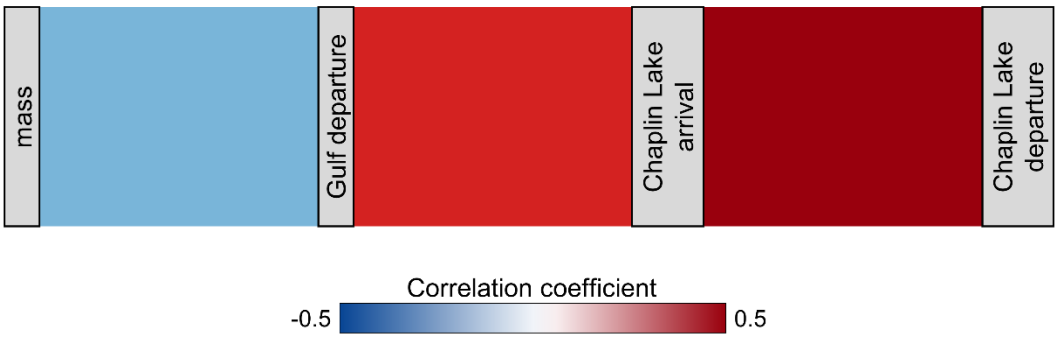


**Figure 6.3.** Sankey diagram showing the correlative strength of associations between Sanderling mass at capture, departure date from the Gulf of Mexico, and staging duration in Chaplin Lake. Path colour represents the strength and direction of correlations among variables, with darker shades of blue and red showing more negative (closer to -0.5) and positive (closer to 0.5) correlations, respectively.

territories and mates (Smith and Moore, 2005). Later arriving individuals exhibit later breeding, which is associated with smaller clutches and offspring relative to birds that arrive earlier (Norris et al., 2004; Smith and Moore, 2005). Later individuals also have less time for renesting or to produce a second brood (Cooper et al., 2010; Smith and Moore, 2005) and have a lower probability of extra-pair mating success or polygyny (Canal et al., 2012; Cooper et al., 2010; Reudink et al., 2009). As a result, migration delays are linked to population declines migratory birds (Baker et al., 2004; Lee et al., 2011; Newton, 2006).

### 6.2.3 Possible alternative pathways and areas for future investigation

This chapter shows how sublethal PAH ingestion can be linked to impaired pre-migratory fuelling, migration delays, and population declines. I focused on linking a single MIE (AhR activation) to a single AO. However, several interacting physiological pathways are likely responsible for the effects observed in exposed individuals. One of the advantages of AOPs is that they are a pragmatic simplification of biology. Interrelated effects and pathways are described by AOP networks, which are a combination of two or more AOPs that share at least one KE (OECD, 2018; Villeneuve et al., 2014b; Vinken, 2013; Vinken et al., 2017). In this section, I discuss biologically plausible alternative and interacting pathways linking PAH exposure to population declines in migratory birds. Figure 6.4 shows how these pathways might be linked in a hypothetical AOP network.

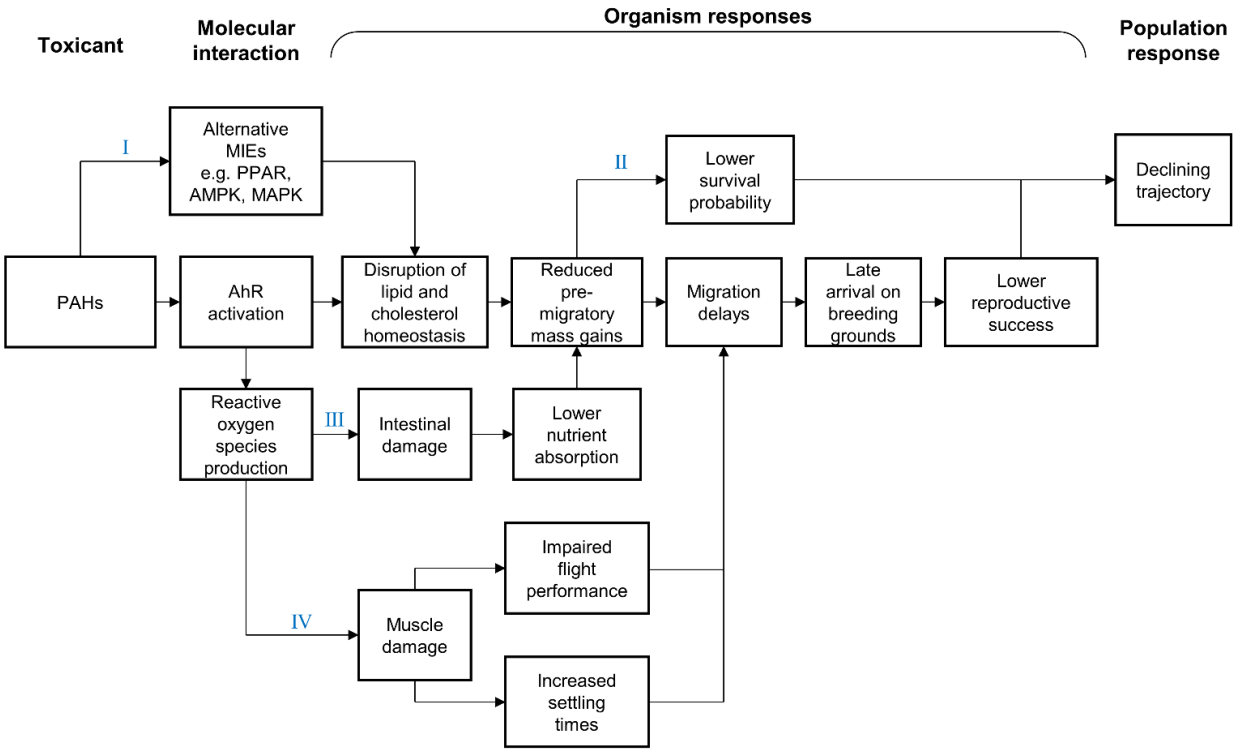


**Figure 6.4.** Hypothetical AOP network linking PAH exposure to population declines via a series of possible interrelated MIEs and KEs at the molecular- and organism-level. Blue roman numerals identify the alternative or co-occurring pathways discussed in the text.

Figure 6.4 shows four possible alternative or co-occurring pathways linking PAH exposure to a declining population trajectory in migratory birds. First, it is possible that PAH exposure initiated other MIEs (pathway I). PAH exposure is known to affect a multitude of cell signalling pathways beyond those controlled by the AhR (Yanyan Zhang et al., 2016). Many of these pathways could have mediated effects observed at the whole organism-level. For example, the peroxisome proliferator-activated receptor (PPAR), AMP-activated protein kinase (AMPK), and mitogen-activated protein kinase (MAPK) signalling pathways are also stimulated by PAH exposure (Yanyan Zhang et al., 2016) and are important regulators of lipid and cholesterol levels, body fat distribution, and overall body mass (Anderson, 2006; Bost et al., 2005; Gehart et al., 2010; Harrington et al., 2007; Long and Zierath, 2006; Srivastava et al., 2012; Tyagi et al., 2011).

A second alternative or co-occurring pathway is for impaired pre-migratory fuelling to directly impact the survival of migratory birds (pathway II). Birds that do not acquire enough food prior to departure can die from starvation on migration (Newton, 2006) or when poor weather conditions or low food availability are encountered at a bird's destination (Marcstrom and Mascher, 1979; Morrison, 1975). Birds weakened by starvation are also more vulnerable to predation (Bijlsma, 1990).

Pathways III and IV are hypothesized to occur following PAH-induced oxidative stress. PAH metabolism often involves the biotransformation of these compounds to reactive metabolites, such as epoxides and quinones. Reactive metabolites can bind to macromolecules, such as DNA, lipids, and proteins, disrupting cellular homeostasis and damaging the affected tissues (Abdel-Shafy and Mansour, 2016; Bhattacharyya et al., 2014). PAH ingestion and metabolism in the gut has previously been shown to cause intestinal damage and lower nutrient absorption in mammals (Bhattacharyya et al., 2014; Diggs et al., 2011; Ribiere et al., 2016). Similar processes in pre-migratory birds could directly impair pre-migratory fuelling. The captive dosing experiment (Chapter 2) and studies in fish species (e.g., sockeye salmon, *Oncorhynchus nerka* (Alderman et al., 2017a) and zebrafish (Lucas et al., 2016)) show that PAH ingestion can also cause muscle damage. Flight and cardiac muscle damage has the potential to lower migratory flight performance (Alderman et al., 2017b; Jenni-Eiermann et al., 2014) and to increase settling times (the time between arrival and the initation of fuelling; Guglielmo et al.,

2001), which would prolong an individual's staging duration and slow its overall migration pace (Hedenström and Alerstam, 1997).

Although this thesis did not directly investigate pathways III and IV, I could test the correlative strength of associations between biomarkers of AhR activation, oxidative stress, muscle damage, and fuel loads using data from the captive dosing experiment (visualized using a Sankey diagram; Figure 6.5). EROD activity was negatively correlated with glutathione-*s*-transferase (*Gstm3*) mRNA expression ($R^2$ = -0.36). Lower *Gstm3* mRNA expression in the liver was correlated with reduced fuel loads ($R^2$ = 0.39) and with greater muscle damage ($R^2$ = -0.22). Alternatively, *Gpx3* expression was weakly correlated with EROD activity and serum creatine kinase concentrations ($R^2$ < 0.08) and was negatively correlated with mass ($R^2$ = -0.20). There is thus preliminary evidence that different antioxidant enzymes may be dissimilarly affected by chronic AhR activation and that changes in their levels of expression could contribute to reduced fuelling and tissue damage. More research is needed to fully understand how PAH-induced oxidative stress might contribute to tissue damage and affect pre-migratory birds.

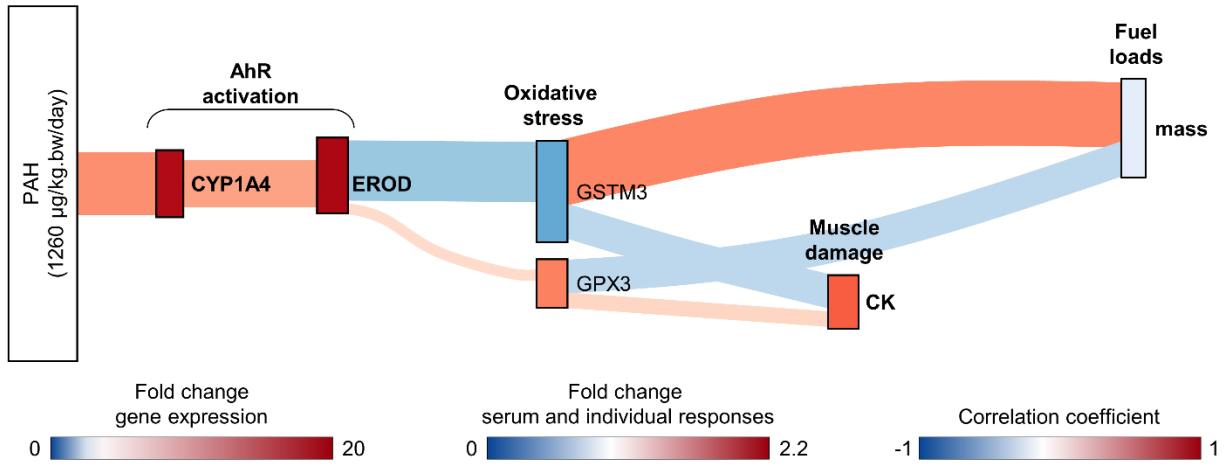


**Figure 6.5.** Sankey diagram showing the correlative strength of associations between gene expression, serum, and individual responses indicative of AhR activation, oxidative stress, muscle damage, and fuel loads in Sanderling orally dosed with 1260 µg/kg bw/day of a commercial PAH mixture over a 21-day pre-migratory fuelling period. Node colours indicate response values, expressed as fold change from controls (range: 0 – 20 for changes in gene expression, 0 – 2.2 for changes serum analytes and mass). Darker reds indicate increases relative to controls, and darker blues indicate decreases relative to controls. Path colours indicate the correlation coefficient between variables: darker blues indicate a more negative correlation (closer to -1) and darker reds indicate a more positive correlation (closer to +1). Path widths are proportional to the strength of the correlation between variables. Boldface type indicates that there was a statistically significant change in a response following PAH dosing. Paths do not necessarily represent a direct biological association between variables.

It is important to note that the captive experiments were performed during Sanderling's autumn pre-migratory fuelling period, whereas field measurements were taken in spring-migrating Sanderling. Northward, spring migrants are typically under greater time constraints than autumn migrants (Hedenström and Alerstam, 1997; Nilsson et al., 2013; Zhao et al., 2017). As well, the hormonal regulation of pre-migratory fuelling differs in spring and autumn migrants (Cornelius et al., 2012). Therefore, separate AOPs may be necessary to describe potential seasonal differences in the toxicology of avian migration. However, seasonal differences in xenobiotic metabolism and toxicities in migratory birds are generally not well understood and this research provides an important step in interpreting this novel area of ecotoxicology. Fully understanding the numerous, interacting signalling cascades responsible for PAH-induced pre-migratory fuelling impairment and the subsequent consequences of reduced pre-migratory mass gains will require further research and would strengthen the hypothesized AOP network.

### 6.4 Conclusions

Long-distance migratory birds are currently experiencing population declines globally (Holmes, 2007; Sanderson et al., 2006; Zockler et al., 2003), and both impaired pre-migratory fuelling (Baker et al., 2004) and staging site oil pollution (Bursian et al., 2017a; Henkel et al., 2012) have been identified as important factors contributing to these declines. There is therefore an urgent need to directly assess and characterize the impacts of PAH exposure on pre-migratory birds. Fully understanding how PAHs affect pre-migratory fuelling, and ultimately avian populations, requires a mechanistic approach that links molecular-level events to adverse outcomes at the population-level. By organizing the data of preceding chapters and existing knowledge into a progression of toxicity events, we can gain a better understanding of how PAHs and other toxicants with similar mechanisms of action can affect avian populations. This work will help to inform avian ecotoxicological risk assessments and efforts to improve the conservation of long-distance migratory birds.

## REFERENCES


Abdel-Shafy, H.I., Mansour, M.S.M., 2016. A review on polycyclic aromatic hydrocarbons: Source, environmental impact, effect on human health and remediation. Egypt. J. Pet. 25, 107–123. doi:10.1016/j.ejpe.2015.03.011

Aeppli, C., Carmichael, C.A., Nelson, R.K., Lemkau, K.L., Graham, W.M., Redmond, M.C., Valentine, D.L., Reddy, C.M., 2012. Oil weathering after the Deepwater Horizon disaster led to the formation of oxygenated residues. Environ. Sci. Technol. 46, 8799–8807. doi:10.1021/es3015138

Aeppli, C., Nelson, R.K., Radović, J.R., Carmichael, C.A., Valentine, D.L., Reddy, C.M., 2014. Recalcitrance and degradation of petroleum biomarkers upon abiotic and biotic natural weathering of Deepwater Horizon oil. Environ. Sci. Technol. 48, 6726–6734. doi:10.1021/es500825q

Aharon-Rotman, Y., Gosbell, K., Minton, C., Klaassen, M., 2016. Why fly the extra mile? Latitudinal trend in migratory fuel deposition rate as driver of trans-equatorial long-distance migration. Ecol. Evol. 6, 6616–6624. doi:10.1002/ece3.2388

AL-Mansour, M.I., 2005. Effects of captivity on basal metabolic rate and body composition in Sanderling bird Calidris alba. Int. J. Zool. Reserach 1, 1–5.

Albers, P.H., 2006. Birds and polycyclic aromatic hydrocarbons. Avian Poult. Biol. Rev. 17, 125–140. doi:10.3184/135704806X212461

Alderman, S.L., Dindia, L.A., Kennedy, C.J., Farrell, A.P., Gillis, T.E., 2017a. Proteomic analysis of sockeye salmon serum as a tool for biomarker discovery and new insight into the sublethal toxicity of diluted bitumen. Comp. Biochem. Physiol. - Part D Genomics Proteomics 22, 157–166. doi:10.1016/j.cbd.2017.04.003

Alderman, S.L., Lin, F., Farrell, A.P., Kennedy, C.J., Gillis, T.E., 2017b. Effects of diluted bitumen exposure on juvenile sockeye salmon: From cells to performance. Environ. Toxicol. Chem. 36, 354–360. doi:10.1002/etc.3533

Alerstam, T., 2011. Optimal bird migration revisited. J. Ornithol. 152, 5–23. doi:10.1007/s10336-011-0694-1

Alerstam, T., 2001. Detours in bird migration. J. Theor. Biol. 209, 319–331. doi:10.1006/jtbi.2001.2266

Alerstam, T., Hedenstrom, A., Akesson, S., 2003. Long-distance migration: evolution and determinants. Oikos 103, 247–260. doi:10.1034/j.1600-0706.2003.12559.x

Alerstam, T., Lindström, Å., 1990. Optimal Bird Migration: The Relative Importance of Time, Energy, and Safety, in: Bird Migration. Springer Berlin Heidelberg, Berlin, Heidelberg, pp. 331–351. doi:10.1007/978-3-642-74542-3_22

Allaire, J.J., Gandrud, C., Russell, K., Yetman, C., 2017. networkD3: D3 JaaScript Network Graphs from R.

Allan, S.E., Smith, B.W., Anderson, K.A., 2012. Impact of the Deepwater Horizon Oil Spill on Bioavailable Polycyclic Aromatic Hydrocarbons in Gulf of Mexico Coastal Waters. Environ. Sci. Technol. 46, 2033–2039. doi:10.1021/es202942q

Alonso-Alvarez, C., Munilla, I., López-Alonso, M., Velando, A., 2007. Sublethal toxicity of the Prestige oil spill on yellow-legged gulls. Environ. Int. 33, 773–781.

doi:10.1016/j.envint.2007.02.012

Anderson, D.H., 2006. Role of lipids in the MAPK signaling pathway. Prog. Lipid Res. 45, 102–119. doi:10.1016/j.plipres.2005.12.003

Andren, H., 1992. Corvid density and nest predation in relation to forest fragmentation: a landscape perspective. Ecology 73, 794–804. doi:10.2307/1940158

Andres, B.A., Smith, P.A., Morrison, R.I.G., Gratto-Trevor, C.L., Brown, S.C., Friis, C.A., 2012. Population estimates of North American shorebirds, 2012. Wader Study Gr. Bull 119, 178–194.

Angrish, M.M., Mets, B.D., Jones, A.D., Zacharewski, T.R., 2012. Dietary fat is a lipid source in 2,3,7,8-tetrachlorodibenzo-ρ-dioxin (TCDD)-elicited hepatic steatosis in C57BL/6 mice. Toxicol. Sci. 128, 377–86. doi:10.1093/toxsci/kfs155

Ankley, G.T., Bennett, R.S., Erickson, R.J., Hoff, D.J., Hornung, M.W., Johnson, R.D., Mount, D.R., Nichols, J.W., Russom, C.L., Schmieder, P.K., Serrrano, J.A., Tietge, J.E., Villeneuve, D.L., 2010. Adverse outcome pathways: A conceptual framework to support ecotoxicology research and risk assessment. Environ. Toxicol. Chem. 29, 730–741. doi:10.1002/etc.34

Arlt, D., Olsson, P., Fox, J.W., Low, M., Part, T., 2015. Prolonged stopover duration characterises migration strategy and constraints of a long-distance migrant songbird. Anim. Migr. 2, 47–62.

Atkinson, P.W., Baker, A.J., Bennett, K.A., Clark, N.A., Clark, J.A., Cole, K.B., Dekinga, A., Dey, A., Gillings, S., González, P.M., Kalasz, K., Minton, C.D.T., Newton, J., Niles, L.J., Piersma, T., Robinson, R.A., Sitters, H.P., 2007. Rates of mass gain and energy deposition in red knot on their final spring staging site is both time- and condition-dependent. J. Appl. Ecol. 44, 885–895. doi:10.1111/j.1365-2664.2007.01308.x

Atshaves, B.P., Martin, G.G., Hostetler, H.A., McIntosh, A.L., Kier, A.B., Schroeder, F., 2010. Liver fatty acid binding protein and obesity. J. Nutr. Biochem. 21, 1015–1032.

Bagby, S.C., Reddy, C.M., Aeppli, C., Fisher, G.B., Valentine, D.L., 2017. Persistence and biodegradation of oil at the ocean floor following *Deepwater Horizon*. Proc. Natl. Acad. Sci. 114, E9–E18. doi:10.1073/pnas.1610110114

Baird, M.F., Graham, S.M., Baker, J.S., Bickerstaff, G.F., 2012. Creatine kinase- and exercise-related muscle damage implications for muscle performance and recovery. J. Nutr. Metab. 2012, 960363. doi:10.1155/2012/960363

Bairlein, F., 2002. How to get fat: Nutritional mechanisms of seasonal fat accumulation in migratory songbirds. Naturwissenschaften 89, 1–10. doi:10.1007/s00114-001-0279-6

Baker, A., Gonzalez, P., Morrison, R.I.G., Harrington, B.A., 2013. Red Knot (Calidris canutus), in: Polle, A.F. (Ed.), The Birds of North America Online. Cornell Lab of Ornithology, Ithaca, New York.

Baker, A.J., Gonzalez, P.M., Minton, C.D.T., Carter, D.B., Niles, L.J., do Nascimento, I., Piersma, T., 2001. Hemisperic problems in the conservation of red knots (Calidris canutus rufa), in: Proceedings of the VI Neotropical Ornithological Congress, International Shorebird Symposium, Moterrey, Mexico. Western Hemisphere Shorebird Reserve Network, Monomet, MA, pp. 21–28.

Baker, A.J., Gonzalez, P.M., Piersma, T., Niles, L.J., de Lima Serrano do Nascimento, I., Atkinson, P.W., Clark, N.A., Minton, C.D.T., Peck, M.K., Aarts, G., 2004. Rapid

population decline in red knots: fitness consequences of decreased refuelling rates and late arrival in Delaware Bay. Proc. R. Soc. B Biol. Sci. 271, 875–882. doi:10.1098/rspb.2003.2663

Balseiro, A., Espí, A., Márquez, I., Pérez, V., Ferreras, M.C., Marín, J.F.G., Prieto, J.M., Má Rquez, I., Pé Rez, V., García Marín, J.F., 2005. Pathological features in marine birds affected by the Prestige's oil spill in the north of Spain. J. Wildl. Dis. 41, 371–378. doi:10.7589/0090-3558-41.2.371

Bank, M.S., Chesney, E., Shine, J.P., Maage, A., Senn, D.B., 2007. Mercury bioaccumulation and trophic transfer in sympatric snapper species from the Gulf of Mexico. Ecol. Appl. 17, 2100–2110. doi:10.1890/06-1422.1

Barton, K., 2017. MuMIn: Multi-model inference.

Bates, D., Machler, M., Bolker, B., Walker, S., 2015. Fitting linear mixed-effects models using lme4. J. Stat. Softw. 67, 1–48. doi:10.18637/jss.v067.i01

Battley, P.F., Warnock, N., Tibbitts, T.L., Gill, R.E.J., Piersma, T., Hassell, C., Douglas, D.C., Mulcahy, D.M., Gartrell, B.D., Schuckard, R., Melville, D.S., Riegen, A.C., 2012. Contrasting extreme long-distance migration patterns in bar-tailed godwits Limosa lapponica. J. Avian Biol. 43, 21–32.

Bayly, N.J., Gómez, C., Hobson, K.A., González, A.M., Rosenberg, K. V, 2012. Fall migration of the Veery (Catharus fuscescens) in northern Colombia: Determining the energetic importance of a stopover site. Auk 129, 449–459. doi:10.1525/auk.2012.11.188

Benedetti, M., Giuliani, E., Regoli, F., 2015. Oxidative metabolism of chemical pollutants in marine organisms: molecular and biochemical biomarkers in environmental toxicology. Ann. N. Y. Acad. Sci. 1340, 8–19.

Berthold, P., Fiedler, W., Schlenker, R., Querner, U., 1998. 25-Year study of the population development of Central European songbirds: A general decline, most evident in long-distance migrants. Naturwissenschaften 85, 350–353. doi:10.1007/s001140050514

Beyer, J., Trannum, H.C., Bakke, T., Hodson, P. V., Collier, T.K., 2016. Environmental effects of the Deepwater Horizon oil spill: A review. Mar. Pollut. Bull. 110, 28–51. doi:10.1016/j.marpolbul.2016.06.027

Bhattacharyya, A., Chattopadhyay, R., Mitra, S., Crowe, S.E., 2014. Oxidative stress: an essential factor in the pathogenesis of gastrointestinal mucosal diseases. Physiol. Rev. 94, 329–54. doi:10.1152/physrev.00040.2012

Bianchini, K., Morrissey, C.A., 2018. Polycyclic aromatic hydrocarbon exposure impairs pre-migratory fuelling in captively-dosed Sanderling (Calidris alba). Ecotoxicol. Environ. Saf. 161, 383–391.

Bijlsma, R.G., 1990. Predation by large falcon species on wintering waders on the Banc d'Arguin, Mauritania. Ardea 78, 75–82.

BirdLife International, 2017. Calidris canutus (amended version of 2016 assessment).

Boehm, P.D., Page, G., Gilfillan, E.S., Bence, A.E., Burns, W.A., Mankiewicz, P.J., 1998. Study of the fates and effects of the Exxon Valdez oil spill on benthic sediments in two bays in Prince William Sound, Alaska. 1. Study design, chemistry, and source fingerprinting. Environ. Sci. Technol. 32, 567–576.

Bolker, B., R Development Core Team, 2017. bbmle: Tools for general maximum likelihood estimation.

Bols, N.C., Schirmer, K., Joyce, E.M., Dixon, D.G., Greenberg, B.M., Whyte, J.J., 1999. Ability of polycyclic aromatic hydrocarbons to induce 7-ethoxyresorufin-O-deethylase activity in a trout liver cell line. Ecotoxicol. Environ. Saf. 44, 118–128.

Bonisoli-Alquati, A., Stouffer, P.C., Turner, R.E., Woltmann, S., Taylor, S.S., 2016. Incorporation of Deepwater Horizon oil in a terrestrial bird. Environ. Res. Lett. 11, 114023. doi:10.1088/1748-9326/11/11/114023

Bost, F., Aouadi, M., Caron, L., Binétruy, B., 2005. The role of MAPKs in adipocyte differentiation and obesity. Biochimie 87, 51–56. doi:10.1016/j.biochi.2004.10.018

Both, C., Visser, M.E., 2001. Adjustment to climate change is constrained by arrival date in a long-distance migrant bird. Nature 411, 296–298.

Braun, E.J., Sweazea, K.L., 2008. Glucose regulation in birds. Comp. Biochem. Physiol. Part B 151, 1–9.

Brewster, D.W., Matsumura, F., 1988. Reduction of adipose tissue lipoprotein lipase activity as a result of in vivo administration of 2,3,7,8-tetrachlorodibenzo-p-dioxin to the guinea big. Biochem. Pharmacol. 11, 2247–2253.

Brewster, D.W., Uriah, L.C., Birnbaum, L.S., 1988. The acute toxicity of 2,3,4,7,8-pentachlorodibenzofuran (4PeCDF) in the male Fischer rat. Fundam. Appl. Toxicol. 11, 236–249.

Briggs, K.T., Gershwin, M.E., Anderson, D.W., 1997. Consequences of petrochemical ingestion and stress on the immune system of seabirds. ICES J. Mar. Sci. 54, 718–725. doi:10.1006/jmsc.1997.0254

Briggs, K.T., Yoshida, S.H., Gershwin, M.E., 1996. The influence of petrochemicals and stress on the immune system of seabirds. Regul. Toxicol. Pharmacol. 23, 145–155.

Brodie, A.E., Azarenko, V.A., 1996. 2,3,7,8-Tetrachlorodibenzo-p-dioxin (TCDD) inhibition of fat cell differentiation. Toxicol. Lett. 84, 55–59.

Brunstrom, B., 1991. Embryolethality and induction of 7-etholyresorufin O-deethylase in chick embryos by polychlorinated biphenyls and polycyclic aromatic hydrocarbons having Ah receptor affinity. Chem. Biol. Interact. 81, 69–77.

Buesen, R., Chorley, B.N., da Silva Lima, B., Daston, G., Deferme, L., Ebbels, T., Gant, T.W., Goetz, A., Greally, J., Gribaldo, L., Hackermüller, J., Hubesch, B., Jennen, D., Johnson, K., Kanno, J., Kauffmann, H.-M., Laffont, M., McMullen, P., Meehan, R., Pemberton, M., Perdichizzi, S., Piersma, A.H., Sauer, U.G., Schmidt, K., Seitz, H., Sumida, K., Tollefsen, K.E., Tong, W., Tralau, T., van Ravenzwaay, B., Weber, R.J.M., Worth, A., Yauk, C., Poole, A., 2017. Applying 'omics technologies in chemicals risk assessment: Report of an ECETOC workshop. Regul. Toxicol. Pharmacol. doi:10.1016/j.yrtph.2017.09.002

Burger, A.E., 1993. Estimating the mortality of seabirds following oil spills: Effects of spill volume. Mar. Pollut. Bull. 26, 140–143. doi:10.1016/0025-326X(93)90123-2

Burger, J., 2017. Avian Resources of the Northern Gulf of Mexico, in: Ward, C.H. (Ed.), Habitats and Biota of the Gulf of Mexico: Before the Deepwater Horizon Oil Spill. Springer Nature, New York, NY, pp. 1353–1477.

Burger, J., Carlucci, S.A., Jeitner, C.W., Niles, L., 2007. Habitat choice, distrubance, and management of foraging shorebirds and gulls at a migratory stopover. J. Coast. Res. 23, 1159–1166. doi:10.2112/04-0393.1

Burger, J., Tsipoura, N., 1998. Experimental oiling of Sanderlings (Calidris alba): Behavior and

weight changes. Environ. Toxicol. Chem. 17, 1154–1158.

Burnham, K., Anderson, D., 2002. Model selection and multimodel inference: a practical information-theoretic approach. Springer-Verlag, New York.

Bursian, S.J., Alexander, C.R., Cacela, D., Cunningham, F.L., Dean, K.M., Dorr, B.S., Ellis, C.K., Godard-Codding, C.A., Guglielmo, C.G., Hanson-Dorr, K.C., Harr, K.E., Healy, K.A., Hooper, M.J., Horak, K.E., Isanhart, J.P., Kennedy, L. V., Link, J.E., Maggini, I., Moye, J.K., Perez, C.R., Pritsos, C.A., Shriner, S.A., Trust, K.A., Tuttle, P.L., 2017a. Overview of avian toxicity studies for the Deepwater Horizon Natural Resource Damage Assessment. Ecotoxicol. Environ. Saf. 142, 1–7. doi:10.1016/j.ecoenv.2017.03.046

Bursian, S.J., Dean, K.M., Harr, K.E., Kennedy, L., Link, J.E., Maggini, I., Pritsos, C., Pritsos, K.L., Schmidt, R.E., Guglielmo, C.G., 2017b. Effect of oral exposure to artificially weathered Deepwater Horizon crude oil on blood chemistries, hepatic antioxidant enzyme activities, organ weights and histopathology in western sandpipers (Calidris mauri). Ecotoxicol. Environ. Saf. doi:10.1016/j.ecoenv.2017.03.045

Butler, P.J., Woakes, A.J., 2001. Seasonal hypothermia in a large migrating bird: saving energy for fat deposition? J. Exp. Biol. 204, 1361–1367.

Butler, R., Peakall, D.B., Leighton, F.A., Borthwick, J., Harmon, R., 1986. Effects of crude oil exposure on standard metabolic rate of Leach's storm-petrel. Condor 88, 248–249.

Campbell, T., Benedet, L., Mann, D., Resio, D., Hester, M.W., Materne, M., 2004. Restoration tools for Louisiana's Gulf shoreline, Ecosystem Restoration Study, Volume 4: Appendix D - Louisiana Gulf Shoreline Restoration Report. Louisiana Coastal Area (LCA), Louisiana.

Camphuysen, C., Leopold, M., 2004. The Tricolor oil spill: characteristics of seabirds found oiled in the Netherlands. Atl. Seabirds 6, 109–128.

Canal, D., Jovani, R., Potti, J., 2012. Male decisions or female accessibility? Spatiotemporal patterns of extra pair paternity in a songbird. Behav. Ecol. 23, 1146–1153.

Carpenter, F.L., Hixon, M.A., Beauchat, C.A., Russell, R.W., Paton, D.C., 1993. Biphasic mass gain in migrant hummingbirds: body composition changes, torpor, and ecological significance. Ecology 74, 1173–1182.

Cavanaugh, K.P., Goldsmith, A.R., Holmes, W.N., Follett, B.K., 1983. Effects of ingested petroleum on the plasma prolactin levels during incubation and the breeding success of paired mallard ducks. Arch. Environ. Contam. Toxicol. 12, 335–341. doi:10.1007/BF01059411

Cavanaugh, K.P., Holmes, W.N., 1987. Effects of ingested petroleum on the development of ovarian endocrine function in photostimulated mallard ducks (Anas platyrhynchos). Arch. Environ. Contam. Toxicol. 16, 247–253. doi:10.1007/BF01055806

Chong, M.F., Fielding, B.A., Frayn, K.N., 2007. Metabolic interaction of dietary sugars and plasma lipids with a focus on mechanisms and de novo lipogenesis. Proc. Nutr. Soc. 66, 52–59.

Clemens, R.S., Rogers, D.I., Hansen, B.D., Gosbell, K., Minton, C.D.T., Straw, P., Bamford, M., Woehler, E.J., Milton I, D.A., Weston, M.A., Venables, B., Weller, D., Hassell, C., Rutherford, B., Onton, K., Herrod, A., Studds, C.E., Choi, C.-Y., Dhanjal-Adams, K.L., Murray, N.J., Skilleter, G.A., Fuller, R.A., 2016. Continental-scale decreases in shorebird populations in Australia. Emu 116, 119–135. doi:10.1071/MU15056

Cohen, E.B., Barrow, W.C.J., Buler, J.J., Deppe, J.L., Farnsworth, A., Marra, P.P., McWilliams,

S.R., Mehlman, D.W., Wilson, R.R., Woodrey, M.S., Moore, F.R., 2017. How do en route events around the Gulf of Mexico influence migratory landbird populations? Condor 119, 327–343.

Cooper, N.W., Murphy, M.T., Redmond, L.J., Dolan, A.C., 2010. Reproductive correlates of spring arrival date in the eastern kingbird Tyrannus tyrannus. Ornitology 152, 143–152.

Cooper, N.W., Sherry, T.W., P, M.P., 2015. Experimental reduction of winter food decreases body condition and delays migration in a long-distance migratory bird. Ecology 96, 1933–1942.

Cornelius, J.M., Boswell, T., Jenni-Eiermann, S., Breuner, C.W., Ramenofsky, M., 2012. Contributions of endocrinology to the migration life history of birds. Gen. Comp. Endocrinol. 190, 47–60. doi:10.1016/j.ygcen.2013.03.027

Couture, L.A., Elwell, M.R., Birnbaum, L.S., 1988. Dioxin-like effects observed in male rats following exposure to octachlorodibenzo-p-dioxin (OCDD) during a 13-week study. Toxicol. Appl. Pharamacology 93, 31–46.

Covino, K.M., Holberton, R.L., Morris, S.R., Covino, K.M., Morris, -S R, 2014. Factors influencing migratory decisions made by songbirds on spring stopover. J. Avian Biol. 46, 73–80. doi:10.1111/jav.00463

Crewe, T.L., Crysler, Z., Taylor, P., 2018. Motus R Book: A walk through the use of R for Motus automated radio-telemetry data [WWW Document]. URL https://motus.org/MotusRBook/index.html (accessed 2.26.18).

Crocker, A.D., Cronshaw, J., Holmes, W.N., 1975. The effect of several crude oils and some petroleum distillation fractions on intestinal absorption in ducklings (Anas platyhynchos). Environ. Physiol. Biochem. 5, 92–106.

Crump, D., Farhat, A., Chiu, S., Williams, K.L., Jones, S.P., Langlois, V.S., 2016. Use of a novel double-crested cormorant ToxChip PCR array and the EROD assay to determine effects of environmental contaminants in primary hepatocytes. Environ. Sci. Technol. 50, 3265–3274. doi:10.1021/acs.est.5b06181

Crump, D., Williams, K.L., Chiu, S., Zhang, Y., Martin, J.W., 2017. Athabasca oil sands petcoke extract elicits biochemical and transcriptomic effects in avian hepatocytes. Environ. Sci. Technol. 51, 5783–5792. doi:10.1021/acs.est.7b00767

Cunningham, F., Dean, K., Hanson-Dorr, K.C., Healy, K., Horak, K., Link, J., Shriner, S., Bursian, S., Dorr, B., 2017. Developent of methods for avian oil toxicity studies using the double crested cormorant (Phalacrocorax auritus). Ecotoxicol. Environ. Saf. 141, 199–208.

de Gelder, S., Saele, O., de Veen, B.T.H., Vos, J., Flik, G., Berntssen, M.H.G., Klaren, P.H.., 2017. The polycyclic aromatic hydrocarbons benzo[a]pyrene and phenanthrene inhibit intestinal lipase activity in rainbow trout (Oncorhynchus mykiss). Comp. Biochem. Physiol. Part C 198, 1–8.

Deepwater Horizon Natural Resource Damage Assessment Trustees, 2016. Deepwater Horizon oil spill: Final Programmatic Damage Assessment and Restoration Plan and Final Programmatic Environmental Impact Statement.

DeLaune, R.D., Gambrell, R.P., Pardue, J.H., Patrick, W.H., 1990. Fate of Petroleum Hydrocarbons and Toxic Organics in Louisiana Coastal Environments. Estuaries 13, 72. doi:10.2307/1351434

Denison, M.S., Nagy, S.R., 2003. Activation of the aryl hydrocarbon receptor by structurally

diverse exogenous and endogenous chemicals. Annu. Rev. Pharmacol. Toxicol. 43, 309–334.

Deppe, J.L., Ward, M.P., Bolus, R.T., Diehl, R.H., Celis-Murillo, A., Zenzal, T.J., Moore, F.R., Benson, T.J., Smolinsky, J.A., Schofield, L.N., Enstrom, D.A., Paxton, E.H., Bohrer, G., Beveroth, T.A., Raim, A., Obringer, R.L., Delaney, D., Cochran, W.W., 2015. Fat, weather, and date affect migratory songbirds' departure decisions, routes, and time it takes to cross the Gulf of Mexico. Proc. Natl. Acad. Sci. 112, E6331–E6338. doi:10.1073/pnas.1503381112

Dietz, M.W., Jenni-Eiermann, S., Piersma, T., 2009. The use of plasma metabolites to predict weekly body-mass change in Red knots. Condor 111, 88–99. doi:10.1525/cond.2009.080112

Diggs, D.L., Huderson, A.C., Harris, K.L., Myers, J.N., Banks, L.D., Rekhadevi, P. V, Niaz, M.S., Ramesh, A., 2011. Polycyclic aromatic hydrocarbons and digestive tract cancers: a perspective. J. Environ. Sci. Health. C. Environ. Carcinog. Ecotoxicol. Rev. 29, 324–57. doi:10.1080/10590501.2011.629974

Doering, J.A., Wiseman, S., Beitel, S.C., Tendler, B.J., Giesy, J.P., Hecker, M., 2012. Tissue specificity of aryl hydrocarbon receptor (AhR) mediated responses and relative sensitivity of white sturgeon (Acipenser transmontanus) to an AhR agonist. Aquat. Toxicol. 114, 125–133. doi:10.1016/j.aquatox.2012.02.015

Dolman, P.M., Sutherland, W.J., 1994. The response of bird populations to habitat loss. Ibis (Lond. 1859). 137, S38–S46.

Dossman, B.C., Mitchell, G.W., Norris, D.R., Taylor, P.D., Guglielmo, C.G., Matthews, S.N., Rodewald, P.G., 2016. The effects of wind and fuel stores on stopover departure behavior across a migratory barrier. Behav. Ecol. 27, 567–574. doi:10.1093/beheco/arv189

Douben, P.E.T., 2003. PAHs: An Ecotoxicological Perspective. John Wiley & Sons.

Drake, K.R.K.L., Thompson, J.E., Drake, K.R.K.L., Zonick, C., 2001. Movements, habitat use, and survival of nonbreeding piping plovers. Condor 103, 259–267. doi:10.1650/0010-5422(2001)103[0259:MHUASO]2.0.CO;2

Duffy, L., Bowyer, R., Testa, J., Faro, J., 1996. Acute phase proteins and cytokines in Alaskan mammals as markers of chronic exposure to environmental pollutants, American Fisheries Society Symposium. 1996.

Duijns, S., Niles, L.J., Dey, A., Aubry, Y., Friis, C., Koch, S., Anderson, A.M., Smith, P.A., 2017. Body condition explains migratory performance of a long-distance migrant. Proc. R. Soc. B Biol. Sci. 284, 20171374. doi:10.1098/rspb.2017.1374

Eisler, R., 2000. Handbook of Chemical Risk Assessement. Health Hazards to Humans, Plants, and Animals. Lewis Publishers, Boca Raton, Florida.

Eisler, R., 1987. Polycyclic aromatic hydrocarbon hazards to fish, wildlife, and invertebrates: a synoptic review.

Elliott, J.E., Harris, M.L., Wilson, L.K., Smith, B.D., Batchelor, S.P., Maguire, J., 2007. Butyltins, trace metals and morphological variables in surf scoter (Melanitta perspicillata) wintering on the south coast of British Columbia, Canada. Environ. Pollut. 149, 114–124.

Ely, C.R., Meixell, B.W., 2016. Demographic outcomes of diverse migration strategies assessed in a metapopulation of tundra swans. Mov. Ecol. 4, 10.

Eng, M.L., Stutchbury, B.J.M., Morrissey, C.A., 2017. Imidacloprid and chlorpyrifos

insecticides impair migratory ability in a seed-eating songbird. Sci. Rep. 7, 15176.

Esler, D., Ballachey, B.E., Bowen, L., Miles, A.K., Dickson, R.D., Henderson, J.D., 2017. Cessation of oil exposure in harlequin ducks after the Exxon Valdez oil spill: Cytochrome P4501A biomarker evidence. Environ. Toxicol. Chem. 36, 1294–1300. doi:10.1002/etc.3659

Esler, D., Trust, K.A., Ballachey, B.E., Iverson, S.A., Lewis, T.L., Rizzolo, D.J., Mulcahy, D.M., Miles, A.K., Woodin, B.R., Stegeman, J.J., Henderson, J.D., Wilson, B.W., 2010. Cytochrome P4501A biomarker indication of oil exposure in harlequin ducks up to 20 years after the Exxon Valdez oil spill. Environ. Toxicol. Chem. 29, 1021–1199. doi:10.1002/etc.129

Espin, S., Ruiz, S., Sanchez-Virosta, P., Lilley, T., Eeva, T., 2017. Oxidative status in relation to metal pollution and calcium availability in pied flycatcher nestlings - A calcium manipulation experiment. Environ. Pollut. 229, 448–458.

Faaborg, J., Holmes, R.T., Anders, A.D., Bildstein, K.L., Dugger, K.M., Gauthreaux, S.A., Heglund, P., Hobson, K.A., Jahn, A.E., Johnson, D.H., Latta, S.C., Levey, D.J., Marra, P.P., Merkord, C.L., Nol, E., Rothstein, S.I., Sherry, T.W., Sillett, T.S., Thompson, F.R.I., Warnock, N., 2010. Conserving migratory land birds in the New World: Do we know enough? Ecol. Appl. 20, 398–418.

Fader, K.A., Nault, R., Zhang, C., Kumagai, K., Harkema, J.R., Zacharewski, T.R., 2017. 2,3,7,8-Tetrachlorodibenzo-p-dioxin (TCDD)-elicited effects on bile acid homeostasis: Alterations in biosynthesis, enterohepatic circulation, and microbial metabolism. Sci. Rep. 7, 5921. doi:10.1038/s41598-017-05656-8

Farmer, A.H., Weins, J.A., 1999. Models and reality: time-energy trade-offs in Pectoral Sandpiper (Calidris melanotos) migration. Ecology 80, 2566–2580.

Finch, T., Pearce-Higgins, J.W., Leech, D.I., Evans, K.L., 2014. Carry-over effects from passage regions are more important than breeding climate in determining the breeding phenology and performance of three avian migrants of conservation concern. Biodivers. Conserv. 23, 2427–2444. doi:10.1007/s10531-014-0731-5

Fletcher, N., Wahlstrom, D., Lundberg, R., Nilsson, C.B., Nilsson, K.C., Stockling, K., Hellmold, H., Hakansson, H., 2005. 2,3,7,8-Tetrachlorodibenzo-p-dioxin (TCDD) alters the mRNA expression of critical genes associated with cholesterol metabolism, bile acid biosynthesis, and bile transport in rat liver: a microarray study. Toxicol. Appl. Pharmacol. 207, 1–24.

Fowler, G.S., Wingfield, J.C., Boersma, P.D., Dee Boesma, P., Boersma, P.D., 1995. Hormonal and reproductive effects of low levels of petroleum fouling in Magellanic penguins (Spheniscus magellanicus). Am. Ornithol. Soc. 112, 382–389.

Fransson, T., Weber, T.P., 1997. Migratory fuelling in blackcaps (Sylvia atricapilla) under perceived risk of predation. Behav. Ecol. Sociobiol. 41, 75–80.

Fraser, R., Heslop, V.R., Murray, F.E.M., Day, W.A., 1986. Ultrastructural studies of the portal transport of fat in chickens. Br. J. Exp. Pathol. 67, 783–791.

Fretwell, S.D., 1980. Evolution of migration in relation to factors regulating bird numbers, in: Keast, A., Morton, E.S. (Eds.), Migrant Birds in the Neotropics. Smithsonian Institution Press, Washington, D.C.

Fry, D.M., Lowenstine, L.J., 1985. Pathology of common mures and cassin's auklets exposed to oil. Arch. Environ. Contam. Toxicol. 14, 725–737.

Gallardo, J., Velarde, E., Arreola, R., 2004. Birds of the Gulf of Mexico and the priority areas for their conservation, in: Wither, K., Nipper, M. (Eds.), Environmental Analysis of the Gulf of Mexico, Publication Series 1. Texas A&M University Press, College Station, TX, pp. 18–194.

Gao, X., Xie, C., Wang, Y., Luo, Y., Yagai, T., Sun, D., Qin, X., Krausz, K.W., Gonzalez, F.J., 2016. The antiandrogen flutamide is a novel aryl hydrocarbon receptor ligand that disrupts bile acid homeostasis in mice through induction of Abcc4. Biochem. Pharmacol. 119, 93–104. doi:10.1016/j.bcp.2016.08.021

Gehart, H., Kumpf, S., Ittner, A., Ricci, R., 2010. MAPK signalling in cellular metabolism: stress or wellness? EMBO Rep. 11, 834–40. doi:10.1038/embor.2010.160

GESAMP, 2007. Estimates of Oil Entering the Marine Environmenta from Seabased Activities. London.

Gill, J.A., Norris, K., Potts, P.M., Gunnarsson, T.G., Atkinson, P.W., Sutherland, W.J., 2001. The buffer effect and large-scale population regulation in migratory birds. Nature 412, 436–438.

Gill, R.E.J., Piersma, T., Hufford, G., Servranckx, R., Riegen, A., 2005. Crossing the ultimate ecological barrier: evidence for an 11 000-km-long nonstop flight from Alaska to New Zealand and eastern Australia by bar-tailed godwits. Condor 1, 1–20.

Gohlke, J.M., Doke, D., Tipre, M., Leader, M., Fitzgerald, T., 2011. A review of seafood safety after the Deepwater Horizon blowout. Environ. Health Perspect. 119, 1062–1069. doi:10.1289/ehp.1103507

Golet, G.H., Seiser, P.E., McGuire, A.D., Roby, D.D., Fischer, J.B., Kuletz, K.J., Irons, D.B., Dean, T.A., Jewett, S.C., Newman, S.H., 2002. Long-term direct and indirect effects of the 'Exxon Valdez' oil spill on pigeon guillemots in Prince William Sound, Alaska. Mar. Ecol. Prog. Ser. 241, 287–304. doi:10.2307/24866124

Gómez, C., Bayly, N.J., Norris, D.R., Mackenzie, S.A., Rosenberg, K. V., Taylor, P.D., Hobson, K.A., Daniel Cadena, C., 2017. Fuel loads acquired at a stopover site influence the pace of intercontinental migration in a boreal songbird. Sci. Rep. 7, 1–11. doi:10.1038/s41598-017-03503-4

Goymann, W., Spina, F., Ferri, A., Fusani, L., 2010. Body fat influences departure from stopover sites in migratory birds: evidence from whole-island telemetry. Biol. Lett. 6, 478–481. doi:10.1098/rsbl.2009.1028

Groh, K.J., Carvalho, R.N., Chipman, J.K., Denslow, N.D., Halder, M., Murphy, C.A., Roelofs, D., Rolaki, A., Schirmer, K., Watanabe, K.H., 2015. Development and application of the adverse outcome pathway framework for understanding and predicting chronic toxicity: I. Challenges and research needs in ecotoxicology. Chemosphere 120, 764–777. doi:10.1016/j.chemosphere.2014.09.068

Grond, K., Ntiamoa-Baidu, Y., Piersma, T., Reneerkens, J., 2015. Prey type and foraging ecology of Sanderlings *Calidris alba* in different climate zones: are tropical areas more favourable than temperate sites? PeerJ 3, e1125. doi:10.7717/peerj.1125

Gudmundsson, G.A., Lindstrom, A., Alerstam, T., 1991. Optimal fat loads and long-distance flights by migrating Knots Calidris canutus, Sanderlings C. alba and Turnstones Arenaria interpres. Ibis (Lond. 1859). 133, 140–152. doi:10.1111/j.1474-919X.1991.tb04825.x

Guglielmo, C.G., 2018. Obese super athletes: fat-fueled migration in birds and bats. J. Exp. Biol. 221, jeb165753.

Guglielmo, C.G., 2010. Move that fatty acid: fuel selection and transport in migratory birds and bats. Integr. Comp. Biol. 50, 336–345.

Guglielmo, C.G., Gerson, A.R., Price, E.R., Hays, Q.R., 2017. The effects of dietary macronutrients on flight ability, energetics, and fuel metabolism of yellow-rumped warblers Setophaga coronata. J. Avian Biol. 48, 133–148.

Guglielmo, C.G., Piersma, T., Williams, T.D., 2001. A sport-physiological perspective on bird migration: evidence for flight-induced muscle damage. J. Exp. Biol. 204, 2683–90.

Guglielmo, C.G., Williams, T.D., 2003. Phenotypic flexibility of body composition in relation to migratory state, age, and sex in the western sandpiper (Calidris mauri). Physiol. Biochem. Zool. 76, 84–98.

Haeusler, R.A., Camastra, S., Nannipieri, M., Astiarraga, B., Castro-Perez, J., Xie, D., Wang, L., Chakravarthy, M., Ferrannini, E., 2016. Increased bile acid synthesis and impaired bile acid transport in human obesity. J. Clin. Endocrinol. Metab. 101, 1935–1944.

Harr, K.E., Reavill, D.R., Bursian, S.J., Cacela, D., Cunningham, F., Dean, K.M., Dorr, B.S., Hanson-Dorr, K.C., Healy, K., Horak, K., Link, J.E., Shriner, S., Schmidt, R.E., 2017a. Organ weights and histopathology of double-crested cormorants (Phalacrocorax auritus) dosed orally or dermally with artificially weathered Mississippi Canyon 252 crude oil. Ecotoxicol. Environ. Saf. 146, 52–61.

Harr, K.E., Rishniw, M., Rupp, T.L., Cacela, D., Dean, K.M., Dorr, B.S., Hanson-Dorr, K.C., Healy, K., Horak, K., Link, J.E., Reavill, D.R., Bursian, S.J., Cunningham, F., 2017b. Dermal exposure to weathered MC252 crude oil results in echocardiographically identifiable systolic myocardial dysfunction in double-crested cormorants (Phalacrocorax auritus). Ecotoxicol. Environ. Saf. 146, 76–82.

Harrington, W.W., Britt, C.S., Wilson, J.G., Milliken, N.O., Binz, J.G., Lobe, D.C., Oliver, W.R., Lewis, M.C., Ignar, D.M., 2007. The effect of PPARα, PPARδ, PPARγ, and PPARpan agonists on body weight, body mass, and serum lipid profiles in diet-induced obese AKR/J mice. PPAR Res. 2007, 1–13. doi:10.1155/2007/97125

Harris, M., Wanless, S., Webb, A., 2011. Changes in body mass of common guillemots Uria aalge in southeast Scotland throughout the year: implication for the release of cleaned birds. Ringing Migr. 20, 134–142.

Harris, M.L., Elliott, J.E., 2011. Effects of polychlorinated biphenyls, dibenzo-p-dioxins and dibenzofurans, and polybrominated diphenyl ethers in wild birds, in: Beyer, W.N., Meador, J.P. (Eds.), Environmental Contaminants in Biota: Interpreting Tisue Concentrations. CRC Press, Boca Raton, Florida, pp. 477–528.

Harrison, R.M., Smith, D.J.T., Luhana, L., 1996. Source apportionment of atmospheric polycyclic aromatic hydrocarbons collected from an urban location in Birmingham, U.K. Environ. Sci. Technol. 30, 825–832. doi:10.1021/es950252d

Harrison, X.A., Blount, J.D., Inger, R., Norris, D.R., Bearhop, S., 2011. Carry-over effects as drivers of fitness differences in animals. J. Anim. Ecol. 80, 4–18. doi:10.1111/j.1365-2656.2010.01740.x

Harvey, S., Philips, J., 1981. Reproductive performance and endocrine responses to ingested petroleum in domestic ducks (Anas platyrynckos). Gen. Comp. Endocrinol. 45, 372–380.

Head, J.A., Jeffery, R.W., Farmahin, R., Kennedy, S.W., 2015. Potency of polycyclic aromatic hydrocarbons (PAHs) for induction of ethoxyresorufin- o -deethylase (EROD) activity in hepatocyte cultures from chicken, pekin duck, and greater scaup. Environ. Sci. Technol. 49,

3787–3794. doi:10.1021/acs.est.5b00125

Hedenström, A., Alerstam, T., 1997. Optimum fuel loads in migratory birds: Distinguishing between time and energy minimization. J. Theor. Biol. 189, 227–234. doi:10.1006/jtbi.1997.0505

Henkel, J.R., Sigel, B.J., Taylor, C.M., 2012. Large-scale impacts of the Deepwater Horizon oil spill: Can local disturbance affect distant ecosystems through migratory shorebirds? Bioscience 62, 676–685. doi:10.1525/bio.2012.62.7.10

Henkel, J.R., Taylor, C.M., 2015. Migration strategy predicts stopover ecology in shorebirds on the northern Gulf of Mexico. Anim. Migr. 2, 63–75. doi:10.1515/ami-2015-0003

Hermier, D., 1997. Lipoprotein metabolism and fattening in poultry. J. Nutr. 127, 805S–808S. doi:10.1093/jn/127.5.805S

Hewson, C.M., Thorup, K., Pearce-Higgins, J.W., Atkinson, P.W., 2016. Population decline is linked to migration route in the Common Cuckoo. Nat. Commun. 7, 1–8. doi:10.1038/ncomms12296

Hiebert, S., 1993. Seasonal Changes in body mass and use of torpor in a migratory hummingbird. Auk 110, 787–797.

Hofmann, A.F., 1999. The continuing importance of bile acids in liver and intestinal disease. Arch. Intern. Med. 159, 2647–2658.

Holmes, R.T., 2007. Understanding population change in migratory songbirds: long-term and experimental studies of Neotropical migrants in breeding and wintering areas. Ibis (Lond. 1859). 149, 2–13.

Hope, D.D., Lank, D.B., Smith, B.D., Ydenberg, R.C., 2011. Migration of two calidrid sandpiper species on the predator landscape: How stopover time and hence migration speed vary with geographical proximity to danger. J. Avian Biol. 42, 522–529. doi:10.1111/j.1600-048X.2011.05347.x

Hope, D.D., Lank, D.B., Ydenberg, R.C., 2014. Mortality-minimizing sandpipers vary stopover behavior dependent on age and geographic proximity to migrating predators. Behav. Ecol. Sociobiol. doi:10.2307/43599531

Horak, K.E., Bursian, S.J., Ellis, C.K., Dean, K.M., Link, J.E., 2017. Toxic effects of orally ingested oil from the Deepwater Horizon spill on laughing gulls. Ecotoxicol. Environ. Saf. 146, 83–90.

Hough, J.L., Baird, M.B., Sfeir, G.T., Pacini, C.S., Darrow, D., Wheelock, C., 1993. Benzo(a)pyrene enhances atherosclerosis in wite carneau and show racer pigeons. Arter. Thromb. 13, 1721–1727.

Houston, A.I., 2000. The strength of selection in the context of migration speed. Proc. Biol. Sci. 267, 2393–2395. doi:10.1098/rspb.2000.1296

Hughes, M.R., Kasserra, C., Thomas, B.R., 1990. Effect of externally applied bunker fuel on body mass and temperature, plasma concentration, and water flux of glaucous-winged gulls, Larus glaucescens. Can. J. Zool. 68, 716–721.

Iwano, S., Shibahara, N., Saito, T., Kamataki, T., 2006. Activation of p53 as a causal step for atherosclerosis induced by polycyclic aromatic hydrocarbons. FEBS Lett. 580, 890–893. doi:10.1016/J.FEBSLET.2006.01.009

Jarjour, C., Frei, B., Elliott, K.H., 2017. Associations between sex, age and species-specific climate sensitivity in migration. Anim. Migr. 4, 23–36. doi:10.1515/ami-2017-0004

Jehl, J.R.J., 1997. Fat loads and flightlessness in Wilson's Phalaropes. Condor 99, 538–543.

Jenni-Eiermann, S., Jenni, L., 1994. Plasma metabolite levels predict individual body-mass changes in a small long-distance migrant, the Garden Warbler. Group 111, 888–899.

Jenni-Eiermann, S., Jenni, L., Smith, S., Costantini, D., 2014. Oxidative stress in endurance flight: an unconsidered factor in bird migration. PLoS One 9, e97650.

Jenni, L., Jenni-Eiermann, S., 1998. Fuel supply and metabolic constraints in migrating birds. Joural Avian Biol. 29, 521–528.

Jenssen, B.M., 1994. Effects of oil pollution, chemically treated oil, and cleaning on the thermal balance of birds. Environ. Pollut. 86, 207–215. doi:10.1016/0269-7491(94)90192-9

Kahle, D., Wickam, H., 2013. ggmap: Spatial visualization with ggplot2. R J. 5, 144–161.

Kirby, J.S., Stattersfield, A.J., Butchart, S.H.M., Evans, M.I., Grimmett, R.F.A., Jones, V.R., O'Sullivan, J., Tucker, G., Newton, I., 2008. Key conservation issues for migratory land- and waterbird species on the world's major flyways. Bird Conserv. Int. 18, S49–S73.

Klaassen, M., Hoye, B.J., Nolet, B.A., Buttemer, W.A., 2012. Ecophysiology of avian migration in the face of current global hazards. Philos. Trans. R. Soc. Lond. B. Biol. Sci. 367, 1719–32. doi:10.1098/rstb.2012.0008

Klaassen, R.H.G., Alerstam, T., Carlsson, P., Fox, J.W., Lindström, Å., 2011. Great flights by great snipes: long and fast non-stop migration over benign habitats. Biol. Lett. 7, 833–835.

Koutsari, C., Ali, A.H., Mundi, M.S., Jensen, M.D., 2011. Storage of circulating free fatty acid in adipose tissue of postabsorptive humans: quantitative measures and implications for body fat distribution. Diabetes 60, 2032–40. doi:10.2337/db11-0154

Labarrere, C.R., 2016. Sanderling (Calidris alba) population structure and pollutant exposure at major winter and migratory stopover sites including Chaplin Lake, Saskatchewan. University of Saskatchewan, Saskatoon, SK, Canada.

Landys, M.M., Piersma, T., Guglielmo, C.G., Jukema, J., Ramenofsky, M., Wingfield, J.C., 2005. Metabolic profile of long-distance migratory flight and stopover in a shorebird. Proc. R. Soc. B Biol. Sci. 272, 295–302.

Latimer, J.S., Zheng, J., 2003. The Sources, Transport, and Fat of PAHs in the Marine Environment, in: Douben, P.E.T. (Ed.), PAHs: An Ecotoxicological Perspective. John Wiley & Sons.

Latta, S.C., Baltz, M.E., 1997. Population limitation in neotropical migratory birds: Comments on Rappole and McDonald (1994). Auk 114, 754–762.

Lattin, C.R., Romero, L.M., 2014. Chronic exposure to a low dose of ingested petroleum disrupts corticosterone receptor signalling in a tissue-specific manner in the house sparrow (Passer domesticus). Conserv. Physiol. 2, cou058.

Lee, J.H., Wada, T., Febbraio, M., He, J., Matsubara, T., Lee, M.J., Gonzalez, F.J., Xie, W., 2010. A novel role for the dioxin receptor in fatty acid metabolism and hepatic steatosis. Gastroenterology 139, 653–663. doi:10.1053/j.gastro.2010.03.033

Lee, S.-D., Ellwood, E.R., Park, S., Primack, R.B., 2011. Late-arriving barn swallows linked to population declines. Biol. Conserv. 144, 2182–2187. doi:10.1016/J.BIOCON.2011.05.009

Lee, S., Hong, S., Liu, X., Kim, C., Jung, D., Yim, U.H., Shim, W.J., Khim, J.S., Giesy, J.P., Choi, K., 2017. Endocrine disrupting potential of PAHs and their alkylated analogues associated with oil spills. Environ. Sci. Process. Impacts 19, 1117–1125. doi:10.1039/C7EM00125H

Legagneux, P., Fast, P.L.F., Gauthier, G., Bety, J., 2012. Manipulating individual state during migration provides evidence for carry-over effects modulated by environmental conditions. Proc. R. Soc. B Biol. Sci. 279, 876–883. doi:10.1098/rspb.2011.1351

Leighton, F.A., 1993. The toxicity of petroleum oils to birds. Environ. Rev. 1, 92–103. doi:10.1139/a93-008

Lemaire, P., Berhaut, J., Lemaire-Gony, S., Lafaurie, M., 1992. Ultrastructural changes induced by benzo[a]pyrene in sea bass (Dicentrarchus labrax) liver and intestine: Importance of the intoxication route. Environ. Res. 57, 59–72. doi:10.1016/S0013-9351(05)80019-2

Li, D., 2017. Birds as pathology-free models of type II diabetes. Austin Endocinology Diabetes Case Reports 2, 1007.

Lind, J., Cresswell, W., 2006. Anti-predation behaviour during bird migration; the benefit of studying multiple behavioural dimensions. J. Ornithol. 147, 310–316. doi:10.1007/s10336-005-0051-3

Lindberg, V., 2000. Uncertainties and error propagation - Part 1, in: Manual on Uncertainties, Graphing, and the Vernier Caliper. Institute of Technology, Rochester, NY.

Liu, Z., Liu, J., Zhu, Q., Wu, W., 2012. The weathering of oil after the Deepwater Horizon oil spill: insights from the chemical composition of the oil from the sea surface, salt marshes and sediments. Environ. Res. Lett. 7, 035302.

Livak, K.J., Schmittgen, T.D., 2001. Analysis of Relative Gene Expression Data Using Real-Time Quantitative PCR and the 2−ΔΔCT Method. Methods 25, 402–408. doi:10.1006/meth.2001.1262

Loecher, M., Ropkins, K., 2015. RgoogleMaps and loa: Unleashing R graphics power on map tiles. J. Stat. Software2 63, 1–18.

Long, Y.C., Zierath, J.R., 2006. AMP-activated protein kinase signaling in metabolic regulation. J. Clin. Invest. 116, 1776–83. doi:10.1172/JCI29044

Louisiana Department of Wildlife and Fisheries, 2016. Elmer's Island Refuge Management Plan.

Lourenço, P.M., Alves, J.A., Reneerkens, J., Loonstra, A.J., Potts, P.M., Granadeiro, J.P., Catry, T., 2016. Influence of age and sex on winter site fidelity of Sanderlings Calidris alba. PeerJ 4, e2517. doi:10.7717/peerj.2517

Lucas, J., Percelay, I., Larcher, T., Lefrancois, C., 2016. Effects of pyrolytic and petrogenic polycyclic aromatic hydrocarbons on 1 swimming and metabolic performance of zebrafish contaminated by 2 ingestion 3 4. Ecotoxicol. Environ. Saf. 132, 145–152. doi:10.1016/j.ecoenv.2016.05.035>

Lyons, J.E., Haig, S.M., 1995. Fat content and stopover ecology of spring migrant Semipalmated Sandpipers in South Carolina. Condor 97, 427–437.

Mackinnon, J., Verkuil, Y.I., Murray, N., 2012. IUCN situation analysis on East and Southeast Asian intertidal habitats, with particular reference to the Yellow Sea (including the Bohai Sea). Occasional Paper of the IUCN Species Survial Commission No. 47. IUCN, Gland, Switzerland and Cambridge, UK.

Macwhirter, B., Austin-Smith, P.J., Kroodsma, D., 2002. Sanderling (Calidris alba), in: Poole, A. (Ed.), The Birds of North America Online. Cornell Lab of Ornithology, Ithaca.

Maggini, I., Kennedy, L. V, Bursian, S.J., Dean, K.M., Gerson, A.R., Harr, K.E., Link, J.E., Pristos, C., Pristos, K., Guglielmo, C.G., 2017a. Toxicological and thermoregilatory effects of feather contamination with artificially weathered MC 252 oil in western sandpipers

(Calidris mauri). Ecotoxicol. Environ. Saf. 146, 118–128.

Maggini, I., Kennedy, L. V, Elliott, K.H., Dean, K.M., MacCurdy, R., Macmillan, A., Pristos, C., Guglielmo, C.G., 2017b. Trouble on takeoff: crude oil on feathers reduces escape performance of shorebirds. Ecotoxicol. Environ. Saf. 141, 171–177.

Maggini, I., Kennedy, L. V, Macmillan, A., Elliott, K.H., Dean, K.M., Guglielmo, C.G., 2017c. Light oiling of feathers increases flight energy expenditure in a migratory shorebird. J. Exp. Biol. 220, 2372–2379.

Marcstrom, V., Mascher, J.W., 1979. Weight and fat in Lapwings and Oystercatchers starved to death during a cold spell in spring. Ornis Scand. 10, 235–240.

Marra, P.P., Hobson, K.A., Holmes, R.T., 1998. Linking winter and summer events in a migratory bird by using stable-carbon isotopes. Science (80-. ). 282, 1884–1886. doi:10.1126/science.282.5395.1884

Mathot, K.J., Lund, D.R., Elner, R.W., 2010. Sediment in stomach contents of Western Sandpipers and Dunlin provide evidence of biofilm feeding. Waterbirds 33, 300–306.

McElroy, A.E., Farrington, J.W., Teal, J.M., 1989. Bioavailability of polycyclic aromatic hydrocarbons in the aquatic environment, in: Varanasi, U. (Ed.), Metabolism of Polycyclic Aromatic Hydrocarbons in the Aquatic Environment. CRC Press, Boca Raton, Florida, pp. 1–39.

Mchale, C.M., Zhang, L., Smith, M.T., 2012. Current understanding of the mechanism of benzene-induced leukemia in humans: implications for risk assessment. Carcinogenesis 33, 240–252. doi:10.1093/carcin/bgr297

McKellar, A.E., Marra, P.P., Ratcliffe, L.M., 2013. Starting over: experimental effects of breeding delay on reproductive success in early-arriving male American redstarts. J. Avian Biol. 44, 495–503. doi:10.1111/j.1600-048X.2013.00180.x

McKinnon, E.A., Fraser, K.C., Stanley, C.Q., Stutchbury, B.J.M., 2014. Tracking from the tropics reveals behaviour of juvenile songbirds on their first spring migration. PLoS One 9, e105605. doi:10.1371/journal.pone.0105605

Meador, J.P., Sommers, F.C., Ylitalo, G.M., Sloan, C.A., 2006. Altered growth and related physiological responses in juvenile Chinook salmon (Oncorhynchus tshawytscha) from dietary exposure to polycyclic aromatic hydrocarbons (PAHs). doi:10.1139/F06-127

Meador, J.P., Stein, J.E., Reichert, W.L., Varanasi, U., 1995. Bioaccumulation of polycyclic aromatic hydrocarbons by marine organisms. Rev Env. Contam Toxicol 143, 79–165. doi:10.1007/978-1-4612-2542-3_4

Mehlem, A., Hagberg, C.E., Muhl, L., Eriksson, U., Falkevall, A., 2013. Imaging of neutral lipids by oil red O for analyzing the metabolic status in health and disease. Nat. Protoc. 8, 1149–1154. doi:10.1038/nprot.2013.055

Meyer-Arendt, K.J., 2011. Grand Isle, Louisiana: a historic US Gulf Coast resort adapts to hurricanes, subsidence and sea level rise, in: Jones, A.L., Phillips, M.R., Phillips, M. (Eds.), Disappearing Destinations: Climate Changes and Future Challenges for Coastal Tourism. CABI.

Moore, F., Yong, W., 1991. Evidence of food-based competition among passerine migrants during stopover. Behav. Ecol. Sociobiol. 28, 85–90. doi:10.1007/BF00180984

Morandin, L.A., O'Hara, P.D., 2016. Offshore oil and gas, and operational sheen occurrence: is there potential harm to marine birds? Environ. Rev. 24, 285–318. doi:10.1139/er-2015-0086

Morrison, R.I.G., 1975. Migration and morphometricso f European Knot and Turnstone on Ellesmere Island, Canada. Bird-Banding 46, 290–301.

Myers, J.P., Sallaberry, M.A., Oritz, E., Castro, G., Gordon, L.M., Maron, J.L., Schick, C.T., Tabilo, E., Antas, P., Below, T., 1990. Migration routes of New World Sanderlings (Calidris alba). Auk 107, 172–180.

National Research Council, 2003. Oil in the Sea III: Inputs, Fates, and Effects. National Academies Press, Washington, D.C. doi:10.1016/0025-326X(80)90170-8

Nault, R., Fader, K.A., Lydic, T.A., Zacharewski, T.R., 2017. Lipidomic evaluation of aryl hydrocarbon receptor-mediated hepatic steatosis in male and female mice elicited by 2,3,7,8-tetrachlorodibenzo-p-dioxin. Chem. Res. Toxicol. 30, 1060–1075. doi:10.1021/acs.chemrestox.6b00430

Neff, J.M., 1985. Polycyclic aromatic hydrocarbons, in: Rand, G.M., Petrocilli, S.R. (Eds.), Fundamentals of Aquatic Toxicology. FMC Corp, Princeton, NJ, pp. 416–454.

Newman, S.H., Anderson, D.W., Ziccardi, M.H., Trupkiewicz, J.G., Tseng, F.S., Christopher, M.M., Zinkl, J.G., 2000. An experimental soft-release of oil-spill rehabilitated American coots (Fulica americana): ii. Effects on health and blood parameters. Environ. Pollut. 107, 295–304.

Newton, I., 2008. The Migration Ecology of Birds. Academic Press, London.

Newton, I., 2006. Can conditions experienced during migration limit the population levels of birds? J. Ornithol. 147, 146–166. doi:10.1007/s10336-006-0058-4

Nilsson, C., Klaassen, R.H.G., Alerstam, T., 2013. Differences in speed and duration of bird migration between spring and autumn. Am. Nat. 181, 837–845. doi:10.1086/670335

Norris, D.R., Marra, P.P., 2007. Seasonal interactions, habitat quality, and population dynamics in migratory birds. The Condor2 109, 535–547.

Norris, D.R., Marra, P.P., Kyser, T.K., Sherry, T.W., Ratcliffe, L.M., 2004. Tropical winter habitat limits reproductive success on the temperate breeding grounds in a migratory bird. Proc. R. Soc. B Biol. Sci. 271, 59–64. doi:10.1098/rspb.2003.2569

Ohiozebau, E., Tendler, B.J., Codling, G., Kelly, E., Giesy, J.P., Jones, P.D., Ohizebau, E., Tendler, B.J., Codling, G., Kelly, E., Giesy, J.P., Jones, P.D., 2017. Potential health risks posed by polycyclic aromatic hydrocarbons in muscle tissues of fishes from the Athabasca and Slave Rivers, Canada. Environ. Geochem. Health 39, 139–160. doi:10.1007/s10653-016-9815-3

Oksanen, J., Blanchet, F.G., Friendly, M., Kindt, R., Legendre, P., McGlinn, D., Minchin, P.R., O'Hara, R.B., Simpson, G.L., Solymos, P., Stevens, M.H.H., Szoecs, E., Wagner, H., 2018. vegan: Community Ecology Package.

Organisation for Economic Co-operation and Development, 2018. Users' Handbook Supplement to the Guidance Document for Developing and Assessing AOPs. Paris.

Organisation for Economic Co-operation and Development, 2017. Revised Gudance Document on Developing and Assessing Adverse Outcome Pathways. Paris.

Ouwehand, J., Both, C., 2017. African departure rather than migration speed determines variation in spring arrival in pied flycatchers. J. Anim. Ecol. 86, 88–97. doi:10.1111/1365-2656.12599

Owens, E.H., Taylor, E., Humphrey, B., 2008. The persistence and character of stranded oil on coarse-sediment beaches. Mar. Pollut. Bull. 56, 14–26.

doi:10.1016/J.MARPOLBUL.2007.08.020

Paruk, J.D., Adams, E.M., Uher-Koch, H., Kovach, K.A., Long, D., Perkins, C., Schoch, N., Evers, D.C., 2016. Polycyclic aromatic hydrocarbons in blood related to lower body mass in common loons. Sci. Total Environ. 565, 360–368. doi:10.1016/j.scitotenv.2016.04.150

Peakall, D.B., Tremblay, J., Kinter, W.B., Miller, D.S., 1981. Endocrine dysfunction in seabirds caused by ingested oil. Environ. Res. 24, 6–14. doi:10.1016/0013-9351(81)90126-2

Perez, C.R., Moye, J., Cacela, D., Dean, K., Pristos, C.A., 2017a. Body mass change in flying homing pigeons externally exposed to deepwater Horizon crude oil. Ecotoxicol. Environ. Saf. 146, 104–110.

Perez, C.R., Moye, J.K., Cacela, D., Dean, K.M., Pritsos, C.A., 2017b. Homing pigeons externally exposed to Deepwater Horizon crude oil change flight performance and behavior. Environ. Pollut. 230, 530–539. doi:10.1016/j.envpol.2017.07.008

Peterson, C.H., Rice, S.D., Short, J.W., Esler, D., Bodkin, J.L., Ballachey, B.E., Irons, D.B., 2003. Long-Term Ecosystem Response to the Exxon Valdez Oil Spill. Science (80-. ). 302, 2082–2086. doi:10.1126/science.1084282

Piatt, J.F., Lensink, C.J., Butler, W., Nysewander, D.R., Nysewander, D.R., 1990. Immediate impact of the "Exxon Valdez" oil spill on marine birds. Auk 107, 387–397. doi:10.2307/4087623

Piatt, J.F., Van Pelt, T.I., 1997. Mass-mortality of guillemots (Uria aalge) in the Gulf of Alaska in 1993. Mar. Pollut. Bull. 34, 656–662. doi:10.1016/S0025-326X(97)00008-8

Piersma, T., 1994. Close to the edge: Energetic bottlenecks and the evolution of migratory pathways in Knots. University of Groningen, Groningen, Netherlands.

Piersma, T., 1987. Hop, jump, or skip? Constraints on migration of arctic waders by feeding, fattening, and flight speed. Limosa 60, 185–194.

Piersma, T., Gill, R.E.J., 1998. Guts don't fly: small digestive organs in obese bar-tailed godwits. Auk 115, 196–203.

Piersma, T., Gudmundsson, G.A., Lilliendahl, K., 1999. Rapid changes in the size of different functional organ and muscle groups during refueling in a long-distance migrating shorebird. Physiol. Biochem. Zool. 72, 405–415.

Pomeroy, A.C., Butler, R.W., Ydenberg, R.C., 2006. Experimental evidence that migrants adjust usage at a stopover site to trade off food and danger. Behav. Ecol. 17, 1041–1045. doi:10.1093/beheco/arl043

Porter, E., Crump, D., Egloff, C., Chiu, S., Kennedy, S.W., 2014. Use of an avian hepatocyte assay and the avian toxchip polymerse chain reaction array for testing prioritization of 16 organic flame retardants. Environ. Toxicol. Chem. 33, 573–582. doi:10.1002/etc.2469

Price, E.R., 2010. Dietary lipid composition and avian migratory flight performance: Development of a theoretical framework for avian fat storage. Comp. Biochem. Physiol. Part A 157, 297–309.

R Core Team, 2017. R: A Language and Environment for Satistical Computing.

Rabalais, N.N., Turner, R.E., Wiseman, W.J., 2002. Gulf of Mexico hypoxia, a.k.a. "The Dead Zone." Annu. Rev. Ecol. Syst. 33, 235–263. doi:10.1146/annurev.ecolsys.33.010802.150513

Ramenofsky, M., 1990. Fat storage and fat metabolism in relation to migration, in: Gwinner, E. (Ed.), Bird Migration: Physiology and Ecopysiology. Springer-Verlag, New York, pp. 241–

231.

Ramenofsky, M., Savard, R., Greenwood, M.R.C., 1999. Seasonal and diel transitions in physiology and behavior in the migratory dark-eyed junco. Comp. Biochem. Physiol. Part A 122, 385–397.

Rappole, J.H., McDonald, M. V, 1994. Cause and effect in population declines of migratory birds. Auk 111, 652–660.

Reddy, C.M., Arey, J.S., Seewald, J.S., Sylva, S.P., Lemkau, K.L., Nelson, R.K., Carmichael, C.A., McIntyre, C.P., Fenwick, J., Ventura, G.T., Van Mooy, B.A.S., Camilli, R., 2012. Composition and fate of gas and oil released to the water column during the Deepwater Horizon oil spill. Proc. Natl. Acad. Sci. 109, 20229–20234. doi:10.1073/pnas.1101242108

Reudink, M.W., Marra, P.P., Kyser, T.K., Boag, P.T., Langin, K.M., Ratcliffe, L.M., 2009. Non-breeding season events influence sexual selection in a long-distance migratory bird. Proceedings. Biol. Sci. 276, 1619–26. doi:10.1098/rspb.2008.1452

Ribiere, C., Peyret, P., Parisot, N., Darcha, C., Dechelotte, P.J., Barnich, N., Peyretaillade, E., Boucher, D., 2016. Oral exposure to environmental pollutant benzo[a]pyrene impacts the intestinal epithelium and induces gut microbial shifts in murine model. Sci. Rep. 6. doi:10.1038/srep31027

Robbins, C.S., Sauer, J.R., Greenberg, R.S., Droege, S., 1989. Population declines in North American birds that migrate to the neotropics. Proc. Natl. Acad. Sci. 86.

Robinson, R.A., Atkinson, P.W., Clark, N.A., 2003. Arrival and weight gain of Red Knot Calidris canutus, Ruddy Turnstone Arenaria interpres and Sanderling Calidris alba staging in Delaware Bay in spring. The Nunnery, Thetford, Norfolk.

Robinson, T.R., Sargent, R.R., Sargent, M.B., 1996. Ruby-throated hummingbird (Archilochus colubris), in: Poole, A. (Ed.), Birds of North America Online. Cornell Lab of Ornithology, Ithaca, New York.

Rocke, T.E., Yuill, T.M., Hinsdill, R.D., 1984. Oil and related toxicant effects on mallard immune defenses. Environ. Res. 33, 343–352.

Rui, L., 2014. Energy metabolism in the liver. Compr Physiol 4, 177–197.

Saleh, M.A., Wilson, B.L., 1999. Analysis of Metal Pollutants in the Houston Ship Channel by Inductively Coupled Plasma/Mass Spectrometry. Ecotoxicol. Environ. Saf. 44, 113–117. doi:10.1006/EESA.1999.1807

Sammarco, P.W., Kolian, S.R., Warby, R.A.F., Bouldin, J.L., Subra, Wilma, A., Porter, S.A., 2013. Distribution and concentrations of petroleum hydrocarbons associated with the BP/Deepwater Horizon oil spill, Gulf of Mexico. Mar. Pollut. Bull. 73, 129–143.

Sandberg, R., Moore, F.R., 1996. Fat stores and arrival on the breeding grounds: reproductive consequences for passerine migrants. Oikos 77, 577–581.

Sanderson, F.J., Donald, P.F., Pain, D.J., Burfield, I.J., van Bommel, F.P.J., 2006. Long-term population declines in Afro-Palearctic migrant birds. Biol. Conserv. 131, 93–105. doi:10.1016/j.biocon.2006.02.008

Santamarina-Fojo, S., Gonzalez-Navarro, H., Freeman, L., Wagner, E., Nong, Z., 2004. Hepatic lipase, lipoprotein metabolism, and atherogenesis. Arterioscler. Thromb. Vasc. Biol. 24, 1750–1754.

Santschi, P.., Presley, B.., Wade, T.., Garcia-Romero, B., Baskaran, M., 2001. Historical contamination of PAHs, PCBs, DDTs, and heavy metals in Mississippi River Delta,

Galveston Bay and Tampa Bay sediment cores. Mar. Environ. Res. 52, 51–79. doi:10.1016/S0141-1136(00)00260-9

Sato, S., Shirakawa, H., Tomita, S., Ohsaki, Y., Hakea, K., Tooi, O., Santo, N., Tohkin Masahiro, Furukawa, Y., Gonzalez, F.J., Komai, M., 2008. Low-dose dioxins alter gene expression related to cholesterol biosynthesis, lipogenesis, and glucose metabolism through the aryl hydrocarbon receptor-mediated pathway in mouse liver. Toxicol. Appl. Pharmacol. 229, 10–19.

Schaub, M., Jenni, L., 2001. Variation of fuelling rates among sites, days and individuals in migrating passerine birds. Funct. Ecol. 15, 584–594. doi:10.1046/j.0269-8463.2001.00568.x

Schaub, M., Jenni, L., Bairlein, F., 2008. Fuel stores, fuel accumulation, and the decision to depart from a migration stopover site. Behav. Ecol. 19, 657–666. doi:10.1093/beheco/arn023

Schick, C.T., 1983. Weight loss in Sanderlings Calidris alba after capture. Wader Study Gr. Bull 38, 33–34.

Schimada, T., Fujii-Kuiyama, Y., 2004. Metabolic activation of polycyclic aromatic hydrocarbons to carcinogens by cytochromes P450 1A1 and 1B1. Cancer Sci. 95, 1–6.

Schmaljohann, H., Lisovski, S., Bairlein, F., 2017. Flexible reaction norms to environmental variables along the migration route and the significance of stopover duration for total speed of migration in a songbird migrant. Front. Zool. 14, 1–16. doi:10.1186/s12983-017-0203-3

Schmaljohann, H., Naef-Daenzer, B., 2011. Body condition and wind support initiate the shift of migratory direction and timing of nocturnal departure in a songbird. J. Anim. Ecol. 80, 1115–1122. doi:10.1111/j.1365-2656.2011.01867.x

Schmittgen, T.D., Livak, K.J., 2008. Analyzing real-time PCR data by the comparative CT method. Nat. Protoc. 3, 1101–1108. doi:10.1038/nprot.2008.73

Schonewille, M., 2016. Cholesterol, bile acid and triglyceride metabolism intertwined. University of Groningen.

Schultz, T.W., Barrera, T.A., Lee, M.C., 1994. Accumulation of mercury in sediments, prey, and shorebirds or Lavaca Bay, Texas. Phase II report. Corpus Christy, Texas Field Office.

Scott, I., Mitchell, P.I., Gudmundsson, G. a., Eaton, M., Ward, R.M., Evans, P.R., 2004. Using radio-transmitters to help monitor the spring migration of Sanderling Calidris alba: Why do some birds stop in Iceland? Bird Study 51, 83–86. doi:10.1080/00063650409461336

Seaman, D.A., 2004. Landscape physiology: plasma metabolites, fattening rates and habitat quality in migratory Western Sandpipers. Simon Fraser University.

Seiser, P.E., Duffy, L.K., David Mcguire, A., Roby, D.D., Golet, G.H., Litzow, M.A., 2000. Comparison of pigeon guillemot, Cepphus columba, blood parameters from oiled and unoiled areas of Alaska eight years after the Exxon Valdez oil spill. Mar. Pollut. Bull. 40, 152–164. doi:10.1016/S0025-326X(99)00194-0

Senner, N.R., Verhoeven, M.A., Abad-Gómez, J.M., Gutiérrez, J.S., Hooijmeijer, J.C.E.W., Kentie, R., Masero, J.A., Tibbitts, T.L., Piersma, T., 2015. When Siberia came to the Netherlands: the response of continental black-tailed godwits to a rare spring weather event. J. Anim. Ecol. 84, 1164–1176. doi:10.1111/1365-2656.12381

Shah, R. V, Patel, S.T., Pilo, B., 1978. Glucose-6-phosphate dehydrogenase and “malic” enzyme activites during adaptive hyperlipogenesis in migratory starling (Sturnus roseus) and white wagtail (Motacilla alba). Can. J. Zool. 56, 2083–2087.

Short, J.W., Irvine, G. V., Mann, D.H., Maselko, J.M., Pella, J.J., Lindeberg, M.R., Payne, J.R., Driskell, W.B., Rice, S.D., 2007. Slightly weathered Exxon Valdez oil persists in Gulf of Alaska beach sediments after 16 years. Environ. Sci. Technol. 41, 1245–1250. doi:10.1021/es0620033

Sikkema, J., de Bont, J.A., Poolman, B., 1995. Mechanisms of membrane toxicity of hydrocarbons. Microbiol Rev 59, 201–222. doi:0146-0749/95/$04.00+0

Sillett, T.S., Holmes, R.T., 2002. Variation in survivorship of a migratory songbird throughout its annual cycle. J. Anim. Ecol. 71, 296–308.

Skagen, S.K., Sharpe, P.B., Waltermire, R.G., Dillon, M.B., 1999. Biogeographical profiles of shorebird migration in midcontinental North America. Biol. Sci. Rep. 167.

Smith, A.D., Mcwilliams, S.R., 2014. What to do when stopping over: behavioral decisions of a migrating songbird during stopover are dictated by initial change in their body condition and mediated by key environmental conditions. Behav. Ecol. 25, 1423–1435. doi:10.1093/beheco/aru148

Smith, L.I., 2002. A tutorial on principal components analysis [WWW Document]. URL http://csnet.otago.ac.nz/cosc453/student_tutorials/prinicpal_components.pdf (accessed 4.6.18).

Smith, R.J., Moore, F.R., 2005. Arrival timing and seasonal reproductive performance in a long-distance migratory landbird. Behav. Ecol. Sociobiol. 57, 231–239. doi:10.1007/s00265-004-0855-9

Snyder, R.A., Ederington-Hagy, M., Hileman, F., Moss, J.A., Amick, L., Carruth, R., Head, M., Marks, J., Tominack, S., Jeffrey, W.H., 2014a. Polycyclic aromatic hydrocarbon concentrations across the Florida Panhandle continental shelf and slope after the BP MC 252 well failure. Mar. Pollut. Bull. 89, 201–208. doi:10.1016/J.MARPOLBUL.2014.09.057

Snyder, R.A., Vesal, A., Welch, C., Barnes, G., Pelot, R., Ederington-Hagy, M., Hileman, F., 2014b. PAH concentrations in Coquina (Donax spp.) on a sandy beach shoreline impacted by a marine oil spill. Mar. Pollut. Bull. 83, 87–91.

Soshilov, A.A., Denison, M.S., 2014. Ligand promiscuity of aryl hydrocarbon receptor agonists and antagonists revealed by site-directed mutagenesis. Mol. Cell. Biol. 34, 1707–19. doi:10.1128/MCB.01183-13

Srivastava, R.A.K., Pinkosky, S.L., Filippov, S., Hanselman, J.C., Cramer, C.T., Newton, R.S., 2012. AMP-activated protein kinase: an emerging drug target to regulate imbalances in lipid and carbohydrate metabolism to treat cardio-metabolic diseases. J. Lipid Res. 53, 2490–514. doi:10.1194/jlr.R025882

Staels, B., Fonseca, V.A., 2009. Bile acids and metabolic regulation: mechanisms and clinical responses to bile acid sequestration. Diabetes Care 32 Suppl 2, S237-45. doi:10.2337/dc09-S355

Stewart, R.L.M., Francis, C.M., Massey, C., 2002. Age-related differential timing of spring migration within sexes in Passerines. Wilson Bull. 114, 264–271.

Stieglitz, J.D., Mager, E.M., Hoenig, R.H., Benetti, D.D., Grosell, M., 2016. Impacts of Deepwater Horizon crude oil exposure on adult mahi-mahi (Coryphaena hippurus) swim performance. Environ. Toxicol. Chem. 35, 2613–2622. doi:10.1002/etc.3436

Studds, C.E., Kendall, B.E., Murray, N.J., Wilson, H.B., Rogers, D.I., Clemens, R.S., Gosell, K., Hassell, C.J., Jessop, R., Melville, D.S., Milton, D.A., Minton, C.D.T., Possingham, H.P.,

Riegen, A.C., Straw, P., Woehler, E.J., Fuller, R.A., 2017. Rapid population decline in migratory shorebirds relying on Yellow Sea tidal mudflats as stopover sites. Nat. Commun. 8, 14895.

Suarez, M.P., Rifai, H.S., Palachek, R., Dean, K., Koenig, L., 2006. Distribution of polychlorinated dibenzo-p-dioxins and dibenzofurans in suspended sediments, dissolved phase and bottom sediment in the Houston Ship Channel. Chemosphere 62, 417–429. doi:10.1016/J.CHEMOSPHERE.2005.04.088

Tanos, R., Murray, I.A., Smith, P.B., Patterson, A., Perdew, G.H., 2012. Role of the Ah receptor in homeostatic control of fatty acid synthesis in the liver. Toxicol. Sci. 129, 372–9. doi:10.1093/toxsci/kfs204

Taylor, P.D., Crewe, T.L., Mackenzie, S.A., Lepage, D., Aubry, Y., Crysler, Z., Finney, G., Francis, C.M., Guglielmo, C.G., Hamilton, D.J., Holberton, R.L., Loring, P.H., Mitchell, G.W., Norris, D.R., Paquet, J., Ronconi, R.A., Smetzer, J.R., Smith, P.A., Welch, L.J., Woodworth, B.K., 2017. The Motus Wildlife Tracking System: a collaborative research network to enhance the understanding of wildlife movement. Avian Conserv. Ecol. 12, art8. doi:10.5751/ACE-00953-120108

Thomas, G.H., Lanctot, R.B., Székely, T., 2006. Can intrinsic factors explain population declines in North American breeding shorebirds? A comparative analysis. Anim. Conserv. 9, 252–258. doi:10.1111/j.1469-1795.2006.00029.x

Till, M., Riebniger, D., Schmitz, H.-J., Schrenk, D., 1999. Potency of various polycyclic aromatic hydrocarbons as inducers of CYP1A1 in rat hepatocyte cultures. Chem. Biol. Interact. 117, 135–150. doi:10.1016/S0009-2797(98)00105-7

Troisi, G., Barton, S., Bexton, S., 2016. Impacts of oil spills on seabirds: Unsustainable impacts of non-renewable energy. Int. J. Hydrogen Energy 41, 16549–16555. doi:10.1016/j.ijhydene.2016.04.011

Troisi, G., Borjesson, L., Bexton, S., Robinson, I., 2007. Biomarkers of polycyclic aromatic hydrocarbon (PAH)-associated hemolytic anemica in oiled wildlife. Environ. Res. 105, 324–329.

Tyagi, S., Gupta, P., Saini, A.S., Kaushal, C., Sharma, S., 2011. The peroxisome proliferator-activated receptor: A family of nuclear receptors role in various diseases. J. Adv. Pharm. Technol. Res. 2, 236–40. doi:10.4103/2231-4040.90879

Urbano, M., Elango, V., Pardue, J.H., 2013. Biogeochemical characterization of MC252 oil:sand aggregates on a coastal headland beach. Mar. Pollut. Bull. 77, 183–191.

Van Gils, J.A., 2004. Foraging Decisions in Digestively Constrained Long-Distance Migrant, the Red Knot (Calidris canutus). University of Groningen, Groningen, The Netherlands.

Vanermen, N., Stienen, E.W.M., De Meulenaer, B., Van Ginderdeuren, K., Degraer, S., 2009. Low dietary importance of polychaetes in opportunistic feeding Sanderlings Calidris alba on Belgian beaches. Ardea 97, 81–87. doi:10.5253/078.097.0110

Villeneuve, D.L., Crump, D., Garcia-Reyero, N., Hecker, M., Hutchinson, T.H., LaLone, C.A., Landesmann, B., Lettieri, T., Munn, S., Nepelska, M., Ottinger, M.A., Vergauwen, L., Whelan, M., 2014a. Adverse outcome pathway development II: Best practices. Toxicol. Sci. 142, 321–330. doi:10.1093/toxsci/kfu200

Villeneuve, D.L., Crump, D., Garcia-Reyero, N., Hecker, M., Hutchinson, T.H., LaLone, C.A., Landesmann, B., Lettieri, T., Munn, S., Nepelska, M., Ottinger, M.A., Vergauwen, L., Whelan, M., 2014b. Adverse outcome pathway (AOP) development I: Strategies and

principles. Toxicol. Sci. 142, 312–320. doi:10.1093/toxsci/kfu199

Villeneuve, D.L., Khim, J.S., Kannan, K., Giesy, J.P., 2002. Relative potencies of individual polycylic aromatic hydrocarbons to induce dioxinlike and estrogenic responses in three cell lines. Environ. Toxicol. 17, 128–137.

Vinken, M., 2013. The adverse outcome pathway concept: A pragmatic tool in toxicology. Toxicology 312, 158–165. doi:10.1016/j.tox.2013.08.011

Vinken, M., Knapen, D., Vergauwen, L., Hengstler, J.G., Angrish, M., Whelan, M., 2017. Adverse outcome pathways: a concise introduction for toxicologists. Arch. Toxicol. 1–11. doi:10.1007/s00204-017-2020-z

Vogel, C.F.A., Matsumura, F., 2003. Interaction of 2,3,7,8-tetrachlorodibenzo-p-dioxin (TCDD) with induced adipocyte differentiation in mouse embryonic fibroblasts (MEFs) involves tyrosine kinase c-Src. Biochem. Pharmacol. 66, 1231–1244. doi:10.1016/S0006-2952(03)00404-0

Wang, Y.-X., 2010. PPARs: diverse regulators in energy metabolism and metabolic diseases. Cell Res. 20, 124–37. doi:10.1038/cr.2010.13

Wang, Z., Liu, Z., Xu, K., Mayer, L.M., Zhang, Z., Kolker, A.S., Wu, W., 2014. Concentrations and sources of polycyclic aromatic hydrocarbons in surface coastal sediments of the northern Gulf of Mexico. Geochem. Trans. 15.

Warnock, N., 2010. Stopping vs. staging: The difference between a hop and a jump. J. Avian Biol. 41, 621–626. doi:10.1111/j.1600-048X.2010.05155.x

Warnock, N., Takekawa, J.Y., Bishop, M.A., 2004. Migration and stopover strategies of individual Dunlin along the Pacific coast of North America. Can. J. Zool. 82, 1687–1697. doi:10.1139/z04-154

Weber, T.P., Ens, B.J., Houston, A.I., 1998. Optimal avian migration: A dynamic model of fuel stores and site use. Evol. Ecol. 12, 377. doi:10.1023/A:1006560420310

Weber, T.P., Houston, A.I., 1997. A general model for time-minimizing avian migration. J. Theor. Biol. 185, 447–458.

Webster, M.S., Marra, P.P., Haig, S.M., Bensch, S., Holmes, R.T., 2002. Links between worlds:unraveling migratory connectivity. Trends Ecol. Evol. 17, 76–83. doi:10.1016/S0169-5347(01)02380-1

Weimerskirch, H., Delord, K., Guitteaud, A., Phillips, R.A., Pinet, P., 2015. Extreme variation in migration strategies between and within wandering albatross populations during their sabbatical year, and their fitness consequences. Sci. Rep. 5, 1–7. doi:10.1038/srep08853

Wickham, H., 2017. scales: Scale Functions for Visualization.

Wickham, H., 2009. ggplot2: Elegant graphics for data analysis. Springer-Verlag New York.

Wilke, C.O., 2017. cowplot: Streamlined plot theme and plot annotations for "ggplot2."

Willie, M., Esler, D., Boyd, W.S., Molloy, P., Ydenberg, R.C., 2017. Spatial variation in polycyclic aromatic hydrocarbon exposure in Barrow's goldeneye (Bucephala islandica) in coastal British Columbia. Mar. Pollut. Bull. 118, 167–179.

Withers, K., 2002. Shorebird use of coastal wetland and barrier island habitat in the Gulf of Mexico. Sci. World 2, 514–536.

Yen, C.-L.E., Nelson, D.W., Yen, M.-I., 2015. Intestinal triacylglycerol synthesis in fat absorption and systemic energy metabolism. J. Lipid Res. 56, 489–501. doi:10.1194/jlr.R052902

Zhang, Y., Dong, S., Wang, H., Tao, S., Kiyama, R., 2016. Biological impact of environmental polycyclic aromatic hydrocarbons (ePAHs) as endocrine disruptors. Environ. Pollut. 213, 809–824. doi:10.1016/j.envpol.2016.03.050

Zhang, Y., Shotyk, W., Zaccone, C., Noernberg, T., Pelletier, R., Bicalho, B., Forese, D.G., Davies, L., Martin, J.W., 2016. Airbone petcoke dust is a major source of polycyclic aromatic hydrocarbons in the Athabasca Oil Sands region. Environ. Sci. Technol. 50, 1711–1720.

Zhao, M., Christie, M., Coleman, J., Hassell, C., Gosbell, K., Lisovski, S., Minton, C., Klaassen, M., 2017. Time versus energy minimization migration strategy varies with body size and season in long-distance migratory shorebirds. Mov. Ecol. 5, 1–12. doi:10.1186/s40462-017-0114-0

Zockler, C., Delany, S., Hagemeijer, W., 2003. Wader populations are declining - how will we elucidate the reasons? Wader Study Gr. Bull. 100, 202–211.

# APPENDIX[1]

[1] Supplementary data are included in this chapter. Figures and tables in the Appendix are presented in the order that they appear in the thesis.

**Table A.1.** Model selection results for linear mixed effects models to explain variation in EROD activity of Sanderling orally exposed to 0 (n = 12), 12.6 (n = 12), 126 (n = 12), or 1260 (n = 13) µg/kg-bw/day of a commercial PAH mixture for 21 days.

| EROD activity models | k[1] | AICc[2] | ΔAICc[3] | w[4] | Evidence ratio[5] |
|---|---|---|---|---|---|
| Intercept only (null) | 3 | 93.2 | 0.0 | 0.3744 | 1.00 |
| Treatment | 6 | 93.4 | 0.2 | 0.3342 | 1.12 |
| Sex | 4 | 94.9 | 1.8 | 0.1544 | 2.42 |
| Treatment + Sex | 7 | 95.4 | 2.2 | 0.1257 | 2.98 |
| Treatment + Sex + Treatment*Sex | 10 | 102.9 | 9.8 | 0.0028 | 133.71 |
| Treatment + Treatment*Sex | 10 | 102.9 | 9.8 | 0.0028 | 133.71 |
| Sex + Treatment*Sex | 10 | 102.9 | 9.8 | 0.0028 | 133.71 |
| Treatment*Sex | 10 | 102.9 | 9.8 | 0.0028 | 133.71 |

[1] k: number of estimated parameters in the model
[2] AICc: Akaike's Information Criterion corrected for small sample sizes
[3] ΔAICc: difference from AICc of the best-approximating model
[4] w: AICc weight
[5] Evidence ratio = w of the best supported model / w of model

**Table A.2.** Model selection results for linear mixed effects models to explain variation in liver lipid content and hepatosomatic index (HSI) of Sanderling orally exposed to 0 (n = 12), 12.6 (n = 12), 126 (n = 12), or 1260 (n = 13) μg/kg-bw/day of a commercial PAH mixture for 21 days.

| Response | Model structure | k[1] | AICc[2] | ΔAICc[3] | w[4] | Evidence ratio[5] |
|---|---|---|---|---|---|---|
| Liver lipid content | Intercept only (null) | 3 | 69.1 | 0.0 | 0.288 | 1.00 |
| | EROD | 4 | 69.9 | 0.7 | 0.199 | 1.45 |
| | Sex | 4 | 70.6 | 1.5 | 0.137 | 2.10 |
| | EROD + Sex | 5 | 71.3 | 2.1 | 0.099 | 2.91 |
| | EROD + EROD*Sex | 5 | 71.3 | 2.1 | 0.099 | 2.91 |
| | EROD*Sex | 5 | 71.3 | 2.1 | 0.099 | 2.91 |
| | EROD + Sex + EROD*Sex | 6 | 73.1 | 4.0 | 0.039 | 7.38 |
| | Sex + EROD*Sex | 6 | 73.1 | 4.0 | 0.039 | 7.38 |
| HSI | Intercept only (null) | 3 | -14.8 | 0.0 | 0.511 | 1.00 |
| | Sex | 4 | -12.6 | 2.2 | 0.171 | 2.99 |
| | EROD | 4 | -12.3 | 2.4 | 0.152 | 3.36 |
| | EROD + Sex | 5 | -10.0 | 4.7 | 0.048 | 10.65 |
| | EROD*Sex | 5 | -10.0 | 4.8 | 0.046 | 11.11 |
| | EROD + EROD*Sex | 5 | -10.0 | 4.8 | 0.046 | 11.11 |
| | Sex + EROD*Sex | 6 | -7.4 | 7.3 | 0.013 | 39.31 |
| | EROD + Sex + EROD*Sex | 6 | -7.4 | 7.3 | 0.013 | 39.31 |

[1] k: number of estimated parameters in the model
[2] AICc: Akaike's Information Criterion corrected for small sample sizes
[3] ΔAICc: difference from AICc of the best-approximating model
[4] w: AICc weight
[5] Evidence ratio = w of the best supported model / w of model

**Table A.3.** Model selection results for linear mixed effects models to explain variation in serum analytes of Sanderling orally exposed to 0 (n = 12), 12.6 (n = 12), 126 (n = 12), or 1260 (n = 13) μg/kg-bw/day of a commercial PAH mixture for 21 days.

| Response | Model structure | k[1] | AICc[2] | ΔAICc[3] | w[4] | Evidence ratio[5] |
|---|---|---|---|---|---|---|
| AST | Intercept only (null) | 5 | 94.0 | 0.0 | 0.539 | 1.00 |
| | Sex | 6 | 96.3 | 2.3 | 0.175 | 3.08 |
| | EROD | 6 | 96.7 | 2.6 | 0.145 | 3.72 |
| | EROD + Sex | 7 | 99.1 | 5.1 | 0.043 | 12.53 |
| | EROD*Sex | 7 | 99.3 | 5.3 | 0.038 | 14.18 |
| | EROD + EROD*Sex | 7 | 99.3 | 5.3 | 0.038 | 14.18 |
| | Sex + EROD*Sex | 8 | 101.8 | 7.8 | 0.011 | 49.00 |
| | EROD + Sex + EROD*Sex | 8 | 101.8 | 7.8 | 0.011 | 49.00 |
| Bile acid | EROD | 7 | 401.4 | 0.0 | 0.272 | 1.00 |
| | EROD + Sex | 8 | 401.8 | 0.4 | 0.218 | 1.25 |
| | Intercept only (null) | 6 | 402.5 | 1.1 | 0.156 | 1.74 |
| | Sex | 7 | 402.5 | 1.2 | 0.152 | 1.79 |
| | EROD*Sex | 8 | 404.4 | 3.0 | 0.060 | 4.53 |
| | EROD + EROD*Sex | 8 | 404.4 | 3.0 | 0.060 | 4.53 |
| | Sex + EROD*Sex | 9 | 405.1 | 3.8 | 0.041 | 6.63 |
| | EROD + Sex + EROD*Sex | 9 | 405.1 | 3.8 | 0.041 | 6.63 |
| β-hydroxybutyrate | Intercept only (null) | 5 | 67.9 | 0.0 | 0.506 | 1.00 |
| | Sex | 6 | 69.5 | 1.6 | 0.230 | 2.20 |
| | EROD | 6 | 70.7 | 2.8 | 0.128 | 3.95 |
| | EROD + Sex | 7 | 72.4 | 4.5 | 0.053 | 9.55 |
| | EROD + EROD *Sex | 7 | 73.6 | 5.7 | 0.030 | 16.87 |
| | EROD*Sex | 7 | 73.6 | 5.7 | 0.030 | 16.87 |
| | Sex + EROD*Sex | 8 | 75.4 | 7.5 | 0.012 | 42.17 |
| | EROD + Sex + EROD*Sex | 8 | 75.4 | 7.5 | 0.012 | 42.17 |
| Cholesterol | Intercept only (null) | 4 | 216.3 | 0.0 | 0.437 | 1.00 |
| | Sex | 5 | 218.1 | 1.8 | 0.175 | 2.50 |
| | EROD | 5 | 218.1 | 1.8 | 0.174 | 2.51 |
| | EROD + Sex | 6 | 220.1 | 3.9 | 0.063 | 6.94 |
| | EROD + EROD*Sex | 6 | 220.4 | 4.2 | 0.055 | 7.95 |
| | EROD*Sex | 6 | 220.4 | 4.2 | 0.055 | 7.95 |
| | Sex + EROD*Sex | 7 | 222.4 | 6.1 | 0.020 | 21.85 |
| | EROD + Sex + EROD*Sex | 7 | 222.4 | 6.1 | 0.020 | 21.85 |
| Creatine kinase | EROD | 6 | 90.2 | 0.0 | 0.5576 | 1.00 |
| | Intercept only (null) | 5 | 92.8 | 2.6 | 0.1546 | 3.61 |
| | EROD*Sex | 7 | 93.8 | 3.6 | 0.0931 | 5.99 |
| | EROD + EROD*Sex | 7 | 93.8 | 3.6 | 0.0931 | 5.99 |
| | EROD + Sex | 7 | 94.7 | 4.4 | 0.0611 | 9.13 |
| | Sex | 6 | 96.8 | 6.5 | 0.0211 | 26.43 |
| | EROD + Sex + EROD*Sex | 8 | 98.3 | 8.1 | 0.0097 | 57.48 |
| | Sex + EROD*Sex | 8 | 98.3 | 8.1 | 0.0097 | 57.48 |

**Table A.3 continued on next page.**

**Table A.3 continued**

| Response | Model structure | k[1] | AICc[2] | ΔAICc[3] | w[4] | Evidence ratio[5] |
|---|---|---|---|---|---|---|
| Glucose | Intercept only (null) | 4 | 202.9 | 0.0 | 0.428 | 1.00 |
| | Sex | 5 | 204.4 | 1.4 | 0.207 | 2.07 |
| | EROD | 5 | 205.0 | 2.0 | 0.154 | 2.78 |
| | EROD + Sex | 6 | 206.6 | 3.7 | 0.067 | 6.39 |
| | EROD + EROD*Sex | 6 | 207.3 | 4.4 | 0.048 | 8.92 |
| | EROD*Sex | 6 | 207.3 | 4.4 | 0.048 | 8.92 |
| | Sex + EROD*Sex | 7 | 208.7 | 5.8 | 0.024 | 17.83 |
| | EROD + Sex + EROD*Sex | 7 | 208.7 | 5.8 | 0.024 | 17.83 |
| GGT | Intercept only (null) | 5 | 87.7 | 0.0 | 0.457 | 1.00 |
| | EROD | 6 | 89.6 | 1.9 | 0.175 | 2.61 |
| | Sex | 6 | 89.7 | 2.0 | 0.170 | 2.69 |
| | EROD + Sex | 7 | 91.7 | 4.0 | 0.063 | 7.25 |
| | EROD + EROD*Sex | 7 | 92.1 | 4.4 | 0.050 | 9.14 |
| | EROD*Sex | 7 | 92.1 | 4.4 | 0.050 | 9.14 |
| | EROD + Sex + EROD*Sex | 8 | 94.2 | 6.5 | 0.018 | 25.39 |
| | Sex + EROD*Sex | 8 | 94.2 | 6.5 | 0.018 | 25.39 |
| Hematocrit | Intercept only (null) | 5 | 634.0 | 0.0 | 0.469 | 1.00 |
| | EROD | 6 | 635.7 | 1.7 | 0.201 | 2.33 |
| | Sex | 6 | 636.4 | 2.4 | 0.138 | 3.40 |
| | EROD + EROD*Sex | 7 | 638.2 | 4.3 | 0.056 | 8.38 |
| | EROD*Sex | 7 | 638.2 | 4.3 | 0.056 | 8.38 |
| | EROD + Sex | 7 | 638.3 | 4.3 | 0.054 | 8.69 |
| | Sex + EROD*Sex | 8 | 641.2 | 7.2 | 0.013 | 36.08 |
| | EROD + Sex + EROD*Sex | 8 | 641.2 | 7.2 | 0.013 | 36.08 |
| Lipase | Sex | 6 | 706.4 | 0.0 | 0.181 | 1.00 |
| | EROD + Sex + EROD*Sex | 8 | 706.5 | 0.1 | 0.173 | 1.05 |
| | Sex + EROD*Sex | 8 | 706.5 | 0.1 | 0.173 | 1.05 |
| | Intercept only (null) | 5 | 706.5 | 0.1 | 0.171 | 1.06 |
| | EROD | 6 | 708.0 | 1.6 | 0.082 | 2.21 |
| | EROD + Sex | 7 | 708.2 | 1.8 | 0.074 | 2.45 |
| | EROD + EROD*Sex | 7 | 708.2 | 1.8 | 0.073 | 2.48 |
| | EROD*Sex | 7 | 708.2 | 1.8 | 0.073 | 2.48 |
| NEFA | EROD | 6 | 14.3 | 0.0 | 0.329 | 1.00 |
| | Intercept only (null) | 5 | 14.8 | 0.5 | 0.254 | 1.30 |
| | EROD + EROD*Sex | 7 | 16.4 | 2.1 | 0.114 | 2.89 |
| | EROD*Sex | 7 | 16.4 | 2.1 | 0.114 | 2.89 |
| | EROD + Sex | 7 | 17.2 | 2.9 | 0.077 | 4.27 |
| | Sex | 6 | 17.5 | 3.2 | 0.065 | 5.06 |
| | EROD + Sex + EROD*Sex | 8 | 19.5 | 5.3 | 0.024 | 13.71 |
| | Sex + EROD*Sex | 8 | 19.5 | 5.3 | 0.024 | 13.71 |

**Table A.3 continued on next page.**

**Table A.3 continued**

| | | | | | | |
|---|---|---|---|---|---|---|
| Triglyceride | Intercept only (null) | 5 | 47.8 | 0.0 | 0.5673 | 1.00 |
| | Sex | 6 | 50.3 | 2.5 | 0.1643 | 3.45 |
| | EROD | 6 | 50.5 | 2.7 | 0.1446 | 3.92 |
| | EROD + Sex | 7 | 53.1 | 5.4 | 0.0389 | 14.58 |
| | EROD*Sex | 7 | 53.4 | 5.6 | 0.0342 | 16.59 |
| | EROD + EROD*Sex | 7 | 53.4 | 5.6 | 0.0342 | 16.59 |
| | Sex + EROD*Sex | 8 | 56.2 | 8.5 | 0.0083 | 68.35 |
| | EROD + Sex + EROD*Sex | 8 | 56.2 | 8.5 | 0.0083 | 68.35 |
| Uric acid | EROD | 6 | 169.5 | 0.0 | 0.334 | 1.00 |
| | Intercept only (null) | 5 | 170.4 | 0.9 | 0.213 | 1.57 |
| | EROD + EROD*Sex | 7 | 171.5 | 2.0 | 0.126 | 2.65 |
| | EROD*Sex | 7 | 171.5 | 2.0 | 0.126 | 2.65 |
| | EROD + Sex | 7 | 172.2 | 2.7 | 0.087 | 3.84 |
| | Sex | 6 | 173.0 | 3.5 | 0.057 | 5.86 |
| | EROD + Sex + EROD*Sex | 8 | 174.4 | 4.9 | 0.029 | 11.52 |
| | Sex + EROD*Sex | 8 | 174.4 | 4.9 | 0.029 | 11.52 |

[1]k: number of estimated parameters in the model
[2]AICc: Akaike's Information Criterion corrected for small sample sizes
[3]ΔAICc: difference from AICc of the best-approximating model
[4]w: AICc weight
[5]Evidence ratio = w of the best supported model / w of model
AST: aspartate aminotransferase, GGT: gamma glutamyl transferase, NEFA: non-esterified fatty acid

**Table A.4.** Factor loadings of the first three principal components (PC) of a principal component analysis of serum analytes measured in Sanderling exposed to 0 (n = 12), 12.6 (n = 12), 126 (n = 12), or 1260 (n = 13) μg/kg-bw/day of a commercial PAH mixture for 21 days.

| | Principal components | | |
|---|---|---|---|
| Response | PC1 | PC2 | PC3 |
| AST | -0.0068 | -0.31 | -0.00063 |
| Bile acid | 0.45 | -0.12 | -0.068 |
| BOHB | -0.41 | -0.26 | -0.19 |
| Cholesterol | 0.032 | -0.52 | 0.035 |
| CK | -0.093 | -0.40 | 0.041 |
| Glucose | 0.28 | -0.083 | -0.0089 |
| GGT | 0.18 | -0.25 | -0.53 |
| Hematocrit | -0.051 | 0.29 | -0.43 |
| Lipase | 0.066 | -0.42 | 0.41 |
| NEFA | -0.28 | -0.25 | -0.46 |
| TG | 0.43 | -0.081 | -0.34 |
| Uric Acid | 0.48 | -0.00087 | 0.034 |

Abbreviations: AST = aspartate aminotransferase, BOHB = β-hydroxybutyrate, CK = creatine kinase, GGT = gamma-glutamyl transferase, NEFA = non-esterified fatty acid, TG = triglyceride

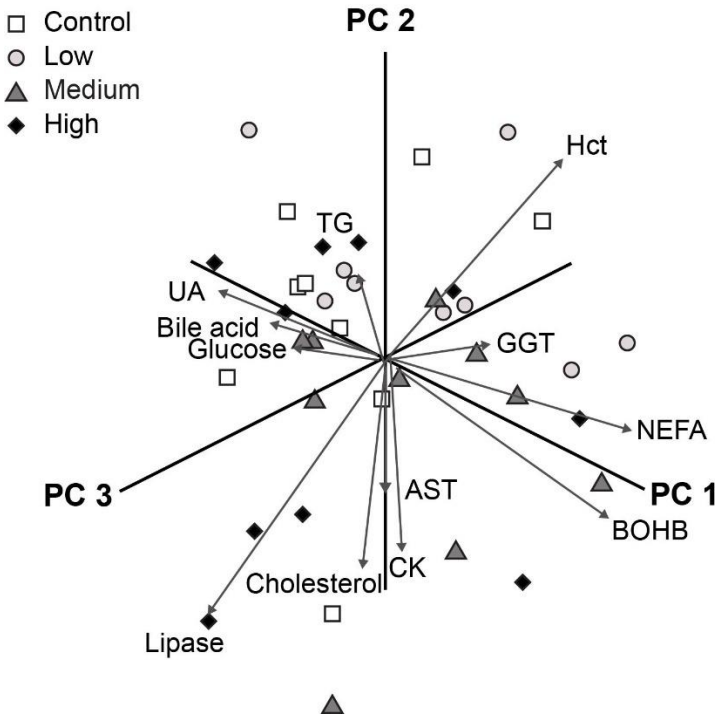


**Figure A.1.** Relationship among serum analytes in Sanderling orally exposed to 0 (Control, white squares), 12.6 (Low, light grey circles), 126 (Medium, dark grey triangles), or 1260 (High, black diamonds) µg/kg-bw/day of a commercial PAH mixture for 21 days. Serum analytes are projected onto the first three principal component axes (PC1, PC2, and PC3) of a principal component analysis, where PC1, PC2, and PC3 explain 29.5, 13.7, and 10.7% of the variance among variables, respectively. AST: aspartate aminotransferase, BOHB: β-hydroxybutyrate, CK: creatine kinase, GGT: gamma glutamyl transferase, Hct: hematocrit, NEFA: non-esterified fatty acid, TG: triglyceride, UA: uric acid.

**Table A.5.** Model selection results for linear mixed effects models to explain variation in values along principal component (PC) axis 1, PC2, and PC3 of a principal component analysis (PCA) describing the relationship among serum analytes in Sanderling orally exposed to 0 (n = 12), 12.6 (n = 12), 126 (n = 12), or 1260 (n = 13) μg/kg-bw/day of a commercial PAH mixture for 21 days.

| Response | Model structure | k[1] | AICc[2] | ΔAICc[3] | w[4] | Evidence ratio[5] |
|---|---|---|---|---|---|---|
| PC1 | Intercept only (null) | 4 | 164.1 | 0.0 | 0.436 | 1.00 |
| | Sex | 5 | 166.4 | 2.4 | 0.134 | 3.25 |
| | EROD | 5 | 166.5 | 2.4 | 0.132 | 3.30 |
| | EROD + EROD*Sex | 6 | 166.5 | 2.9 | 0.104 | 4.19 |
| | EROD*Sex | 6 | 166.9 | 2.9 | 0.104 | 4.19 |
| | EROD + Sex | 6 | 169.0 | 4.9 | 0.037 | 11.78 |
| | EROD + Sex + EROD*Sex | 7 | 169.6 | 5.6 | 0.027 | 16.15 |
| | Sex + EROD*Sex | 7 | 169.6 | 5.6 | 0.027 | 16.15 |
| PC2 | EROD | 5 | 134.2 | 0.0 | 0.369 | 1.00 |
| | Intercept only (null) | 4 | 135.1 | 0.8 | 0.241 | 1.53 |
| | EROD + EROD*Sex | 6 | 137.0 | 2.7 | 0.094 | 3.93 |
| | EROD*Sex | 6 | 137.0 | 2.7 | 0.094 | 3.93 |
| | EROD + Sex | 6 | 137.0 | 2.8 | 0.093 | 3.97 |
| | Sex | 5 | 137.7 | 3.4 | 0.066 | 5.59 |
| | Sex + EROD*Sex | 7 | 139.9 | 5.7 | 0.022 | 16.77 |
| | EROD + Sex + EROD*Sex | 7 | 139.9 | 5.7 | 0.022 | 16.77 |
| PC3 | Intercept only (null) | 4 | 125.6 | 0.0 | 0.514 | 1.00 |
| | Sex | 5 | 127.9 | 2.2 | 0.169 | 3.04 |
| | EROD | 5 | 128.0 | 2.3 | 0.159 | 3.23 |
| | EROD + Sex | 6 | 130.3 | 4.7 | 0.049 | 10.49 |
| | EROD + EROD*Sex | 6 | 130.6 | 5.0 | 0.043 | 11.95 |
| | EROD*Sex | 6 | 130.6 | 5.0 | 0.043 | 11.95 |
| | EROD + Sex + EROD*Sex | 7 | 133.2 | 7.5 | 0.012 | 42.83 |
| | Sex + EROD*Sex | 7 | 133.2 | 7.5 | 0.012 | 42.83 |

[1] k: number of estimated parameters in the model
[2] AICc: Akaike's Information Criterion corrected for small sample sizes
[3] ΔAICc: difference from AICc of the best-approximating model
[4] w: AICc weight
[5] Evidence ratio = w of the best supported model / w of model

**Table A.6.** Model selection results for linear mixed effects models to explain the variation in hepatic expression of 9 target genes in Sanderling orally exposed to 0, 12.6, 126, or 1260 µg/kg-bw/day of a commercial PAH mixture for 21 days. The global model included the fixed effect of treatment plus the random effects of cohort and sampling time.

| Response | Model structure | k[1] | AICc[2] | ΔAICc[3] | w[4] | Evidence ratio[5] |
|---|---|---|---|---|---|---|
| CYP1A4 | Intercept only (null) | 4 | 139.1 | 0.0 | 0.70 | 1.00 |
| | Treatment | 7 | 140.8 | 1.7 | 0.30 | 2.33 |
| CYP7B1 | Intercept only (null) | 4 | 45.9 | 0.0 | 0.96 | 1.00 |
| | Treatment | 7 | 52.4 | 6.6 | 0.04 | 24.0 |
| GPX3 | Intercept only (null) | 4 | 142.9 | 0.0 | 0.96 | 1.00 |
| | Treatment | 7 | 149.1 | 6.2 | 0.04 | 24.0 |
| GSTM3 | Intercept only (null) | 4 | 41.4 | 0.0 | 0.76 | 1.00 |
| | Treatment | 7 | 43.7 | 2.3 | 0.24 | 3.17 |
| HMGCR | Intercept only (null) | 4 | 128.7 | 0.0 | 0.91 | 1.00 |
| | Treatment | 7 | 133.4 | 4.6 | 0.09 | 10.1 |
| LBFABP | Treatment | 7 | 144.9 | 0.0 | 0.53 | 1.00 |
| | Intercept only (null) | 4 | 145.1 | 0.3 | 0.47 | 1.13 |
| LIPC | Treatment | 7 | 125.4 | 0.0 | 0.89 | 1.00 |
| | Intercept only (null) | 4 | 129.6 | 4.2 | 0.11 | 8.09 |
| SLCO1A2 | Intercept only (null) | 4 | 112.5 | 0.0 | 0.97 | 1.00 |
| | Treatment | 7 | 119.1 | 6.6 | 0.04 | 24.3 |

[1] k: number of estimated parameters in the model
[2] AICc: Akaike's Information Criterion corrected for small sample sizes
[3] ΔAICc: difference from AICc of the best-approximating model
[4] w: AICc weight
[5] Evidence ratio = w of the best supported model / w of model
Abbreviations: CYP1A4 = cytochrome P450 1A4, CYP7B1 = cytochrome P450 7B1, GPX3 = glutathione peroxidase 3, GSTM3 = glutathione S-transferase 3, HMGCR = 3-hydroxy-3-methylglutaryl-coenzyme A reductase, LBFABP = liver basic fatty acid binding protein 1, LIPC = hepatic lipase, SLCO1A2 = solute carrier organic anion transporter family, member 1A2

**Table A.7.** Model selection results for linear mixed effects models to explain differences in mass among Gulf of Mexico staging areas. Global model included the fixed effects of staging area, year, and age, plus the random effect of capture date and handling time.

| Response | Species | Fixed effects | k[1] | AICc[2] | ΔAICc[3] | w[4] | Evidence ratio[5] |
|---|---|---|---|---|---|---|---|
| Mass | Sanderling | year | 6 | -184.1 | 0.0 | 0.900 | 1.00 |
| | | intercept only (null) | 4 | -178.6 | 5.5 | 0.056 | 16.1 |
| | | year + age | 8 | -177.9 | 6.3 | 0.039 | 23.1 |
| | | age | 6 | -172.3 | 11.9 | 0.002 | 450 |
| | | area + year | 8 | -171.1 | 13.0 | 0.001 | 900 |
| | | area | 6 | -168.6 | 15.6 | <0.001 | >900 |
| | | area + year + age | 10 | -165.1 | 19.1 | <0.001 | >900 |
| | | area + age | 8 | -162.2 | 21.9 | <0.001 | >900 |
| | Red knot | area + year + age | 8 | 244.2 | 0.0 | 0.690 | 1.00 |
| | | year + age | 7 | 246.6 | 2.4 | 0.204 | 3.38 |
| | | area + age | 7 | 248.5 | 4.3 | 0.079 | 8.73 |
| | | age | 6 | 250.7 | 6.5 | 0.027 | 25.6 |
| | | area + year | 6 | 265.2 | 21.1 | <0.001 | >690 |
| | | year | 5 | 268.2 | 24.0 | <0.001 | >690 |
| | | area | 5 | 271.4 | 27.3 | <0.001 | >690 |
| | | intercept only (null) | 4 | 275.2 | 31.1 | <0.001 | >690 |

[1] k: number of estimated parameters in the model
[2] AICc: Akaike's Information Criterion corrected for small sample sizes
[3] ΔAICc: difference from AICc of the best-approximating model
[4] w: AICc weight
[5] Evidence ratio = w of the best supported model / w of model

**Table A.8.** Model selection results for linear mixed effects models to explain differences in plasma metabolites and fattening index among Gulf of Mexico staging areas. Global models included the fixed effects of staging area, year, and age, plus the random effects of capture date, capture time, and handling time.

| Response | Species | Fixed effects | k[1] | AICc[2] | ΔAICc[3] | w[4] | Evidence ratio[5] |
|---|---|---|---|---|---|---|---|
| TG | Sanderling | intercept only (null) | 5 | 59.1 | 0.0 | 0.789 | 1.00 |
| | | year | 6 | 62.7 | 3.6 | 0.132 | 5.98 |
| | | area | 7 | 65.3 | 6.2 | 0.036 | 21.9 |
| | | age | 7 | 65.9 | 6.8 | 0.027 | 29.2 |
| | | area + year | 8 | 67.6 | 8.5 | 0.011 | 71.7 |
| | | year + age | 8 | 69.6 | 10.5 | 0.004 | 197 |
| | | area + age | 9 | 72.4 | 13.3 | 0.001 | 789 |
| | | area + year + age | 10 | 75.0 | 15.9 | <0.001 | >789 |
| | Red knot | intercept only (null) | 5 | 18.0 | 0.0 | 0.648 | 1.00 |
| | | year | 6 | 20.8 | 2.8 | 0.159 | 4.08 |
| | | area | 6 | 20.9 | 2.9 | 0.149 | 4.35 |
| | | area + year | 7 | 25.0 | 7.0 | 0.019 | 34.1 |
| | | age | 7 | 25.2 | 7.2 | 0.018 | 36.0 |
| | | area + age | 8 | 28.8 | 10.8 | 0.003 | 216 |
| | | year + age | 8 | 28.9 | 10.9 | 0.003 | 216 |
| | | area + year + age | 9 | 33.6 | 15.6 | <0.001 | >648 |
| BOHB | Sanderling | year | 6 | 84.8 | 0.0 | 0.569 | 1.00 |
| | | intercept only (null) | 5 | 86.6 | 1.8 | 0.236 | 2.41 |
| | | area + year | 8 | 88.9 | 4.0 | 0.076 | 7.49 |
| | | year+ age | 8 | 89.0 | 4.2 | 0.070 | 8.13 |
| | | age | 7 | 90.9 | 6.0 | 0.028 | 20.3 |
| | | area | 7 | 92.2 | 7.3 | 0.015 | 37.9 |
| | | area + year + age | 10 | 93.9 | 9.0 | 0.006 | 94.8 |
| | | area + age | 9 | 96.9 | 12.1 | 0.001 | 569 |
| | Red knot | intercept only (null) | 5 | 47.4 | 0.0 | 0.676 | 1.00 |
| | | year | 6 | 49.9 | 2.5 | 0.196 | 3.45 |
| | | area | 6 | 51.8 | 4.4 | 0.074 | 9.14 |
| | | age | 7 | 53.7 | 6.3 | 0.029 | 23.3 |
| | | area + year | 7 | 54.9 | 7.5 | 0.016 | 42.3 |
| | | year + age | 8 | 56.7 | 9.3 | 0.007 | 96.6 |
| | | area + age | 8 | 58.4 | 11.0 | 0.003 | 225 |
| | | area + year + age | 9 | 62.4 | 15.0 | <0.001 | >676 |

**Table A.8 continued on next page.**

**Table A.8 continued**

| Response | Species | Fixed effects | k[1] | AICc[2] | ΔAICc[3] | w[4] | Evidence ratio[5] |
|---|---|---|---|---|---|---|---|
| UA | Sanderling | intercept only (null) | 5 | 35.3 | 0.0 | 0.680 | 1.00 |
| | | year | 6 | 37.1 | 1.7 | 0.286 | 2.38 |
| | | age | 7 | 42.7 | 7.4 | 0.017 | 40.0 |
| | | area | 7 | 43.8 | 8.5 | 0.010 | 68.0 |
| | | year + age | 8 | 44.6 | 9.3 | 0.007 | 97.1 |
| | | area + year | 8 | 47.6 | 12.3 | 0.001 | 680 |
| | | area + age | 9 | 51.4 | 16.1 | <0.001 | >680 |
| | | area + year + age | 10 | 55.3 | 20.0 | <0.001 | >680 |
| | Red knot | intercept only (null) | 5 | 19.3 | 0.0 | 0.489 | 1.00 |
| | | year | 6 | 20.2 | 0.9 | 0.311 | 1.57 |
| | | area | 6 | 22.3 | 3.0 | 0.108 | 4.53 |
| | | age | 7 | 24.0 | 4.7 | 0.046 | 10.6 |
| | | area + year | 7 | 25.1 | 5.8 | 0.028 | 17.5 |
| | | year + age | 8 | 26.7 | 7.4 | 0.012 | 40.8 |
| | | area + age | 8 | 28.2 | 9.0 | 0.006 | 81.5 |
| | | area + year + age | 9 | 32.6 | 13.3 | <0.001 | >489 |
| FI | Sanderling | area + year | 8 | 175.0 | 0.0 | 0.370 | 1.00 |
| | | year | 6 | 175.7 | 0.7 | 0.262 | 1.41 |
| | | intercept only (null) | 5 | 177.2 | 2.2 | 0.125 | 2.96 |
| | | area + year + age | 10 | 178.3 | 3.3 | 0.071 | 5.21 |
| | | year + age | 8 | 178.4 | 3.3 | 0.069 | 5.36 |
| | | area | 7 | 178.6 | 3.6 | 0.060 | 6.17 |
| | | age | 7 | 180.0 | 5.0 | 0.030 | 12.3 |
| | | area + age | 9 | 181.8 | 6.8 | 0.012 | 30.8 |
| | Red knot | intercept only (null) | 5 | 77.0 | 0.0 | 0.340 | 1.00 |
| | | area | 6 | 77.6 | 0.6 | 0.247 | 1.38 |
| | | year | 6 | 78.8 | 1.8 | 0.137 | 2.48 |
| | | age | 7 | 79.0 | 2.0 | 0.125 | 2.72 |
| | | area + age | 8 | 80.5 | 3.5 | 0.059 | 5.76 |
| | | area + year | 7 | 81.0 | 4.0 | 0.046 | 7.39 |
| | | year + age | 8 | 81.4 | 4.4 | 0.038 | 8.95 |
| | | area + year + age | 9 | 84.3 | 7.3 | 0.009 | 37.8 |

[1] k: number of estimated parameters in the model
[2] AICc: Akaike's Information Criterion corrected for small sample sizes
[3] ΔAICc: difference from AICc of the best-approximating model
[4] w: AICc weight
[5] Evidence ratio = w of the best supported model / w of model
Abbreviations: TG = triglyceride, BOHB = β-hydroxybutyrate, UA = uric acid, FI = fattening index

**Table A.9.** Model selection results for linear mixed models to compare Sanderling and Red knot departure dates at different Gulf of Mexico staging areas. Global model included the fixed effects of species, staging area, and year.

| Response | Fixed effects | k[1] | AICc[2] | ΔAICc[3] | w[4] | Evidence ratio[5] |
|---|---|---|---|---|---|---|
| Departure | species + area + year | 7 | 433.6 | 0.0 | 0.529 | 1.00 |
| | area + year | 6 | 433.8 | 0.2 | 0.467 | 1.13 |
| | species | 3 | 446.0 | 12.5 | 0.001 | 529 |
| | area | 4 | 446.8 | 13.2 | <0.001 | >529 |
| | intercept only (null) | 2 | 447.1 | 13.5 | <0.001 | >529 |
| | species + area | 5 | 447.2 | 13.7 | <0.001 | >529 |
| | species + year | 5 | 449.0 | 15.4 | <0.001 | >529 |
| | year | 4 | 449.9 | 16.3 | <0.001 | >529 |

[1] k: number of estimated parameters in the model
[2] AICc: Akaike's Information Criterion corrected for small sample sizes
[3] ΔAICc: difference from AICc of the best-approximating model
[4] w: AICc weight
[5] Evidence ratio = w of the best supported model / w of model

**Table A.10.** Model selection results for linear mixed effects models to examine the factors influencing Sanderling and Red knot departure dates from the Gulf of Mexico. Global models included the fixed effects of mass, fattening index (FI), staging area, and year. Capture date was included as a random effect in all models.

| Response | Species | Fixed effects | k[1] | AICc[2] | ΔAICc[3] | w[4] | Evidence ratio[5] |
|---|---|---|---|---|---|---|---|
| Departure | Sanderling | area + year | 6 | 159.6 | 0.0 | 0.549 | 1.00 |
| | | FI + area + year | 7 | 160.5 | 0.9 | 0.355 | 1.55 |
| | | mass + area + year | 7 | 164.6 | 5.0 | 0.045 | 12.2 |
| | | FI + mass + area + year | 8 | 165.7 | 6.2 | 0.025 | 22.0 |
| | | FI + area | 6 | 167.4 | 7.8 | 0.011 | 49.9 |
| | | area | 5 | 167.5 | 7.9 | 0.010 | 54.9 |
| | | mass + area | 6 | 172.0 | 12.5 | 0.001 | 549 |
| | | FI + year | 5 | 172.2 | 12.6 | 0.001 | 549 |
| | | FI + mass + area | 7 | 172.2 | 12.7 | <0.001 | >549 |
| | | year | 4 | 172.5 | 12.9 | <0.001 | >549 |
| | | FI | 4 | 174.2 | 14.6 | <0.001 | >549 |
| | | intercept only (null) | 3 | 174.8 | 15.2 | <0.001 | >549 |
| | | FI + mass + year | 6 | 176.7 | 17.1 | <0.001 | >549 |
| | | mass + year | 5 | 176.8 | 17.2 | <0.001 | >549 |
| | | FI + mass | 5 | 178.4 | 18.9 | <0.001 | >549 |
| | | mass | 4 | 178.8 | 19.2 | <0.001 | >549 |
| Departure | Red knot | area + year | 5 | 84.2 | 0.0 | 0.373 | 1.00 |
| | | area | 4 | 85.7 | 1.5 | 0.175 | 2.13 |
| | | year | 4 | 86.4 | 2.2 | 0.127 | 2.94 |
| | | intercept only (null) | 3 | 87.6 | 3.4 | 0.070 | 5.33 |
| | | FI + area | 5 | 87.8 | 3.6 | 0.061 | 6.11 |
| | | FI + area + year | 6 | 88.1 | 3.8 | 0.055 | 6.78 |
| | | FI | 4 | 88.5 | 4.3 | 0.044 | 8.48 |
| | | FI + year | 5 | 88.5 | 4.3 | 0.044 | 8.48 |
| | | mass | 4 | 90.7 | 6.5 | 0.015 | 24.9 |
| | | mass + area | 5 | 90.9 | 6.7 | 0.013 | 28.7 |
| | | mass + year | 5 | 91.6 | 7.4 | 0.009 | 41.4 |
| | | mass + area + year | 6 | 92.4 | 8.2 | 0.006 | 62.2 |
| | | FI + mass | 5 | 93.0 | 8.7 | 0.005 | 74.6 |
| | | FI + mass + area | 6 | 94.9 | 10.6 | 0.002 | 187 |
| | | FI + mass + year | 6 | 95.7 | 11.4 | 0.001 | 373 |
| | | FI + mass + area + year | 7 | 99.2 | 15.0 | <0.001 | >373 |

[1] k: number of estimated parameters in the model
[2] AICc: Akaike's Information Criterion corrected for small sample sizes
[3] ΔAICc: difference from AICc of the best-approximating model
[4] w: AICc weight
[5] Evidence ratio = w of the best supported model / w of model

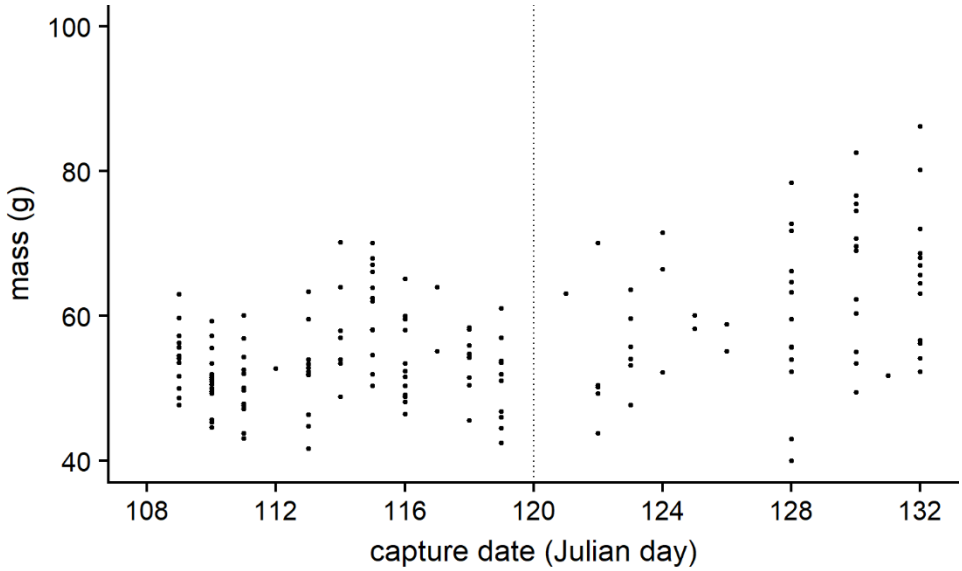


**Figure A.2.** Relationship between mass at capture and capture date for Sanderling trapped in the Gulf of Mexico. The vertical dashed line indicates the date when Sanderling ramped up fuelling (Julian day 120).

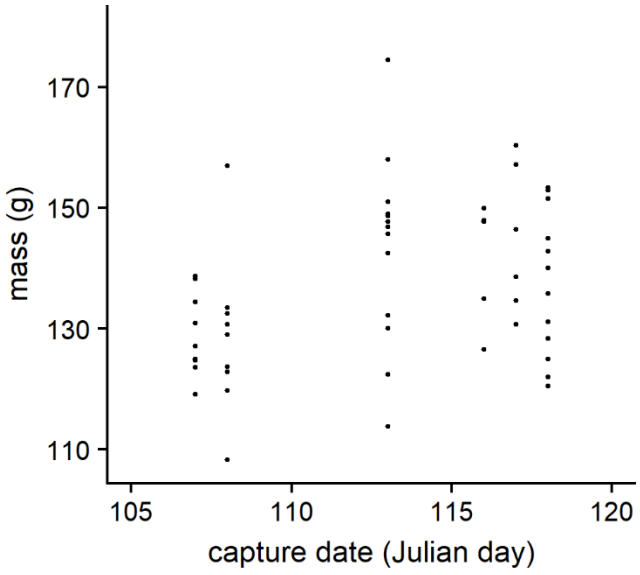


**Figure A.3.** Relationship between mass at capture and capture date for Red knots trapped in the Gulf of Mexico.

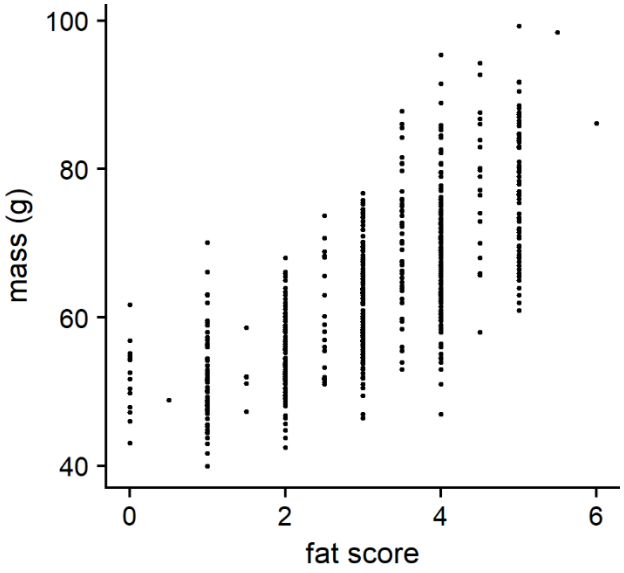


**Figure A.4.** Relationship between fat score and mass at capture of Sanderling in the Gulf of Mexico and Chaplin Lake.

**Table A.11.** Model selection results for linear mixed effects models to explain the variation in Sanderling corrected stopover duration and departure dates among trapping areas in the Gulf of Mexico. Global models included fixed effects of trapping area and year, plus the random effect of capture date.

| Response | Model structure | k[1] | AICc[2] | ΔAICc[3] | w[4] | Evidence ratio[5] |
|---|---|---|---|---|---|---|
| Stopover duration | trapping area + year | 7 | 321.2 | 0.0 | 0.995 | 1.00 |
| | year | 5 | 332.8 | 11.6 | 0.003 | 332 |
| | trapping area | 5 | 333.7 | 12.4 | 0.002 | 498 |
| | intercept only (null) | 3 | 337.8 | 16.6 | <0.001 | >995 |
| Departure date | intercept only (null) | 3 | -123.7 | 0.0 | 1.000 | 1 |
| | trapping area | 5 | -108.6 | 15.0 | <0.001 | >1000 |
| | year | 5 | -108.5 | 15.2 | <0.001 | >1000 |
| | trapping area + year | 7 | -100.1 | 23.6 | <0.001 | >1000 |

[1] k: number of estimated parameters in the model
[2] AICc: Akaike's Information Criterion corrected for small sample sizes
[3] ΔAICc: difference from AICc of the best-approximating model
[4] w: AICc weight
[5] Evidence ratio = w of the best supported model / w of model

**Table A.12.** Model selection results for linear mixed effects models to examine the effect of mass at capture on corrected stopover duration and departure dates of Sanderling in the Gulf of Mexico. The global model included fixed effects of mass at capture and year, plus the random effect of capture date.

| Response | Model structure | k[1] | AICc[2] | ΔAICc[3] | w[4] | Evidence ratio[5] |
|---|---|---|---|---|---|---|
| Stopover duration | year | 6 | 333.9 | 0.0 | 0.592 | 1.00 |
| | mass + year | 7 | 335.1 | 1.3 | 0.316 | 1.87 |
| | intercept only (null) | 4 | 338.9 | 5.0 | 0.048 | 12.3 |
| | mass | 5 | 339.1 | 5.2 | 0.044 | 13.5 |
| Departure date | year | 6 | 335.5 | 0.0 | 0.548 | 1.00 |
| | mass + year | 7 | 336.5 | 1.0 | 0.340 | 1.61 |
| | intercept only (null) | 4 | 339.7 | 4.2 | 0.068 | 8.06 |
| | mass | 5 | 340.6 | 5.1 | 0.044 | 12.5 |

[1] k: number of estimated parameters in the model
[2] AICc: Akaike's Information Criterion corrected for small sample sizes
[3] ΔAICc: difference from AICc of the best-approximating model
[4] w: AICc weight
[5] Evidence ratio = w of the best supported model / w of model

**Table A.13.** Model selection results for linear models to examine the effect of Gulf of Mexico departure date on Sanderling migratory travel time. The global model included fixed effects of departure date and year.

| Response | Model structure | k[1] | AICc[2] | ΔAICc[3] | w[4] | Evidence ratio[5] |
|---|---|---|---|---|---|---|
| Travel time | departure date + year | 5 | 147.8 | 0.0 | 0.310 | 1.00 |
| | departure date | 3 | 148.0 | 0.1 | 0.290 | 1.07 |
| | year | 4 | 148.2 | 0.3 | 0.270 | 1.15 |
| | intercept only (null) | 2 | 149.6 | 1.8 | 0.130 | 2.38 |

[1] k: number of estimated parameters in the model
[2] AICc: Akaike's Information Criterion corrected for small sample sizes
[3] ΔAICc: difference from AICc of the best-approximating model
[4] w: AICc weight
[5] Evidence ratio = w of the best supported model / w of model

**Table A.14.** Model selection results for linear models to explain variation in migratory travel time among Sanderling from different Gulf of Mexico trapping areas. The global model included fixed effects of trapping area and year.

| Response | Model structure | k[1] | AICc[2] | ΔAICc[3] | w[4] | Evidence ratio[5] |
|---|---|---|---|---|---|---|
| Travel time | intercept only (null) | 2 | 149.6 | 0.0 | 0.573 | 1.00 |
| | trapping area + year | 5 | 151.6 | 2.0 | 0.211 | 2.72 |
| | year | 3 | 152.3 | 2.7 | 0.149 | 3.85 |
| | trapping area | 4 | 153.9 | 4.3 | 0.068 | 8.43 |

[1] k: number of estimated parameters in the model
[2] AICc: Akaike's Information Criterion corrected for small sample sizes
[3] ΔAICc: difference from AICc of the best-approximating model
[4] w: AICc weight
[5] Evidence ratio = w of the best supported model / w of model

**Table A.15.** Model selection results for linear models to explain variation in Sanderling arrival dates in Chaplin Lake. The global model included fixed effects of travel time, Gulf of Mexico departure date, year, and the interaction of Gulf of Mexico departure date and travel time.

| Response | Model structure | k[1] | AICc[2] | ΔAICc[3] | w[4] | Evidence ratio[5] |
|---|---|---|---|---|---|---|
| Arrival date | travel time + departure date | 4 | 98.7 | 0.0 | 0.481 | 1.00 |
| | departure date + travel time:departure date | 4 | 99.2 | 0.5 | 0.366 | 1.31 |
| | departure date + travel time + travel time:departure date | 5 | 102.1 | 3.4 | 0.087 | 5.53 |
| | travel time + departure date + year | 6 | 104.9 | 6.2 | 0.022 | 21.9 |
| | departure date + year + travel time:departure date | 6 | 105.2 | 6.5 | 0.019 | 25.3 |
| | travel time | 3 | 105.4 | 6.7 | 0.017 | 28.3 |
| | intercept only (null) | 2 | 108.1 | 9.4 | 0.005 | 96.2 |
| | departure date | 3 | 109.5 | 10.8 | 0.002 | 241 |
| | travel time + year | 5 | 110.6 | 11.9 | 0.001 | 481 |
| | travel time + departure date + year + travel time:departure date | 7 | 112.1 | 13.4 | <0.001 | >481 |
| | year | 4 | 113.1 | 14.5 | <0.001 | >481 |
| | departure date + year | 5 | 116.4 | 17.7 | <0.001 | >481 |

[1] k: number of estimated parameters in the model
[2] AICc: Akaike's Information Criterion corrected for small sample sizes
[3] ΔAICc: difference from AICc of the best-approximating model
[4] w: AICc weight
[5] Evidence ratio = w of the best supported model / w of model

**Table A.16.** Model selection results for linear models to explain variation in Chaplin Lake arrival dates among Sanderling from different Gulf of Mexico trapping areas. The global model included fixed effects of trapping area and year.

| Response | Model structure | k[1] | AICc[2] | ΔAICc[3] | w[4] | Evidence ratio[5] |
|---|---|---|---|---|---|---|
| Arrival date | trapping area | 4 | 126.1 | 0.0 | 0.88 | 1.00 |
| | intercept only (null) | 2 | 131.5 | 5.4 | 0.058 | 15.2 |
| | year | 4 | 132.1 | 6.0 | 0.043 | 20.5 |
| | trapping area + year | 6 | 133.7 | 7.6 | 0.020 | 44.0 |

[1] k: number of estimated parameters in the model
[2] AICc: Akaike's Information Criterion corrected for small sample sizes
[3] ΔAICc: difference from AICc of the best-approximating model
[4] w: AICc weight
[5] Evidence ratio = w of the best supported model / w of model

**Table A.17.** Model selection results for linear models to examine the relationship between Sanderling arrival and departure dates in Chaplin Lake. The global model included fixed effects of arrival date and year.

| Response | Model structure | k[1] | AICc[2] | ΔAICc[3] | w[4] | Evidence ratio[5] |
|---|---|---|---|---|---|---|
| Departure date | arrival date | 3 | 108.9 | 0.0 | 0.073 | 1.00 |
| | arrival date + year | 5 | 111.0 | 2.1 | 0.025 | 2.92 |
| | intercept only (null) | 2 | 117.0 | 8.1 | 0.013 | 5.62 |
| | year | 4 | 121.6 | 12.7 | 0.001 | 73.0 |

[1] k: number of estimated parameters in the model
[2] AICc: Akaike's Information Criterion corrected for small sample sizes
[3] ΔAICc: difference from AICc of the best-approximating model
[4] w: AICc weight
[5] Evidence ratio = w of the best supported model / w of model

**Table A.18.** Model selection results for linear models to explain the variation in Chaplin Lake stopover durations among Sanderling from different Gulf of Mexico trapping areas. The global model included fixed effects of trapping area and year.

| Response | Model structure | k[1] | AICc[2] | ΔAICc[3] | w[4] | Evidence ratio[5] |
|---|---|---|---|---|---|---|
| Stopover duration | trapping area | 4 | 113.6 | 0.0 | 0.828 | 1.00 |
| | year | 4 | 117.7 | 4.1 | 0.106 | 7.81 |
| | trapping area + year | 6 | 119.7 | 6.1 | 0.040 | 20.7 |
| | intercept only (null) | 2 | 120.4 | 6.9 | 0.027 | 30.7 |

[1] k: number of estimated parameters in the model
[2] AICc: Akaike's Information Criterion corrected for small sample sizes
[3] ΔAICc: difference from AICc of the best-approximating model
[4] w: AICc weight
[5] Evidence ratio = w of the best supported model / w of model

**Table A.19.** Model selection results for linear mixed effects models to explain variation in Sanderling stopover duration and departure date in Chaplin Lake. Global model included fixed effects of trapping area and year, plus the random intercept of capture date.

| Response | Model structure | k[1] | AICc[2] | ΔAICc[3] | w[4] | Evidence ratio[5] |
|---|---|---|---|---|---|---|
| Stopover duration | trapping area + year | 8 | 748.2 | 0.0 | 1.000 | 1.00 |
| | trapping area | 6 | 762.6 | 14.4 | <0.001 | >1000 |
| | year | 5 | 764.9 | 16.7 | <0.001 | >1000 |
| | intercept only (null) | 3 | 774.5 | 26.3 | <0.001 | >1000 |
| Departure date | trapping area + year | 8 | 3676.2 | 0.0 | 1.000 | 1.00 |
| | trapping area | 6 | 3725.1 | 48.9 | <0.001 | >1000 |
| | year | 5 | 3747.4 | 71.3 | <0.001 | >1000 |
| | intercept only (null) | 3 | 3798.4 | 122.2 | <0.001 | >1000 |

[1] k: number of estimated parameters in the model
[2] AICc: Akaike's Information Criterion corrected for small sample sizes
[3] ΔAICc: difference from AICc of the best-approximating model
[4] w: AICc weight
[5] Evidence ratio = w of the best supported model / w of model

**Table A.20.** Model selection results for linear mixed effects models to examine the effect of mass at capture on the minimum stopover duration and departure date of Sanderling in Chaplin Lake. Global models included fixed effects of mass at capture and year, plus the random effect of capture date.

| Response | Model structure | k[1] | AICc[2] | ΔAICc[3] | w[4] | Evidence ratio[5] |
|---|---|---|---|---|---|---|
| Stopover duration | mass + year | 7 | 638.5 | 0.0 | 0.958 | 1.00 |
| | year | 6 | 645.3 | 6.8 | 0.032 | 29.9 |
| | mass | 5 | 647.6 | 9.1 | 0.010 | 95.8 |
| | intercept only (null) | 4 | 633.1 | 24.6 | <0.001 | >958 |
| Departure date | mass | 5 | 660.5 | 0.0 | 0.420 | 1.00 |
| | mass + year | 7 | 660.9 | 0.4 | 0.340 | 1.24 |
| | year | 6 | 662.0 | 1.5 | 0.196 | 2.14 |
| | intercept only (null) | 4 | 665.1 | 4.5 | 0.043 | 9.77 |

[1] k: number of estimated parameters in the model
[2] AICc: Akaike's Information Criterion corrected for small sample sizes
[3] ΔAICc: difference from AICc of the best-approximating model
[4] w: AICc weight
[5] Evidence ratio = w of the best supported model / w of model